

A POSTURE CONTROL MODEL AND BALANCE TEST
FOR THE PREDICTION OF RELATIVE POSTURAL STABILITY
With Special Consideration to the Problem of Falling in the Elderly

by

BRIAN EDWARD MAKI

Bachelor of Applied Science (Honours)
Mechanical Engineering, University of British Columbia, 1979

Master of Science in Mechanical Engineering
Massachusetts Institute of Technology, 1982

A THESIS

submitted in partial fulfillment
of the requirements for the degree of

DOCTOR OF PHILOSOPHY

in the

BIOENGINEERING UNIT
UNIVERSITY OF STRATHCLYDE

Glasgow
September, 1987

ABSTRACT

A balance testing methodology was developed, based on a posture control model which defines relative stability by the degree to which a transient postural perturbation would cause the centre-of-pressure on the feet to approach the limits of the base-of-support. To minimize anticipatory adaptations and to ensure subject safety, the balance test used a small-amplitude continuous random or pseudorandom perturbation. The data were used to identify an input-output model, which was then used to predict large-amplitude transient response. The test perturbation was an anterior-posterior acceleration of a platform on which the subject stood. Pilot experiments were performed to determine appropriate perturbation parameters.

Testing of sixty-four normal subjects demonstrated highly significant ageing-related decreases in predicted stability. No significant sex-related differences were found. Predicted stability increased when the subjects were blindfolded. In using the balance test to identify balance-impaired individuals, the blindfolded results and the eyes-open/blindfolded ratio provided higher success rates than the eyes-open results. Depending on the modelling method used, the balance test was able to identify up to three of five vestibular patients and five of five elderly fallers, at a false positive rate of 25% in the normal subjects.

Correlations between the balance test results and measures of spontaneous postural sway were weak, except in the normal young adult subjects. Comparison with transient tests showed the balance test to yield reasonably accurate predictions of small-amplitude transient response, but to overestimate the large-amplitude response; however, the transient test results may have been confounded by adaptive effects.

It was concluded that the balance test provides a sensitive functional measure of the changes in postural control that are known to occur in ageing. Although it shows promise as a tool for identifying balance impairments, larger numbers of balance-impaired subjects must be tested.

ACKNOWLEDGEMENTS

I would like to express my deep appreciation to Geoff Fernie for his guidance and support and for first stimulating my interest in this project. I would also like to thank Professor J.P. Paul and Dr. A.C. Nicol for their guiding comments and advice.

I gratefully acknowledge the funding support provided by the Medical Research Council of Canada, via operating grant MA-8025. The work was conducted at the West Park Research laboratory of the Department of Surgery, University of Toronto.

The people in the laboratory at West Park Research are deserving of much thanks for their invaluable help and advice over the past four years, as well as for their participation as volunteers in the experiments: Gerry Griggs, Jean Holden, Pam Holliday, Brock Irwin, Richard Lobb, Kevin Lunau and Gloria Redmond. In particular, I would like to acknowledge the assistance received from Gerry Griggs, Brock Irwin and Richard Lobb in constructing the apparatus and instrumentation, and from Pam Holliday and Franca Iannotta in recruiting the subjects and performing the experiments.

I would also like to thank all of the volunteers who participated in the experiments, as well as Dr. Cyril Gryfe and Ruth Miller of the Baycrest Centre for Geriatric Care for recruiting the elderly faller subjects.

Finally, and above all, I would like to thank my wife, Ellen, for her much-needed advice and assistance, and for her unflagging support, understanding and patience. I dedicate this thesis to her, to my mother, Irene Maki, and to the memory of my father, Harvey Maki.

TABLE OF CONTENTS

	<u>Page</u>
TITLE PAGE	i
ABSTRACT	ii
ACKNOWLEDGEMENTS	iii
TABLE OF CONTENTS	iv
LIST OF FIGURES	xi
LIST OF TABLES	xiii
LIST OF ABBREVIATIONS AND SYMBOLS	xiv
CHAPTER 1. INTRODUCTION	
1.1 Statement of thesis	1
1.2 Description of the problem	1
1.3 Scope of the thesis	2
1.4 Outline of the thesis	3
CHAPTER 2. REVIEW OF CURRENT KNOWLEDGE	
2.1 Functional anatomy and physiology of postural control	5
2.1.1 The regulated plant: the skeletal linkage	5
2.1.1.1 Inverted pendulum model	5
2.1.1.2 Multi-link models	6
2.1.2 The controller: the neural centres and pathways	7
2.1.3 The actuators: the motor system	9
2.1.4 The feedback transducers: the sensory receptors	10
2.1.4.1 Somatosensors	10
2.1.4.2 The vestibular system	11
2.1.4.3 The visual system	12
2.2 Methods for the study of postural control	13
2.2.1 Measurement methods	13
2.2.2 Spontaneous sway experiments	14
2.2.3 Induced sway experiments	15
2.2.4 Sensory stimulation and disruption	17
2.3 Existing knowledge about posture control mechanisms	18
2.3.1 The stretch reflex	19
2.3.2 Vestibular reflexes	19
2.3.3 Visual reflexes	20

	<u>Page</u>
2.3.4 Organization of postural responses	21
2.4 Causes of falling in the elderly	23
2.4.1 Effects of ageing: incidence and severity of perturbations	24
2.4.2 Effects of ageing: postural performance	25
2.4.3 Epidemiological studies of falling	26
2.4.3.1 Circumstances of falls	26
2.4.3.2 Characteristics of fallers	27
2.4.4 Prediction of falling liability	29
 CHAPTER 3. THE POSTURE CONTROL MODEL AND BALANCE TEST	
3.1 The posture control model	32
3.1.1 A general conceptual model	32
3.1.2 Stability	32
3.1.3 The simplified model	33
3.2 Simulation of falling situations	34
3.2.1 Difficulties with transient-waveform tests	34
3.2.2 Continuous-waveform tests	35
3.2.3 The test perturbation	36
3.3 The testing methodology	37
 CHAPTER 4. THE PERTURBATION PLATFORM	
4.1 Design requirements	38
4.1.1 Introduction	38
4.1.2 Review of the literature	39
4.1.3 Simulation of balancing responses	39
4.1.4 Summary	40
4.2 Mechanical design	41
4.2.1 Drive train	41
4.2.2 Power supply	43
4.2.3 Structural components	43
4.2.4 Visual surround and safety structures	44
4.3 Control system	45
4.3.1 Design and fine-tuning	45
4.3.2 Performance	47

	<u>Page</u>
4.4 Instrumentation	47
4.4.1 Position, velocity and acceleration transducers	47
4.4.2 Force plates	48
4.4.3 Computer and computer interface	50
4.5 Calibration and performance of the instrumentation	52
4.5.1 The calibration jig	52
4.5.2 Linear potentiometer	52
4.5.3 Force plates	53
4.5.4 Accelerometer	56
4.6 Safety features	57
 CHAPTER 5. SELECTION OF THE PERTURBATION PARAMETERS	
5.1 Introduction	59
5.2 General requirements	59
5.2.1 Persistent excitation	59
5.2.2 Accuracy of identification	59
5.2.3 Stationarity	60
5.2.4 Human tolerance and safety	60
5.3 Perturbation parameters	60
5.3.1 Waveform	60
5.3.2 Power spectrum	62
5.3.3 Bandwidth	62
5.3.4 Amplitude	64
5.3.5 Duration	65
5.4 Experimental methods used in the pilot tests	65
5.4.1 Subjects	65
5.4.2 Test procedure	65
5.4.3 Protocol	66
5.4.4 Analysis	67
5.5 Results and discussion	68
5.5.1 Waveform	68
5.5.2 Power spectrum	69
5.5.3 Bandwidth	69
5.5.4 Amplitude	69
5.5.5 Duration	70
5.6 Conclusions	71

CHAPTER 6. EXPERIMENTAL AND ANALYTICAL METHODS

6.1	Test perturbations	73
6.2	Subjects	74
6.3	Testing procedure	75
6.4	Protocol	76
6.5	System identification methods	77
6.5.1	Cross-spectral analysis	78
6.5.2	Least squares and maximum likelihood methods	79
6.6	Estimation of the saturation amplitude	80
6.7	Quantification of spontaneous sway	81
6.8	Prediction of transient response	81
6.9	Statistical analyses	82
6.9.1	Statistical models	82
6.9.2	Analysis of balance test responses	83
6.9.3	Analysis of spontaneous sway measures	83
6.9.4	Analysis of transient responses	84

CHAPTER 7. EXPERIMENTAL RESULTS

7.1	Balance test responses	86
7.1.1	Comparison of system identification models	86
7.1.2	Comparison of tests	89
7.1.3	Age and sex differences in normal subjects	90
7.1.4	Identification of balance-impaired individuals	90
7.1.5	Validation of the statistical models	92
7.2	Spontaneous sway measures	93
7.2.1	Comparison with balance test responses	93
7.2.2	Responses in normal subjects	94
7.2.3	Identification of balance-impaired individuals	95
7.2.4	Validation of the statistical models	95
7.3	Transient responses	97
7.3.1	Dependence of actual response on perturbation amplitude	97
7.3.2	Comparison of actual and predicted responses	98
7.3.3	Functional definition of the base-of-support	99
7.3.4	Validation of the statistical models	99

CHAPTER 8. DISCUSSION

8.1	Rationale for the experimental and analytical methodology	101
8.1.1	The test perturbation	101
8.1.2	The testing procedures	102
8.1.3	The experimental protocol	103
8.1.4	The methods of analysis	104
8.2	Balance test responses	107
8.2.1	Age and sex differences in normal subjects	107
8.2.2	Comparison of tests	109
8.2.3	Influence of vision	111
8.2.4	Balance test responses in the balance-impaired groups	114
8.2.5	Identification of balance-impaired individuals	117
8.3	Spontaneous sway	120
8.3.1	Comparison with balance test responses	120
8.3.2	Age-related differences in normal subjects	121
8.3.3	Sex-related differences in normal subjects	123
8.3.4	Identification of balance-impaired individuals	124
8.4	Transient test responses	125
8.4.1	Linearity	125
8.4.2	Comparison of actual and predicted response	128
8.4.3	Functional definition of the base-of-support	128
8.5	An assessment of the posture control model	130
8.5.1	Relation to current theories of postural control	130
→ 8.5.2	Limitations	132
8.5.3	Validation of the posture control model	134
8.6	An assessment of the balance test	135
8.6.1	The test perturbation	135
→ 8.6.2	Measurement and computational accuracy	138
8.6.2.1	Sources of error	138
8.6.2.2	Simulation of effects of errors	140
8.6.3	System identification methods	142
8.6.4	Estimation of the saturation amplitude	144
8.6.5	Linearity	145
8.6.6	Modulation of balance test responses	147

	<u>Page</u>
↗ 8.6.7 Repeatability	150
↗ 8.6.8 Validation of the balance test	151
8.7 Suggested improvements to the balance test	153
8.7.1 The perturbation platform	153
8.7.2 The testing procedure and protocol	154
8.8 ↗ Directions for future research	155
CHAPTER 9. SUMMARY	159
REFERENCES	162
APPENDIX A. ANALYSIS AND SIMULATION OF THE POSTURE CONTROL SYSTEM	
A.1 Derivation of a simplified dynamic model	179
A.1.1 Single-link sub-saturation model	179
A.1.2 Two-link saturated base-of-support model	183
A.2 Simulation methods	185
A.3 Simulation results	186
A.3.1 Influence of shear forces	186
A.3.2 Perturbation bandwidth requirements	187
A.3.3 Perturbation amplitude requirements	188
A.3.4 Effects of ageing on balancing responses	189
A.3.5 Effects of changes in feedback gain	190
A.3.6 Sensory thresholds	191
A.4 Limitations of the simulation model	192
APPENDIX B. SYSTEM IDENTIFICATION WITH PSEUDORANDOM INPUTS	
B.1 Theory	195
B.1.1 Random input	196
B.1.2 Pseudorandom input	197
B.2 Simulation example	199
B.3 Conclusion	201
APPENDIX C. PILOT EXPERIMENTS TO ASSESS REPEATABILITY	
C.1 Introduction	203

	<u>Page</u>
C.2 Methodology	203
C.2.1 Subjects	203
C.2.2 Testing procedure	203
C.2.3 Test perturbations	204
C.2.4 Protocol	204
C.2.5 Analysis	204
C.3 Results	205
C.4 Discussion	207
C.4.1 Adaptation to the test procedure	207
C.4.2 Adaptation to the test perturbation	208
C.4.3 Random variability	208
C.4.4 Limitations	209

LIST OF FIGURES

	<u>Page</u>
2.1 Conceptual model of the posture control system	5a
2.2 Organization of the neural centres and pathways	8a
2.3 Functional anatomy of the lower extremity	10a
3.1 The anterior-posterior stability margin	33a
3.2 The linear-nonlinear cascade posture control model	34a
4.1 Schematic of the perturbation platform	41a
4.2 Speed-torque characteristics	42a
4.3 Drive train	43a
4.4 Platform carriage and supporting structures	44a
4.5 Safety structures and framework	45a
4.6 Polyurethane foam enclosure and visual surround	46a
4.7 Frequency response of the platform	47a
4.8 Vertical-force measurements	48a
4.9 Horizontal-force measurements	49a
4.10 Free-body diagram of force plate	50a
4.11 The calibration jig	52a
4.12 Frequency response of right force plate	55a
5.1 Comparison of waveforms	68a
5.2 Comparison of power spectra	69a
5.3 Effect of input amplitude	70a
5.4 Effect of changes in duration	71a
7.1 Example data from pseudorandom test	86a
7.2 Example transfer function estimates: cross-spectral model	87a
7.3 Example transfer function estimates: least squares and maximum likelihood models	87
7.4 Example transient response predictions	88a
7.5 Example spontaneous sway results	93a
7.6 Example transient test results	97a

	<u>Page</u>
8.1 Influence of nonlinearity on saturation amplitude estimates	145a
A.1 Free-body diagram: single-link sub-saturation model	179a
A.2 Approximate linear model of the posture control system	182a
A.3 Free-body diagram: two-link saturated base-of-support model	183a
A.4 Example frequency response	186a
A.5 Example unit pulse responses	187a
A.6 Effects of changes in feedback gain	188a
A.7 Effects of changes in dead time	189a
A.8 Effects of changes in height and weight	190a
A.9 Effect of feedback gain on peak responses	191a
A.10 Ankle kinematics: pseudorandom perturbation	192a
A.11 Ankle kinematics: transient perturbation	193a
B.1 The measurement problem	195a
B.2 Simulation results for purely random noise	199a
B.3 Simulation results for random noise plus nonlinearity	200a
B.4 Simulation results for "nonharmonic" pseudorandom input	201a
C.1 Results of repeatability tests: pseudorandom waveform	206a
C.2 Results of repeatability tests: random waveform	206

LIST OF TABLES

	<u>Page</u>
4.1 Perturbation parameters used by other investigators	39a
4.2 Performance of the force plates	54a
6.1 Characteristics of the normal subjects	74a
6.2 Characteristics of the balance-impaired subjects	75a
6.3 Outline of the protocol	76a
7.1 Comparison of the system identification models	88
7.2 Comparison of the continuous-waveform tests	89a
7.3 Saturation amplitude: age and sex differences in normal subjects	90a
7.4 Saturation amplitude: classification of balance-impaired subjects	91a
7.5 Saturation amplitude: summary of subject classification	91
7.6 Comparison of spontaneous sway measures with saturation amplitude	94a
7.7 Spontaneous sway: age and sex differences in normals	95a
7.8 Spontaneous sway: classification of balance-impaired subjects	96a
7.9 Spontaneous sway: summary of subject classification	96
7.10 Transient response: regression versus perturbation amplitude	98a
7.11 Comparison of actual and predicted transient response	99a
7.12 Stepwise regression: maximum centre-of-pressure displacement versus foot dimensions	100a
8.1 Results of simulation of measurement and computational error	141a
A.1 Simulation parameters	185a
C.1 Test-to-test and day-to-day variability: coefficients of variation	205a
C.2 Summary of regression versus day and test number	207a

LIST OF ABBREVIATIONS AND SYMBOLS

ACC	- waveform with flat acceleration spectrum
ACCEL	- acceleration (of the perturbation platform)
ADC	- analog-to-digital converter
ADL	- activities of daily living
AIC	- Akaike Information Criterion
ANOVA	- analysis of variance
a-p	- anterior-posterior
BF	- blindfolded
BOS	- base-of-support
CFREQ	- spectral centroidal frequency (of spontaneous COP displacement)
CNS	- central nervous system
COG	- centre-of-gravity
COP	- centre-of-pressure
CS	- cross-spectral (system identification method)
CV	- coefficient of variation
DAC	- digital-to-analog converter
DC	- direct current
DISP	- spectral dispersion (of spontaneous COP displacement)
EMG	- electromyography
EO	- eyes open
FFT	- Fast Fourier Transform
FM	- frequency modulation
HPRN	- harmonic pseudorandom (waveform)
LN	- linear-nonlinear (cascade model)
LS	- least squares (system identification method)
MFREQ	- mean frequency (of spontaneous COP displacement)
ML	- maximum likelihood (system identification method)
m-l	- medial-lateral
MTP	- metatarsophalangeal (joints)
NHPRN	- nonharmonic pseudorandom (waveform)
PNS	- peripheral nervous system
POS	- waveform with flat position spectrum

- PRN - pseudorandom (waveform)
- p - probability value (observed level of significance)
- R² - coefficient of determination
- R_a² - coefficient of determination, adjusted for degrees of freedom
- RAN - random (waveform)
- RANGE - peak-to-peak range (of spontaneous COP displacement)
- RMS - root-mean-square (in general, or in specific reference to spontaneous COP displacement)
- RPM - revolutions per minute
- SA - saturation amplitude
- SCR - silicon controlled rectifier
- S/N - signal-to-noise ratio
- SPEED - average speed (of spontaneous COP displacement)
- VEL - waveform with flat velocity spectrum

- α - level of significance
- Δ COP - peak COP displacement in the unit pulse response .

CHAPTER 1. INTRODUCTION

1.1 STATEMENT OF THESIS

The posture control model hypothesizes that relative postural stability can be quantified by the degree to which a transient postural perturbation causes the centre-of-pressure on the feet to approach the limits of the base-of-support.

The primary objectives of this thesis were to: (1) develop a balance testing methodology based on the posture control model, (2) investigate the balance test responses in normal young and elderly adult subjects, and (3) begin to evaluate the ability of the balance test to identify balance-impaired individuals.

1.2 DESCRIPTION OF THE PROBLEM

Postural instability and falling are major problems faced by many elderly people. An estimated 28% of community-dwelling elderly people fall each year (Prudham and Evans, 1981). In a study of an institutionalized ambulatory elderly population, Gryfe et al (1977) reported an annual incidence rate of 668 falls per 1000 residents.

Although an estimated 71% (Sehested and Severin-Nielsen, 1977) to 83% (Gryfe et al, 1977) of falls in the elderly result in no significant injury, the injuries that do occur can have serious consequences. Indeed, falls are the leading cause of accidental death in persons aged 65 or older (Metropolitan Life, 1978). One of the more serious results of a fall is fracture of the proximal femur. In the United States, there are 200,000 hip fractures each year, of which 84% occur in the population 65 and older (Baker and Harvey, 1985). The associated health care costs have been estimated at two billion dollars. Other consequences of falls in the elderly include soft tissue injuries, as well as other types of fractures (most commonly, fractures of the upper extremity) (Gryfe et al, 1977). In addition to acute injuries, the experience of having fallen can lead to the "post-fall syndrome", a severe dread of falling which limits mobility and independence (Isaacs, 1983).

There is a need to develop an appropriate balance test which could be used to identify individuals who are at-risk, before they

experience a debilitating fall, thereby allowing preventative measures to be taken (e.g. balance training programs, walking aids, pharmacotherapy, withdrawal of inappropriate pharmacotherapies). If successful in predicting falling liability, such a balance test could also be used in experimental investigations of causal and preventative factors (e.g. environmental lighting, footwear, drugs).

Although the present work has been aimed at the problem of falling in the elderly, the proposed balance test could find application in the diagnosis and follow-up of other balance-impaired patient groups.

Another potential application is in the area of occupational health and safety. Conceivably, the large numbers of falls and associated injuries that occur in the work environment (National Safety Council, 1979) could be reduced by matching workers to job classifications on the basis of postural performance. Alternatively, the balance test could be used to monitor the effects of neurotoxic substances to which workers might be exposed. The balance test could be used in designing safer living and working environments (e.g. effect of lighting level) or in predicting balance responses in unusual environments (e.g. effect of hypoxia, as in high-altitude flight).

1.3 SCOPE OF THE THESIS

The first part of the thesis work focused on the development of the posture control model and the associated balance testing methodology. The balance test quantifies the balancing response to a postural perturbation, applied by accelerating the platform on which the subject stands. Thus, the initial work included the development of the perturbation platform and the selection of appropriate perturbation characteristics. Pilot experiments were performed on a small number of healthy normal subjects to aid in the selection of the perturbation parameters.

The balance test responses in normal subjects were determined, based on testing of 32 young and 32 elderly healthy normal adults. Age- and sex-related differences were evaluated, as were the effects of vision-deprivation (i.e. blindfolding). The ability of

the balance test to identify balance-impaired individuals was assessed, in a preliminary manner, by testing 5 patients with vestibular lesions and 5 elderly subjects with a documented history of falling, and comparing the results to the normal values. The results obtained in the eyes-open tests were compared to traditional measures of spontaneous postural sway.

The balance test predicts the transient response of the posture control system, based on the measured response to a continuous platform motion. The correlation between predicted and actual transient response was evaluated, using data from transient tests performed on the normal young adult subjects.

Conclusive validation of the posture control model and balance testing methodology will require testing of larger numbers of subjects. This work is beyond the scope of the present thesis.

1.4 OUTLINE OF THE THESIS

A review of the literature is presented in Chapter 2. This review focuses on the physiology and biomechanics of postural control and the existing methods for quantifying postural stability and falling liability.

The posture control model and balance test are presented in Chapter 3, along with the underlying rationale. Chapter 4 describes the design, calibration and performance testing of the perturbation platform used in the balance tests, while the selection of the perturbation characteristics is discussed in Chapter 5.

The experimental and analytical methods are detailed in Chapter 6. The experimental results are presented in Chapter 7, including: (1) balance test responses in normal subjects, (2) ability of the balance test to identify balance-impaired individuals, (3) comparison of the balance test results with those obtained using conventional measures of spontaneous postural sway, and (4) comparison of the predictions with actual measurements of transient response.

In Chapter 8, the experimental results are discussed. The results are compared to findings of other investigators, the extent to which the results validate the posture control model and balance

test methodology is evaluated, the assumptions and limitations of the model and test methodology are summarized, and suggestions for future work are presented. The conclusions of the thesis are summarized in Chapter 9.

Appendix A presents a simplified analysis of the dynamics of postural control and describes the simulations that were performed. The simulation results were used in designing the perturbation platform, and in evaluating the experimental methods and results. In designing the test perturbation, problems in using certain types of pseudorandom waveforms were identified; these are discussed in Appendix B. Appendix C describes pilot experiments performed to assess the test-to-test and day-to-day repeatability of the balance test responses.

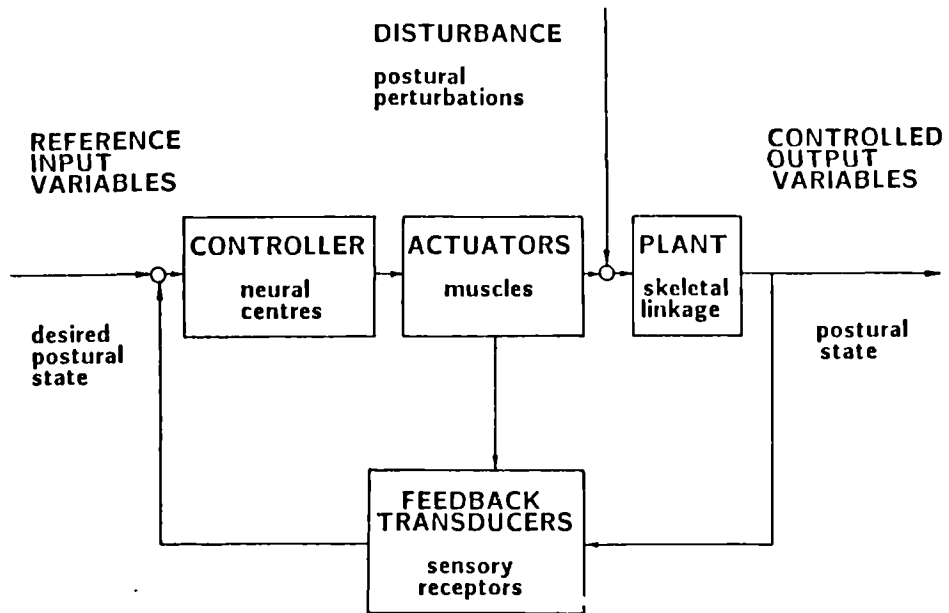


Fig 2.1 Conceptual model of the posture control system.

CHAPTER 2. REVIEW OF CURRENT KNOWLEDGE

2.1 FUNCTIONAL ANATOMY AND PHYSIOLOGY OF POSTURAL CONTROL

The posture control system can be conceptualized as a negative feedback system which acts to maintain the skeletal linkage in an upright position, in opposition to destabilizing perturbations. Neural centres process feedback from the sensory receptors and send commands to the muscles, which then generate stabilizing moments at the joints. In control engineering parlance, the skeletal linkage is the "plant" to be regulated, the neural centres and pathways are the "controllers", the muscles are the "actuators" and the sensory receptors are the "feedback transducers" (see fig 2.1).

2.1.1 The Regulated Plant: The Skeletal Linkage

For simplicity, the skeleton is often represented as a planar linkage of rigid segments, while the complex kinematics of the joints are approximated as simple frictionless pinned connections. However, since the skeletal linkage has over 200 degrees-of-freedom (Barin, 1983), further simplification is necessary to permit the dynamics of the linkage to be analyzed. In most cases, models have been limited to four or fewer degrees-of-freedom. In particular, the single degree-of-freedom "inverted pendulum" model has received much attention. Most studies of postural control have focussed on motion in the sagittal plane, primarily because bipedal stance affords the least stability in the anterior-posterior direction.

2.1.1.1 Inverted pendulum model

The single-link inverted pendulum is the simplest model for the skeletal dynamics. Here, the motion is restricted to a single degree-of-freedom: sagittal plane rotation at the ankle. The inertial properties are represented by a single lumped mass located at the centre-of-gravity (COG), although an additional rotational inertia about the COG may also be included. The actuator is a moment generator at the ankle.

McGhee and Kuhner (1970) and Nashner (1970, 1971 and 1972) were among the earliest to use the inverted pendulum model. Subsequently, Gurfinkel (1973) extended the model to include a triangular foot. Several experimental studies, however, have

indicated that the inverted pendulum model is often deficient. For example, during quiet standing, significant rotation has been found to occur at the neck, hip and/or knee, in addition to ankle rotation (Barin, 1980). In response to applied perturbations, the ankle and hip have been found to show anti-phasic motion at higher frequencies (e.g. 3 Hz) (Tokita et al, 1984).

Soames and Atha (1980) also concluded that the inverted pendulum model is deficient, based on their failure to demonstrate any strong correlations between measurements of spontaneous postural sway and parameters of physique (e.g. body height and weight); however, in this case, the conclusion must be questioned. In contending that the inverted pendulum model necessarily implies a strong linear relationship between sway and physique, these authors failed to allow for inter-subject differences in postural control parameters.

2.1.1.2 Multi-link models

Multi-link models comprise a number of segments, each of which is represented by a mass, COG location and rotational inertia about the COG. Moment generators are located at each joint. In general, these models have been limited to motion in the sagittal plane. Golliday and Hemami (1976) analyzed the stability of a two-link model with motion occurring at the ankle and hip. The three-link model extended the earlier models to include knee motion (Camana et al, 1977; Hemami and Jaswa, 1978). Four-link models, consisting of the shank, thigh, torso and head, have been presented by Koozekanani et al (1980), Stockwell et al (1981) and Barin (1983). Hatze (1980) presented a 17-link model.

Barin (1983) evaluated one-, two- and four-link models by comparing experimental measurements of centre-of-pressure (COP) displacement with model predictions based on measurements of joint rotations. For voluntary self-induced swaying motions, he found that the four-link model produced substantially better fits between the measured and predicted COP values; however, for sway responses to applied perturbations, he found negligible differences between the two- and four-link models. In both situations, the one-link model produced inferior COP predictions.

2.1.2 The Controller: The Neural Centres and Pathways

The most basic functional unit of the nervous system is the neuron (nerve cell) which transmits electrical impulses (action potentials) by means of electrochemical activity in the cell membrane. Integration occurs through temporal and spatial summation of action potentials, at the synapses (junctions) between neurons (or between neurons and muscle cells). This summation changes the membrane potential of the neuron or muscle fibre (postsynaptic effect), or affects transmission across the synapse (presynaptic effect). In either case, the end result may be either inhibitory or excitatory. If and when the membrane potential of the postsynaptic neuron exceeds the firing threshold, an action potential is transmitted.

The central nervous system (CNS) includes the brain and spinal cord. The nerves which extend from the CNS form the peripheral nervous system (PNS). The peripheral nerves are composed of afferent neurons, which convey information from peripheral receptors to the CNS, and efferent neurons, which pass signals from the CNS to the muscles.

In the simplest terms, the brain comprises: (1) the cerebral cortex, the "highest" centre where voluntary commands originate, (2) the cerebellum, which acts to coordinate motor control, and (3) the brain stem, which relays signals between the higher centres and the spinal cord. Higher centre commands are carried from the CNS to the PNS via descending tracts in the spinal cord, while sensory information is returned via ascending tracts. The descending tracts originate in the cortex and in the nuclei (masses of nerve cells) of the brain stem. Both the cortex and cerebellum influence the activity of the brain stem nuclei. In all of the neural "circuits", the final pathway is formed by the alpha motoneurons. These pass directly (i.e. without any synapses) from the spinal cord to the motor units of the muscle.

The descending pathways influence the alpha motoneurons by: (1) synapsing directly on the alpha motoneurons, (2) synapsing on the gamma motoneurons, which influence the alpha motoneurons via the muscle spindle reflex arc (see Sections 2.1.4.1 and 2.3.1), and (3) synapsing on interneurons (i.e. spinal cord neurons) which

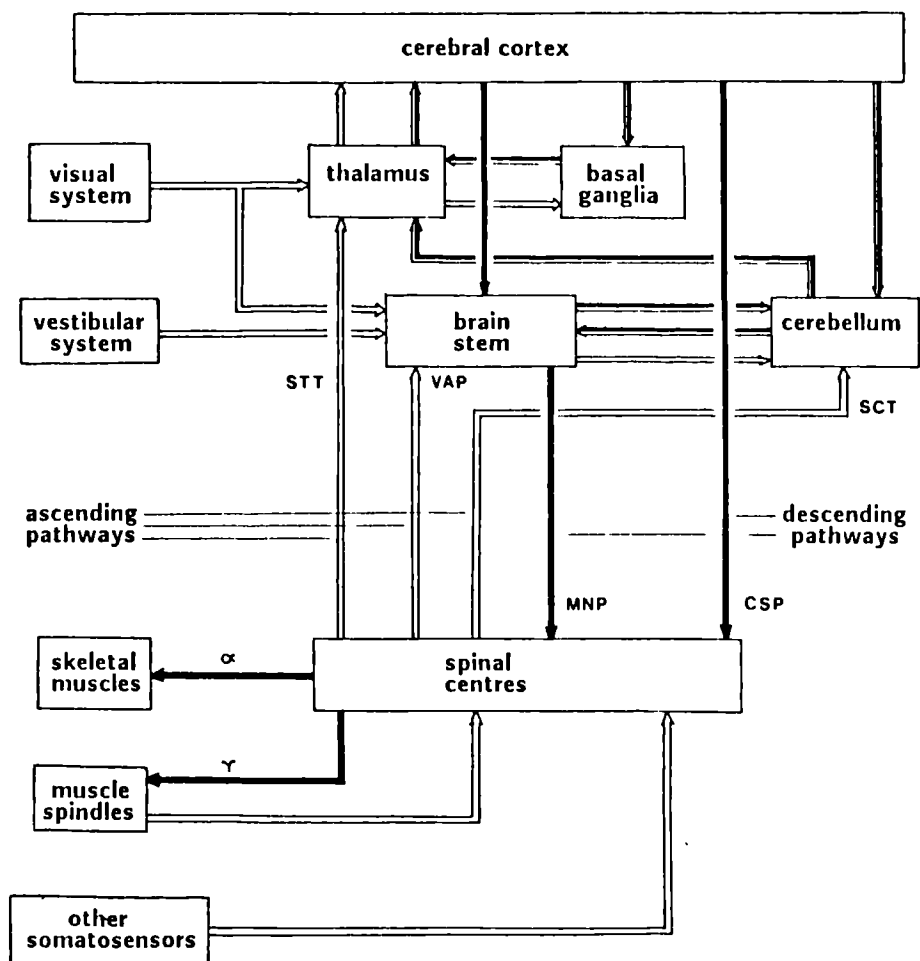

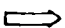




Fig 2.2 Organization of the neural centres and pathways.

- Legend:
- CSP = corticospinal pathway (pyramidal tracts)
 - MNP = multineuronal pathways
 - STT = spinothalamic tract
 - SCT = spinocerebellar tract
 - VAP = various ascending pathways
 - α = alpha motoneurons
 - γ = gamma motoneurons
-  motor commands
 sensory feedback
 command monitoring (hypothesized function)
 command correction (hypothesized function)

synapse on the alpha motoneurons. There are two major pathways: (1) the corticospinal pathway (or pyramidal tracts), which travel directly from the cerebral cortex, and (2) the multineuronal pathways, which originate in the cerebral cortex but synapse in the nuclei of the cerebrum and brainstem before descending to the level of the motoneurons. The tracts in the multineuronal pathways are named according to the nuclei of origin, e.g. the vestibulospinal tract descends from the vestibular nuclei.

As will be discussed in Section 2.1.4, sensory feedback is provided by somatosensory, vestibular and visual receptors. Somatosensory information is passed to the higher centres via the spinocerebellar tracts and various other ascending pathways. These afferent neurons are subject to inhibitory control from descending tracts. Vestibular afferents travel to the vestibular nuclei in the brainstem. Some visual afferents also travel to the brainstem, while others travel to the thalamus (an integrating centre for sensory inputs) and on to the visual cortex.

The cerebellum is intimately involved in the control and coordination of movement. According to present theory, the cerebellum receives information about an intended movement from cortical and subcortical centres ("efference copy") and information about the actual movement from the sensory systems ("afference copy"). If there is a discrepancy between the efferent and afferent information, error signals are sent to the cortical and subcortical centres where new commands are generated.

The basal ganglia (collections of subcortical nuclei) also play an important role in the control of movement. The basal ganglia receive input from the cortex and thalamus and project mainly to the thalamus; they have no direct projections to the spinal cord. While it was once thought that the basal ganglia were involved primarily in postural control, more recent evidence indicates that they also play an important role in the initiation and control of other types of movements.

The functional anatomy of the neural "circuitry" is depicted in figure 2.2. See Kandel and Schwartz (1981) for a comprehensive review of neural anatomy and physiology.

2.1.3 The Actuators: The Motor System

The skeletal muscles, in concert with the skeletal linkage, function as the actuators of the posture control system. The smallest functional unit is the motor unit: the muscle fibres innervated by a single alpha motoneuron. The total muscle force results from the summation of the tension developed by each of the motor units in the muscle. The muscle force is modulated by recruitment of motor units and by modulation of the motoneuronal firing frequencies. The force generated by the muscle is dependent on the muscle length, velocity of contraction (or lengthening) and level of neural activation. The dynamics of the force generation are dependent on the viscoelastic properties of the serial and parallel connective tissues. The joint moment generated by the muscle is dependent on the skeletal moment arm, which varies according to the angle of the joint. A review of muscle mechanics is provided by Winter (1979c).

Because muscles produce only tensile forces, a pair of opposing muscles (antagonists) is required to control the motion at a joint. Hence, for balancing motions in the sagittal plane, a minimum of six muscles is needed to independently control the motion at the ankle, knee and hip joints. Nashner and McCollum (1985) have identified a set of six major muscles and muscle groups as follows:

- (1) ankle flexion - tibialis anterior
- (2) ankle extension - gastrocnemius
- (3) knee flexion - gastrocnemius and hamstrings
- (4) knee extension - quadriceps
- (5) hip flexion - quadriceps and abdominals
- (6) hip extension - hamstrings and paraspinals.

It should be noted that, strictly speaking, the abdominals and paraspinals are flexors and extensors of the spine, rather than the hip. Note also that the actions of the muscles listed above are not necessarily limited to the sagittal plane. For example, tibialis anterior both flexes and inverts the foot, while the hamstrings rotate the thigh (when the hip is extended).

In addition to the muscles listed above, the soleus, an ankle extensor, and a number of hip muscles (gluteals, tensor fasciae

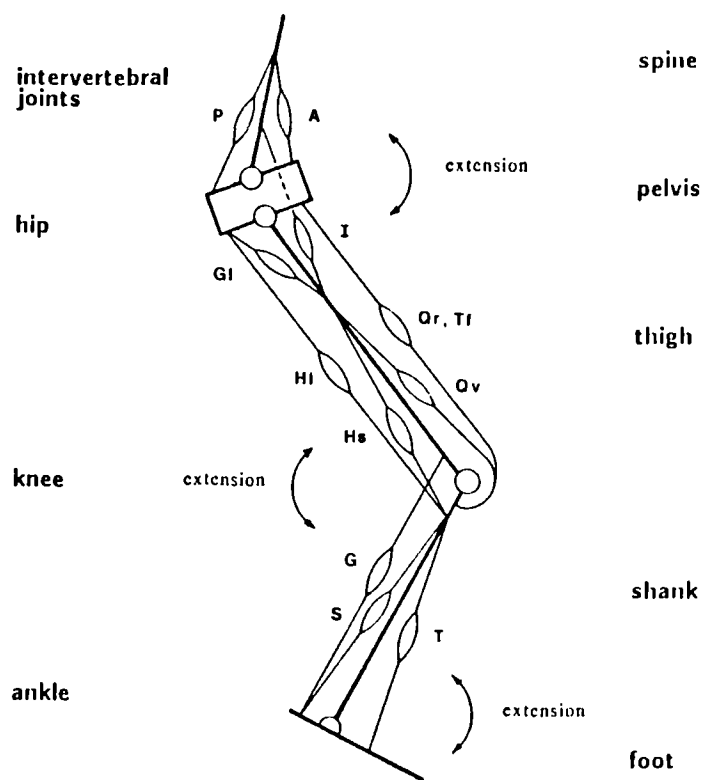


Fig 2.3 Functional anatomy of the lower extremity (sagittal plane).

- Legend:
- G - gastrocnemius
 - S - soleus
 - T - tibialis anterior
 - Qr - quadriceps: rectus femoris
 - Qv - quadriceps: vastus medialis, lateralis and intermedius
 - Hs - hamstrings: biceps femoris (short head)
 - Hl - hamstrings: biceps femoris (long head), semitendinosus and semimembranosus
 - A - abdominals
 - P - paraspinals
 - G1 - gluteals
 - I - iliopsoas
 - Tf - tensor fasciae latae

latae, iliopsoas) are important contributors to the maintenance of static posture (e.g. Carlsöö, 1972).

Several of the above muscles cross two joints and therefore perform dual functions, in particular: gastrocnemius, quadriceps (rectus femoris), hamstrings (semimembranosus, semitendinosus and long head of biceps femoris) and iliopsoas.

Figure 2.3 diagrams the functional anatomy of the lower extremity in the sagittal plane.

2.1.4 The Feedback Transducers: The Sensory Receptors

Sensory feedback occurs via three major sensory modalities: somatosensory, vestibular and visual.

2.1.4.1 Somatosensors

Somatosensory inputs are provided by a number of different types of mechanoreceptors. These sensors are said to be "somatosensory" because they are located in the somatic tissues of the body (i.e. skin, muscles, ligaments, joints and fascia). They are "mechanoreceptors" in that they respond to mechanical deformation of the receptor or adjacent cells.

Proprioception (i.e. information about the relative position and motion of the body segments) is provided by sensory nerve endings within the joints. Several different types of sensory endings (both encapsulated and unencapsulated) are located in the joint capsule and in the surrounding ligaments. These endings are actually tension receptors, but provide information about the angular displacement of the joint and the rate of displacement.

Further proprioceptive information is furnished by spindle receptors which are interspersed throughout the muscles. The muscle spindles respond to changes in muscle length and to rate of lengthening. Each spindle is composed of several small intrafusal muscle fibres which lie in parallel with the extrafusal fibres of the muscle. The central regions of the intrafusal fibres are innervated by sensory nerves which are excited when the muscle is stretched. Efferent gamma motoneurons, which innervate the non-receptor end regions of the intrafusal fibres, act to control the threshold and sensitivity of the spindle.

Active muscle tension is sensed by the Golgi tendon organs. Each organ is located in series with a small number of extrafusal muscle fibres. Although they do respond to passive muscle stretch, the tendon organs are far more sensitive to active muscle contraction. Unlike the spindles, the tendon organs have no efferent innervation. Early investigators maintained that the main role of the tendon organs was to protect the muscle from overstretching; however, more recent evidence suggests that they play a much more important role in motor control. For example, Houk (1976) has suggested that the tendon organs, in concert with the spindles, provide the sensory feedback in a control loop that regulates muscle stiffness.

Cutaneous touch receptors and subcutaneous pressure receptors located on the plantar aspects of the feet provide information about the contact forces between the feet and the supporting surface. Deep pressure receptors located in the tissues of the feet and leg respond to pressure changes, resulting primarily from muscle contraction. Relatively little is known about the role that the touch and pressure receptors play in postural control (Watanabe and Okubo, 1981).

A comprehensive review of the anatomy and physiology of the somatosensors is provided by Brodal (1981).

2.1.4.2 The vestibular system

The labyrinthine organs of the vestibular system are located in each inner ear. Each organ comprises a system of membranous sacs and tubes that lie within the temporal bone. The sacs and tubes are filled with fluid (endolymph), as is the space between the membranes and the bone (perilymph).

Each labyrinth has two sacs (the sacculus and the utriculus) which are approximately orthogonal. Each sac contains a patch of sensory hair cells (the macula) which are embedded in the otolith, a membrane containing numerous calcium carbonate crystals (the otoconia). Displacements of the otoconia, as a result of gravitational or inertial forces, bend and excite the underlying hair cells. Thus, the otoliths function as accelerometers, sensitive to both gravitational force and linear acceleration.

Each labyrinth has three semicircular canals which are approximately orthogonal. At one end of each canal, there is a patch of sensory hair cells (the crista ampullaris) that projects into a membrane (the cupula) that closes off the end of the canal. Angular accelerations of the head produce movements of the endolymph fluid within the canal, and the resulting deflection of the cupula stimulates the hair cells. Although the canals are excited by the angular accelerations of the head, the dynamic characteristics of the canal-endolymph-cupula system act to integrate the acceleration, yielding an output that is proportional to angular velocity (over an estimated frequency range of 0.02 to 50 Hz) (Wilson and Melvill Jones, 1979a).

A detailed description of the anatomy and physiology of the vestibular labyrinths is provided by Wilson and Peterson (1980).

2.1.4.3 The visual system

The lens and cornea of the eye focus light rays from external objects into an image on the photoreceptors of the retina. The peripheral areas of the retina provide the widest angle sensitivity, whereas the more central areas (i.e. the fovea) have a higher visual acuity. Detailed descriptions of the anatomy and physiology of the eye and the retina are provided by Westheimer (1980) and Brown (1980).

In postural control, the visual system serves to sense the orientation and motion of the head with respect to the external environment (Brandt et al, 1986). By itself, the visual signal is ambiguous: it may be interpreted as self-motion or object-motion. In "afferent motion perception", the visual signal is derived from relative shifts of the visual image on the retina. Fore-aft head movements are detected primarily from the change in image size that results from the changing eye-object distance; however, fore-aft movements can also be detected from changes in binocular disparity. "Efferent motion perception" is derived by monitoring the neural drive required to fixate the retinal image of a moving target during pursuit eye movements.

Although the peripheral retina provides adequate visual information for postural control, it has been suggested that the

central retina may also play an important role in "fine-tuning" the postural responses (Brandt et al, 1986).

2.2 METHODS FOR THE STUDY OF POSTURAL CONTROL

Skilled clinicians can often identify balance-impaired individuals on the basis of qualitative observations. However, in order to identify more subtle impairments, to monitor changes in the course of treatment, to perform controlled studies of causal or preventative factors, or to investigate the neurophysiology of postural control, a quantifiable balance test is needed.

One quantitative approach is to measure the spontaneous postural sway of subjects as they stand quietly on a rigid floor. An alternate approach is to measure the response to an applied postural perturbation. Information about the relative contributions of the different sensory subsystems has been gained through studies in which one or more of the sensory channels is stimulated or disrupted.

2.2.1 Measurement Methods

Measured variables include: (1) displacement of the centre-of-pressure (COP) on the feet, (2) translational motion at selected anatomical landmarks, (3) rotational motion at selected joints, (4) moment of force at selected joints, and (5) electromyographic (EMG) measurements of muscle activity.

COP is measured by means of a force plate, a rigid platform supported by a number of strain gauge or piezoelectric elements which measure the forces applied to the plate by the subject's feet. See Winter (1979b) for a more detailed discussion of these devices.

Body motion at selected anatomical landmarks or marker locations can be measured using: (1) the electromechanical linkage method (e.g. rotary potentiometers with wires attached to the subject), (2) the stereometric method (using photodetectors, video cameras, film cameras, magnetometers or hypersonic transducers), or (3) the accelometric method (using accelerometers mounted on the subject). If desired, the measured motions can be used to determine the rotational motion at the joints, or potentiometric electrogoniometers (another type of electromechanical linkage) can

be used to make these measurements directly. The accelometric method and many of the stereometric methods require some form of transducer (or reflector) to be worn by the subject, while the electrogoniometer presents an even greater encumbrance. Many of the linkage methods have the disadvantage of imposing a mechanical load on the subject. See Chao (1978) for a review of kinematic measurement methods.

Moment of force at the ankle can be estimated from force plate data. Estimation of the moments at other joints requires additional measurements of the joint kinematics and the dimensions and (in some cases) the inertial properties of the body segments (Winter, 1979b).

EMG is recorded using surface electrodes, which are taped to the skin over the muscle, or using wire or needle electrodes, which are inserted directly into the muscle. Surface electrodes are more widely used in posture control studies because they are safer and easier to apply, and because the output is more representative of the overall activity of the muscle (rather than an isolated motor unit). See Winter (1979d) for a more detailed discussion.

2.2.2 Spontaneous Sway Experiments

Many investigators have studied the spontaneous postural sway of subjects as they stand quietly on a stationary floor (for reviews, see Begbie, 1967; Terekhov, 1976; Cernacek, 1980; Okubo, 1980; and Njiokiktjien, 1980). Some investigators have chosen to amplify the destabilizing effect of spontaneous sway by having the subjects stand on a narrow beam or on a seesaw (e.g. Dietz et al, 1980).

In most spontaneous sway studies, the investigators measured either COP displacement (e.g. Black et al, 1982), translational motion at selected anatomical landmarks (e.g. Dornan et al, 1978), or rotational motion at selected joints (e.g. Ishida and Miyazaki, 1985). In at least one study (Ishida and Miyazaki, 1985), COP measurements were used to estimate ankle moment. A somewhat different approach involves measuring the maximum time interval over which subjects are able to maintain stability while standing on one leg (e.g. Potvin et al, 1980; Stones and Kozma, 1987).

Spontaneous sway has been characterized in terms of: (1) time domain measures that quantify the amplitude, range, speed or direction of sway (e.g. Hufschmidt et al, 1980), and (2) frequency domain measures derived from power spectrum estimates (e.g. Benseal and Dzendolet, 1968; Hayes et al, 1985). Some investigators have used autoregressive time series models (e.g. Brauer and Seidel, 1980). Roy et al (1985) have developed a random "diffusion process" model.

In general, spontaneous sway measurements characterize the output of the posture control system without any quantitative measurement of the input, and hence cannot be used to identify an input-output model of the system. An input-output model is desirable because it characterizes the system itself (not just the system output measured over some arbitrary interval in time) and can be used to predict the response of the system to other inputs. Even if used only as a comparative measure, the small-amplitude spontaneous sway measures may bear little relation to the postural performance in typical falling situations, which involve much larger amplitudes of sway. Small- and large-amplitude responses may differ because of nonlinearities in the posture control system (e.g. sensory thresholds, increased passive muscle stiffness for small displacements).

Ishida and Miyazaki (1985) attempted to identify an input-output model for spontaneous sway, treating ankle angle as the input and ankle moment as the output (assuming inverted pendulum sway). However, the lack of an independent input can lead to serious bias errors in the model estimates (van Lunteren, 1979a).

2.2.3 Induced Sway Experiments

Some of the problems associated with measurements of spontaneous sway can be overcome by applying a postural perturbation to the subject and measuring some aspect of the induced sway response. A number of variables have been used to characterize the response, including: (1) EMG activity in various muscles or muscle groups (e.g. Nashner, 1976; Gurfinkel et al, 1976; Nashner, 1977; Nashner and Woollacott, 1979; Allum and

Budingen, 1979; Hibino, 1980; Diener et al, 1984; Tokita et al, 1984); (2) translation of body landmarks and/or rotation of joints (e.g. Gantchev et al, 1972a and 1972b; Andres and Anderson, 1980; Hibino, 1980; Ishida and Imai, 1980; Andres, 1982; Tokita et al, 1984); (3) forces and/or COP on the feet (e.g. Ishida and Imai, 1980; Diener et al, 1984); and (4) ankle moment (e.g. Meyer and Blum, 1978; Ishida and Imai, 1980).

Induced sway measurements have been used in system identification experiments and in more basic neurophysiological studies. The goal of the system identification study is to develop an input-output model of the posture control system. The applied perturbation is treated as the model input and the induced sway response(s) as the output(s). In many neurophysiological studies, the perturbation is viewed primarily as a stimulus, that is, a means to elicit postural responses. The responses are then analyzed in a comparative manner. Typically, EMG responses are of prime interest in these types of experiments.

Perturbations are most commonly applied by moving the platform on which the subject stands. The platform motion may be rotational, translational or both, and may be transient (e.g. ramps, pulses, steps) or continuous (e.g. sinusoidal, random or pseudorandom). Table 4.1 (in Chapter 4) illustrates the wide variety of different platform perturbation signals that have been used by various investigators.

In some studies, perturbations have been applied by pushing or pulling on the subject (e.g. Isaacs, 1983); however, these types of perturbations are difficult to apply in a controlled manner. Somewhat more controlled forces have been applied using systems of pulleys and weights (Wolfson et al, 1986). Another more controlled approach has been to suddenly release the wire supporting a leaning subject (Do et al, 1982), or to apply a sudden force or displacement to a handle grasped by the subject (Traub et al, 1980; Cordo and Nashner, 1982).

Several investigators have applied perturbations during gait, using: (1) motion of a platform incorporated into the surface of a walkway (Nashner, 1980), (2) sudden acceleration or deceleration of a treadmill (Berger et al, 1984), (3) electrical stimulation of the

foot (Belanger and Patla, 1984), or (4) trip wires (Grimes, 1979).

Typically, in the system identification studies, a linear transfer function model is used to characterize one or more components of the posture control system (e.g. Gantchev and Popov, 1973; Meyer and Blum, 1978; Hibino, 1980; Ishida and Imai, 1980; Andres, 1982; Tokita et al, 1984). A linear model may be a reasonable approximation for a limited range of perturbation amplitudes; however, this approach may fail to yield accurate information with regard to relative postural stability. A fall occurs when the system is disturbed by a large-amplitude perturbation which causes the system to become unstable. In this situation, the linear approximation may no longer be valid, as saturation-like nonlinearities come into play, i.e. limitations on muscle strength, joint range of motion, support surface friction, COP displacement, etc.

2.2.4 Sensory Stimulation and Disruption

In order to gain information about the organization of postural responses and the contributions of the different sensory modalities, it is necessary to perform experiments in which one or more of these modalities is selectively stimulated, blocked or disrupted. However, in performing these types of experiments, it is important to recognize that the posture control system will often compensate for deficits in one sensory modality through a "reweighting" of the remaining inputs (Nashner, 1981). In no way can the contributions of the different senses be assumed to be additive.

Vision is easily blocked by instructing the subjects to close their eyes or by having them wear blindfolds. Visual cues can be distorted by moving the visual field (Brandt et al, 1986). Another approach is to "stabilize" the visual input by servoing the motion of a movable visual surround to the motion of the head (e.g. Nashner and Berthoz, 1978). Any change in visual input is nulled out by the motion of the visual surround. Alternatively, the servo approach can be used to amplify or attenuate the visual stimulus in a controlled manner.

Somatosensory inputs from the lower extremity can be

diminished, with minimal restriction of motor capabilities, by means of ischemic blocking (using a tourniquet) (e.g. Allum et al, 1982). Apparently, the large-diameter muscle spindle and Golgi tendon organ afferents are most readily affected by the loss of blood supply. Muscle spindle inputs can be disturbed by applying vibration (e.g. Eklund, 1969). The plantar mechanoreceptors can be stimulated by standing the subject on an array of "shotgun" balls, modulating the stimulation by changing the spacing between the balls (Watanabe and Okubo, 1981). Standing the subjects on compliant foam rubber alters ankle and plantar somatosensory inputs (e.g. Pyykkö et al, 1986), but also alters the effective mechanical stiffness of the ankle. Somatosensory inputs are eliminated in lower limb amputees (e.g. Fernie and Holliday, 1978); however, the sensory and motor deficits cannot be delineated.

Nashner (1970, 1971, 1976 and 1982) has "stabilized" somatosensory inputs from the ankle by servoing platform tilt to ankle rotation. Any change in ankle angle is nulled out through rotation of the support surface. It should be noted that this approach eliminates kinematic ankle cues, but fails to nullify the touch and pressure receptors or the Golgi tendon organs.

Vestibular inputs are the most difficult to block. One approach has been to test patients with unilateral or bilateral peripheral vestibular lesions (e.g. Nashner et al, 1982). Alternatively, comparison of sitting and standing responses to ankle rotations may yield information about the relative contributions of the vestibular and somatosensory reflexes, since the vestibular stimulation is much reduced during the seated tests (Allum and Keshner, 1986). Vestibular inputs can be enhanced through electrical or caloric (i.e. thermal) stimulation of the vestibular organs (e.g. Nashner and Wolfson, 1974).

2.3 EXISTING KNOWLEDGE ABOUT POSTURE CONTROL MECHANISMS

Postural control is achieved through a number of reflex systems, which are apparently organized in a hierarchial manner (Nashner, 1981). There is, however, some controversy in the literature regarding the relative importance of these systems.

2.3.1 The Stretch Reflex

The stretch reflex is mediated primarily by the muscle spindles and is excited by muscle stretch, with secondary contributions from simultaneously excited cutaneous and joint receptors. The afferent signals excite alpha motoneurons and thereby cause a muscle contraction. The stretch reflex can be conceptualized as a negative feedback system that acts to oppose changes in muscle length (Houk and Henneman, 1974) and which tends to linearize the muscle properties (Nichols and Houk, 1973).

In the monosynaptic stretch reflex, the spindle afferents synapse directly on the alpha motoneurons; however, experimental evidence indicates that the monosynaptic stretch reflex plays an insignificant role in normal postural control (Gurfinkel et al, 1976; Nashner, 1976).

A longer latency reflex (referred to as the functional, long latency or transcortical stretch reflex) is also apparently mediated by somatosensors but is thought to involve higher level neural processing. This processing may involve spinal, brainstem or transcortical neural pathways (e.g. Ghez and Shinoda, 1978; Chan et al, 1979). These reflexes are functionally much stronger than the monosynaptic reflexes and occur in the ankle flexors and extensors at a latency of approximately 100 ms, compared to monosynaptic latencies of 45-50 ms. Nashner et al (1982) argue that these longer latency reflexes (which they refer to as "automatic postural responses" or "rapid postural adjustments") are the dominant stabilizing influence. They found negligible differences in the balancing responses of normal subjects and patients with vestibular deficits, whether or not vision was deprived or "stabilized", as long as somatosensory inputs were not disrupted. As further evidence, they observed similar patterns of response to both platform rotations and translations, even though the visual and vestibular inputs are quite different for these two types of perturbations (Nashner, 1977).

2.3.2 Vestibular Reflexes

The vestibulospinal reflex involves neural connections between the labyrinth afferents and the alpha motoneurons. The

contribution of this reflex to dynamic balancing responses is thought to be mediated primarily by the semicircular canals. The otoliths are primarily involved in the "static" (i.e. low frequency) component of the reflex, although they may also play a role in the dynamic component, particularly in response to vertical accelerations (Wilson and Melvill Jones, 1979b). Afferent influences from neck proprioceptors tend to counter the vestibulospinal reflex, so that changes in head attitude relative to the body produce no reflex responses at the limbs (Roberts, 1978).

In contrast to Nashner's conclusion that the functional stretch reflex is the dominant stabilizing influence, Allum and Keshner (1986) claim that vestibulospinal reflexes contribute approximately 65% of sway stabilization in normal subjects, compared to 35% for the somatosensory reflexes. Their conclusions were based on comparisons of seated and standing responses to ankle rotations.

The vestibular system contributes to the maintenance of appropriate head position with respect to the body via the vestibulocollic reflex. In this reflex, neural connections between the labyrinth afferents and the neck muscles act to stabilize the head with respect to the external environment (Wilson and Melvill Jones, 1979b). Cervical proprioceptors in the vertebrae of the neck participate in the cervicocollic reflex which may act to cancel the effects of the vestibulocollic reflex and thereby maintain the head in line with body. This is necessary if the vestibular system is to act as the primary sensor for sway stabilization (Allum and Keshner, 1986).

The vestibular system interacts with the visual system via the vestibulo-ocular reflex. Neural connections between the labyrinth afferents and the ocular muscles act to stabilize the eyes with respect to the environment, thereby allowing the eyes to focus despite movement of the head (Wilson and Melvill Jones, 1979b).

2.3.3 Visual Reflexes

From the review of the role of vision in posture provided by Brandt et al (1986), it is clear that changes in visual conditions

can have a substantial influence on spontaneous postural sway. Eye closure increases spontaneous sway, while changes in the visual environment (e.g. eye-object distance, illumination level) also affect the spontaneous sway.

In the case of rapid balancing responses, many investigators believe that visually-mediated responses are too slow to make a significant contribution. Responses to movements of a visual surround were found to be slow, with latencies of 0.5-2 s (Lestienne et al, 1977). Allum and Pfaltz (1985) found that eye closure produced only slight changes in the responses to platform tilts, in normal subjects. Nashner et al (1982) found that a patient who was completely devoid of vestibular function was unable to maintain balance using visual inputs alone, i.e. when somatosensory inputs were nulled.

In contrast, electrophysiological studies in goldfish and monkeys (see review by Nashner, 1981) have demonstrated very rapid visually-evoked responses in the vestibular nuclei. Human experiments in which the visual stimulus was normal, nulled out or amplified, have demonstrated that vision can influence rapid postural responses (Nashner and Berthoz, 1978). The early postural responses to platform translations were found to be attenuated in cases where the visual stimulus conflicted with other sensory information.

2.3.4 Organization of Postural Responses

Nashner (1981) has suggested that, at the lowest hierarchical level, stabilizing postural responses are organized into a limited number of stereotyped patterns of muscle activation (synergies). Since the selection of the appropriate synergy is dependent only on the nature of the postural configuration at the time of the perturbation, the use of synergies reduces the problem of motor coordination to a simple "decision-making" process which can occur automatically.

The synergistic responses utilize a weighted combination of somatosensory, vestibular and visual inputs. At least some of the experimental evidence suggests that local somatosensory inputs predominate under normal environmental conditions (see

Section 2.3.1); hence, the functional stretch reflex is expected to be the predominant control loop at this level of the hierarchy.

Nashner and coworkers (Nashner, 1981; Nashner and McCollum, 1985; Horak and Nashner, 1986) have identified three major synergies: the suspensory synergy, and the hip and ankle sway synergies. In the suspensory synergy, coordinated activation of muscles on opposite aspects of the leg (gastrocnemius and quadriceps; or tibialis anterior and hamstrings) produces upward or downward thrust of the leg, with the largest motions occurring at the knee joint. This synergy counteracts changes in the height of the COG.

In the sway synergies, coordinated activation of muscles on the same anterior or posterior aspect of the leg and trunk (gastrocnemius, hamstrings and paraspinals; or tibialis anterior, quadriceps and abdominals) produces corrective actions at the hip and ankle that counteract anterior-posterior sway. In the ankle synergy, the relative contributions of the thigh and trunk muscles are set to counterbalance the knee moment generated by the ankle muscles, thereby stabilizing the knee and restricting the body motion primarily to ankle rotation (i.e. inverted pendulum sway). In the hip synergy, the ankle muscles do not contract, and the sway in a particular direction is countered by the antagonists of the thigh and trunk muscles used in the ankle synergy. Here, the hip and ankle rotation is anti-phasic (e.g. ankles extend while hip flexes), and additional rotation now occurs at the knee, resulting in some vertical motion of the COG.

According to Nashner et al (1982), when changing environmental conditions cause the automatic synergic responses to produce erroneous results, slower-acting central mechanisms reorganize the responses, making use of vestibular and visual as well as somatosensory information to resolve any conflicts. The contributions of the different reflex systems are then reweighted according to the environmental conditions and circumstances of the balancing task. The vestibular inputs are thought to provide the orientational reference against which conflicts in somatosensory and visual inputs are identified. This hypothesis is based on evidence that vestibular deficient patients cannot cope effectively

with disturbances in the somatosensory and visual inputs, and the observation that the vestibular system is the only sensory system that provides an orientational reference unaffected by changes in environmental conditions.

The reweighting of the sensory inputs to the "low-level" automatic responses occurs rapidly (e.g. over a small number of experimental trials) and continuously (Nashner et al, 1982). The reweighting process is thought to represent a higher level in the fixed control hierarchy, in which actual sensory input is compared to an "internal model" of anticipated sensory input. In contrast, truly adaptive changes in postural strategy are thought to involve modification of the internal model itself. Typically, these changes occur over much longer periods of time (e.g. days or weeks). An example would be the reversal of the vestibulo-ocular reflexes that occurs when subjects wear reversing prisms (e.g. Gonshor and Melvill Jones, 1976).

2.4 CAUSES OF FALLING IN THE ELDERLY

A fall occurs when the body is subjected to a perturbation such that the posture control system is unable to maintain stability. For a given individual, incidence of falling is dependent on: (1) incidence of perturbations, (2) severity of perturbations, and (3) ability of the posture control system to maintain balance when subjected to a perturbation. Perturbations may result from interaction with the external environment (e.g. slips, trips, missteps, jostles or self-initiated displacements), they may occur as a result of internal physiological disturbances which disrupt the metabolism of the CNS (e.g. cardiac arrhythmias, hypoglycemia), or there may be a combination of internal and external factors (e.g. postural hypotension) (see review by Isaacs, 1983). Self-initiated perturbations may result, in some cases, from a failure to make the necessary anticipatory postural adjustments in performing voluntary movements (e.g. Brown and Frank, 1987).

In their analysis of falls, Wild et al (1981) distinguished between "ordinary" and "extraordinary" displacements of the body, which are either "initiated" (by the subject, in the course of

his/her activities) or "imposed" (by the external environment). In addition, Isaacs (1983) cited the possibility of initiating corrective responses to illusory displacements that were detected but never actually occurred. While extraordinary displacements (e.g. slipping on an unseen patch of ice) might cause anyone to fall, Wild et al (1981) suggested that ageing may diminish the ability to recover from ordinary displacements (e.g. tripping on a carpet).

Hinchcliffe (1983) has identified a sequence of "rescue" reactions to postural perturbations consisting of sway reactions, staggering (i.e. stepping) and sweeping reactions (i.e. using the limbs as inertia paddles). Should these responses fail, "fall-breaking" reactions then occur (e.g. using the upper limbs to break the fall or to protect the face and head).

2.4.1 Effects of Ageing: Incidence and Severity of Perturbations

For a given individual, the incidence and severity of external perturbations is dependent on many factors, including gait pattern, ability to detect and avoid environmental hazards, and activity level and lifestyle.

Increased variability in foot placement during gait has been shown to occur with ageing (Guimaraes and Isaacs, 1980), and would be expected to result in an increased incidence of slips, trips and missteps. On the other hand, adaptations such as reduced walking speed and decreased stride length (e.g. Guimaraes and Isaacs, 1980; O'Brien et al, 1983) may tend to reduce both incidence and severity of perturbations, by increasing the duration of the more stable double-support phase (Gillis et al, 1986).

Decline in visual acuity (e.g. Kornzweig, 1980), gaze stability (e.g. Leibowitz and Shupert, 1985) and cognitive processes (e.g. Potvin et al, 1980) might result in a reduced ability to identify external hazards, whereas slower and poorer coordination of psychomotor responses (e.g. Spirduso, 1980) might reduce the ability to avoid external hazards that are identified. Conversely, the more sedentary lifestyle adopted by many elderly would tend to reduce exposure to environmental hazards and to the postural demands of vigorous occupational and recreational

activities.

Internal perturbations which affect brain perfusion can be expected to increase with ageing, associated with postural hypotension, postprandial hypotension, reduction in baroreflex sensitivity, reduction in cerebral blood flow, carotid sinus hypersensitivity and development of cardiac arrhythmias (Lipsitz, 1985). The cervical spondylosis that occurs in ageing may increase liability for temporary obstruction of the vertebral arteries when turning the head (Isaacs, 1983).

2.4.2 Effects of Ageing: Postural Performance

The performance of the posture control system is expected to decline as a result of ageing. Age-related deterioration in the important sensory modalities, such as vision (e.g. Kornzweig, 1980), vestibular function (e.g. Graybiel and Fregly, 1966; Black et al, 1977; Kenshalo, 1979) and somatosensory proprioception (e.g. Kenshalo, 1979; Wyke, 1979; MacLennan et al, 1980), are well documented. The speed of the balance response is expected to decrease with ageing, as a result of reduced conduction velocity in the peripheral and central nervous systems (Dorfman and Bosley, 1979; Strenge and Hedderich, 1982) and slowing of muscle contraction (Davies and White, 1983).

Reduction in muscle strength with ageing has been demonstrated (Larsson et al, 1979; Aniansson et al, 1980; Young et al, 1984; Young et al, 1985), associated with decreases in size and number of muscle fibres and number of motoneurons (Campbell et al, 1973; Larsson et al, 1979; Grimby and Saltin, 1983; Lexell et al, 1983). In addition, elderly muscle has been shown to be more susceptible to fatigue (Davies and White, 1983).

Degenerative age-related changes observed in motor cortex neurons and spinal motoneurons have been hypothesized to interfere with: (1) relaxation of "antigravity" muscles, producing decrements in motor performance and agility, (2) normal recruitment of motor units, leading to fatiguability and secondary muscle atrophy, and (3) gamma motoneuron control of the muscle spindles (Scheibel, 1979).

In view of these physiological changes, it is not surprising

that the following results have been demonstrated in elderly subjects: (1) deteriorated balancing synergies in which muscle contractions are delayed and occur in a reversed sequence (Woollacott et al, 1982a, 1982b and 1986), (2) more extreme and less effective responses to impulsive force perturbations (Wolfson et al, 1986), (3) increased sway in response to rotational platform perturbations (Holliday and Fernie, 1985), and (4) increase in spontaneous postural sway (Sheldon, 1963; Hasselkus and Shambes, 1975; Black et al, 1977; Overstall et al, 1977; Fernie and Holliday, 1978; Era and Heikkinen, 1985; Hayes et al, 1985).

2.4.3 Epidemiological Studies of Falling

Epidemiological studies of falling have been plagued by a number of methodological problems (Isaacs, 1983). Falls occur infrequently and are often unwitnessed. Subject populations tend to be biased toward more severe injury-causing falls, as these are the falls that tend to be reported. Studies that rely on anecdotal self-reports of falls may produce unreliable results. In many cases, subjects are unable to explain their falls, may arbitrarily choose a reasonable explanation (e.g. "I must have tripped"), or may even forget that a fall occurred.

Additional problems stem from the retrospective nature of many of these studies. Typically, there is no control group (Perry, 1982b). In studies where comparisons to age-matched controls are made, subjective assessments may be biased by prior knowledge as to whether or not a particular subject is a faller (Tinetti et al, 1986). Retrospective studies may detect abnormalities in subjects who fell, but there is no guarantee that these abnormalities were present at the time of the fall (Perry, 1982b); in fact, they may have developed as a result of the fall.

In view of the many methodological problems, the results discussed in this section should be viewed with some degree of caution.

2.4.3.1 Circumstances of falls

Sheldon (1960), in a retrospective study of 500 falls that resulted in medical treatment, concluded that almost half resulted from environmental factors. In a survey of 150 falls that resulted

in hospital emergency room treatment, Waller (1974) found that rough or slippery ground accounted for 54% of the falls in healthy subjects but only 14% in subjects with acute or chronic health problems. Based on the results of a survey of 963 elderly, Exton-Smith (1977) found that tripping was reported most prevalently as the cause of falling, but only in the younger elderly subjects (under 75). In a prospective one-year study of 100 healthy elderly, Gabell et al (1985) found that 15 of the 22 falls that were reported were caused by slips or trips, associated largely with poor ground conditions and/or inappropriate footwear.

Ashley et al (1977), in a prospective study of falls occurring over a five-year period in an institutionalized yet ambulatory elderly population, found the most common activity associated with falls to be walking to or from a toilet. They noted a clustering of falls prior to death, in some patients. No relation was found between time of day and incidence of falling.

In a retrospective study of 125 falls reported by patients to their doctor, Wild et al (1980 and 1981) found that 42% of the falls occurred during level-surface gait, 4% occurred while turning during gait, 11% occurred during stairway ascent or descent, and 30% occurred during other ordinary activities of daily living. Ten per cent of the falls occurred in darkness and another 10% in dim light. Environmental hazards (excluding stairways and poor lighting) were judged to play a role in 12% of the falls.

Based on a review of epidemiological studies, Perry (1982b) concluded that environmental hazards, such as stairs and floor obstacles, are more important causes of falling in younger and healthier elderly, and that the institutionalized elderly have a greater tendency to fall during "trivial" activities, such as getting out of a chair. Nickens (1985), in a similar review, agreed that environmental hazards tend to become a less important factor as age increases.

2.4.3.2 Characteristics of fallers

Epidemiological studies suggest that the following characteristics may be associated with falling: (1) female sex, (2) advanced age, (3) isolation (i.e. single, divorced or widowed

marital status), (4) depression, (5) poor self-perceived health status, (6) consumption of hypnotics, sedatives, tranquilizers, anti-hypertensives or alcohol, (7) pre-existing disease (e.g. heart disease, stroke, arthritis), (8) deteriorated gait and/or mobility, and (9) deteriorated balance (Wild et al, 1980 and 1981; Campbell et al, 1981; Prudham and Evans, 1981; Perry, 1982a and 1982b). Other balance-related factors that are often cited include dizziness, vertigo, syncope, and "drop attacks" (Perry, 1982b).

Gabell et al (1985) found a group of fallers (identified prospectively) to show a significantly greater prevalence of the following factors, when compared to nonfallers: (1) absent or abnormal plantar reflex, (2) failure to wear prescribed glasses, (3) foot problems, (4) self-perceived disability, and (5) prolonged post-rest depression of pulse pressure. In a substudy, these authors also found a greater prevalence for deteriorated gait following "photo-stress" (i.e. a change from dim to bright lighting) in the fallers.

Tobis et al (1981 and 1985) found that elderly fallers were more likely to experience errors in visual perception of verticality or horizontality. Whipple et al (1987) found diminished strength and power in the knee and ankle flexor and extensor muscles of elderly fallers, compared to age-matched controls. Gordon et al (1982) suggested that cardiac arrhythmias are an important factor in falls; however, Kirshen et al (1984) were unable to identify fallers using cardiovascular measures. Brocklehurst et al (1982) found a significant correlation between falling history and proprioception (in subjects aged 75-84), but no correlation with visual acuity, vibration sense or vestibular function. Other studies have failed to show any correlation between falling and measurements of postural hypotension (Wild et al, 1980 and 1981) or vibration sense (MacLennan et al, 1980).

Sheldon (1963) first suggested that increased postural sway may be related to a greater tendency to fall. Overstall et al (1977) attempted to relate postural sway to falls and reported that fallers sway more than nonfallers, provided that the fall was not caused by a trip. Wild et al (1980) reported that a group of elderly fallers showed a higher incidence of obvious balance

impairments, compared to an age-matched control group. Brocklehurst et al (1982) found a significant correlation between falling history and spontaneous sway (with eyes closed), but only in subjects aged 75-84. Fernie et al (1982) and Kirshen et al (1984) demonstrated increased mean levels of spontaneous sway in groups of elderly fallers, compared to elderly control groups. Gabell et al (1985) also measured spontaneous sway, and found a increased tendency for fallers to show an "inverse Romberg ratio" (i.e. greater stability with eyes closed than with eyes open); however, this finding was not statistically significant. Using an impulsive force perturbation applied at the waist, Wolfson et al (1986) found that a group of elderly fallers had significantly poorer balance scores (rated according to a nine-level grading scale) and lost their balance significantly more often, compared to elderly nonfallers.

In all of the balance studies described above (except for Fernie et al, 1982 and Gabell et al, 1985), the balance tests were performed after one or more falls had occurred; thus, it is unclear whether the measured deterioration in balance was a cause or a result of the fall. Since the falling data were obtained retrospectively, largely through interviews with the fallers, the accuracy of the data must be questioned. In contrast, Gabell et al (1985) monitored the falling of the subjects prospectively for a period of one year, after performing the spontaneous sway tests. Fernie et al (1982) also monitored the falling prospectively for one year, but performed three sets of sway tests at five-week intervals, starting eight months into the fall-monitoring period. In this study, institutionalized yet ambulatory subjects were used in order to improve the accuracy of the falling data, by allowing observation and reporting of the falls by the clinical staff.

2.4.4 Prediction of Falling Liability

Although transient internal physiological disturbances are undoubtedly an important factor in many falls, a large percentage of falls cannot be explained in this way (Wild et al, 1980). It appears likely that many falls occur in response to a slip, trip, misstep, jostle or self-induced perturbation, in situations where

the posture control mechanisms are unable to maintain balance. The incidence and severity of these perturbations is very difficult to predict; therefore, assessment of the posture control system and its ability to recover from perturbations may be the most reliable single predictor of falling liability. However, in order to obtain the most accurate predictions, it may be necessary to consider postural performance in combination with other predictor variables.

Only a few studies have assessed the ability of balance tests to predict falling liability in individual subjects. Fernie et al (Bartlett et al, 1986) and Kirshen et al (1984) attempted to use spontaneous sway measures to make these predictions, but met with limited success. Fernie reported a misclassification rate of 43%, for both faller and nonfaller groups (based on a sample of 119 fallers and 86 nonfallers). In Kirshen's results, 9 of 17 fallers (53%) and 37 of 49 controls (76%) were classified correctly. Although they did not explicitly analyze misclassification rates, Wolfson et al (1986) noted that 11 of 13 individuals who scored very poorly in response to their impulse force test had a history of multiple falls.

Whereas Fernie et al (1982) and Kirshen et al (1984) used measurements of spontaneous sway, induced sway tests might be expected to provide better assessment of postural control in relation to falling liability (see Section 2.2). Wolfson et al (1986) did use a perturbation in their test, but evaluated the responses subjectively (albeit with a panel of blinded observers). In addition, the relationship of their test perturbation (i.e. a backward force applied at the waist) to the perturbations that occur in actual falls must be questioned.

A number of investigators have attempted to correlate falling with multiple predictor variables. Morse (1986), using a rating scale based on previous history of falling, presence of a secondary diagnosis, intravenous therapy, use of ambulatory aids, gait and mental status, discriminated 80% of fallers from controls. The assessments of gait and mental status were subjective. Kirshen et al (1984) combined indices of cardiovascular status with spontaneous sway measurements, but found no improvement over the results obtained using sway as the only predictor variable.

Tinetti et al (1986) developed a fall risk index based on nine factors: mobility, morale, mental status, distant vision, hearing, postural hypotension, results of back examination, postadmission medications, and admission activities of daily living. For each factor, the subject was scored to be either normal or abnormal, and the overall fall risk score was defined as the number of abnormal scores. All 14 subjects who had risk scores of seven or more were found, prospectively, to be recurrent fallers. The mobility score (based on graded subjective assessments of performance in a number of simple gait and balance manoeuvres) was found to be the best single predictor of recurrent falling.

CHAPTER 3. THE POSTURE CONTROL MODEL AND BALANCE TEST

3.1 THE POSTURE CONTROL MODEL

3.1.1 A General Conceptual Model

As discussed in Chapter 2 and illustrated in figure 2.1, the posture control system can be conceptualized as a negative feedback system which acts to maintain the inherently unstable skeletal linkage in an upright position, in opposition to destabilizing perturbations. Neural centres process the feedback provided by somatosensory, vestibular and visual sensors and send commands to the muscle actuators, which then generate stabilizing moments at the joints.

Nonlinearities include small-amplitude sensory thresholds and large-amplitude saturation-like effects, e.g. limitations on sensor response, joint range of motion, muscle strength, support surface friction, displacement of the centre-of-pressure (COP) on the feet, etc. Other nonlinearities include the dynamics of the skeletal linkage, as well as the dynamic transfer characteristics of the sensors, actuators and neural processors.

3.1.2 Stability

In order to predict falling liability, the relative stability of the posture control system must be assessed. In analyzing stability, it is necessary to consider nonlinear effects. Postural instability and falling are expected to occur when the system is disturbed by a relatively large perturbation; therefore, the large-amplitude saturation-like nonlinear effects are expected to be of prime importance.

It is hypothesized that the limitation on COP displacement imposed by the finite length of the base-of-support (BOS) (i.e. the feet) is the dominant saturation-like nonlinearity that affects postural instability and falling. Once the COP reaches the anterior or posterior perimeter of the BOS, generation of further stabilizing ankle moment (as in the ankle synergy) or shear force (as in the hip synergy) will cause the foot to rotate, i.e. the heel or the toes will leave the ground. In general, a more complex balance-recovery manoeuvre must be executed at this point (or soon

stability margin = $\min (s_1, s_2)$

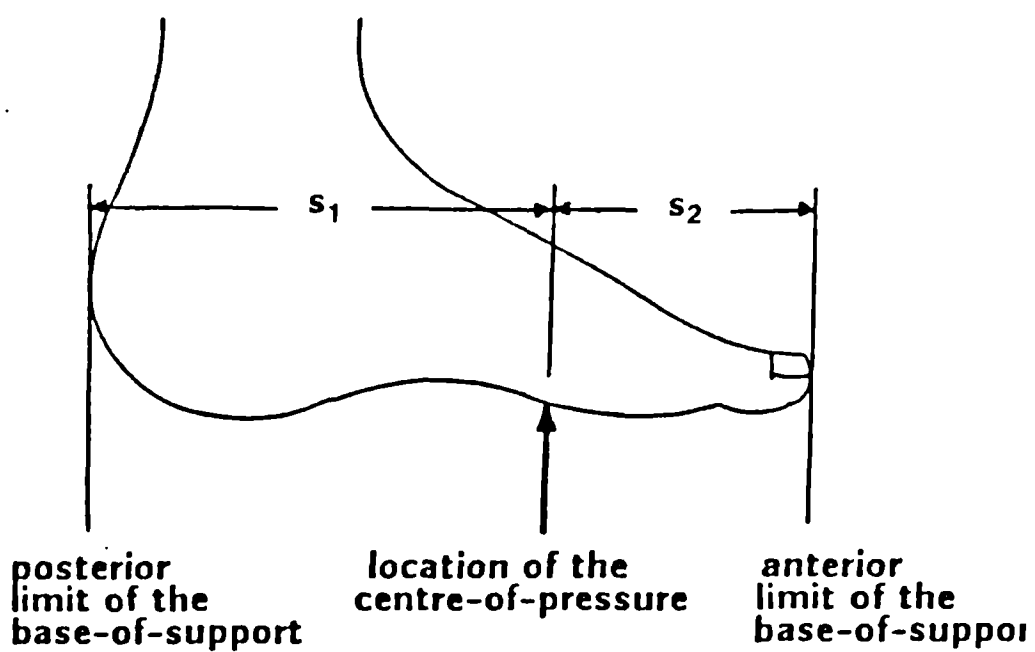


Fig 3.1 The anterior-posterior stability margin.

after) in order to avoid falling, e.g. grab a handrail, wave arms, initiate a step or modify a step already in progress. The dynamics of BOS saturation are discussed further in Section 8.5.2 and Appendix A.1.2.

Koozekanani et al (1980) have suggested that the posture control system may act to maximize the "stability margin", the distance between the COP and the nearest margin of the BOS (see fig 3.1). Individuals who have larger stability margins will be better able to withstand a wider range of destabilizing perturbations without resorting to more complex balance-recovery manoeuvres, and therefore may be less likely to fall.

3.1.3 The Simplified Model

Based on the stability margin concept, the simplified posture control model is represented by a linear-nonlinear (LN) cascade: a linear dynamic component followed by a static nonlinearity (see fig 3.2). The input to the system is a postural perturbation and the output is the resulting displacement of the COP. The nonlinear component of the LN-cascade is a saturation-like nonlinearity, where the saturation limits reflect the finite length of the BOS. The complex nonlinear sub-saturation dynamics of the closed-loop system shown in figure 2.1 are approximated by the linear component of the LN-cascade: a time-invariant, linear transfer function.

When BOS saturation occurs, the system must switch to a new control mode in order to maintain stability, i.e. a more complex balance-recovery manoeuvre must be initiated. Within the framework of the posture control model postulated by Droulez et al (1985), the system operates in a "conservative" mode at sub-saturation amplitudes, i.e. continuous closed-loop servocontrol. When BOS saturation occurs, the system switches to a "projective" mode, selecting an appropriate motor program from a pre-established repertoire.

Because of the time delays associated with the selection and initiation of the more complex projective manoeuvres, it is expected that optimal postural stability will be achieved by minimizing reliance on these manoeuvres, instead utilizing the conservative mode of operation to the greatest extent possible. If

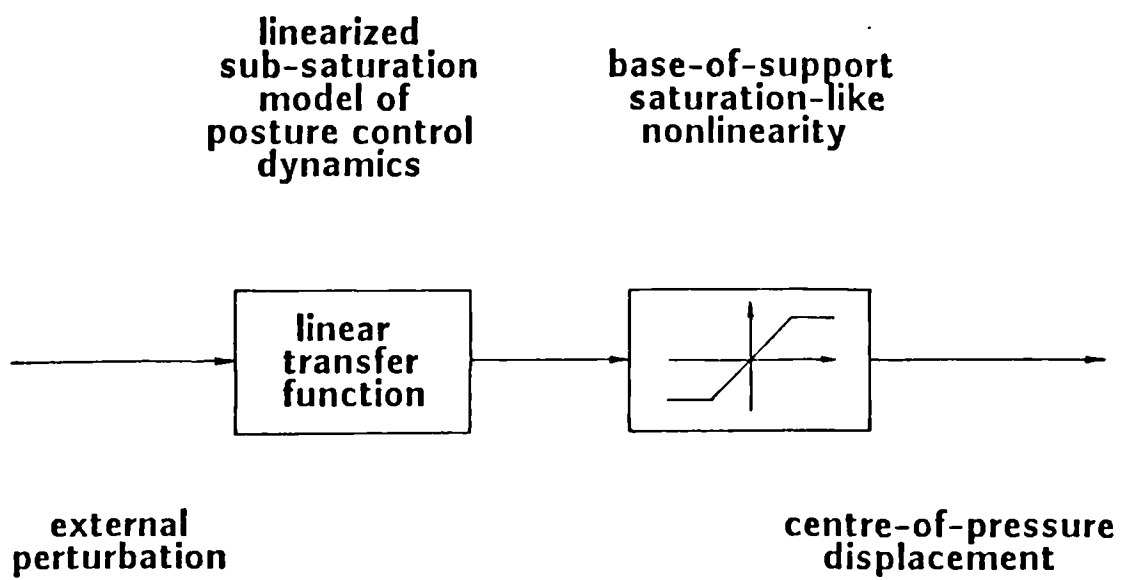


Fig 3.2 The linear-nonlinear cascade posture control model.

this is true, then relative postural stability can be defined in terms of the size of the conservative operating range. For the BOS saturation model, this involves determining the range of perturbations that each individual can withstand without saturating the BOS.

The rationale behind the posture control model is discussed further in Section 8.5.1.

3.2 SIMULATION OF FALLING SITUATIONS

Although some falls may result from internal physiological disturbances (e.g. transient ischemia of the cerebellum or brainstem), it appears that many falls in the elderly occur in situations where the posture control mechanisms are unable to correct for unexpected displacements (i.e. perturbations) of the body (Wild et al, 1981). These perturbations may occur during gait or whilst engaging in activities of daily living (ADL), and may be self-induced and/or externally imposed.

Gait perturbations, such as slips, trips, missteps and "jostles" (e.g. bumping into external objects), are all self-induced to some extent. Self-induced ADL perturbations may occur in standing up, turning, reaching for objects, bending to pick up objects or applying forces to unstable objects that suddenly "give way". Some of these perturbations may result from a failure to make the necessary anticipatory postural adjustments in performing the voluntary movements. Examples of externally imposed perturbations include sudden gusts of wind, sudden accelerations experienced while standing in a moving vehicle and jostles applied by other people.

In order to predict falling liability, the balance test should characterize the response to these types of transient perturbations.

3.2.1 Difficulties with Transient-Waveform Tests

A transient waveform would provide the best simulation of the sudden perturbations that provoke falls; however, a transient balance test presents several difficulties. The safety of such a test is a major concern, particularly in dealing with "frail" elderly subjects.

Even if the risk of injury is reduced through the use of a safety harness, handrails or padded surfaces, subject apprehension may distort the balance response. For example, heightened apprehension may cause subjects to "brace" themselves through co-contraction of antagonist muscle groups. Anticipatory responses of this nature are unlikely to occur (at least not to the same extent) in actual falling situations, where balance is perturbed suddenly and unexpectedly.

In order to achieve accurate identification of "noisy" systems using transient waveforms, the test must be repeated a number of times and the results averaged (Rake, 1980). However, repetitive testing with transient waveforms can lead to adaptive changes in postural synergies and/or initial posture (Nashner, 1976; Horak et al, 1985; Moore et al, 1986). These adaptations degrade the identification of a time-invariant model. Moreover, they represent anticipatory effects that are unlikely to occur in actual falls.

3.2.2 Continuous-Waveform Tests

One solution to the problems associated with transient perturbations is to use a safe small-amplitude continuous-waveform perturbation in the balance test and to predict large-amplitude transient response using the continuous-waveform test results. Through appropriate choice of amplitude, power spectrum and bandwidth, a continuous perturbation can be designed to minimize apprehension and risk of falling. Large-amplitude response can be predicted from small-amplitude tests provided that the posture control system is approximately linear over the range of perturbation amplitudes used in the measurements and predictions. If the waveform is unpredictable to the subject, then the test should elicit posture control system behaviour similar to that occurring in actual falling situations.

Sinusoidal waveforms have the disadvantage of predictability (Stark, 1968). Subjects are able to adapt to this type of perturbation and, in moving platform tests, may learn to "ride" the platform (Andres, 1982). As a result, the measured response may not be indicative of the response in typical falling situations. The perturbation can be made unpredictable by using random or

pseudorandom waveforms. Stark (1968) reported that a pseudorandom waveform composed of a sum of as few as three sinusoids cannot be predicted by human subjects.

3.2.3 The Test Perturbation

To allow extrapolation of the balance test results to everyday postural performance and falling behaviour, the test perturbation should simulate a typical falling circumstance in terms of: (1) kinematics, that is, the relative motion of the body segments, and (2) sensory input, that is, the visual, vestibular and somatosensory cues.

In an ideal simulation of a slip, trip or misstep, the perturbation would be applied to the supporting foot during gait, an approach used by Nashner (1980). Obviously, however, the need for a continuous-waveform perturbation precludes this approach. Instead, a postural perturbation can be applied by moving a platform on which the subject stands. By restricting the number of degrees of freedom of the perturbation motion, the complexity of the posture control model can be reduced.

Platform rotation (i.e. tilt) might simulate overstepping a kerb or stairway tread, but otherwise does not simulate the kinematics of typical falls. Furthermore, the resulting sensory cues may be inconsistent. For example, a "toes-up" platform rotation induces a backward falling motion yet results in ankle dorsi-flexion, yielding proprioceptive cues consistent with a forward fall. The resulting reflexes act to further destabilize the body (Nashner, 1976; Diener et al, 1984).

An anterior-posterior (a-p) translational platform acceleration approximates the kinematics of typical falling situations in that it creates a relative a-p acceleration between the feet and the upper body. Provided that the visual field moves with the platform, the predominant visual, somatosensory and vestibular sensory feedback is directly related to the swaying motion of the body relative to the platform, consistent with a fall relative to the platform frame of reference. One exception lies in the vestibular otoliths, which record the linear acceleration of the head in an absolute reference frame. The implications of the

incongruence between the otoliths and the other sensory modalities are discussed in Section 8.6.1. Other limitations of the translational platform perturbation are also discussed in this section.

3.3 THE TESTING METHODOLOGY

The proposed balance test is based on the LN-cascade posture control model described above. The relative stability of different individuals is quantified in terms of the nominal "saturation amplitude", the transient perturbation amplitude at which the resulting COP displacement would saturate (or equal the length of) the BOS. To ensure subject safety and to minimize anticipatory adaptations, the transient response is determined indirectly. A small-amplitude random or pseudorandom a-p perturbation is applied by accelerating the platform on which the subject stands, and the resulting acceleration and COP measurements are used to identify the linear component of the LN-cascade model. The linear transfer function is then used to predict large-amplitude transient response, thereby allowing the saturation amplitude to be estimated.

A more detailed discussion of the balance testing methodology is presented in Chapter 6. The rationale is discussed further in Section 8.1. The design of the perturbation platform and the selection of the perturbation characteristics are detailed in Chapters 4 and 5, respectively.

CHAPTER 4. THE PERTURBATION PLATFORM

4.1 DESIGN REQUIREMENTS

4.1.1 Introduction

As discussed in Chapter 3, the perturbation to be used in the balance test is a random (RAN) or pseudorandom (PRN), anterior-posterior (a-p), translational platform acceleration. In order to allow the transient response predictions from the RAN or PRN tests to be assessed, the platform must also be able to generate appropriate transient perturbations. The analysis requires measurement of the platform acceleration and the centre-of-pressure (COP) displacement. The ability to measure the COP of each foot separately is needed to allow investigation of the functional length of the base-of-support (BOS).

In meeting the above requirements, it is essential that the platform design satisfies the need for subject safety and tolerance. Furthermore, the platform must not generate extraneous sensory cues (e.g. excessive noise or vibration) that might affect balancing responses.

The design specifications for the perturbation system must include requirements for: (1) bandwidth, (2) range of motion, (3) maximum speed, (4) maximum thrust and (5) maximum power. The thrust and power specifications depend on the perturbation waveform and the loading imposed by the experimental subject. For a deadweight load, the required thrust is equal to the product of the platform acceleration and the mass of the load. Swaying motion of the load, however, may change the thrust requirements.

For the measurement systems, the bandwidth capabilities must exceed the bandwidth of the perturbation. The measurement accuracy should be as high as possible, subject to instrumentation cost and availability constraints. The measurement errors are specified in Section 4.5 and the effects of these magnitudes of error on the balance test results are discussed in Section 8.6.2.

Upper bounds for the design specifications were estimated by requiring a capability to exceed the frequency response and stability limitations of the physiological posture control system. These limitations were estimated by reviewing the existing

TABLE 4.1 - PERTURBATION PARAMETERS USED BY OTHER INVESTIGATORS

INVESTIGATOR	PERTURBATION PARAMETERS +					
	TYPE OF MOTION	POSITION WAVEFORM	POWER SPECTRUM	FREQUENCY RANGE (Hz)	AMPLITUDE	DURATION
Honjo (1957)	rot-ap	ramp?	N/A	N/A	4-20 deg/s	N/A
Nashner (1971-77)	rot-ap	ramp?	N/A	N/A	0.15-6 deg/s	N/A
	tra-ap	ramp?	N/A	N/A	0-5 in/s	N/A
Gantchev et al (1972)	rot-ap	sine	N/A	0.2-1.0	3 deg	?
	tra-ap	sine	N/A	0.2-1.4	36 mm	?
Litvintsev (1973)	tra-ap, ml	ramp?	N/A	N/A	?	N/A
Walsh (1973)	rot-ap, ml	sine	N/A	0.06-0.7	0.3 deg	20 s
Gurfinkel et al (1976)	tra-ap	sine	N/A	0.2-2.0	5 cm	40 cycles
	rot-ap	sine	N/A	0.2-2.0	1,2 deg	40 cycles
		ramp	N/A	N/A	0.1-0.2 deg, 0.6 deg/s	N/A
Meyer et al (1978)	rot-ap	sine	N/A	0.1-1.0	?	160 s
		random	?	? -1.0	0.5 deg max	160 s
		ramp	N/A	N/A	0.6 deg, 15 deg/s	N/A
Allum et al (1979)	rot-ap	ramp	N/A	N/A	1-4 deg, 30-50 deg/s	N/A
Nashner et al (1979-81)	rot-ap	h-sine	N/A	2,4	5 deg, 20 deg/s	N/A
	tra-ap	h-sine	N/A	2,4	8 cm, 30 cm/s	N/A
	tra-vt	h-sine	N/A	2,4	5 cm, 20 cm/s	N/A
Hibino (1980)	rot-ap	sine	N/A	0.1-3.0	5 deg	?
Ishida et al (1980)	tra-ap	BPRN	bell-shaped	0.2-2.0	?	?
Andres (1982)	tra-ap	ramp	N/A	N/A	7.5 cm/s	N/A
		sine	N/A	0.2-0.8	6-18 cm/s	20 s
		PRN	?	0.1-2.0	4-10 cm/s max	20 s
Diener et al (1984)	rot-ap	ramp	N/A	N/A	2-8 deg, 10-100 deg/s	N/A
Tokita et al (1984)	tra-ap	PRN	?	0.1-5.0	10 cm max	?

+ NOTE: rot = rotational, tra = translational, ap = anterior-posterior, ml = medial-lateral, vt = vertical, h-sine = half-sine, PRN = pseudorandom, BPRN = binary pseudorandom, N/A = not applicable.

knowledge about the dynamic characteristics of posture control responses, and by performing computer simulations of balancing responses to various platform motions. In addition, consideration was given to the perturbation parameters used by other investigators.

4.1.2 Review of the Literature

Andres and Anderson (1980) developed a detailed list of design requirements for "postural measurement systems". For the "stimulus delivery system", they arrived at the following requirements: (1) peak-to-peak range of 30.5 cm, (2) maximum speed of 30.5 cm/s, and (3) upper frequency response limit of 3.0 Hz. The authors presented no specific rationale for their recommendations, although they apparently perceived a need to test a wider range of perturbations than previous investigators. No requirements were reported for the lower frequency response limit or for the maximum acceleration, thrust or power.

Perturbation parameters used by other investigators are listed in table 4.1. For translational perturbations, the maximum values that have been reported are as follows: (1) peak-to-peak range of 10 cm, (2) peak speed of 30 cm/s, and (3) upper frequency limit of 5.0 Hz. For platform translations, the smallest lower frequency limit reported in the literature is 0.1 Hz. For rotational perturbations, the frequency range has extended as low as 0.06 Hz, with an upper limit of 3.0 Hz. No specifications for acceleration, thrust or power were found in the literature.

Review of the existing experimental evidence suggested that an upper frequency of 5.0 Hz would exceed the functional bandwidth of the posture control system (see Section 5.3.3). Analysis of the sensory feedback modalities indicated that the visual field should move with the platform in order to simulate the sensory cues of a fall relative to the platform frame of reference (see Sections 3.2.3 and 8.6.1).

4.1.3 Simulation of Balancing Responses

Computer simulations were performed to investigate the COP displacement response to horizontal platform translations, with the aim of estimating appropriate upper limits for the platform design

specifications. The simulation methods and results are detailed in Appendix A.

The results of the simulations suggested that a perturbation bandwidth of 0.1-5.0 Hz would be adequate to identify the relevant dynamic characteristics of the posture control system. The simulations indicated that the 0.1 Hz limit would be low enough to identify a flat low-frequency asymptote in the frequency response. Simulated COP responses at frequencies higher than 5.0 Hz were too small to be of any functional significance.

Using an inverted pendulum model of the balancing response, the simulations indicated that an acceleration pulse with an amplitude of 1.5 m/s^2 and a duration of 0.3 s would be sufficient to cause subjects to lose their balance (i.e. for the COP to reach the limits of the BOS). This perturbation would require a peak speed of 0.45 m/s and, to allow for both acceleration and deceleration, a range of 0.14 m. For a 100 kg (95th percentile male) subject, this waveform would require a peak thrust and power of 0.12 kN and 15 W, respectively, to be delivered to the subject.

To arrive at a worst-case estimate, the subject was simulated by a 100 kg deadweight. In order to topple the deadweight, the following perturbation characteristics were required: peak acceleration of 2.6 m/s^2 , peak speed of 0.78 m/s, range of 0.23 m, peak thrust of 0.26 kN and peak power of 0.20 kW.

For PRN and RAN waveforms, the acceleration, speed, thrust and power requirements were smaller, compared to the pulse waveform. However, the PRN and RAN range requirements were larger, with estimated values of 0.39 m and 0.60 m for the inverted pendulum and deadweight models, respectively.

4.1.4 Summary

Based on the results presented above, the following specifications were formulated for the perturbation system: (1) range of motion of 0.6 m, (2) maximum speed of 1.5 m/s, (3) maximum acceleration of 5 m/s^2 , (4) maximum thrust of 0.5 kN, (5) maximum power of 0.5 kW, and (6) bandwidth of 0.1-5.0 Hz. Note that the specifications were deliberately overestimated to ensure that the platform would have the capability of perturbing balance

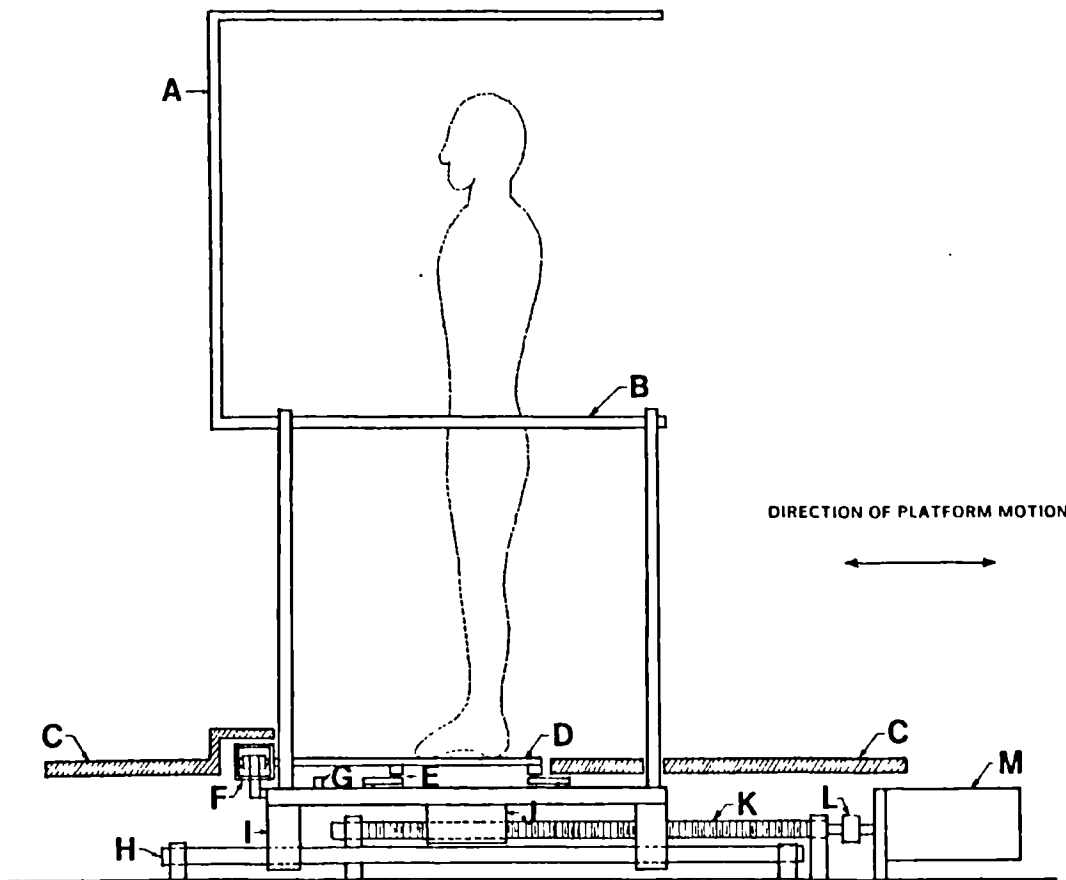


Fig 4.1 Schematic of the perturbation platform.

- Legend:
- A = visual surround
 - B = safety handrail
 - C = safety cover
 - D = force plate
 - E = vertical-force load cell and ball transfer
 - F = horizontal-force load cell and ball transfers
 - G = accelerometer
 - H = ball bushing shaft
 - I = ball bushing
 - J = tandem ball nut
 - K = ball screw
 - L = flexible coupling
 - M = DC servomotor plus tachometer
- Note: linear potentiometer not shown

to the point of instability during transient tests.

4.2 MECHANICAL DESIGN

The overall platform design is illustrated schematically in figure 4.1.

4.2.1 Drive Train

It was found that the design requirements could be satisfied using a direct-current (DC) servo-motor. Compared to hydraulic or pneumatic systems, the use of a motor has several advantages, including: (1) no need for a special hydraulic or pneumatic power supply (resulting in lower cost and greater portability), and (2) no problems with fluid or air leakage. In addition, if a DC permanent-magnet motor is used, the performance characteristics are far more linear, thereby facilitating the control of the device.

Computer simulations were performed to determine the motor speed-torque requirements. In contrast to the simulations described earlier, these simulations included the effects of the inertia and compliance of the drive train itself, in order to determine the speed and torque required at the motor. Pulse, PRN and RAN waveforms were simulated, using the "worst-case" amplitudes determined in the previous simulations. A 100 kg deadweight load was used to represent the subject.

By comparing manufacturers' motor performance graphs with simulation-generated plots of the speed-torque requirements, an appropriate motor was selected (Inland Motor, model TT-2954D2; Industrial Drives Division, Kollmorgen Corp., Radford, Virginia). The selected motor uses a samarium cobalt magnet and has a peak speed of 2300 RPM, a peak torque of 37.2 Nm, and a power rating of 2.1 kW. The performance characteristics of this motor are shown in figure 4.2, along with the simulated speed-torque requirements.

The rotational motion of the motor shaft is converted into a linear translation by means of a ball screw. The ball screw is essentially a lead screw in which the thread-to-thread contact has been replaced by recirculating ball bearings, resulting in much greater mechanical efficiency, smoother operation (minimal stiction) and longer life than a conventional lead screw. By using a preloaded tandem ball nut, backlash is virtually eliminated. The

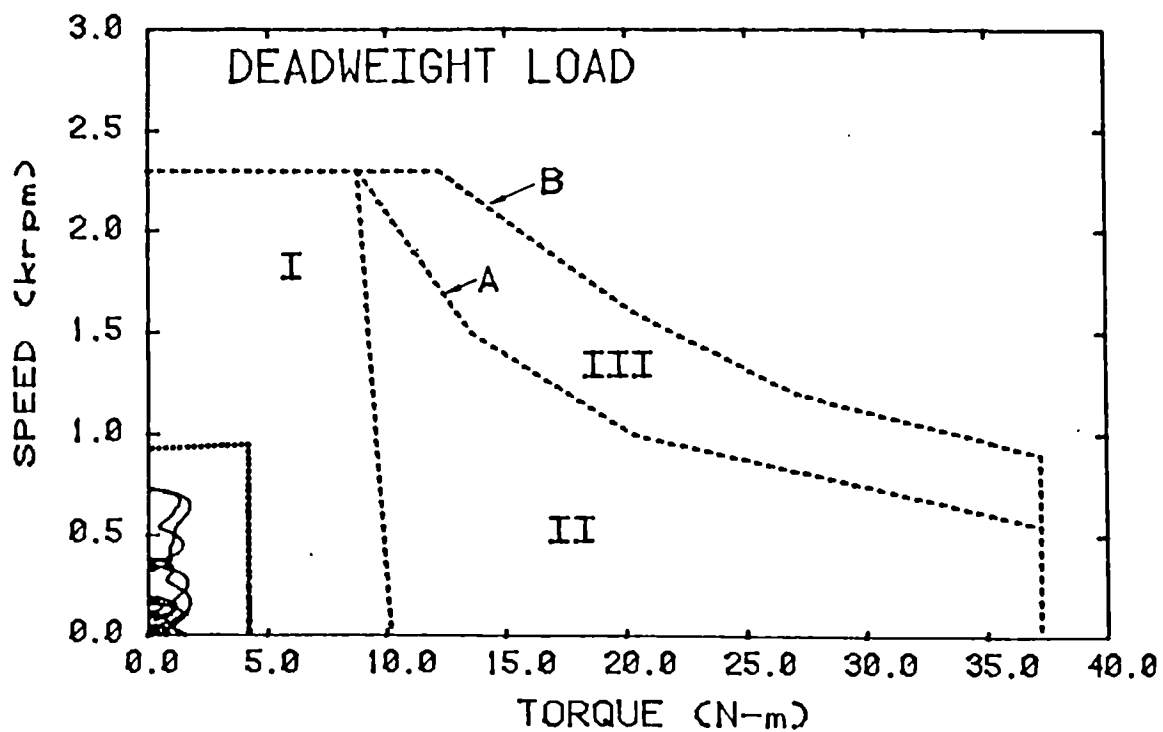
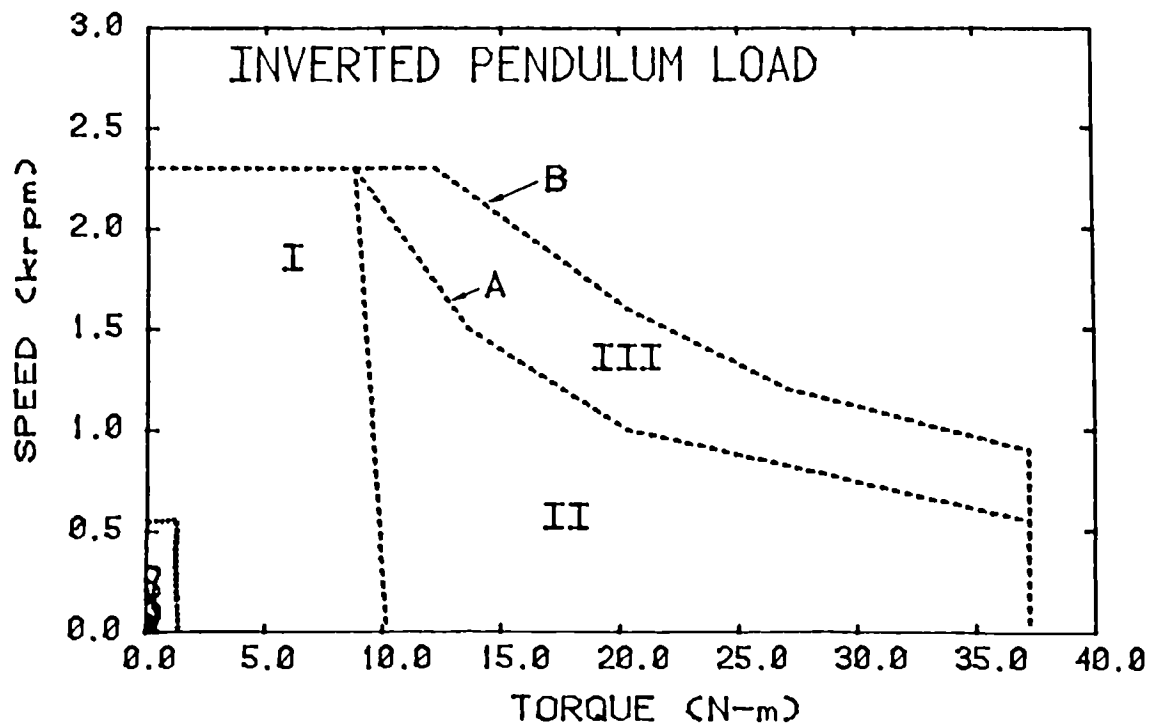


Fig 4.2 Speed-torque characteristics.

Legend: simulated speed-torque requirements:
 solid line = pseudorandom waveform
 dotted line = pulse waveform
 motor performance limits (dashed lines):
 I = continuous duty zone
 II = intermittent duty zone
 III = acceleration/deceleration zone
 A = 2.1 kW motor rating
 B = 3.4 kW commutation limit

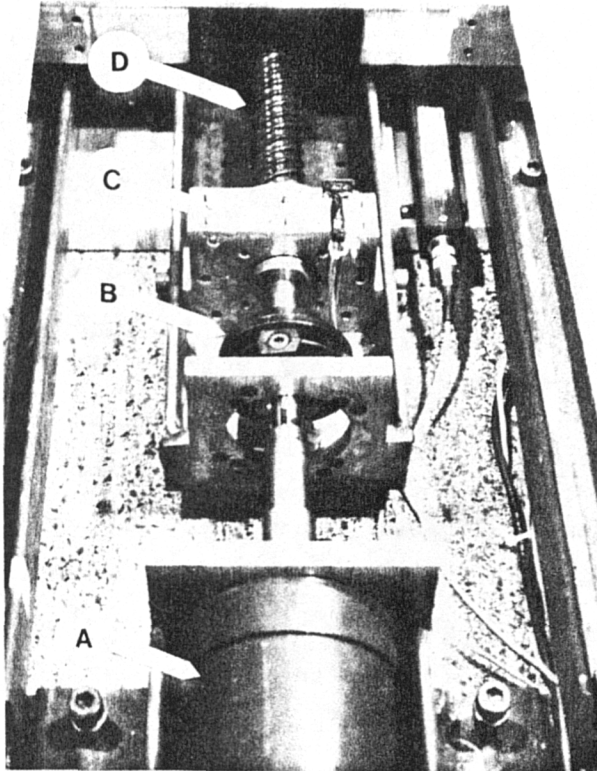


Fig 4.3 Drive train.

Legend: A = motor
B = flexible coupling
C = pillow block for angular contact bearings
D = ball screw

ball screw (Dynatorq, model D-58; Rockford Ball Screw Co., Rockford, Illinois) and ball nut (Dynatorq, model RP-58) have a lead of 1.875 inches (48 mm) and a pitch diameter of 1.5 inches (38 mm).

The tandem ball nut is mounted on the underside of the platform carriage (i.e. the moving part of the platform). The ball screw is supported at both ends by tandem angular contact bearings (Fafnir, model 7205W; Fafnir Bearing Division of Textron Inc., New Britain, Connecticut), mounted in custom-designed pillow blocks which in turn are bolted to the base of the platform. These bearings support the thrust generated by the drive train in accelerating the platform.

The ball screw is connected to the motor shaft by means of a flexible coupling (Centaflex with Zytel element, model 2-2; Lovejoy Inc., Downers Grove, Illinois). The flexible coupling minimizes wear and stiction due to misalignment of the two shafts. This particular model of coupling is relatively stiff in torsion and was selected to ensure minimal reduction in the frequency response of the drive train.

The flexible coupling also serves to damp motor vibrations. To further reduce transmission of motor vibration, the motor is mounted directly to the floor, separate from the rest of the platform. The vibration of the motor itself was reduced by decreasing the amplitude of the bias current; however, excessive reduction in bias current was found to result in jerky platform operation. Thus, the adjustment of the bias current entailed a compromise between platform vibration and jerky platform movement.

The drive train design meets or exceeds all of the design requirements. The maximum range of motion is 0.6 m, the maximum speed is 1.83 m/s, and the maximum thrust is 4.9 kN. As illustrated in figure 4.2, the power rating of the motor far exceeds the power requirements. Based on a total inertial load of 0.0143 kg-m² (due to the rotational inertia of the motor, ball screw and coupling, plus the "reflected" inertia associated with the mass of the carriage and a 100 kg subject) and a torsional stiffness of 1.24 kNm/rad (associated with the flexible coupling), the resonant frequency of the perturbation system was calculated to

be approximately 47 Hz, far exceeding the bandwidth requirement of 5 Hz.

A photograph of the motor end of the drive train is shown in figure 4.3.

4.2.2 Power Supply

A silicon-controlled-rectifier (SCR) amplifier (Inland Motor model TPA/1-12040-603-2954D2; Industrial Drives Division, Kollmorgen Corp., Radford, Virginia) is used to drive the motor. This amplifier was designed by the motor manufacturer specifically for the purpose of driving the model-2954D2 motor. It provides full-wave, three-phase rectification, and therefore has a control bandwidth extending to approximately 30 Hz (Electrocraft, 1980), far exceeding the design requirements. Operation is bi-directional and fully regenerative (i.e. the motor is braked dynamically, instead of "coasting" to a stop).

An SCR amplifier generates the required power efficiently and at relatively low cost (Electrocraft, 1980). Linear amplifiers are better suited to lower power applications, whereas the other types of switching amplifiers (e.g. pulse-width modulation) require a DC power supply.

4.2.3 Structural Components

The platform carriage is supported by four ball bushings (Super Ball Bushing, model SPB-24-ADV; Thomson Industries, Manhasset, New York) on two parallel case-hardened steel shafts (38 mm in diameter and 160 cm in length: 46 cm between centre-lines). Each shaft is supported at the ends and in the middle by shaft support blocks (Thomson model SB-24), which in turn are mounted on a steel channel section, 15 cm wide and 160 cm long. The pillow blocks supporting the ball screw are mounted on a 120 cm length of this same steel channel. The three lengths of steel channel are bolted to a 25 mm thick plate of aluminum (76 cm long and 61 cm wide) which in turn is bolted to the concrete floor.

The carriage and force plates are constructed of 6 mm thick aluminium-alloy plating, reinforced with a grid-like network of aluminium-alloy angle section. The carriage is 76 cm long and 61 cm wide, while each force plate is 39 cm long and 30 cm wide.

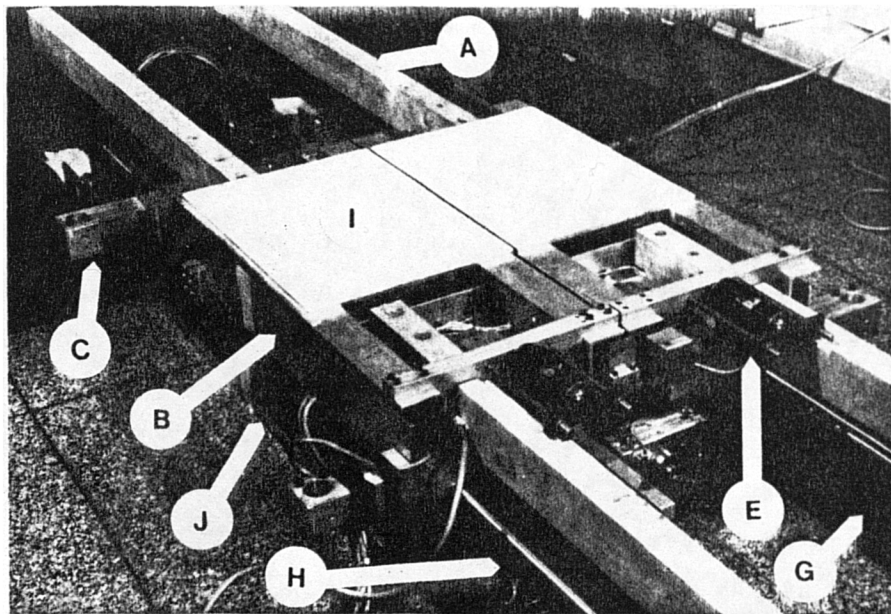
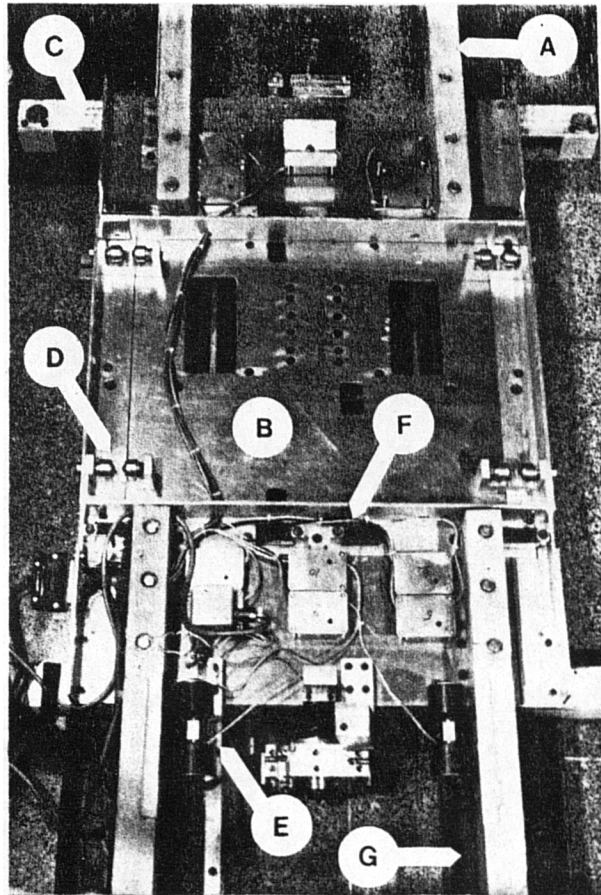


Fig 4.4 Platform carriage and supporting structures
(top = without force plates, bottom = with force plates).

Legend: A = beams to support safety cover, B = carriage
 C = struts to support visual field/handrail framework
 D = lateral-constraint ball transfers
 E = horizontal-force load cell, with ball transfers
 F = vertical-force load cell, G = steel channel
 H = ball bushing shaft, I = force plate, J = base-plate

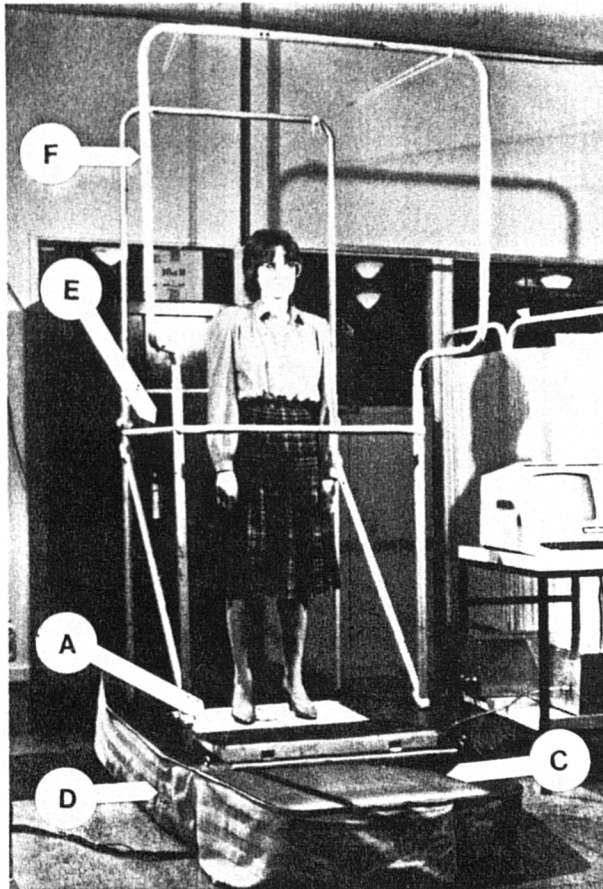
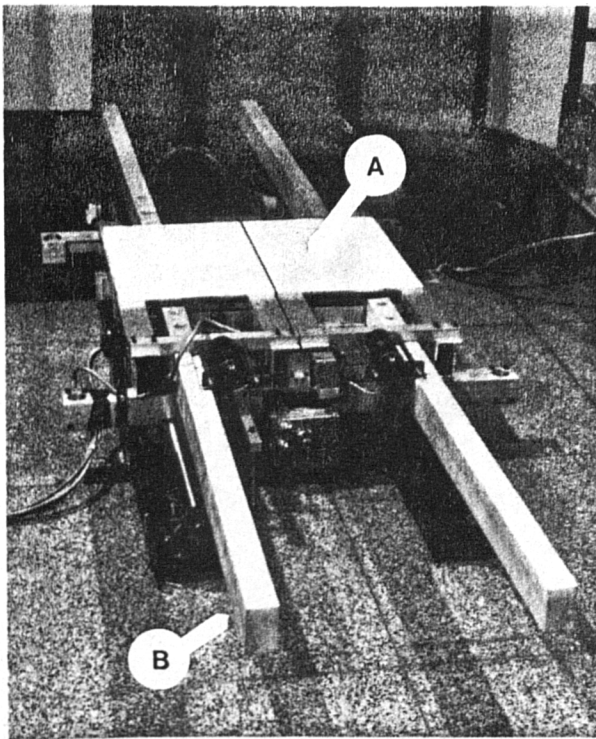


Fig 4.5 Safety structures and framework
(top = without safety cover, bottom = with safety cover).

Legend: A = force plates B = beams to support safety cover
C = safety cover D = fabric skirt
E = handrails F = framework for visual surround

The structural components were designed to minimize deflections that might cause binding in the ball nut or ball bushings. High stiffness is also needed in order to achieve an adequate frequency response in the COP measurements. The design was aimed at achieving a frequency response exceeding 10 Hz under the worst-case loading conditions (100 kg subject standing on one leg at the centre of one platform). At the same time, the components of the platform carriage were designed to minimize the mass, thereby reducing the inertial load on the motor.

Photographs of the platform carriage and supporting structures are shown in figure 4.4.

4.2.4 Visual Surround and Safety Structures

Safety handrails and a framework to support the visual surround are attached to the platform carriage. The handrails and framework are constructed of lightweight aluminum-alloy tubing (outer diameter of 25 mm). The handrails and exposed areas of the framework are wrapped with a covering of high-density polyurethane foam (6 mm thick).

The visual surround consists of rigid styrofoam panels (25-50 mm thick) strapped to the front, sides and top of the tubular framework. The front panel is approximately 70 cm from the eyes; laterally, the distance is approximately 40 cm on each side. A poster is mounted at eye level on the front panel. Two incandescent light fixtures (60 watts each) are installed to the rear of the subject.

A plywood panel, mounted on softwood beams cantilevered to the platform carriage, serves to cover the supporting structures and drive train. The panel overhangs the carriage by 60 cm at each end. A fabric skirt is attached to the perimeter of the plywood cover to further conceal the undercarriage and to prevent dust from entering the drive train components. Rubber treading is stapled to the top surface to prevent subjects from slipping while getting on or off the platform.

Sheets of polyurethane foam (75 mm thick) are used to pad the lower half of the handrail framework, to the front and sides of the subject. In addition, a foam-padded styrofoam block (approximately

60 cm wide, 60 cm deep and 150 cm high) can be strapped into place behind the subject, if desired. In the event of a fall, the foam surfaces cushion the impact and limit the distance that the subject falls. The front and rear surfaces are slightly inclined, to better "catch" the subject should a forward or backward fall occur.

Handrails and padded surfaces were selected in preference to a safety harness. Even if the safety harness is designed to move in unison with the platform, the swaying motion of the subject relative to the harness may still provide some degree of sensory feedback, via the cutaneous or deep pressure receptors. Although it may be possible to minimize the sensory feedback through careful design of the harness, there are other problems inherent to the safety harness approach. In particular, there is a possibility that the restraining forces exerted by the harness could induce bone fracture or soft tissue injury, particularly in "frail" elderly subjects. In addition, wearing the harness might tend to increase the apprehension of the subjects, thereby altering their balancing responses.

Photographs of the platform, with and without the safety cover, are presented in figure 4.5. The polyurethane foam enclosure is shown in figure 4.6.

4.3 CONTROL SYSTEM

4.3.1 Design and Fine-Tuning

The platform carriage is controlled as a positional servomechanism, using an additional velocity feedback loop to provide damping and increased stability. In addition, the SCR amplifier has a built-in current feedback loop, which improves the system performance by making the output torque relatively independent of the motor speed. Positional control was chosen to avoid the drift problems that can occur in velocity or acceleration control.

Initial settings for the feedforward gain and velocity feedback gain were estimated through classical control-system design procedures (e.g. Ogata, 1970a), based on measurements of the open-loop frequency response. The performance was then fine-tuned experimentally. Starting with the initial gain estimates, the

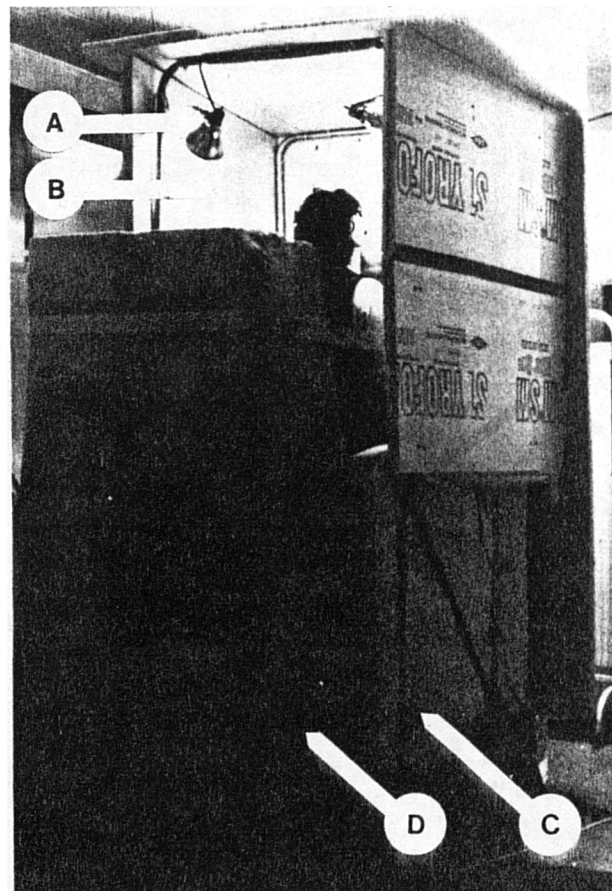
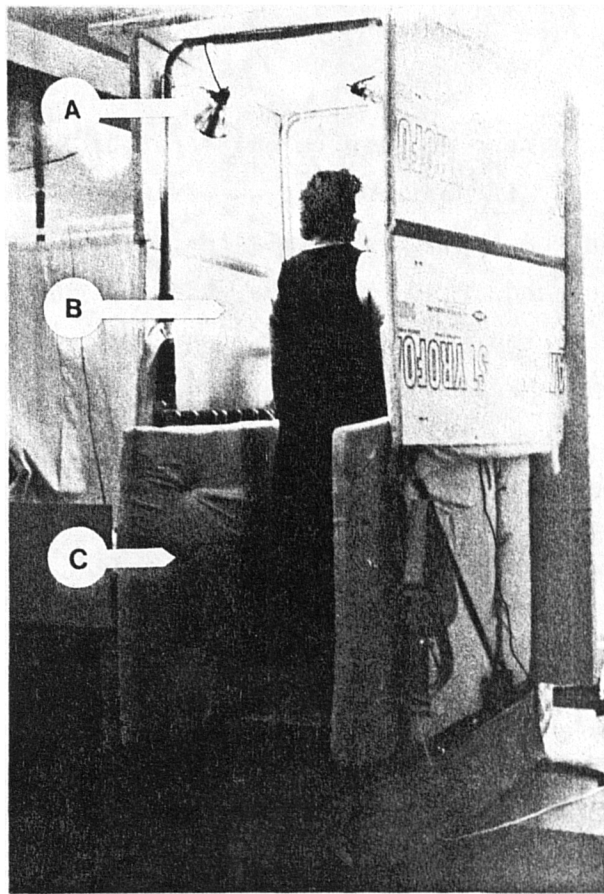


Fig 4.6 Polyurethane foam enclosure and visual surround (top = without rear enclosure, bottom = with rear enclosure).

Legend: A = lighting fixture B = visual surround
 C = foam padding D = padded styrofoam block

effects of small adjustments in the gain values were assessed by measuring the resulting closed-loop frequency response, using dead-weight loads of 40 to 100 kg to simulate the experimental subject. During these tests, the platform was controlled to move in a pseudorandom fashion, allowing the frequency response to be determined using cross-spectral nonparametric methods (see Section 6.5). For each setting of feedforward gain, the velocity feedback gain was adjusted to give a slightly underdamped transient response (damping coefficient ≈ 0.7). The performance was found to be relatively independent of the load. This is to be expected, as the inertia of the drive train is two to three times greater than the inertia due to the dead-weight load.

Although increase in feedforward gain improved the frequency response, this also seemed to increase the jerkiness or "cogging" in the platform operation. This problem may be a result of the stiction in the system. In response to binding, the control system generates a large error signal, because of the high gain setting. The binding is freed, but overshoot occurs and the control system must then decelerate the carriage, allowing binding to occur again, and the cycle of "slip-overshoot-stick" is repeated. The overshoot problem may be exacerbated by the discrete nature of the SCR amplifier response. A large error signal will cause the amplifier to switch on at an early "firing angle". This results in a heavy surge of power, as the SCR cannot switch off again until the 60 Hz half-cycle is over (Electrocraft, 1980).

To achieve the desired platform performance (i.e. -3 dB at 5 Hz, or better) without sacrificing smoothness of operation, the position command signal is passed through a "precompensator", which compensates for the attenuation and phase lag in the closed-loop frequency response of the platform. The precompensator is simply a first-order high-pass digital filter with a transfer function approximately equal to the inverse of the measured closed-loop frequency response. It differs from a conventional compensator in that it is placed outside of the feedback loops. The filtering of the command signal is performed offline, prior to the start of the test.

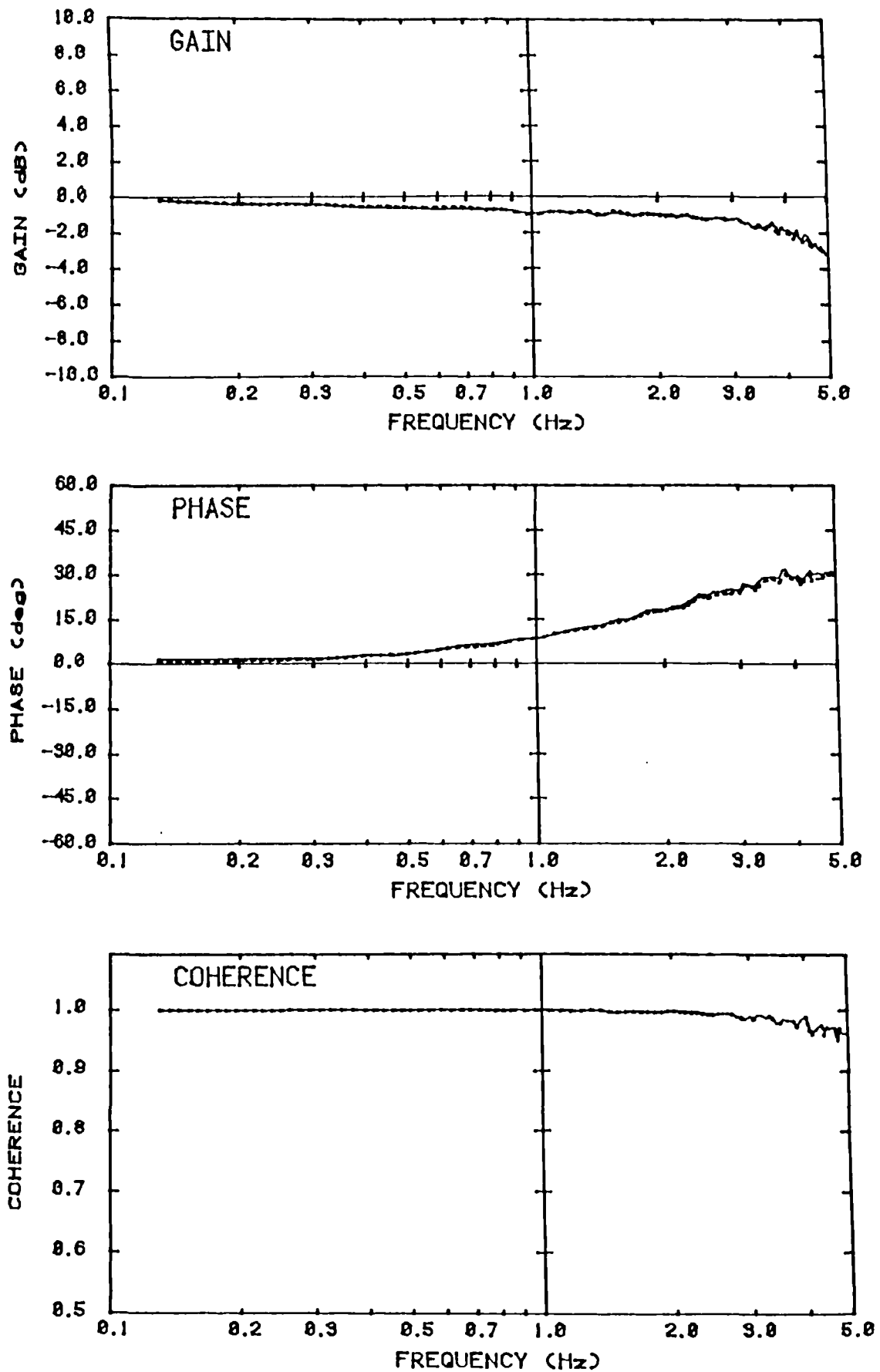


Fig 4.7 Frequency response of the platform
(input = desired acceleration, output = measured acceleration).

Legend: solid line = 44 kg subject
dashed line = 85 kg subject

4.3.2 Performance

Using the precompensator, the gain and phase characteristics of the platform frequency response were found to be flat to within approximately 3 dB and 30 degrees, respectively, for frequencies up to 5.0 Hz, the highest frequency tested. The response was found to be largely independent of the inertial load on the platform, for loads ranging from 40 to 100 kg. Similar results were obtained for both the position and acceleration frequency response. Examples of the acceleration frequency response (measured with actual subjects on the platform) are shown in figure 4.7. The frequency response estimates were derived from PRN-waveform tests, using cross-spectral analysis (see Section 6.5).

4.4 INSTRUMENTATION

4.4.1 Position, Velocity and Acceleration Transducers

The carriage position is measured with a high-precision linear potentiometer (Longfellow, model LF-S-24/600-0-D5; Waters Manufacturing Inc., Wayland, Massachusetts). This potentiometer has a range of 60 cm and a maximum nonlinearity of 0.1% over this range. Because the resistive element is a conductive plastic filament, the resolution is "infinite", allowing for smoother and more accurate positional control of the carriage motion, compared to finite-resolution wirewound potentiometers.

A tachometer (Inland Motor, model TGF-1800-00), integral to the motor, provides a measure of the motor speed. The tachometer signal is approximately proportional to the translational velocity of the platform carriage, but may differ slightly because of backlash or torsional "windup" in the drive train. The small inaccuracies are not important, because the velocity signal is used only in a secondary feedback loop (to provide damping and improve stability).

The potentiometer and tachometer signals are passed to high input-impedance buffer and amplifier circuits. Separate circuits: (1) provide amplification, (2) subtract the feedback signals from the computer-generated position command signal, and (3) allow the feedforward gain and the velocity feedback gain to be adjusted.

Acceleration is measured with a high-sensitivity

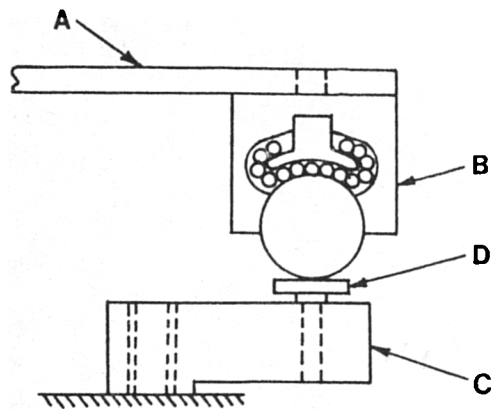
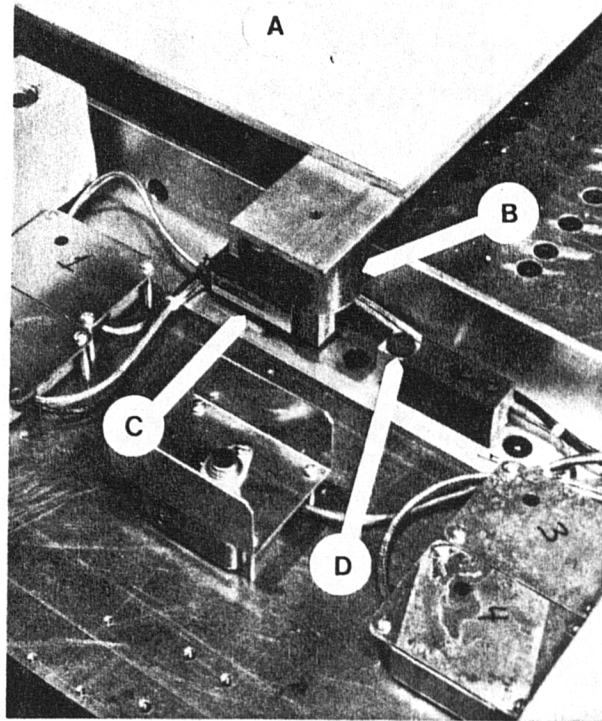


Fig 4.8 Vertical-force measurements.

Legend: A = force plate, B = ball transfer, C = load cell
D = hardened steel button

piezoresistive accelerometer (Endevco, model 2265-20, Endevco, San Juan Capistrano, California). This accelerometer has a range of ± 20 g and a frequency response of 0-200 Hz, with a combined nonlinearity and hysteresis error less than or equal to $\pm 2\%$ of the reading. An instrumentation amplifier amplifies the output of the accelerometer while providing common-mode rejection.

Although the accelerometer is mounted on the platform carriage, it provides an accurate measure of the acceleration applied to the subject, over the frequency range of interest, because the coupling between the carriage and the force plates (on which the subject stands) is very stiff. The most compliant element in the coupling is the horizontal-force load cell. A worst-case calculation, based on the load cell stiffness and a 100 kg deadweight load, showed the natural frequency of the coupling to exceed 50 Hz.

4.4.2 Force Plates

Two custom-built force plates are mounted side-by-side on the top of the platform carriage. Each plate is supported by four load cells, one at each corner. These load cells measure the vertical force on each plate. In addition, a single load cell, mounted at the front of each plate, measures the a-p horizontal force (in the process, transmitting the thrust from the drive train to the force plate). The top surface of each force plate is covered by a vinyl tile (2 mm thick). The vinyl prevents subjects from slipping, and provides electrical and thermal insulation.

The load cells are of the bending-beam, strain-gauge design (Minibeam, model MB-250; Interface, Inc., Scottsdale, Arizona). Each load cell has a rated capacity of ± 250 lb (1.1 kN), with nonlinearity and hysteresis less than 0.03% and 0.02% of full scale, respectively. Strain-gauge load cells were selected in preference to piezoelectric designs because of their better low-frequency response, smaller nonlinearity and hysteresis, and lower cost. Commercially-available force plates were avoided because of their relatively large mass and high cost.

In using uniaxial load cells, it was necessary to devise some means for eliminating cross-talk between the vertical and

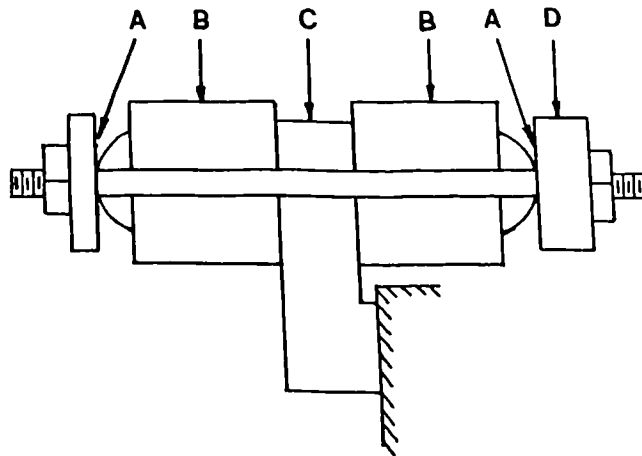
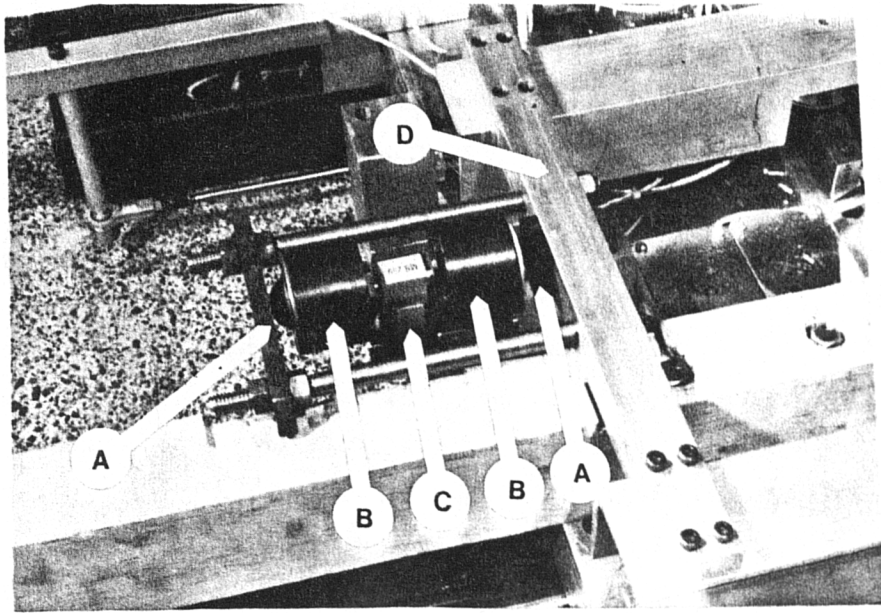


Fig 4.9 Horizontal-force measurements.

Legend: A = hardened steel surface, B = ball transfer
C = load cell, D = frame (attached to force plate)

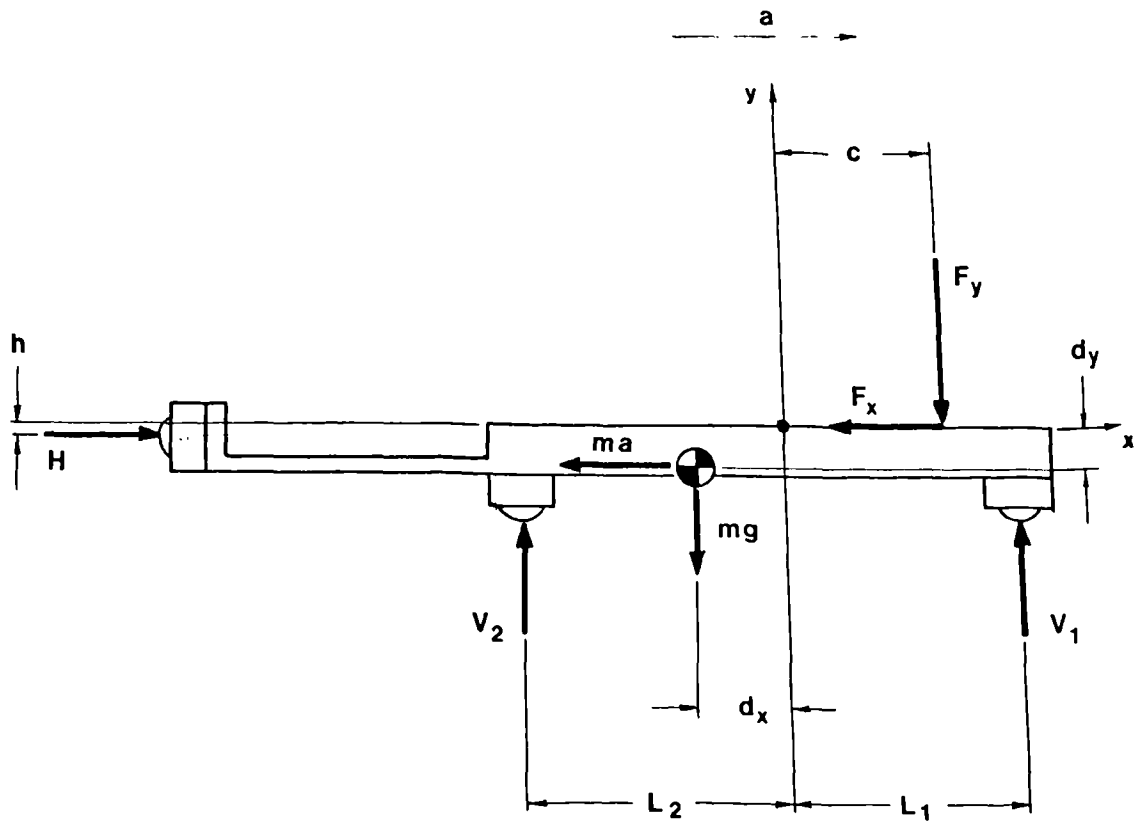
horizontal force measurements. Multi-axis load cells would allow both horizontal and vertical forces to be measured, but are expensive and tend to have a relatively high level of cross-talk.

Instead, cross-talk was minimized by placing a high-precision ball transfer (Autotrack, model 1061; Autotrack Ltd., Freddich, Worcestershire) between each load cell and the force plate. The ball transfer is essentially a large-diameter (25 mm) ball supported by a bed of recirculating small-diameter (3 mm) balls resting in a hemispherical cup. Because the large ball is free to rotate, the ball transfer can transmit only normal loads to the load cell, thereby eliminating cross-talk.

For the vertical-force load cells, the ball transfers are mounted on the underside of each force plate. Each ball transfer mates with a hardened steel "button" mounted on the underlying load cell (see fig 4.8). A somewhat different mounting arrangement is used for the horizontal-force load cells, in order to transmit and measure the thrust forces in both forward and backward directions. Tandem ball transfers, mounted on the load cell, mate with hardened-steel surfaces on a box-frame attached to the front end of the force plate (see fig 4.9).

Lateral horizontal forces are not measured. In order to prevent the force plates from moving laterally, without affecting the a-p and vertical force measurements, two pairs of 12 mm ball transfers (Autotrack, model 1151) are used to constrain each force plate.

The a-p horizontal forces acting on the platform affect the measurement of COP. As illustrated in figure 4.10, these forces include the thrust force delivered via the drive train, the shearing force exerted by the subject's foot and, in accordance with D'Alembert's principle, a fictitious inertial force associated with the acceleration of the platform. The horizontal forces create a rotational moment which must be counter-balanced by the vertical forces generated at the load cells. Unless appropriate corrections are made, the changes in the vertical forces will result in an error in COP measurement. The apparatus was designed to minimize the moment created by the horizontal forces, thereby minimizing the magnitude of correction needed.



From moment equilibrium:

$$c = \frac{V_1 L_1 - V_2 L_2 + Hh + mgd_x - mad_y}{F_y}$$

where:

- c = centre-of-pressure location
- H = force at horizontal-force load cell
- m = mass of force plate
- a = acceleration of platform carriage
- F_x, F_y = forces at subject's feet
- V_1, V_2 = forces at front, back vertical-force load cells

Note: dimensions h and d_y are exaggerated.

Fig 4.10 Free-body diagram of force plate.

The moment was minimized in two ways. First, the moment due to the inertial force was reduced by minimizing the force plate mass and by locating the force plate centre-of-gravity as close as possible to the upper force plate surface. Secondly, the moment arm between the thrust and shear forces was minimized, by locating the thrust axis as close as possible to the upper surface of the force plate. By projecting a laser beam through the hole in the horizontal-force load cell (i.e. along the thrust axis) and adjusting the load cell height until the beam was tangential to the force plate surface, the moment arm between the thrust and shear forces was reduced to less than 0.5 mm, the radius of the laser beam.

4.4.3 Computer and Computer Interface

The positional command signal is generated by a VAX 11/730 minicomputer (Digital Equipment Corporation, Maynard, Massachusetts). The same computer is used to sample and store the data from the transducers and force plates. Input/output is performed via the DMF32 parallel port of the VAX, driven by custom-written software. The DMF32 is connected to a 12-bit analog-to-digital converter (ADC) (Datel, model MDAS-16; Datel Systems, Inc., Mansfield, Massachusetts) and a 16-bit digital-to-analog converter (DAC) (Burr-Brown, model DAC70; Burr-Brown, Tucson, Arizona). The ADC system includes a 16-channel multiplexor and a sample-and-hold amplifier. Although simultaneous sampling is not achieved, the maximum "jitter" between channels is only 20 μ s. The sampling rate is controlled by the system clock on the VAX.

The 12-bit resolution of the ADC limits the resolution of the position measurements to 0.18 mm, the velocity measurements to 0.0095 m/s, the acceleration measurements to 0.0053 m/s², and the load cell measurements to 0.12 N. The resolution of the COP measurements is dependent on the magnitude and position of the load. A typical value is 0.1 mm (for a 225 N load at the centre of the force plate).

The VAX is designed for timesharing amongst multiple users. In order to prevent the VAX from periodically "swapping" the

platform control program out of memory, it is necessary to "lock" the program into memory and to suspend all other "processes" running on the computer. Because the DMF32 parallel port of the VAX is designed primarily for operating a line printer, the operation is relatively slow. Input/output operations are further slowed by hardwired time delays in the control lines, which were required to prevent spurious pulses generated by the DMF32 from interfering with the control of the ADC and DAC. In the end, the maximum sampling rate that could be achieved was approximately 16.7 Hz (a cycle consisting of sampling 13 ADC channels and sending out a value on the DAC).

To prevent aliasing, each transducer signal (i.e. position, velocity and acceleration, plus the ten load cell outputs) is passed through a low-pass filter prior to sampling. The filters are second order, with 3 dB attenuation at 6 Hz. The filter characteristics were selected to prevent aliasing while minimizing amplitude and phase distortion over the frequency range of interest (i.e. up to 5 Hz). The filters are a standard operational amplifier design (e.g. Webster, 1978).

To allow for smooth platform operation, the DAC output (i.e. the position command signal) is passed through a modified integrator. The integrator re-sets to the DAC value at each new sample point in the command signal. Between sample points, the integrator produces a straight-line interpolation.

There was concern that the maximum sampling rate of 16.7 Hz might be too slow to accurately measure the data. The problem was investigated by recording the data simultaneously on an FM tape recorder. The tape was then played back at a slower rate (one-eighth of the recording speed), passing the output through the anti-aliasing filters prior to digitization. In this way, the sampling rate was increased from 16.7 to 133.3 Hz and the signal bandwidth was increased from 6 to 48 Hz. For transient tests, comparison of the data obtained at the two different sampling rates showed substantial differences in the acceleration measurements, but not in the COP measurements. The transient acceleration power spectrum showed substantial energy at frequencies above 6 Hz, but little energy at frequencies higher than 15 Hz. For PRN tests, the

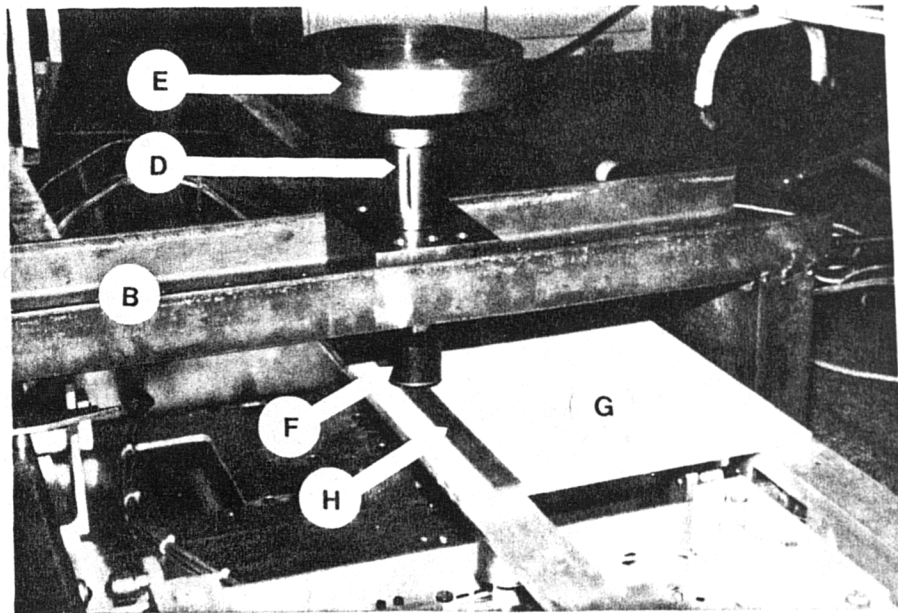
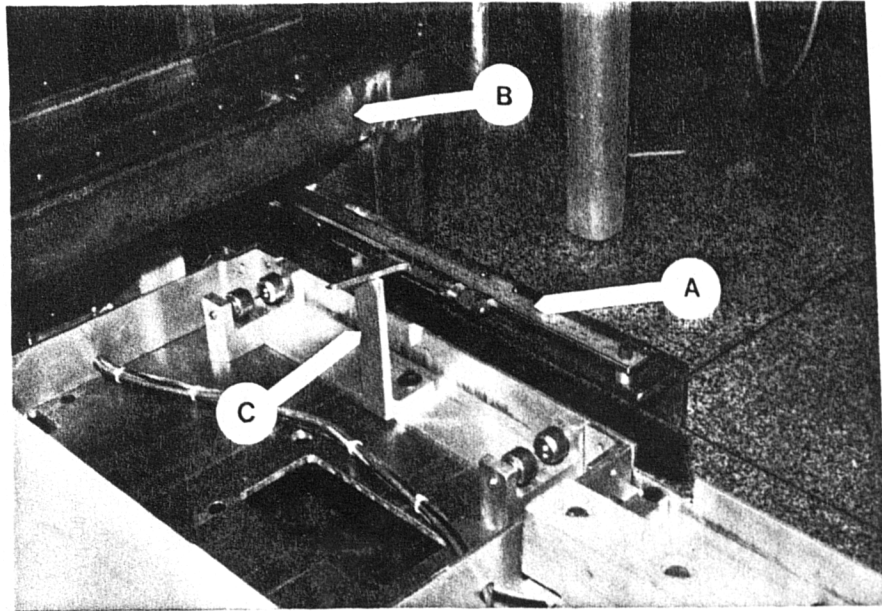


Fig 4.11 The calibration jig
(top shows vernier calipers, bottom shows post and platter assembly).

Legend: A = vernier calipers B = bridge,
 C = contacting post on carriage
 D = ball bushing supporting the vertical post
 E = platter F = ball transfer
 G = force plate H = sheet metal strip

differences between the results obtained at the two sampling rates were negligible.

To allow for more accurate measurements of acceleration during transient tests, a single-channel ADC (Burr-Brown, model ADC80AG-12; Burr-Brown, Tucson, Arizona) is used to sample the data at a rate of 100 Hz. The ADC is interfaced to an HP9845A microcomputer (Hewlett Packard, Palo Alto, California) via an anti-aliasing filter (second order, -3 dB at 15 Hz). Custom-written software synchronizes the sampling with the sampling performed by the VAX, and transfers the data (offline) from the HP9845A to the VAX.

4.5 CALIBRATION AND PERFORMANCE OF THE INSTRUMENTATION

4.5.1 The Calibration Jig

The calibration jig is shown in figure 4.11. The jig forms a bridge across the platform, at the midpoint of the range of travel, and is bolted to the base of the platform. On the jig are mounted: (1) a 36 cm vernier caliper, which is used to calibrate the linear potentiometer, and (2) a platter and post assembly, which is used to apply loads to the force plates at known locations.

4.5.2 Linear Potentiometer

The linear potentiometer was calibrated by moving the platform to various positions, measuring the actual position with the vernier caliper (which contacted a rigid post attached to the platform) and recording the potentiometer wiper voltage. The caliper could be mounted in either of two positions, allowing the potentiometer to be calibrated over the entire 60 cm range of motion. The resolution of the caliper was 0.02 mm.

A linear regression was performed on the recorded potentiometer voltages versus the measured position values, in order to determine the calibration coefficient. This regression yielded a correlation coefficient exceeding 0.999, indicating a very strong linear relationship. The accuracy of the calibration was tested by regressing actual versus calculated positions for a new series of data. This analysis yielded a regression slope of 1.0002, a y-intercept of 0.0106 mm and a correlation coefficient exceeding 0.999. The mean error of the measurements was 0.00362 mm

and the standard deviation of the error was 0.278 mm. Note that these errors are likely due, in large part, to the finite resolution of the ADC (see Section 4.4.3).

The natural frequency of the potentiometer mounting was calculated to be 210 Hz (based on the mass of the wiper shaft assembly and the stiffness of the arm used to couple the wiper shaft to the platform carriage), well above the 5 Hz operating bandwidth of the platform. Although the frictional drag of the wiper (4.5 N maximum) will cause the coupling to deflect, the resulting error in the position measurements was calculated to be less than 0.02 mm.

4.5.3 Force Plates

In the calibration jig, the vertical post is free to slide within a ball bushing. Because there is negligible friction, the vertical load applied to the force plate is equal to the weight of the mass supported on the platter, plus the weight of the platter and post. The lateral position of the post is adjustable. The fore-aft position, relative to the force plates, is adjusted by moving the platform carriage backward or forward underneath the calibration jig.

A hardened steel point is inserted at the bottom end of the post, to apply the load accurately at a desired point. This is used for static calibrations. Alternatively, a ball transfer can be inserted instead of the steel point. This allows for dynamic calibrations, where the platform carriage is controlled to move back and forth underneath the ball transfer. During the calibration and testing procedures, a thin sheet of steel is taped to the force plate, to prevent damage to the vinyl covering. The displacement of the load location relative to the force plate (i.e. the COP) is equal and opposite to the displacement of the platform carriage relative to the calibration jig. Thus, the actual COP is measured by the linear potentiometer.

In the static calibration, loads between 200 and 500 N were applied at various locations on each force plate. Linear regressions were performed against the measured load cell voltages, in order to determine the calibration coefficients for measuring

TABLE 4.2 - PERFORMANCE OF THE FORCE PLATES

TEST + LOADING ++			MEASUREMENT ERROR +++		
	LOAD (N)	POSN (mm)	VERTICAL FORCE (%) MEAN \pm SD	MOMENT (%) MEAN \pm SD	CENTRE-OF-PRESSURE (mm) MEAN \pm SD
<u>LEFT FORCE PLATE</u>					
static	++++	++++	0.453 \pm 0.311	0.081 \pm 0.960	0.026 \pm 0.386
PRN	203	0	1.42 \pm 0.353	-0.856 \pm 6.26	-0.937 \pm 0.777
	332	-100	-0.444 \pm 0.335	-0.722 \pm 4.59	-0.912 \pm 0.760
		0	0.813 \pm 0.268	-0.680 \pm 4.74	-0.831 \pm 0.395
		100	-6.62 \pm 0.154	-5.78 \pm 3.93	-0.733 \pm 0.143
	480	0	-0.069 \pm 0.148	-0.903 \pm 4.70	-0.897 \pm 0.257
pulse (+ve)	203	0	0.903 \pm 0.486	1.68 \pm 3.83	-1.19 \pm 0.693
	332	0	1.65 \pm 0.326	1.03 \pm 2.59	-0.026 \pm 1.16
	480	0	0.319 \pm 0.296	0.885 \pm 3.57	-0.815 \pm 0.550
pulse (-ve)	203	0	1.08 \pm 0.667	1.13 \pm 1.80	-0.703 \pm 0.764
	332	0	1.73 \pm 0.557	0.699 \pm 0.637	-0.988 \pm 0.956
	480	0	0.446 \pm 0.336	0.224 \pm 0.838	-0.769 \pm 0.471
<u>RIGHT FORCE PLATE</u>					
static	++++	++++	0.397 \pm 0.320	0.251 \pm 0.600	0.001 \pm 0.385
PRN	203	0	1.11 \pm 0.221	-1.31 \pm 7.26	-1.28 \pm 0.672
	332	-100	0.678 \pm 0.311	0.160 \pm 0.869	0.263 \pm 0.594
		0	0.498 \pm 0.285	0.622 \pm 1.95	0.555 \pm 0.363
		100	0.418 \pm 0.195	0.486 \pm 1.90	0.535 \pm 0.349
	480	0	0.354 \pm 0.127	-0.861 \pm 4.08	-0.672 \pm 0.377
pulse (+ve)	203	0	1.45 \pm 0.544	1.18 \pm 4.28	-1.04 \pm 0.580
	332	0	-0.058 \pm 0.357	0.475 \pm 0.683	0.291 \pm 0.651
	480	0	0.536 \pm 0.231	0.442 \pm 2.91	-0.611 \pm 0.596
pulse (-ve)	203	0	0.989 \pm 0.423	0.334 \pm 2.50	-0.945 \pm 0.438
	332	0	-0.202 \pm 0.340	0.647 \pm 2.34	1.00 \pm 0.396
	480	0	0.539 \pm 0.188	-0.138 \pm 1.58	-0.629 \pm 0.433

NOTE: + PRN = pseudorandom; pulse direction +ve forward, -ve backward; PRN amplitude was 0.3 m/s² (RMS); pulse amplitude was 1.0 m/s²;
 ++ POSN = medial-lateral position of load with respect to centre of force plate;
 +++ for static tests, error estimates based on 275 data points (5 loads at each of 55 locations); for dynamic tests, COP error estimates based on 4035 data points (PRN tests) or 18 data points (pulse tests); moment percentage error estimates omitted data points within 5 mm of force plate centre (resulting in 3900 data points for PRN tests, 18 points for pulse tests);
 ++++ loads and load locations same as for calibration (see text).

vertical force and the associated moment (the COP can then be calculated by dividing the moment by the force). The loads were applied at intervals of 30 mm in the a-p direction, over a range of 30 cm, and at intervals of 50 mm in the medial-lateral (m-l) direction, over a range of 20 cm. Thus, for each force plate, the calibration "grid" consisted of five a-p lines and eleven m-l lines. Five different loads were applied at each point, yielding a total of 275 data points for each force plate.

The horizontal-force load cells were calibrated using a system of wires, pulleys and weights to apply known horizontal loads to the force plates. Fourteen loads were applied, ranging from ± 20 N to ± 300 N.

The linear regressions of horizontal force, vertical force and moment (due to vertical force) versus the load cell voltages produced correlation coefficients exceeding 0.999, indicating very strong linear relationships.

A second set of static measurements was made to test the accuracy of the calibration coefficients. The procedures were identical to those described above. For the horizontal-force measurements, the mean errors were 1.53% and -0.53% and the error standard deviations were 2.76% and 4.04%, for the left and right force plates, respectively. The results for the vertical force measurements are listed in table 4.2 (see "static test").

The frequency response of each force plate was determined by controlling the platform carriage to move back and forth in a pseudorandom manner underneath the applied load. Using cross-spectral methods (see Section 6.5), the frequency response was estimated, treating the calculated COP as the output and the actual COP (as measured by the linear potentiometer) as the input. As illustrated in figure 4.12, the frequency response was flat, showing little gain or phase distortion in the measured COP over the frequency range tested (up to 5.0 Hz).

As discussed earlier, the platform was designed to minimize the need for inertial and shear-force corrections. Tests were performed to determine whether in fact these corrections could be neglected. Using the data from dynamic PRN tests with loads applied via the calibration jig, stepwise regressions were

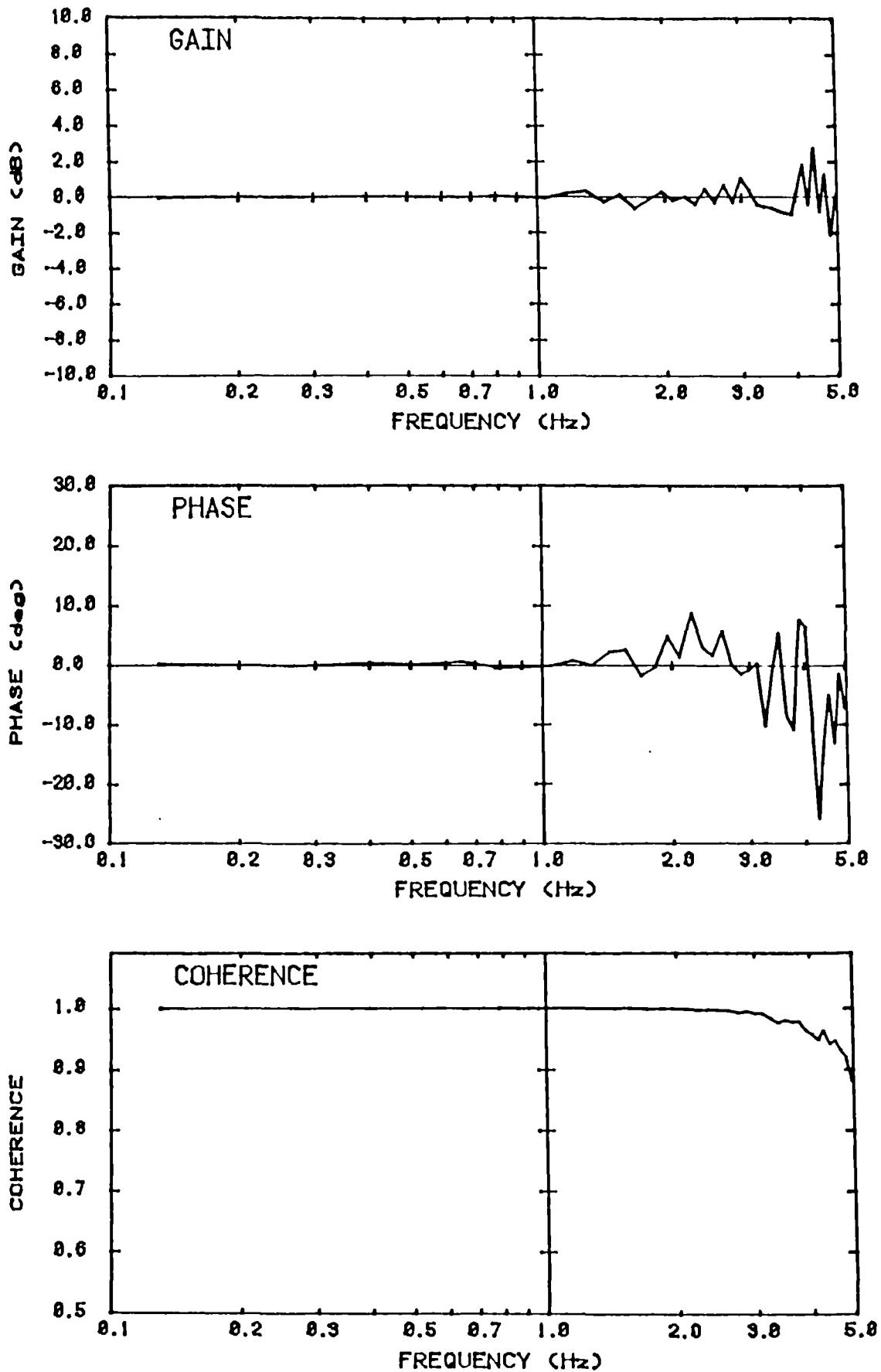


Fig 4.12 Frequency response of right force plate
 (input = actual centre-of-pressure location, output = measured
 centre-of-pressure location).

performed on the applied moment (due to the vertical force) versus the vertical-force load cell, horizontal-force load cell and accelerometer voltages. The applied moment was calculated as the product of the vertical force (i.e. the weight of the load) and the actual COP (recorded by the linear potentiometer). Note that this simple regression approach was possible only because the dynamics of the force plate measurements were negligible. It is assumed that the dynamics of the acceleration and shear-force measurements are also negligible (over the frequency range of interest).

Regression of the applied moment versus the vertical-force load cell voltages alone resulted in a very strong linear relationship, with a correlation coefficient exceeding 0.9999. Inclusion of the inertial and shear-force terms produced a negligible increase in the correlation coefficient. Furthermore, in analyzing an independent set of data, inclusion of these terms produced no reduction in the error between the actual and calculated moment values. These results indicate that the inertial and shear corrections were not significant relative to other sources of noise in the measurements.

In the calibration-jig tests, the applied shear load is small. To better simulate test conditions, PRN tests were performed carrying a deadweight load. In this situation, the applied moment is proportional to the platform acceleration. Stepwise regression of the accelerometer voltage (indicating the applied moment) versus the vertical-force and horizontal-force load cell voltages showed that inclusion of the shear force term in the regression produced negligible improvements in the regression error or in the correlation between the actual and calculated moment values.

In order to assess the accuracy of the calibration under actual test conditions, a set of dynamic performance tests was performed, using the calibration jig to apply loads with time-varying COP. Both PRN and transient platform motions were tested, with waveforms representative of the perturbations later used in the actual experiments. The loads ranged from approximately 200 to 500 N. Actual and measured values were compared for the vertical force, for the applied moment and for the COP. As above, the actual vertical forces were determined by

weighing the applied deadweight loads, the actual COP values were recorded by the linear potentiometer, and the actual moment was calculated as the product of the actual force and the actual COP. The "measured" COP, force and moment values were calculated from the vertical-force load cell measurements, using the results of the static calibration. For each test, the error means and standard deviations were calculated.

The results of the dynamic performance tests are summarized in table 4.2. It should be noted that some of the error can be attributed to errors in determining the actual values for COP and vertical load; therefore, the performance errors reported in the table are conservative estimates. The errors in the actual COP values are due primarily to "slop" in the calibration jig post-and-platter assembly, as a result of which the actual load location may differ from the linear potentiometer reading. This error is estimated to be approximately ± 0.5 mm. The accuracy of the vertical force values is limited by the accuracy and resolution of the scale used to weigh the deadweight loads. This error is approximately ± 1 N. The effect of the error in determining the true COP is disproportionately large at small values of the COP; therefore, in calculating the percentage error in the moment measurements, COP locations within 5 mm of the force plate centre were excluded.

4.5.4 Accelerometer

The calibration coefficient for the accelerometer was supplied by the manufacturer. The frequency response specification (0-200 Hz) far exceeds the operating bandwidth of the perturbation platform.

The static calibration of the accelerometer was checked using a modified phonograph turntable. The accelerometer was mounted at various known radii (using locating holes accurately machined on a mill) and the turntable was rotated at various constant speeds (33.3, 45 and 78 RPM). Average angular velocity during each revolution was measured by using an optical sensor to time the revolutions. Knowing the radius and rotational speed, the centripetal acceleration could then be calculated.

Based on applied accelerations ranging from 0.3 to 5.0 m/s², regression between measured and actual accelerations showed a correlation coefficient of 0.997. The error appeared to be relatively independent of the acceleration level, with a mean value of 0.035 m/s² and a standard deviation of 0.062 m/s². This error estimate is conservative, because much of the error is likely an artifact of the testing procedure itself. In particular, error can be attributed to fluctuations in the turntable speed and the accelerometer inclination occurring during each turntable revolution.

The accuracy of the accelerometer under dynamic conditions was checked by double-differentiating the platform displacement measured by the linear potentiometer and comparing this to the accelerometer signal. The double-differentiation was performed using an analog circuit. Using data from a sinusoidal test at 0.5 Hz (amplitude = 0.5 m/s²), regression between the accelerometer signal and the double-differentiated position signal produced a correlation coefficient of 0.977. As in the turntable tests, the error appeared to be relatively independent of the acceleration level. The mean error was 0.0051 m/s² and the error standard deviation was 0.050 m/s². Similar results were obtained in tests at 1 and 5 Hz. Even though the position signal was low-pass filtered, there was still substantial amplification of the higher-frequency noise, as a result of the double-differentiation. Because of this source of inaccuracy in the testing procedure, the above error estimate is conservative.

4.6 SAFETY FEATURES

A safety handrail is provided so that subjects can stop themselves from falling, should they lose their balance. In the event that a fall does occur, the platform is designed to minimize the risk of sustaining a serious injury. The plywood cover prevents contact with the hard surfaces, sharp edges, and rotating components of the drive train and supporting structures. Polyurethane foam pads provide cushioning and limit the distance of any fall.

There are a number of automatic safety features that will shut

down the platform should a malfunction occur. If the carriage begins to move beyond the allowed range of travel, it will activate a set of photosensor detectors, which will turn off the motor. A backup system of mechanical switches is also provided, in case the photosensors fail. Viscoelastic foam (Temperfoam) pads are provided to cushion the impact of the carriage with the mechanical end-stops. The maximum velocity of the platform is limited by a circuit which monitors the tachometer output and shuts down the motor should the pre-set limit be exceeded.

In addition to these automatic safety features, there are three shutoff switches that can be activated manually, at any time, to shut off the motor. One of these switches is connected to the amplifier via a long cable, allowing the operator to carry this switch in his/her hand at all times.

The software that controls the platform operation is designed so that the actual position of the platform is measured and the position command signal is set to this value before the operator is instructed to turn on the motor. This prevents the platform from suddenly jumping from its existing position to another position when the motor is turned on. During the initialization procedure, the position signal is checked for unrealistic values that might indicate malfunction of the position transducer.

There is no risk of electrical shock to the subject. The motor and amplifier are isolated from the platform by the nonconducting element in the flexible coupling. The plywood cover prevents the subjects from contacting the motor itself; the amplifier is at a remote location. All of the instrumentation signals passing from the platform involve small DC voltages and therefore present no risk. Even if this were not the case, the subject is insulated from any possible shock, because of the vinyl and polyurethane coverings on the force plates and handrails, respectively.

CHAPTER 5. SELECTION OF THE PERTURBATION PARAMETERS

5.1 INTRODUCTION

As discussed in Chapter 3, the balance testing methodology requires the identification of a linear, time-invariant, input-output model of the posture control system. The "system identification" is achieved by applying a measurable postural perturbation (the input) to the subject and measuring the resulting centre-of-pressure (COP) displacement (the output).

The particular perturbation signal used in the balance test may have a substantial influence on the accuracy of the system identification and on the interpretation of the results. As was illustrated in table 4.1 (in Chapter 4), a wide variety of different perturbation signals has been used by various investigators. Andres and Anderson (1980) pointed out the need for accurate quantification of perturbation signals; however, the criteria by which perturbation parameters are selected have not been adequately addressed in the literature.

Pertinent parameters include waveform, power spectrum, bandwidth, amplitude and test duration. In this chapter, the selection of these parameters is discussed in the light of general requirements for persistent excitation, accurate identification, stationarity, and subject safety and tolerance. Also discussed are pilot experiments which were performed to resolve specific issues.

5.2 GENERAL REQUIREMENTS

5.2.1 Persistent Excitation

A minimum requirement for system identification is that the input signal "persistently excites" the dynamics of the system over the measurement period (Isermann, 1980). This means that the frequency content of the input must exercise the system over the range of frequencies for which the model is needed.

5.2.2 Accuracy of Identification

Selection of appropriate input parameters can help to minimize random error and bias in the model estimates. In fact, it is possible to design optimal input signals that minimize model errors, given constraints on the measurement time, the sampling

rate and the amplitude and power characteristics of the input and output signals (Goodwin and Payne, 1977). However, in general, the design of truly optimal input signals requires detailed prior knowledge of the system model and noise characteristics (Box and Jenkins, 1976), information which is generally not available *a priori*.

5.2.3 Stationarity

Identification of a time-invariant model requires that the characteristics of the system do not change over the measurement period, that is, the system must be stationary. The stationarity of the posture control responses will be affected by fatigue and by changes in balancing strategy (e.g. postural synergy, body configuration, tonic postural "set", etc). Fatigue will become a factor if the duration of the test is excessively long. In order to minimize adaptive changes, the test perturbation must be unpredictable.

5.2.4 Human Tolerance and Safety

The test perturbation must be safe, that is, the risk of falling must be minimized. The subjects' perception of the risk must also be minimized, since subject apprehension could result in response strategies that would be unlikely to occur in everyday life. For example, subjects might "brace" themselves through increased co-contraction of antagonist muscle groups. Discomfort is another factor that could influence the response. High frequency vibration can induce discomfort, as can excessively long measurement periods.

5.3 PERTURBATION PARAMETERS

5.3.1 Waveform

As discussed in Chapter 3, the test perturbation is a continuous random or pseudorandom waveform. Although random waveforms could conceivably have the advantage of greater unpredictability, pilot repeatability experiments (detailed in Appendix C) provided no evidence of increased adaptation in pseudorandom tests. None of the six subjects tested exhibited any significant test-to-test trends in the balance test results, within

a given testing session, regardless of which type of waveform was used ($p > 0.05$).

In general, random waveforms require longer measurement times in order to "average out" the inherent statistical variability, compared to periodic pseudorandom waveforms (Gibb, 1982). As a further disadvantage, the use of random waveforms leads to "leakage" distortion, associated with the truncation of the signals into finite time records. Although leakage can be reduced by multiplying the data by an appropriate window function, the windowing will in itself introduce some distortion. In contrast, pseudorandom waveforms are "self-windowing", in that the period of the waveform can be selected to equal the data record length, thereby eliminating any leakage (Gibb, 1982).

If the system has a significant degree of nonlinearity, then the resulting distortion products can create random error and/or bias in the linearized model estimates. The bias error may be particularly severe for certain types of pseudorandom inputs. For pseudorandom inputs, nonlinearities generate harmonics in the response at frequencies that are integer multiples of the frequency components in the input signal. In addition, intermodulation terms are generated at frequencies that are sums and differences of the input frequencies (Gibb, 1982). Because the pseudorandom input is periodic, the harmonic and intermodulation terms in the response are also periodic and do not tend to "average out", as in the case of a random input. As a result, the linear model estimates at the harmonic and intermodulation frequencies are biased.

The bias error can be reduced by using pseudorandom waveforms in which none of the frequency components are integer multiples of other frequencies in the signal (van Lunteren, 1985). By restricting the analysis to those frequencies present in the input, harmonic distortion is prevented from affecting the results. In addition, because of the reduced number of frequency components in the input signal, intermodulation distortion is reduced. In practice, the same benefits can be derived by stipulating that the input frequencies include no small-integer multiples, since the higher harmonics in the output of a nonlinear system tend to be small in amplitude (Ogata, 1970b). Note that caution must be

exercised in using "nonharmonic" waveforms, as the decreased frequency resolution may allow sharp peaks or troughs in the system frequency response to pass undetected.

Pseudorandom waveforms can be generated in a number of forms. Maximum-length binary signals are widely used in system identification applications (Graupe, 1976); however, they have the disadvantage that the shape of the power spectrum cannot be changed readily (Eykhoff, 1974). Moreover, the frequency components in these signals are integer multiples. Greater flexibility is attained by using a signal composed of a sum of a number of sinusoids with random phase angles. Any desired (discrete) power spectrum can be achieved through appropriate selection of the amplitudes and frequencies of the sinusoids (van den Bos and Krol, 1979).

The issues associated with the use of pseudorandom waveforms are discussed in greater detail in Appendix B.

5.3.2 Power Spectrum

The power spectrum specifies the distribution of the perturbation power over the selected frequency range. In general, it is desirable to increase the power at frequencies where the system frequency response is low, so as to increase the signal-to-noise ratio in the response measurements at those frequencies. Ideally, an optimal input power spectrum could be selected so as to compensate for the system frequency response, yielding equal signal-to-noise ratios at all frequencies in the measured response. In practice, however, this can only be achieved using an iterative approach, since optimal input design requires *a priori* information about the system characteristics.

5.3.3 Bandwidth

The frequency content of the perturbation signal must allow for persistent excitation, that is, it must exercise the posture control system over the range of frequencies needed for the model. Here, the model is to be used to predict the response to transient perturbations simulating slips, trips, missteps, jostles and self-initiated "activities of daily living" (ADL) displacements. Unfortunately, the frequency content of these perturbations cannot

be predicted *a priori*. An idealized transient perturbation, i.e. a pulse, has a power spectrum that is flat from 0 Hz up to an upper frequency that depends on the duration and shape of the pulse (e.g. Doebelin, 1980).

Five seconds is a conservative estimate for the maximum duration of the balancing responses to typical fall-provoking perturbations. Since the components of the posture control system with settling times greater than 5 s (i.e. time constants $> \sim 1.7$ s) will be too slow to make a significant contribution to the balance recovery, there is no need for the balance test to excite and identify these components. On this basis, 0.1 Hz ($\sim (1/1.7)$ rad/s) is a reasonable lower limit for the frequency content of the test perturbation. As was shown in table 4.1 in Chapter 4, other investigators have typically used a lower frequency limit of 0.1-0.2 Hz, although values as low as 0.06 Hz have been reported. Inverted pendulum simulations suggested that a lower limit of 0.1 Hz would be adequate to identify a flat low-frequency asymptote in the frequency response (see Appendix A.3.2).

There is reason to avoid an unnecessarily small lower frequency limit. Nashner (1970, 1971) has suggested that the vestibular otoliths may predominate at frequencies below 0.1 Hz; if this is true, then perturbation energy at frequencies lower than 0.1 Hz might tend to accentuate the incongruence (inherent to the balance test) between the otoliths and the other sensory modalities (see Sections 3.2.3 and 8.6.1). Note also that an overly small frequency limit will needlessly increase instrumentation costs by increasing the range of motion requirements for the perturbation platform (assuming a flat acceleration spectrum).

For the upper frequency limit, most investigators have used a frequency of 1-3 Hz, although values as high as 5 Hz have been reported. Typically, results show a decrease in response with increasing frequency. For example, data from Ishida and Imai (1980) show attenuation of approximately 20 dB as the frequency increases from 0.2 Hz to 2 Hz (using a platform acceleration input and an output proportional to COP displacement). Assuming this "roll-off" continues at higher frequencies, the responses at

frequencies much greater than 2 Hz will likely be too small to be of major functional significance. In general agreement with these findings, inverted pendulum simulations predicted that the COP response will be insignificant at frequencies exceeding 5 Hz (see Appendix A.3.2).

In selecting the upper frequency limit, subject tolerance must also be considered, since exposure to high frequency vibration can lead to discomfort and fatigue. The poorest tolerance is generally in the range from 4 to 8 Hz (Chaney, 1965).

An upper frequency limit of 5 Hz would seem to be a reasonable compromise between the need to identify the predominant dynamic characteristics of the posture control system and the need for subject tolerance. The extra instrumentation costs required to measure accurately the small responses at higher frequencies and to generate higher frequency perturbations do not appear to be justified.

5.3.4 Amplitude

Selection of the perturbation amplitude is governed by three considerations: (1) signal-to-noise ratio in the measurements of the input and output, (2) linearity of the model, and (3) subject safety and tolerance. The need to measure signals accurately in the presence of measurement noise calls for large input amplitudes, whereas safety and tolerance concerns require small amplitudes. Linear modelling is best served by moderate amplitudes. If the amplitude is too small, then certain sensory components may not be stimulated, due to threshold effects. Alternatively, if the amplitude is too large, then large-amplitude saturation-like nonlinearities may be excited. In general, a linear model will only apply over a limited range of perturbation amplitudes.

With random and pseudorandom waveforms, the particular "realization" of the waveform can be selected so as to minimize the "peak factor", the ratio of the peak amplitude to the root-mean-square (RMS) amplitude (van den Bos, 1974). This allows for maximum energy transfer to the system, within the constraints on peak amplitude imposed by safety considerations and the need to avoid nonlinear saturation effects.

5.3.5 Duration

In order to minimize random error in the model estimates, the measurement time must be maximized. However, in a practical experiment, the measurement time will be limited by subject fatigue and tolerance.

5.4 EXPERIMENTAL METHODS USED IN THE PILOT TESTS

Pilot experiments were performed to obtain quantitative data that would aid in the selection of the perturbation waveform, power spectrum, bandwidth, amplitude and duration. These experiments were performed using the perturbation platform described in Chapter 4. Thus, the test perturbation was an anterior-posterior translational platform acceleration, with a visual field that moved with the platform. A linear nonparametric transfer function (or frequency response) model of the posture control system was identified, treating the platform acceleration as the input and the COP displacement as the output. Although the model could be determined equally well using platform position or velocity as the input variable, acceleration has the clearest physical interpretation, in that the destabilizing moments (acting on the body segments) that result from the platform motion are directly related to the platform acceleration (e.g. see Appendix A.1.1).

5.4.1 Subjects

The eight subjects (four males and four females) who participated in the experiments were all healthy, normal adults with no obvious neurological or musculoskeletal deficits. The subjects ranged in age from 19 to 40.

5.4.2 Test Procedure

For each test, the subject was instructed to stand relaxed, with feet comfortably spaced and arms at sides, and to look straight ahead. Headphones were used to listen to "Muzak"® (i.e. bland monotonous music) so as to mask any auditory cues from the motor and to distract the subject from consciously modifying his/her motion. Prior to the first test, the outlines of the feet were traced, to allow changes in foot position to be detected and to allow the same positioning to be repeated in subsequent tests.

Tests varied from 3 to 5 minutes in duration. The platform motion was controlled to start and end gradually, with no sudden changes in acceleration. During the tests, the subjects were observed to determine whether they grabbed the handrail, waved their arms or moved their feet. At the end of each test, the subjects were allowed a 2-3 minute seated rest. The maximum duration of any single testing session was 1.5 hours.

5.4.3 Protocol

Five subjects were each tested using three different waveforms: (1) a pseudorandom input composed of a sum of harmonic sinusoids (HPRN), (2) a "nonharmonic" pseudorandom input composed of a sum of sinusoids, none of which were small-integer multiples (NHPRN), and (3) a bandlimited and amplitude-limited random input approximating Gaussian white noise (RAN). Subjects were tested three times for each waveform, in random order.

To construct the RAN waveform, zero-mean Gaussian white noise (generated by applying a normalizing transformation to the output of a multiplicative congruential random number generator) was "clipped" (limiting the amplitude to ± 3 standard deviations) and then bandpass filtered, with cutoffs (-1 dB) at 0.1 and 5.0 Hz (-30 dB rejection at 0.08 and 5.3 Hz). The two pseudorandom signals both had a period of 15.36 s, and were constructed as a sum of equal-amplitude sinusoids having random phase angles uniformly distributed between 0 and 360 degrees. The frequencies of the sinusoids ranged from 0.13 to 4.95 Hz. The HPRN signal comprised 76 sinusoids, spaced at equal frequency intervals of 0.065 Hz. The NHPRN version comprised 15 sinusoids, at the following frequencies: 2, 3, 5, 8, 11, 14, 18, 21, 25, 29, 35, 43, 51, 61 and 76 cycles per 15.36 s period. The three perturbation waveforms all had the same flat acceleration power spectrum envelope (RMS amplitude = 0.2 m/s^2 for HPRN and RAN, 0.09 m/s^2 for NHPRN; peak factor ≈ 3.8). The duration of each waveform was 5 minutes.

Three of the five subjects were also tested using an HPRN waveform with a period of 7.68 s. This waveform comprised 40 sinusoids ranging from 0.13 Hz to 5.2 Hz, spaced at equal frequency intervals of 0.13 Hz. The amplitude characteristics were similar to those of the longer-period HPRN waveform.

Three subjects were each tested using three different input power spectra: (1) flat acceleration power spectrum (ACC), (2) flat velocity power spectrum (VEL), and (3) flat position power spectrum (POS). Subjects were tested three times for each spectrum, in random order. All three spectra used a "nonharmonic" pseudorandom waveform, with the same frequency content as the NHPRN signal described above. The peak factors of the different spectra were approximately equal (2.3 for ACC, 2.6 for VEL, 2.5 for POS). For each spectrum, the amplitude was adjusted approximately to the upper limit of the subject's tolerance, that is, the highest amplitude at which the subject could balance without grabbing a handrail, waving his/her arms or moving his/her feet. The duration of each test was approximately 3 minutes.

Three subjects were tested at different amplitudes using the NHPRN waveform. Each subject was tested three times at each of five RMS amplitudes, in random order: 0.05, 0.1, 0.15, 0.2 and 0.25 m/s². (None of the subjects were able to withstand amplitudes larger than 0.25 m/s² without moving their feet or grabbing a handrail.) The duration of each test was approximately 3 minutes.

5.4.4 Analysis

Treating the platform acceleration as the system input and the COP displacement as the output, the data were fitted with a nonparametric linear transfer function (or frequency response) model. The method of "averaging periodograms" was used (Bendat and Piersol, 1971b and 1980). First, the data were divided into segments of equal length, discarding the first segment so as to eliminate any transient response. Then, for each segment, the input-output cross-spectrum, the input auto-spectrum and the output auto-spectrum were estimated. These spectral estimates were averaged, and the frequency response was estimated as the ratio of the average cross-spectrum divided by the average input auto-spectrum. The coherence function was estimated as the squared magnitude of the average cross-spectrum divided by the product of the input and output auto-spectra.

The spectral estimates were made using a Fast Fourier Transform (FFT) algorithm (Carter and Ferrie, 1979; Rabiner et al,

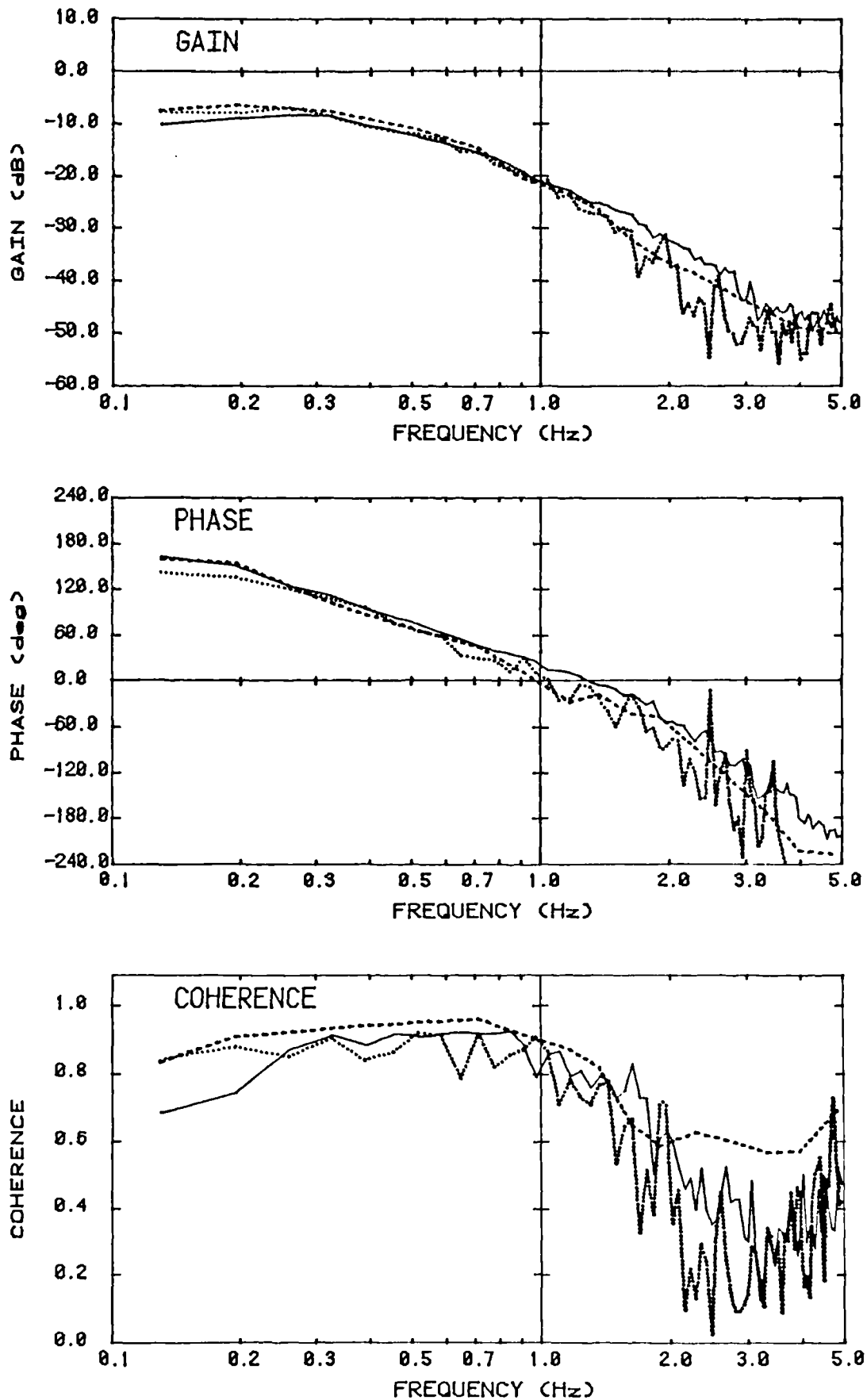


Fig 5.1 Comparison of waveforms.

Legend: solid line - random (RAN)
dotted line - harmonic pseudorandom (HPRN)
dashed line - nonharmonic pseudorandom (NHPRN)

1979). The FFT "length" was chosen to be 256 points, resulting in a segment duration of 15.36 s and a spectral resolution of 0.065 Hz. To reduce the variance of the estimates, segments were overlapped by 50% (Welch, 1967). In tests using random inputs, the data in each segment were windowed (using a Hamming window) in order to reduce the "leakage" (i.e. truncation distortion) (Gibb, 1982). This was not necessary for the pseudorandom inputs. Since the segment length was chosen to equal the period of these inputs (15.36 s), leakage could not occur. Nonetheless, in the comparisons of the random and pseudorandom inputs, the pseudorandom data were analyzed both with and without windowing, to ensure that any observed differences were not due to the windowing itself. In the remaining analyses, the pseudorandom data were not windowed.

5.5 RESULTS AND DISCUSSION

5.5.1 Waveform

It is tempting to compare results obtained using different waveforms on the basis of the coherence function, as the coherence is supposed to indicate the "goodness-of-fit" of a noise-free, linear, single-input/single-output model. However, for nonlinear systems, this interpretation of the coherence function applies only to random inputs (see Appendix B). For NHPRN inputs, reduction in coherence (from unity) indicates approximately the amount of "noise" in the output measurements (due to measurement noise and/or unmeasured inputs that are uncorrelated with the measured input), but does not reflect the linearity of the system. For HPRN inputs, the coherence cannot be interpreted in a useful way.

Typical results are shown in figure 5.1. The large frequency-to-frequency fluctuations in the HPRN frequency response estimate are actually bias errors due to the periodic distortion generated by nonlinearities in the system. The RAN estimate is much smoother, but still appears to exhibit somewhat greater variability than the NHPRN estimate. The variability is due in part to the randomness inherent to the RAN input. The lower coherence of the RAN estimate, compared to the NHPRN estimate, suggests that there is also substantial nonlinear distortion in the RAN model estimate. The frequency response derived using the RAN

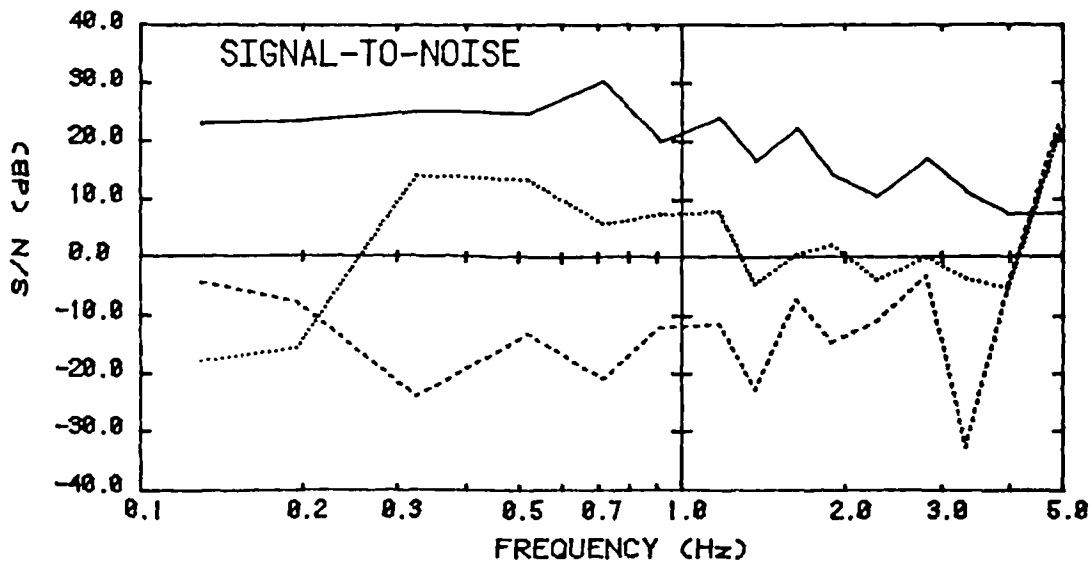
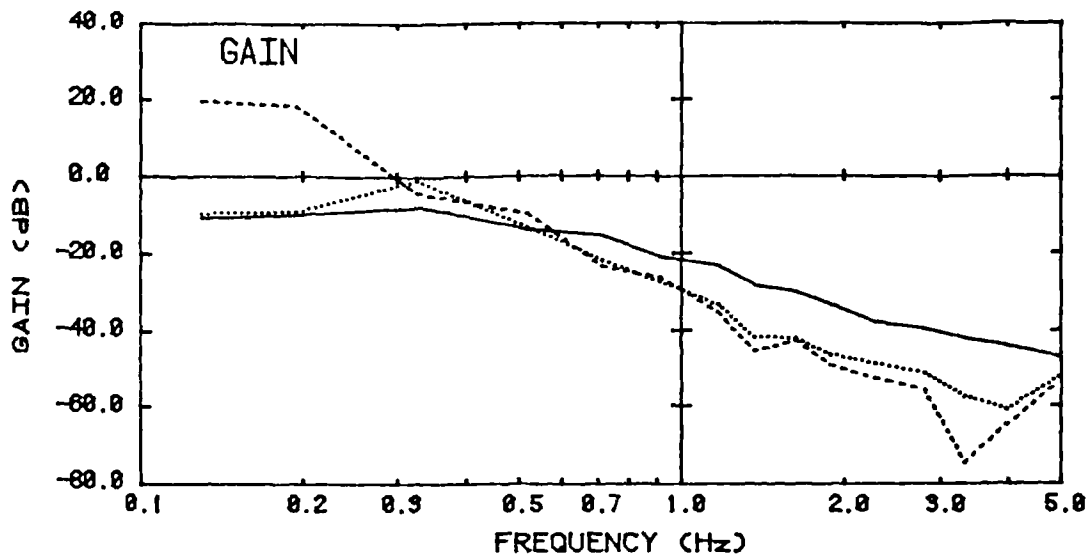
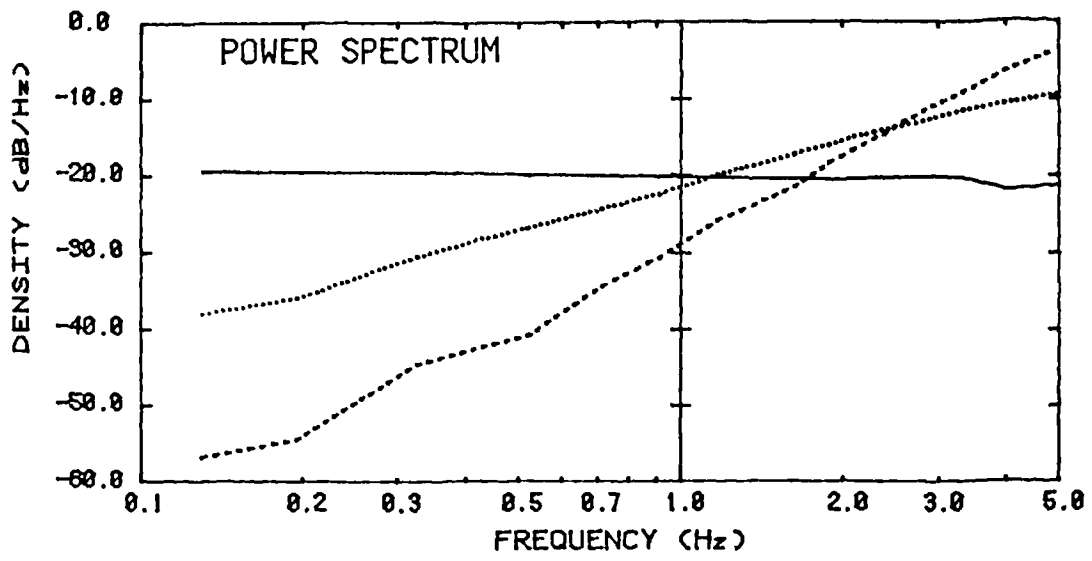


Fig 5.2 Comparison of power spectra (NHPRN waveform).

Legend: solid line - flat acceleration (ACC)
dotted line - flat velocity (VEL)
dashed line - flat position (POS)

Note: input power spectra are in terms of acceleration (m/s^2)

input exhibits no sharp peaks or troughs; therefore, the reduced frequency resolution of the NHPRN input is not a problem.

Some subjects felt that they were able to recognize and predict certain features of the smaller-period HPRN waveform, particularly when made aware that the perturbation was in fact periodic. Increase in the period to 15.36 s seemed to eliminate the predictability, in both the HPRN and NHPRN waveforms.

5.5.2 Power Spectrum

Figure 5.2 shows typical results obtained using the ACC, VEL and POS input power spectra.

Because a NHPRN waveform was used, reductions in coherence (from unity) indicate approximately the relative amount of "noise" in the output. The signal-to-noise ratio, $S/N(f)$, can be calculated from the coherence (γ^2), as follows: $S/N(f) = \gamma^2(f) / (1 - \gamma^2(f))$, where f denotes frequency. Compared to the ACC spectrum, the VEL spectrum resulted in markedly reduced S/N over the entire frequency range, with the exception of the highest frequency (4.95 Hz). The POS spectrum also yielded high S/N at the highest frequency, but the S/N was extremely low over the rest of the frequency range (in fact, the S/N was less than 0 dB, indicating that the noise was larger in magnitude than the signal).

Compared to the ACC spectrum, the VEL and POS spectra were perceived by the subjects to be very uncomfortable.

5.5.3 Bandwidth

The frequency range used in the experimental tests was approximately 0.1 to 5.0 Hz. As is evident in figure 5.1, the lower frequency limit was sufficiently small to allow a low-frequency asymptote of the frequency response gain to be determined. At the high-frequency limit, there was sufficient attenuation (-40 dB) to define a high-frequency asymptote.

5.5.4 Amplitude

Typical results are shown in figure 5.3 (data shown are for one subject, three tests at each amplitude). In raising the amplitude from 0.05 to 0.1 m/s², substantial changes in the

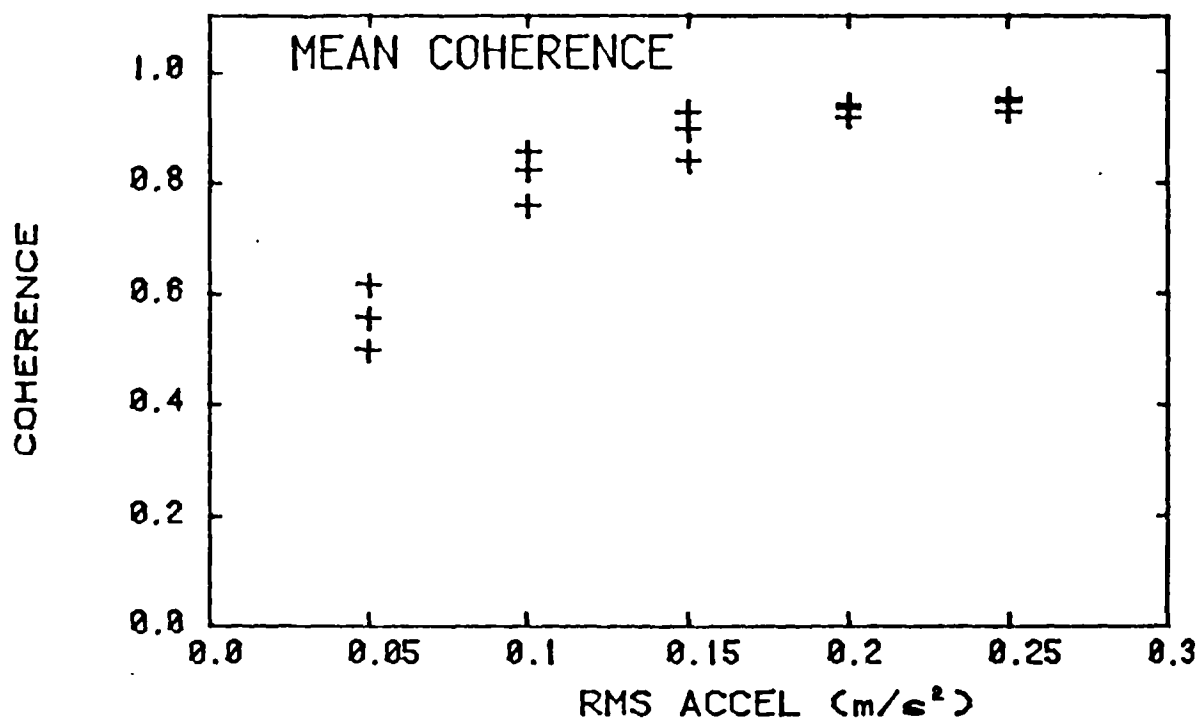
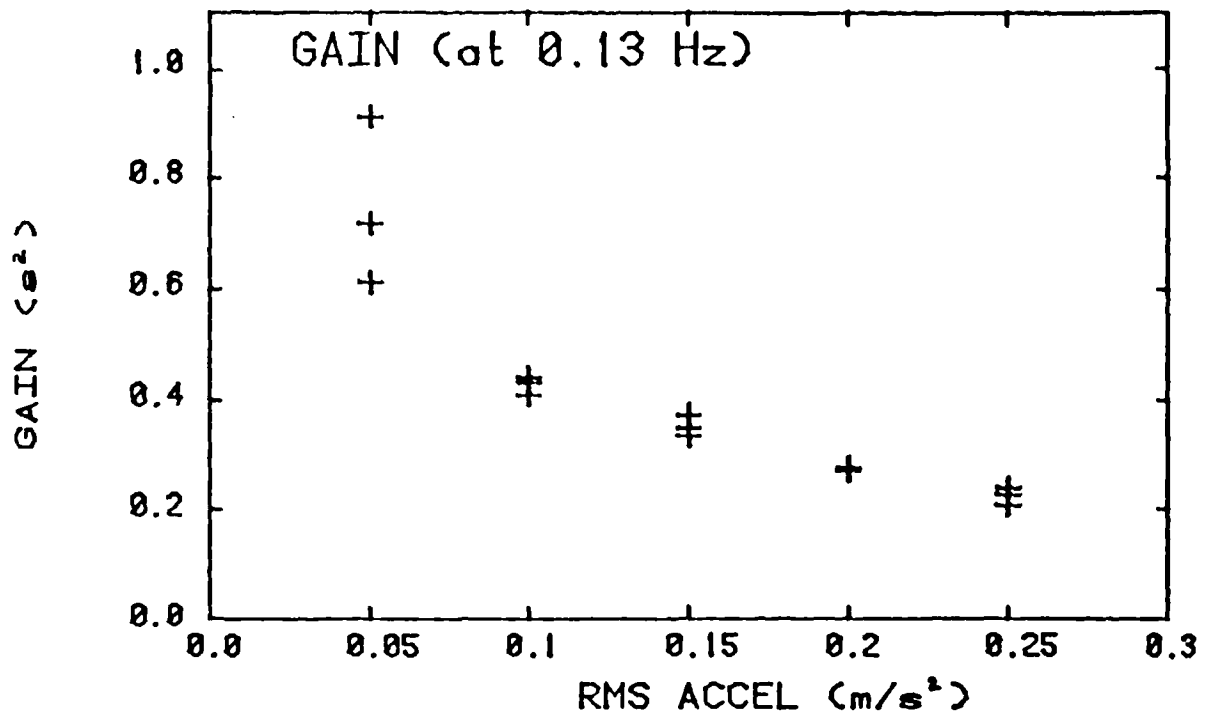


Fig 5.3 Effect of input amplitude
(NHPRN waveform; same subject, three tests at each amplitude).

frequency response (as quantified by gain values at 0.13 Hz) and improvements in mean coherence occurred; however, there was relatively little change as the amplitude was increased further. In general, the best amplitude will depend on the waveform and its frequency content. The optimal amplitude may also depend on the postural stability of the subject, although the healthy young adults tested here all showed similar results. For the NHPRN waveform and healthy young adults tested here, the RMS amplitude should exceed 0.05 m/s^2 in order to achieve acceptable signal-to-noise ratios in the response measurements. RMS amplitudes exceeding 0.25 m/s^2 are likely to result in loss of balance.

5.5.5 Duration

The maximum test duration of 5 minutes was used in testing five subjects. All five subjects were able to tolerate this duration. Moreover, this duration was sufficient to achieve reasonably accurate results. In the experimental analysis, the 5 minutes of data were divided into 19 segments of 15.36 s duration. Using 50% overlap of adjacent segments, a total of 37 segments was obtained. According to approximate formulae derived for nonparametric frequency response estimates and random Gaussian inputs (Doebelin, 1980), averaging over 37 segments of data will yield gain estimates accurate to within 10% with 95%-probability, assuming a coherence of 0.8 or greater. The actual variance in the estimates may be slightly greater than this because overlapped data segments were used (Welch, 1967).

For pseudorandom inputs, the required duration will be less. Using a random input, some of the variance in the frequency response estimates is due to the inherent variability in the input signal. For a deterministic pseudorandom input, the variance is less (due only to random noise and unmeasured inputs) and therefore can be reduced to an acceptable level by averaging a smaller number of data segments.

Lacking a general method for estimating the required duration for pseudorandom inputs (van Lunteren, 1979b), the effects of changes in duration were assessed experimentally, in a qualitative

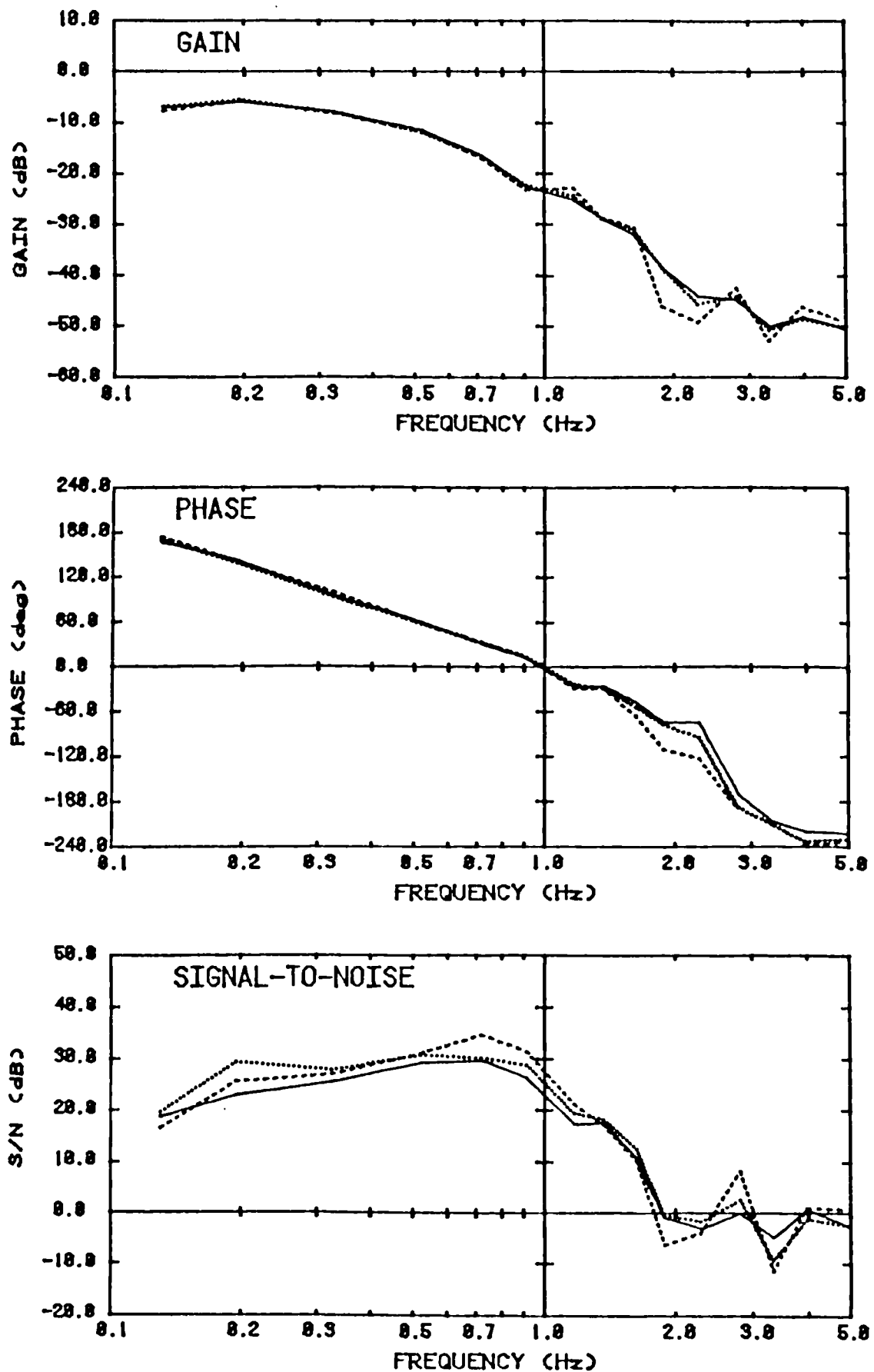


Fig 5.4 Effect of changes in duration (NHPRN waveform).

Legend: solid line - 5 minutes
dotted line - 2.5 minutes
dashed line - 1.25 minutes

manner, using the data from the waveform-comparison tests. Frequency response estimates were made using all 5 minutes of the data, the first 50% of the data and the first 25% of the data. As illustrated in figure 5.4, reduction to 50% typically resulted in only small changes in the estimates (maximum change in gain < 2 dB, maximum change in phase angle < 10 degrees), whereas reduction to 25% resulted in substantially larger changes. In terms of the signal-to-noise ratio (S/N), the effects of the reductions in test duration were relatively small, and the changes that did occur were not consistent, with increases in S/N at some frequencies and decreases at other frequencies. Note, however, that caution must be exercised in interpreting the S/N results, as the accuracy of the S/N estimates is dependent on the test duration.

In order to assess whether the 5-minute duration was too long and thereby causing systematic changes in the system characteristics (e.g. due to fatigue or adaptation), each test was analyzed for stationarity. The output data were divided into nineteen 15.36 s segments, the variance of each segment was calculated and a "runs test" (Bendat and Piersol, 1971a) was performed on the variance estimates. The data for the HPRN and NHPRN inputs each showed significant nonstationarity (at $\alpha = 0.05$) in only one of 15 tests. None of the 15 RAN tests showed significant nonstationarity.

5.6 CONCLUSIONS

(1) A "nonharmonic" pseudorandom perturbation and a random perturbation both yielded more accurate identification of a linear transfer function model than a harmonic pseudorandom signal. For a given measurement duration, the "nonharmonic" pseudorandom waveform is expected to yield more accurate estimates than the random waveform. In the pseudorandom signals, a period of 15.36 s seemed to be sufficiently long to make the perturbation unpredictable.

(2) A flat acceleration power spectrum yielded higher signal-to-noise ratios and was better tolerated by subjects, compared to spectra that were flat in velocity or position. A bandwidth of approximately 0.1-5.0 Hz was adequate to identify a low- and a high-frequency asymptote in the frequency response, and

was tolerated well by subjects (using a flat acceleration spectrum).

(3) The optimal amplitude will depend on the waveform, and may also depend on the characteristics of the subject population. For the "nonharmonic" pseudorandom waveform and healthy young adults tested here, it was determined that the RMS amplitude should be greater than 0.05 m/s^2 , but should not exceed 0.25 m/s^2 .

(4) Using a random input, a test duration of 5 minutes yielded acceptably accurate results, but was not so long as to cause adaptive or fatigue-related nonstationarity, at least in healthy young adults. For pseudorandom inputs, reduction of the duration to 2.5 minutes did not appear to substantially change the results.

CHAPTER 6. EXPERIMENTAL AND ANALYTICAL METHODS

This chapter describes the details of the experimental and analytical methods. The underlying objectives of the experiments were outlined in Chapter 1, and the general rationale for the balance testing methodology was developed in Chapter 3. The rationale underlying many of the details of the testing procedure and protocol is explained in Section 8.1.

6.1 TEST PERTURBATIONS

The perturbation used in the balance test was a pseudorandom (PRN) or random (RAN), anterior-posterior (a-p), translational acceleration of the platform on which the subject stood. A visual surround moved with the platform.

The PRN acceleration signal had a period of 15.36 s, and was constructed as a sum of 15 sinusoids of equal amplitude and random phase angle. The frequencies ranged from 0.13 to 4.95 Hz (2, 3, 5, 8, 11, 14, 18, 21, 25, 29, 35, 43, 51, 61 and 76 cycles per 15.36 s period). The phase angles were uniformly distributed between 0 and 360 degrees, and were generated using a multiplicative congruential random number generator. The duration of the PRN waveform was 185 s. See figure 7.1 (in Chapter 7) for an example plot of the acceleration waveform measured during an actual PRN test.

The RAN waveform was constructed by bandpass filtering a signal approximating zero-mean Gaussian white noise. The Gaussian noise was generated by applying Marsaglia's polar transformation (Kennedy and Gentle, 1980) to the output of a multiplicative congruential random number generator. The noise was filtered digitally, with bandpass cutoffs (-1 dB) at 0.1 and 5.0 Hz and -30 dB rejection at 0.08 and 5.3 Hz. Prior to filtering, the random noise was "clipped", limiting the amplitude to ± 3 standard deviations. The duration of the RAN waveform was 310 s.

The PRN and RAN signals were scaled to yield root-mean-square (RMS) acceleration amplitudes of 0.075, 0.10 and 0.15 m/s². The peak factors (ratios of peak amplitude to RMS amplitude) were minimized by using a trial-and-error approach to determine appropriate "seed" values for the random number generator used in generating the waveforms. The peak factor was 3.28 for the RAN

TABLE 6.1

CHARACTERISTICS OF THE NORMAL SUBJECTS

	MALES		FEMALES	
	MEAN \pm SD	RANGE	MEAN \pm SD	RANGE
YOUNG NORMALS (16 males, 16 females)				
age (years)	24.2 \pm 5.2	20 - 37	26.1 \pm 5.8	20 - 40
height (m)	1.76 \pm 0.079	1.63 - 1.93	1.63 \pm 0.101	1.44 - 1.78
weight (kN)	0.701 \pm 0.096	0.599 - 0.981	0.553 \pm 0.068	0.418 - 0.676
foot length (m) +	0.259 \pm 0.013	0.240 - 0.285	0.232 \pm 0.015	0.195 - 0.248
ELDERLY NORMALS (16 males, 16 females)				
age (years)	68.9 \pm 5.9	61 - 79	69.4 \pm 3.8	63 - 75
height (m)	1.74 \pm 0.035	1.70 - 1.80	1.54 \pm 0.050	1.45 - 1.62
weight (kN)	0.760 \pm 0.080	0.683 - 0.944	0.594 \pm 0.070	0.418 - 0.688
foot length (m) +	0.261 \pm 0.012	0.231 - 0.280	0.229 \pm 0.011	0.211 - 0.248

+ NOTE: average of left and right foot lengths, measured in the a-p direction with the feet in the test position.

signal; four different realizations of the PRN waveform were constructed, with peak factors ranging from 2.06 to 2.30.

Transient perturbations were designed to comprise an initial square-wave acceleration pulse, a constant-velocity interval, and a final square-wave deceleration pulse. The duration of each pulse was 0.3 s; the total duration was 0.72 s. Six pulse amplitudes were used: 0.5, 1.0, 1.5, 2.0, 2.5 and 3.0 m/s². In all cases, the platform translation was in the backward direction. See figure 7.6 (in Chapter 7) for example plots of the acceleration waveform measured during actual transient tests.

The perturbations were applied using the platform described in Chapter 4. The selection of the continuous-waveform perturbation parameters was based primarily on the results of the pilot experiments described in Chapter 5. The design of the transient waveform was also based on the results of pilot tests on healthy young adults. For all three pilot subjects tested, the lowest amplitude was easily tolerated, whereas the larger amplitudes provoked loss of balance.

6.2 SUBJECTS

The characteristics of the normal subjects are summarized in table 6.1. Sixty-four normal subjects were tested: 32 between the ages of 20 and 40, and 32 between the ages of 61 and 79, with equal numbers of males and females in each age group. These subjects were screened for neurological, visual, cardiovascular and musculo-skeletal disorders, for history of falling and for use of drugs that might affect balance. The screening was performed through the oral administration of a questionnaire.

Also tested were five patients with unilateral peripheral vestibular lesions and five elderly subjects with a history of falling (see table 6.2). At the time of the balance testing, all of the vestibular patients were unable to complete successfully one or more clinical balance tests (i.e. stand toe-to-heel for 60 s, stand on one leg for 30 s, walk a straight line toe-to-heel) with eyes closed. Two of the five patients (V2 and V5) were also unable to complete one or more tests with eyes open. The fallers were residents of a residential-care complex for the elderly. All were

CHARACTERISTICS OF THE BALANCE-IMPAIRED SUBJECTS

	DESCRIPTION OF IMPAIRMENT	SEX	AGE (years)	HEIGHT (m)	WEIGHT (kN)	FOOT + LENGTH (m)
VESTIBULAR PATIENTS						
V1	right labyrinthectomy motorcycle accident 23 weeks post-op.	male	38	1.76	0.850	0.270
V2	right vest. neurectomy Meniere's disease 11 weeks post-op.	female	50	1.65	0.750	0.265
V3	left vest. neuronitis 39 weeks since onset	male	42	1.75	0.699	0.262
V4	right vest. neurectomy Meniere's disease 4.5 weeks post-op.	male	40	1.61	0.485	0.249
V5	left labyrinthectomy Meniere's disease 39 weeks post-op.	male	61	1.69	0.757	0.266
ELDERLY FALLERS						
F1	2 falls in past year	female	83	1.50	0.549	0.233
F2	4 falls in past year	female	82	1.45	0.659	0.218
F3	2 falls in past year	female	75	1.48	0.481	0.229
F4	1 fall in past year	female	86	1.43	0.427	0.240
F5	2 falls in past year	male	83	1.69	0.730	0.245

+ NOTE: average of left and right foot lengths, measured in the a-p direction with the feet in the test position.

ambulatory and had experienced one or more falls during the previous year (but none within the previous month). The falling histories reported by the subjects were verified by the nursing staff at the residence.

6.3 TESTING PROCEDURE

Prior to the first test, the outlines of the feet were traced on a piece of paper which was taped to the force plates. The foot tracings were used to detect changes from the initial foot position. In addition, they allowed the same positioning to be repeated in subsequent tests, and facilitated the measurement of the foot dimensions. The subjects were instructed to "stand with feet comfortably spaced", with the backs of their heels flush against a vertical panel (orientated at right angles to the direction of platform motion). The panel was removed prior to each test. The tests were performed in stocking feet.

In testing the elderly subjects and vestibular patients, padding was installed to the rear of the subjects, for additional safety. In order to reduce the apprehension of some of the elderly fallers, the experimenter stood behind these subjects during the tests, ready to "catch" them if necessary.

For each test, the subjects were instructed to "stand relaxed as if waiting in a queue", with arms at sides, and to look straight ahead at a poster mounted on the visual surround. Headphones were used to listen to "Muzak"® (i.e. bland monotonous music), except during the measurements of spontaneous sway. During the tests, the subjects were observed to determine whether they grabbed the handrail, waved their arms, raised their heels or toes, or otherwise moved their feet.

In the continuous-waveform tests, the platform motion was controlled to start and end gradually, with no sudden changes in acceleration. Subjects were warned "that the test would begin in a few seconds", approximately 3 s in advance of the start of the platform motion. A 2-3 minute seated rest was allowed between tests. For the transient tests, the interval between the advance warning and the start of the test was randomized, varying from 3 to 8 s, and the rest period was allowed after every set of 3 trials.

TABLE 6.3

OUTLINE OF THE PROTOCOL

TEST	DESCRIPTION	WAVEFORM	AMPLITUDE + (m/s ²)	VISUAL INPUT	NO. OF TRIALS
STATIC TEST					
S1	spontaneous	N/A	N/A	eyes open	1
CONTINUOUS-WAVEFORM TESTS					
C1	learning	pseudorandom	0.10	eyes open	1
C2	amplitude 1	pseudorandom	0.10	eyes open	1
C3	amplitude 2	pseudorandom	0.075 or 0.15 ++	eyes open	1
C4	random	random	0.075, 0.10 or 0.15 +++	eyes open	1
C5	blindfolded	pseudorandom	0.075 or 0.10 ++	blindfolded	1
TRANSIENT-WAVEFORM TESTS (YOUNG NORMAL SUBJECTS ONLY)					
T1	learning	pulse	0.5	eyes open	1
T2	amplitude 1	pulse	0.5	eyes open	3
T3	amplitude 2	pulse	1.0 ++++	eyes open	3
T4	amplitude 3	pulse	1.5 ++++	eyes open	3
T5	amplitude 4	pulse	2.0 ++++	eyes open	3
T6	amplitude 5	pulse	2.5 ++++	eyes open	3
T7	amplitude 6	pulse	3.0 ++++	eyes open	3

NOTE: + root-mean-square amplitude for continuous waveforms, pulse amplitude for transient waveforms;
 ++ used higher amplitude only if subject tolerated "amplitude 1";
 +++ used highest amplitude tolerated in previous tests;
 ++++ tested only if subject tolerated at least one trial at next lowest amplitude.

Various anthropometric measurements were made, including height, weight, armspan and a number of foot dimensions. The foot dimensions were measured with the feet in the same position as in the balance tests, and included a-p foot length, a-p and vertical location of the flexion-extension ankle axes, and a-p location of the first and fifth metatarsal heads (most anterior point, determined through palpation). The approximate location of each ankle axis was estimated by palpating the most lateral and most medial points on the malleoli and applying "correction factors" determined by Inman and Isman (1969). A-p foot length was measured from the most posterior point on the calcaneus to the most anterior point on the phalanges. The a-p locations of the other anatomical features were also measured relative to the most posterior point on the calcaneus.

Subjects were tested for gross deficits in visual acuity (Snellen eyechart), vibration sense (ability to sense tuning fork vibration), and range of motion at the ankle, knee and hip (passive motion tests). A written questionnaire was used to assess the normal activity level and to determine the pre-test activities, i.e. eating, exercise, sleep and use of drugs or alcohol. Subjects were excluded if they had consumed any alcohol or balance-affecting drugs on the day of the test.

6.4 PROTOCOL

The test protocol is summarized in table 6.3. The first part of the protocol was the same for all subjects (with the exceptions noted below). In test S1, spontaneous sway was measured as the subject stood quietly on the platform for 77 s. Tests C1 to C5 involved the continuous-waveform perturbations. The RAN waveform was used in test C4; the other tests used the PRN waveform. A different waveform realization was used for each PRN test.

Test C1 was a learning trial, to allow the subject to gain familiarity with the continuous-perturbation test procedure. The same amplitude was used in test C2. If the subject was able to "tolerate" the perturbation in test C2 without saturating the base-of-support (BOS) (i.e. raising heels or toes) or resorting to compensatory motions (i.e. grabbing handrails, waving arms or

moving feet), the amplitude was increased in test C3. Otherwise, the amplitude was reduced. The RAN-perturbation test, test C4, was performed at the largest amplitude that the subject had "tolerated" in the previous PRN tests. Test C5 was performed with the subject blindfolded. The test-C2 amplitude was used for this test provided that the subject had "tolerated" this amplitude previously; otherwise, the lowest amplitude was used.

It was necessary to modify the protocol for some of the elderly fallers. In subjects F3, F4 and F5, the learning trial (test C1) was performed at the lowest amplitude, to help reduce apprehension. The lowest amplitude was also used in test C2 for subject F2 and in the blindfolded test (test C5) for subjects F2 and F5. In all fallers except F1 (the first faller tested), tests C3 and C4 were omitted, so as to minimize fatigue.

After the completion of the continuous-waveform tests, the normal young subjects were also tested with transient waveforms. An initial learning trial was conducted, at the smallest amplitude. Subjects were then tested at each amplitude three times, starting at the smallest value and progressing up to the maximum amplitude that could be tolerated. If the subject grabbed the handrail, waved his/her arms or moved his/her feet in all three trials at a given amplitude, then no higher amplitudes were tested.

6.5 SYSTEM IDENTIFICATION METHODS

Treating platform acceleration as the system input and a-p centre-of-pressure (COP) displacement as the output, the data were fitted with a linear transfer function model. Three system identification methodologies were used to fit the linear transfer function: (1) cross-spectral analysis, (2) ordinary least squares and (3) maximum likelihood. In all three methods, models of different order and dead time were fit, and the optimal model structure was determined using the Akaike Information Criterion (AIC) (Akaike, 1974):

$$AIC = N (\ln 2\pi + 2 \ln \lambda) + 2m; \quad \lambda^2 = (1/N) \sum_{n=1}^N e^2(n)$$

where N is the number of data points, e(n) are the model-fit errors (or "residuals") and m is the number of estimated parameters in the

model. In all three methods, the optimal model structure was determined separately for each set of test data.

6.5.1 Cross-Spectral Analysis

The cross-spectral (CS) method was used to estimate the nonparametric transfer function (i.e. the frequency response), using the method of "averaging periodograms" to make the necessary spectral estimates (Bendat and Piersol, 1971b and 1980). First, the data were divided into segments of equal length (using 50% overlap, as suggested by Welch (1967)), discarding the first segment to eliminate the transient response. Then, for each segment, the input-output cross-spectrum, the input auto-spectrum and the output auto-spectrum were estimated, using a 256-point Fast Fourier Transform (FFT) algorithm (Carter and Ferrie, 1979; Rabiner et al, 1979). Since the segment length was equal to the period of the PRN inputs (15.36 s), truncation distortion (i.e. "leakage") could not occur (Gibb, 1982); therefore, no windowing was performed for the PRN tests. For the RAN tests, the data segments were multiplied by a Hamming window prior to performing the FFT's.

The spectral estimates for the data segments were averaged, and the frequency response was estimated as the ratio of the average cross-spectrum divided by the average input auto-spectrum. The coherence function was estimated as the squared magnitude of the average cross-spectrum divided by the product of the input and output auto-spectra.

Each estimated frequency response was fitted with parametric transfer function models, using a conjugate gradient search algorithm (Seidel, 1975). The models were constrained to be of "minimum-phase" (i.e. all poles and zeros in the left-hand Laplace-plane). In calculating the model-fit cost function, the frequency response estimates were weighted by the coherence estimates. The full parametric model was of the form:

$$H(s) = Ke^{-\tau s} \frac{b_3 s^3 + b_2 s^2 + b_1 s + 1}{a_4 s^4 + a_3 s^3 + a_2 s^2 + a_1 s + 1}$$

where s is the Laplace operator. The order of the full model was selected to allow for the steepest high-frequency roll-off

(80 dB/decade) observed in the frequency response plots. Constraining the order of the numerator to be less than the order of the denominator, all reduced forms of the full model were fit. For each set of test data, the optimal model was selected as the one with the minimum AIC value (based on the fit between the nonparametric frequency response and the parametric transfer function).

6.5.2 Least Squares and Maximum Likelihood Methods

Both the least squares (LS) and maximum likelihood (ML) methods fit a discrete model directly to the time domain data (e.g. Åström, 1980; Strojic, 1980). The model is of the form:

$$A(d) y(n) = d^k B(d) x(n) + \lambda C(d) e(n) \quad n = 1, N$$

where A, B and C are polynomials in d of order m, d is the backward shift operator, y(n) is the sampled COP output, x(n) is the sampled acceleration input, λ is the noise intensity, e(n) is the equation error (or residual), and N is the number of data points. In the LS case, $\lambda = 1$ and $C(d) = 1$.

The LS model was fitted using the discrete square root filtering algorithm, while the ML model was fit using a combined Gauss-Newton and Newton-Raphson iterative algorithm (Wieslander, 1980). The initial parameter estimates required for the ML iterations were obtained using the LS method. The starting COP value was subtracted from the COP data prior to fitting the models.

The LS and ML identifications were performed using a commercially-available software package, IDPAC (Scientific Systems, Cambridge, Massachusetts). The capabilities of the software limited the maximum model order to 14 for the LS model and 8 for the ML model. Each set of test data was fitted with dead times between 0.0 and 0.3 s. As required by the LS and ML models, the dead times were integer multiples of the sample interval (0.06 s). The upper limit of 0.3 s was estimated from the results of the CS analysis.

The LS model was fitted first. For each value of the dead time, models of decreasing order were fitted (starting with the maximum order) until the minimum AIC value was reached. The dead

time and model order combination that resulted in the lowest AIC value overall was chosen as the final LS model structure. The optimal dead time determined for the LS model was used in the ML model. The order of the ML model was determined by fitting models of decreasing order until the minimum AIC value was reached.

For each set of test data, statistical tests were performed to validate the assumptions of the system identification models. For both the LS and ML models, the residuals were tested for independence by means of the nonparametric run test (e.g. Bendat and Piersol, 1971a). In addition, the ML residuals were tested for normality using the chi-square goodness-of-fit test (e.g. Walpole and Meyers, 1972). These tests were performed automatically by the IDPAC software.

6.6 ESTIMATION OF THE SATURATION AMPLITUDE

Transient response to a negative unit pulse in platform acceleration was predicted by performing a digital simulation of the linear transfer function. The pulse had a duration of 0.06 s and an amplitude of $-(1/0.06)$ m/s², and is referred to as a "negative unit pulse" because the "area" (i.e. the integral with respect to time) was equal to -1.

For the LS and ML models, the simulations were performed by direct implementation of the difference equations, at a sample interval of 0.06 s. For the CS model, a sample interval of 0.01 s was used, in order to allow the dead time to be represented more accurately. In simulating the CS models, each model was represented as a cascade of first- and/or second-order systems. Transformation from the Laplace domain to the discrete time domain was accomplished by means of the bilinear transformation, followed by the inverse z-transform (e.g. Stearns, 1975).

The nominal saturation amplitude (SA) was calculated from the relation: $BOS = (SA) (\Delta COP)$, where BOS is the average a-p length of the feet (as defined in Section 6.3) and ΔCOP is the peak COP displacement in the predicted unit pulse response (see fig 7.4 in Chapter 7).

6.7 QUANTIFICATION OF SPONTANEOUS SWAY

Spontaneous a-p COP fluctuations measured during the 77 s static tests were quantified by means of time domain and frequency domain measures. The time domain measures included: (1) root-mean-square COP displacement relative to the mean COP location (RMS), (2) range of COP displacement (RANGE), and (3) average speed of COP displacement (SPEED). SPEED was calculated as SP / T , where SP is the total a-p sway path and T is the duration of the test. These three variables were analyzed in a non-normalized form and after normalization with respect to the length of the BOS. In addition, the time domain data were used to estimate the "mean frequency" of sway as follows: $MFREQ = SP / (4\sqrt{2} \text{ RMS } T)$ (Hufschmidt et al, 1980).

The frequency domain measures were calculated from the power spectrum of the COP displacement. The power spectrum (or spectral density function) was estimated using the method of "averaging periodograms" described in Section 6.5.1. A 256-point FFT was used, giving a segment duration of 15.36 s and a frequency resolution of 0.065 Hz. Segments were overlapped by 50%, yielding a total of nine segments. A Hamming window was used.

The power spectrum was characterized by the centroidal frequency and dispersion (Vanmarcke, 1972). These parameters are defined in terms of the moments of the spectral density function $G(f)$, where $\lambda_i = \int f^i G(f) df$ is the i th moment. The centroidal frequency quantifies where the spectrum is concentrated along the frequency axis and is calculated as: $CFREQ = \sqrt{\lambda_2 / \lambda_0}$. The dispersion quantifies the spread of the spectrum about the centroidal frequency and is calculated as: $DISP = \sqrt{1 - \lambda_1^2 / \lambda_0 \lambda_2}$. The dispersion ranges from 0 to 1. CFREQ and DISP were estimated over the frequency range 0.065 to 4.95 Hz.

6.8 PREDICTION OF TRANSIENT RESPONSE

Transient responses were predicted (for the young adult subjects) by performing digital simulations, using the CS, LS and ML models identified from the balance tests. The input for each simulation was the measured acceleration data from an actual transient test.

The simulations were performed using the methods described in Section 6.6. The LS and ML model simulations were performed at a sample interval of 0.06 s, and hence used the acceleration data that were sampled at 16.7 Hz as the input. For the CS model, a sample interval of 0.01 s was used; therefore, the CS simulation used the acceleration data that were sampled at 100 Hz.

For each simulation, the peak anterior COP displacement was found. The peak anterior COP displacement in the actual transient test data was also found, as was the peak backward platform acceleration. The "gain" of the response was estimated as the peak COP displacement (i.e. the measured value) divided by the peak backward platform acceleration

6.9 STATISTICAL ANALYSES

6.9.1 Statistical Models

The statistical analyses were based on regression and analysis of variance (ANOVA) models. Details of the statistical models and analytical methods can be found in numerous textbooks (e.g. Montgomery, 1984a; Neter et al, 1985a). The statistical analyses were performed using a commercially-available software package, Minitab (Pennsylvania State University, University Park, Pennsylvania).

For each analysis, the assumptions of the statistical model were tested qualitatively, by: (1) plotting the residuals in time sequence (to assess independence), (2) plotting the residuals as a function of the fitted values (to assess uniformity of variance), and (3) constructing histograms and normal probability plots of the residuals (to assess normality) (Montgomery, 1984b). In cases where violations were suspected, quantitative tests were also performed. The residuals were tested for normality and independence using the Wilk-Shapiro test (e.g. Ryan et al, 1982) and the nonparametric run test (e.g. Bendat and Piersol, 1971a), respectively. The ANOVA models were tested for uniform variance using Bartlett's test (e.g. Neter et al, 1985b).

In the ANOVA models where subjects were treated as blocks (i.e. no subject interaction terms), possible subject-treatment interaction was assessed by plotting the treatment means versus the

treatment levels for each subject and then comparing these plots. In cases where interaction was suspected, the Tukey test for interaction was performed (e.g. Neter et al, 1985c).

6.9.2 Analysis of Balance Test Responses

The Δ COP values obtained using the CS, LS and ML models were compared by means of linear regression and by one-way ANOVA with blocking on subjects. The Duncan multiple range test was used to compare the means in a pairwise manner. These analyses were performed using the data from all of the subjects. In addition, separate analyses were performed for the young-normal, elderly-normal, vestibular-patient and elderly-faller subject groups.

One-way ANOVA with blocking on subjects was used to compare the SA values obtained from the different continuous-waveform tests. The Duncan multiple range test was then used to compare the means in a pairwise manner. The young normals, elderly normals, vestibular patients and elderly fallers were analyzed separately.

A two-way ANOVA was used to test for age- and sex-related differences in the SA scores of the normal subjects. This analysis was performed for the eyes-open (EO) and blindfolded (BF) results and for the EO/BF ratio. The EO condition was represented by the test-C2 data or by the "best" test, i.e. the test at the largest perturbation amplitude that each subject was able to "tolerate" without resorting to compensatory manoeuvres (i.e. grabbing handrails, waving arms, raising heels or toes, or moving feet).

For each balance-impaired subject, a percentile score was calculated by comparing the individual's SA with the SA distribution estimated for the normal subjects. Each subject was compared to the appropriate age group. Subjects with scores lying below a selected percentile level were classified as balance-impaired. For the EO/BF ratio, a two-tailed criterion was used.

6.9.3 Analysis of Spontaneous Sway Measures

The spontaneous sway measures were compared to the test-C2 SA results by means of linear regression. In addition, these measures were analyzed for age- and sex-related differences and the ability

to identify the balance-impaired individuals was assessed, using the methods described above. For most of the variables, it was necessary to perform a transformation on the data in order to achieve a normal distribution and uniform variance, so that the ANOVA and regression models could be applied. The appropriate transformations were determined using the procedures detailed by Neter et al (1985b).

6.9.4 Analysis of Transient Responses

The dependence of the transient response on perturbation amplitude was analyzed by means of linear regression. The initial learning trials were excluded, as were any tests in which "loss of balance" occurred. Here, loss of balance was defined as grabbing a handrail, moving the feet, lifting the heels or toes, or waving the arms. In the regression, the dependent variable was the response gain (i.e. the peak anterior COP displacement divided by the peak backward platform acceleration). The independent variable was the peak backward platform acceleration. In order to determine the linear or curvilinear function that best fit the data, a regression was also performed on the logarithmic transformations of the gain and acceleration values.

The percentage errors between the actual and predicted peak COP displacements were compared for different perturbation amplitudes, by means of a one-way ANOVA with blocking on subjects. Test-C2 and "best" test CS, LS and ML models were used to predict the transient responses. As above, the analysis excluded the initial learning trials and any tests in which loss of balance occurred. Also excluded were subjects who were unable to maintain balance at more than one amplitude. Because of the unequal numbers of samples at each amplitude, it was necessary to use a regression approach to perform the ANOVA. In order to compare the mean percentage error values in a pairwise manner, subjects with empty "cells" were eliminated, i.e. subjects who failed (in all three trials) to maintain balance at one or more of the amplitudes. Tukey's test was then used to compare the means.

In an attempt to develop a functional definition for the anterior limit of the BOS in terms of anatomical features, the peak

anterior COP displacement was found for those transient tests in which the subjects lifted their heels (but performed no other balance-recovery manoeuvres). A stepwise linear regression was then performed, regressing maximum COP displacement versus the following a-p foot dimensions: L, MT1, MT5, A, [L - A], [MT1 - A], and [MT5 - A] (where L is the foot length; MT1 and MT5 are the distances between the back of the foot and the first and fifth metatarsal heads, respectively; A is the distance between the ankle and the back of the foot). The analyses were performed for the left, right and overall COP. In analyzing the left and right COP, the corresponding set of foot dimensions was used. In analyzing overall COP, the average foot dimensions were used.

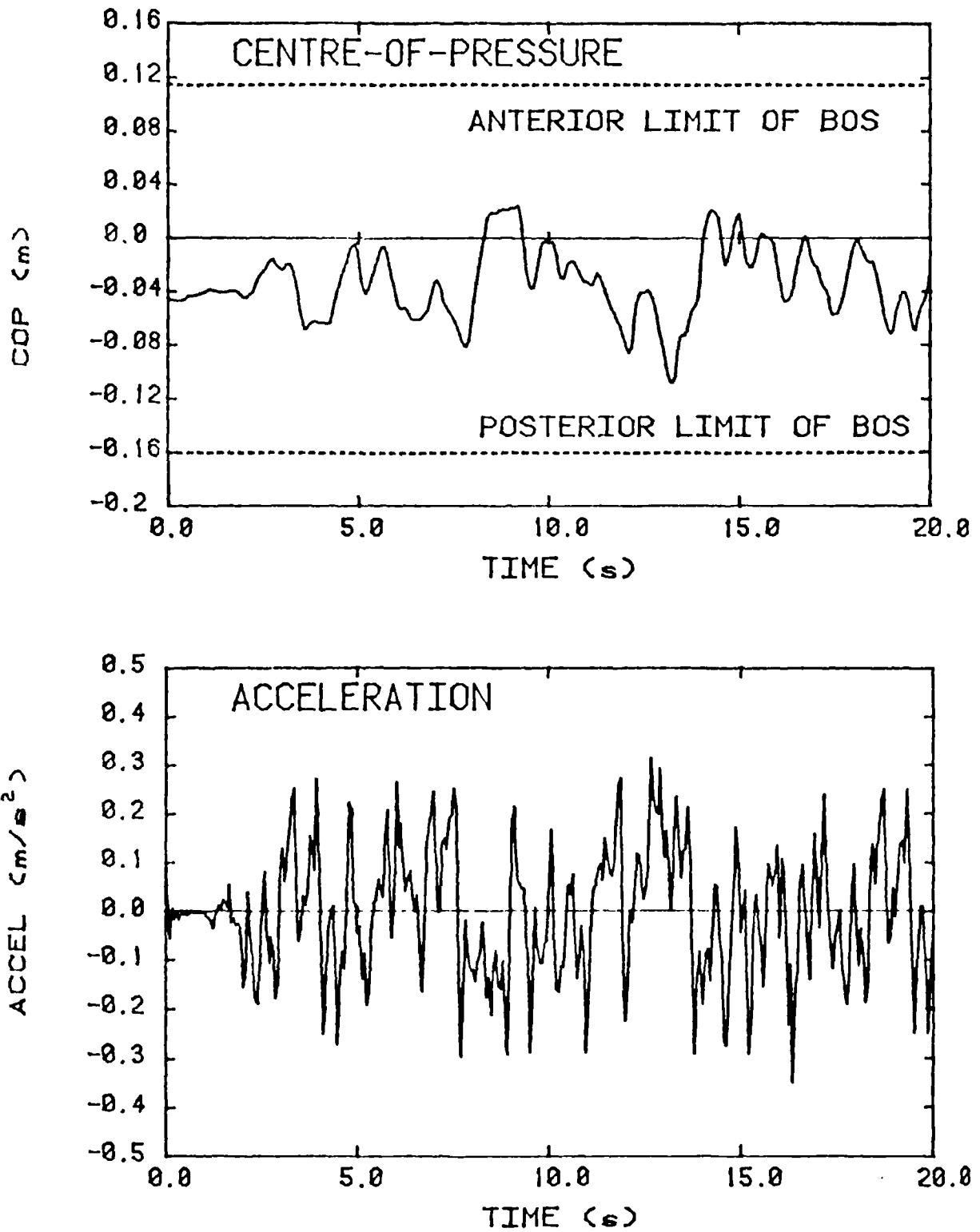


Fig 7.1 Example data from pseudorandom test: platform acceleration and resulting a-p COP displacement (initial 20 s from 185 s test).

CHAPTER 7. EXPERIMENTAL RESULTS

7.1 BALANCE TEST RESPONSES

Figure 7.1 shows a 20 s segment of data from the start of a sample pseudorandom (PRN) test. Figure 7.2 shows the corresponding nonparametric frequency response estimate along with the fitted parametric transfer function, obtained using the cross-spectral (CS) model. The results obtained using the least squares (LS) and maximum likelihood (ML) models are shown in figure 7.3 (transformed from the discrete-time domain to the frequency domain). Figure 7.4 shows the corresponding transient unit pulse response predictions obtained using these models.

7.1.1 Comparison of System Identification Models

Table 7.1 compares the results obtained using the CS, LS and ML models, based on the test-C2, test-C5 and "best-test" data. The models were compared in terms of the peak centre-of-pressure displacement (ΔCOP) in the predicted unit pulse response. The tabulated results were derived using the data from all subjects. Separate analyses of the young normals, elderly normals, vestibular patients and elderly fallers showed similar results.

The LS and ML estimates showed the strongest linear relationship, as evidenced by the large values for the coefficient of determination (R_a^2). In general, however, the estimates from all three models were in fairly close agreement. Except for the test-C5 CS-model comparisons, T-tests gave no evidence that the regression slopes were not equal to one or that the offsets were not zero ($p > 0.1$).

For most subjects, the ΔCOP estimates changed only a few percent in using a different model. However, in two tests, the CS model produced ΔCOP estimates that differed substantially (i.e. 20-30%) from the LS and ML values. One of these "outliers" was the test-C2 (and "best-test") result for an elderly normal subject; the other was the test-C5 result for a young normal subject. Even when these "outliers" were omitted from the analyses, the CS-model comparisons still showed the weakest linear relationships (i.e. the lowest R_a^2 values).

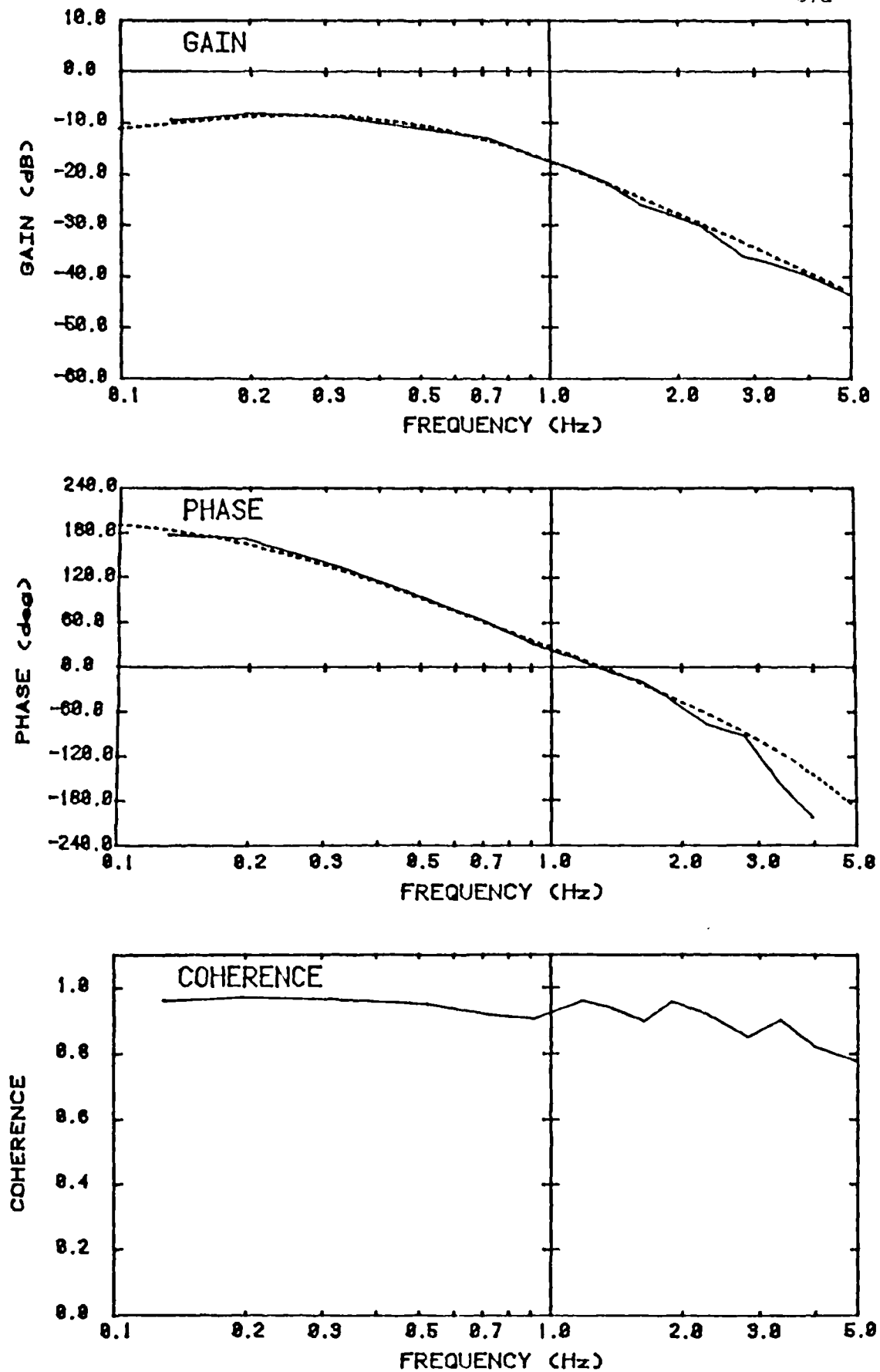


Fig 7.2 Example transfer function estimates: cross-spectral model.

Legend: solid line - nonparametric frequency response
dashed line - parametric transfer function

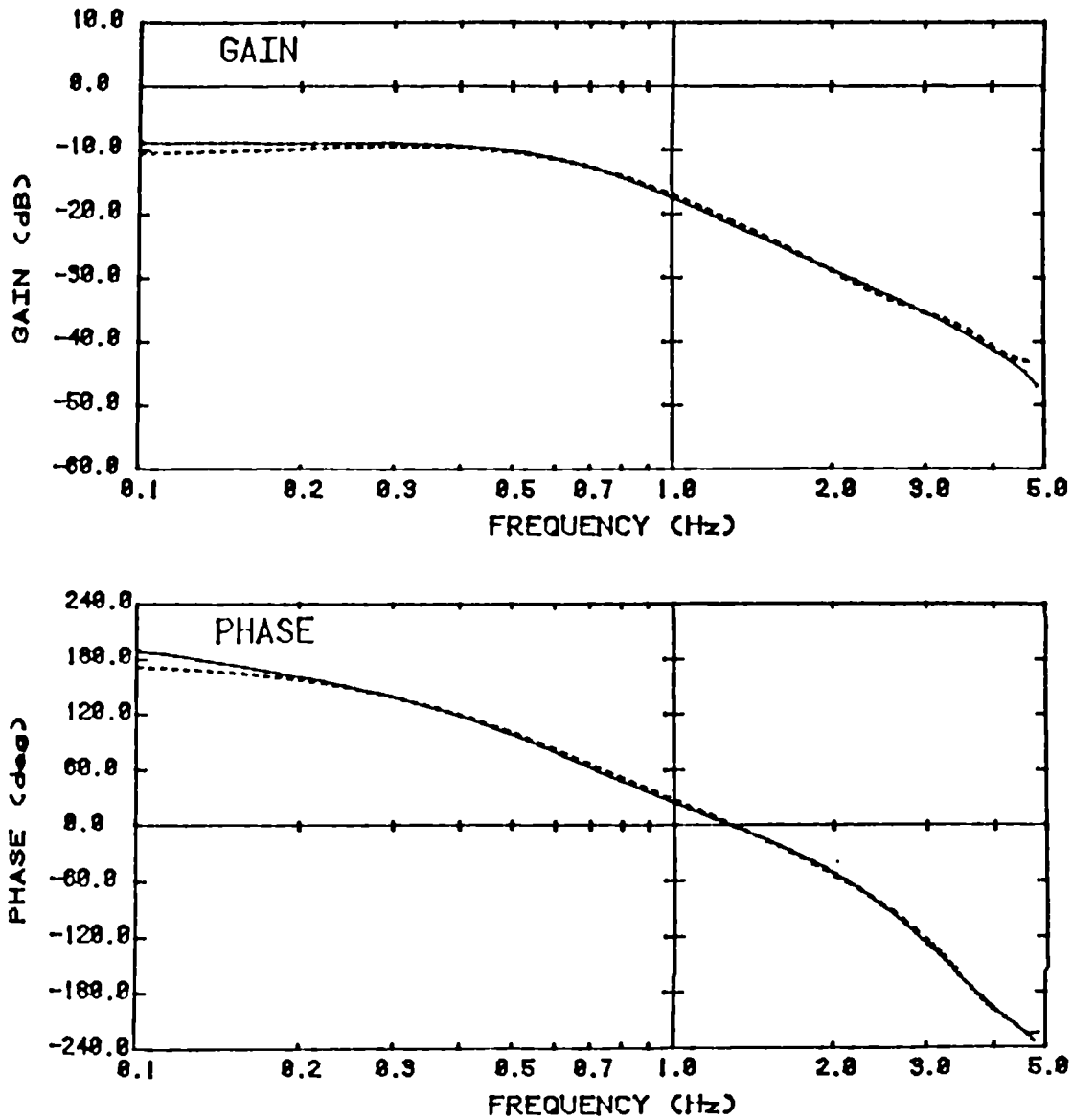


Fig 7.3 Example transfer function estimates: least squares and maximum likelihood models.

Legend: solid line - maximum likelihood model
dashed line - least squares model

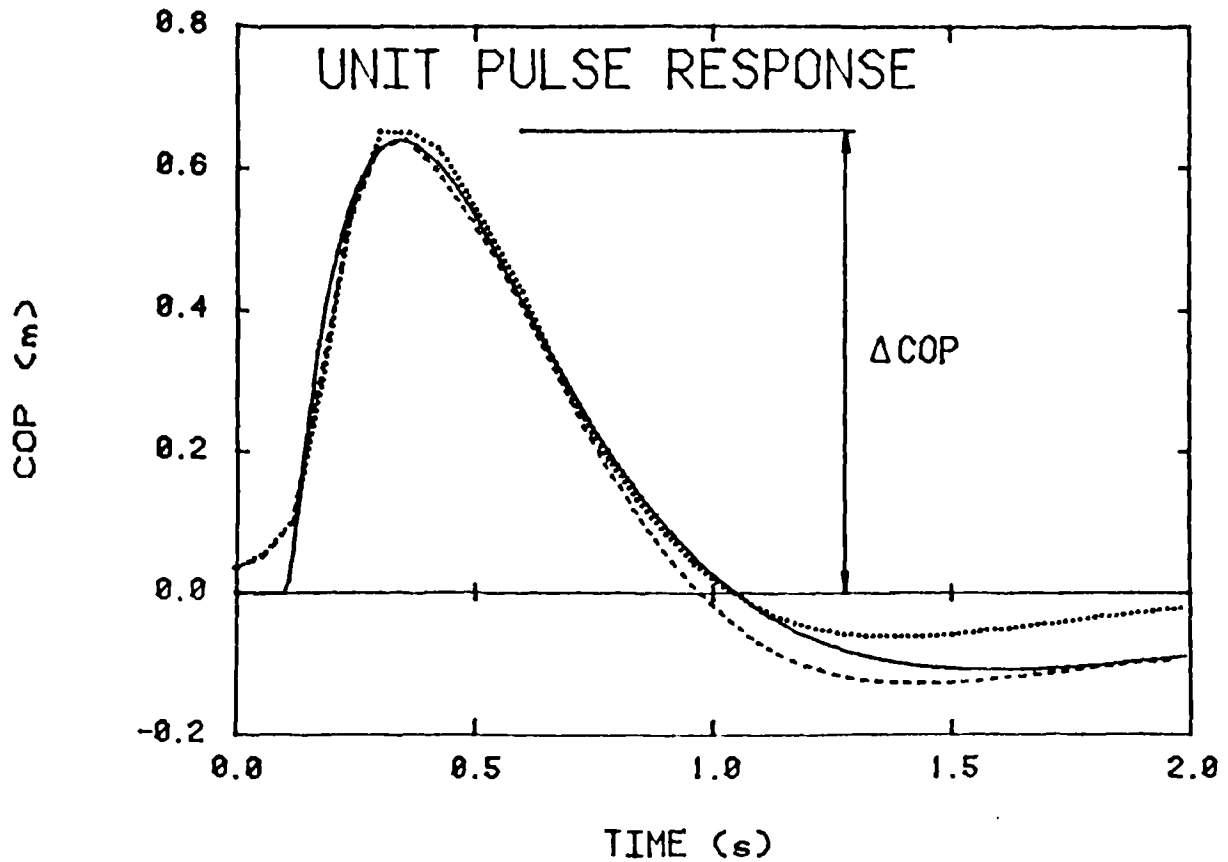


Fig 7.4 Example transient response predictions: centre-of-pressure displacement resulting from unit acceleration pulse at time = 0 s.

Legend: solid line - cross-spectral model
dotted line - least squares model
dashed line - maximum likelihood model

TABLE 7.1

COMPARISON OF THE SYSTEM IDENTIFICATION MODELS (Δ COP PREDICTIONS)

COMPARISON +	LINEAR REGRESSION ++			% DIFFERENCE +++	
	OFFSET	SLOPE	R_a^2 (%)	MEAN \pm SD	RANGE
<u>TEST C2</u>					
LS vs CS	0.0245	0.979	84.1	1.23 \pm 5.74	-27.5 : 11.2
ML vs CS	0.0175	0.974	84.6	-0.23 \pm 5.57	-30.1 : 7.6
LS vs ML	0.00991	1.00	98.5	1.48 \pm 1.87	-1.9 : 8.0
<u>"BEST" TEST</u>					
LS vs CS	0.0121	1.01	86.1	2.31 \pm 5.75	-27.5 : 12.7
ML vs CS	0.0135	0.987	86.2	0.46 \pm 5.69	-30.1 : 11.0
LS vs ML	0.00121	1.02	99.2	1.86 \pm 1.48	-1.8 : 5.8
<u>TEST C5</u>					
LS vs CS	0.166***	0.784***	82.8	3.19 \pm 6.15	-12.8 : 22.8
ML vs CS	0.152***	0.784***	83.5	1.12 \pm 6.05	-12.4 : 22.3
LS vs ML	0.0237	0.986	96.3	2.08 \pm 2.50	-3.8 : 7.8

NOTE: + CS, LS and ML = cross-spectral, least squares and maximum likelihood models;

++ offset (y-intercept) is constant term in regression (m); slope is dimensionless; R_a^2 is coefficient of determination, adjusted for degrees of freedom;

+++ % difference for A vs B = (100%)(A-B)/B; estimates for mean and standard deviation (SD) based on 74 subjects;

*** indicates offset \neq 0 or slope \neq 1, $p < 0.001$; $p > 0.1$ in all other cases (T-test, degrees of freedom = 72).

TABLE 7.2

COMPARISON OF THE CONTINUOUS-WAVEFORM TESTS

TEST DESCRIPTION	SATURATION AMPLITUDE: MEAN \pm STD DEV \pm		
	CS MODEL ++	LS MODEL	ML MODEL
<u>YOUNG NORMALS</u>			
C1 learning	0.366 \pm 0.050	0.356 \pm 0.049	0.361 \pm 0.050
C2 amplitude 1	0.361 \pm 0.041	0.362 \pm 0.049	0.367 \pm 0.051
C3 amplitude 2	0.353 \pm 0.051	0.344 \pm 0.053	0.350 \pm 0.055
C4 random	0.390 \pm 0.041	0.377 \pm 0.040	0.381 \pm 0.041
C5 blindfolded	0.395 \pm 0.045	0.374 \pm 0.034	0.382 \pm 0.037
<u>ELDERLY NORMALS</u>			
C1 learning	0.309 \pm 0.059	0.303 \pm 0.054	0.307 \pm 0.055
C2 amplitude 1	0.301 \pm 0.038	0.295 \pm 0.039	0.299 \pm 0.040
C3 amplitude 2	0.299 \pm 0.050	0.292 \pm 0.053	0.298 \pm 0.053
C4 random	0.343 \pm 0.039	0.326 \pm 0.039	0.331 \pm 0.039
C5 blindfolded	0.338 \pm 0.048	0.334 \pm 0.044	0.341 \pm 0.045
<u>VESTIBULAR PATIENTS</u>			
C1 learning	0.386 \pm 0.033	0.371 \pm 0.034	0.378 \pm 0.038
C2 amplitude 1	0.377 \pm 0.030	0.359 \pm 0.031	0.367 \pm 0.033
C3 amplitude 2	0.356 \pm 0.039	0.340 \pm 0.038	0.349 \pm 0.037
C4 random	0.393 \pm 0.031	0.375 \pm 0.036	0.386 \pm 0.036
C5 blindfolded	0.394 \pm 0.053	0.390 \pm 0.029	0.397 \pm 0.030
<u>ELDERLY FALLERS</u>			
C1 learning	0.327 \pm 0.027	0.320 \pm 0.010	0.342 \pm 0.029
C2 amplitude 1	0.321 \pm 0.034	0.314 \pm 0.025	0.317 \pm 0.027
C5 blindfolded	0.321 \pm 0.041	0.315 \pm 0.026	0.316 \pm 0.030

NOTE: + estimates based on 32 young normals, 32 elderly normals and 5 vestibular patients; for elderly fallers, 4 subjects for test C1 and 5 subjects for tests C2 and C5;

++ CS, LS and ML = cross-spectral, least squares and maximum likelihood models.

Although the differences between the models were generally small, the analyses of variance (ANOVA's) did indicate that these differences were significant ($p < 0.05$). The multiple range tests indicated that the LS model produced significantly higher Δ COP estimates, on the average, compared to the CS and ML models ($p < 0.05$).

7.1.2 Comparison of Tests

Table 7.2 lists descriptive statistics for the saturation amplitude (SA) values obtained for the different continuous-waveform tests, using the CS, LS and ML models.

For both the young and the elderly normals, the ANOVA's found significant differences between the tests ($p < 0.001$). The Duncan multiple range test showed that the "random" (test C4) and "blindfolded" (test C5) tests produced the largest mean SA values ($p < 0.01$). In the elderly subjects, there were no significant differences between the other three PRN tests ($p > 0.05$). However, for the young subjects, analysis of the CS estimates demonstrated significant differences between the "learning" test (test C1) and the "amplitude 2" test (test C3), whereas the LS and ML results showed significant differences between the "amplitude 1" (test C2) and "amplitude 2" (test C3) tests ($p < 0.01$).

The ANOVA's also showed significant test differences for the vestibular patients ($p < 0.05$). The multiple range tests indicated that the mean test-C3 result was significantly lower ($p < 0.05$) when compared to tests C1, C4 and C5 (CS and ML models) or when compared to tests C4 and C5 (LS model). In addition, the test-C2 mean was significantly lower than the test-C5 mean, for the ML model. None of the other differences were found to be significant ($p > 0.05$).

For the elderly fallers, the analysis was limited to tests C1, C2 and C5. The test-C1 results were excluded for subject F2, who grabbed the handrail extensively during this test. Based on the remaining four subjects, the ANOVA's showed significant test-related differences in the ML results ($p < 0.001$), but no significant differences when using the CS and LS models ($p > 0.1$). For the ML model, the multiple range test showed the test-C1 mean to be significantly higher than the other test results ($p < 0.05$).

TABLE 7.3

SATURATION AMPLITUDE: AGE AND SEX DIFFERENCES IN NORMAL SUBJECTS

MODEL +	SATURATION AMPLITUDE: MEAN \pm STD DEV ++				F-VALUES +++		
	YOUNG	ELDERLY	MALES	FEMALES	AGE	SEX	INTER
<u>EYES OPEN: TEST C2</u>							
CS	0.361 \pm 0.041	0.301 \pm 0.038	0.335 \pm 0.045	0.328 \pm 0.054	36.2***	0.616	0.208
LS	0.362 \pm 0.049	0.295 \pm 0.039	0.331 \pm 0.051	0.326 \pm 0.061	36.7***	0.261	0.0804
ML	0.367 \pm 0.051	0.299 \pm 0.040	0.336 \pm 0.051	0.330 \pm 0.062	34.9***	0.286	0.178
<u>EYES OPEN: "BEST" TEST</u>							
CS	0.353 \pm 0.051	0.301 \pm 0.047	0.328 \pm 0.048	0.326 \pm 0.063	17.7***	0.0165	1.68
LS	0.344 \pm 0.053	0.294 \pm 0.053	0.318 \pm 0.053	0.320 \pm 0.064	14.2**	0.0179	1.74
ML	0.350 \pm 0.055	0.300 \pm 0.054	0.325 \pm 0.054	0.326 \pm 0.066	13.3**	0.0100	1.77
<u>BLINDFOLDED</u>							
CS	0.395 \pm 0.045	0.338 \pm 0.048	0.366 \pm 0.047	0.367 \pm 0.061	23.2***	0.0001	0.668
LS	0.374 \pm 0.034	0.334 \pm 0.044	0.354 \pm 0.039	0.353 \pm 0.049	16.9**	0.0192	0.833
ML	0.382 \pm 0.037	0.341 \pm 0.045	0.363 \pm 0.042	0.361 \pm 0.051	15.6**	0.0286	0.737
<u>EYES OPEN / BLINDFOLDED: TEST C2</u>							
CS	0.918 \pm 0.067	0.895 \pm 0.073	0.918 \pm 0.073	0.895 \pm 0.067	1.58	1.58	0.224
LS	0.968 \pm 0.090	0.886 \pm 0.068	0.935 \pm 0.094	0.919 \pm 0.086	16.5**	0.567	0.514
ML	0.960 \pm 0.086	0.880 \pm 0.067	0.927 \pm 0.086	0.913 \pm 0.088	17.1**	0.553	0.213
<u>EYES OPEN / BLINDFOLDED: "BEST" TEST</u>							
CS	0.893 \pm 0.075	0.891 \pm 0.086	0.896 \pm 0.077	0.888 \pm 0.084	0.00455	0.146	1.29
LS	0.919 \pm 0.100	0.881 \pm 0.093	0.896 \pm 0.090	0.903 \pm 0.106	2.39	0.0809	0.963
ML	0.914 \pm 0.096	0.879 \pm 0.089	0.894 \pm 0.083	0.900 \pm 0.104	2.27	0.0761	1.27

NOTE: + CS, LS and ML = cross-spectral, least squares, and maximum likelihood models;

++ 16 males and 16 females in each age group;

+++ F-VALUES: test for significant differences between means, related to age, sex or age-sex interaction; degrees of freedom = 1,60;

*** indicates significant difference, $p < 0.0001$; ** $p < 0.001$; $p > 0.1$ in all other cases.

Using the data from all five subjects, paired T-tests showed no significant differences between the test-C2 and test-C5 results ($p > 0.8$).

7.1.3 Age and Sex Differences in Normal Subjects

Table 7.3 summarizes the results of the analysis of the normal subject data, obtained using the CS, LS and ML models. Results are presented for the eyes-open (EO) and blindfolded (BF) test conditions and for the EO/BF ratio. Both the test-C2 data and the "best" test data were used to represent the EO condition.

The ANOVA showed no significant interaction in any of the analyses; therefore, separate age and sex effects can be assessed ($p > 0.1$). For the EO and BF data, the ANOVA's showed highly significant differences between the two age groups regardless of the model or test ($p < 0.001$). In all cases, the mean SA was larger in the young subjects. For the test-C2 EO/BF data, the LS and ML models showed significant age differences ($p < 0.001$) but the CS model did not ($p > 0.1$). In the cases where the differences were significant, the young subjects had the higher mean EO/BF ratios. No significant sex-related difference was found in any of the analyses ($p > 0.1$).

7.1.4 Identification of Balance-Impaired Individuals

The percentile scores of the balance-impaired subjects are listed in table 7.4. Results are shown for the CS, LS and ML models, using either test C2 or the "best" test to represent the EO condition.

Table 7.5 summarizes the results of the subject classification based on a 25% critical-area criterion ($\alpha = 0.25$). Use of a 25% criterion was found to give a better tradeoff between false positive and false negative rates, compared to 5% and 10% criteria. Note that the critical area was divided into two tails in analyzing the EO/BF data. Thus, for the 25%-criterion, subjects were classified as abnormal if their score was below the 12.5th percentile or above the 87.5th percentile. Overall, subjects were classified as balance-impaired if at least one of their EO, BF or EO/BF results was abnormal.

TABLE 7.4

SATURATION AMPLITUDE: CLASSIFICATION OF BALANCE-IMPAIRED SUBJECTS

SUBJECT	PERCENTILE SCORE BASED ON SATURATION AMPLITUDE								
	EYES OPEN			BLINDFOLDED			EYES OPEN/BLINDFOLDED		
	CS +	LS	ML	CS	LS	ML	CS	LS	ML
<u>TEST G2</u>									
vestibular patients:									
V1	88	77	82	78	71	78	69	71	69
V2	57	56	51	50	71	69	60	37	32
V3	25*	22*	22*	4***	38	23*	97**	20	34
V4	83	56	62	30	39	51	99***	70	68
V5	96	83	87	99	99	98	12*	4**	9*
elderly fallers:									
F1	59	57	58	19*	33	33	98***	86	88*
F2	74	79	83	23*	18*	14*	99***	99***	99***
F3	29	41	32	13*	21*	15*	89*	85	88*
F4	97	93	90	84	73	70	84	90*	88*
F5	62	59	58	48	28	25*	69	93*	95**
<u>"BEST" TEST</u>									
vestibular patients:									
V1	86	85	87	same as above			78	84	82
V2	31	32	33	same as above			19	14	15
V3	30	24*	24*	same as above			96**	23	36
V4	34	40	39	same as above			48	46	34
V5	93	76	79	same as above			18	10*	16
elderly fallers:									
F1	57	66	65	same as above			96**	91*	91*
F2	70	72	75	same as above			98***	99***	99***
F3	34	44	36	same as above			87	79	80
F4	94	86	82	same as above			81	84	81
F5	60	57	55	same as above			68	88*	90*

NOTE: + CS, LS and ML = cross-spectral, least squares and maximum likelihood models;

* balance-impaired at $\alpha = 0.25$ criterion, ** at $\alpha = 0.10$, *** at $\alpha = 0.05$ (one-tailed for eyes-open and blindfolded, two-tailed for eyes-open/blindfolded ratio).

TABLE 7.5

SATURATION AMPLITUDE: SUMMARY OF SUBJECT CLASSIFICATION ($\alpha = 0.25$)

DATA +	PERCENTAGE OF SUBJECTS CLASSIFIED CORRECTLY ++											
	YOUNG NORMALS			ELDERLY NORMALS			VESTIBULAR PATIENTS			ELDERLY FALLERS		
	CS	LS	ML	CS	LS	ML	CS	LS	ML	CS	LS	ML
	+++											
<u>TEST C2</u>												
EO	78	75	72	72	69	69	20	20	20	0	0	0
BF	75	72	66	72	75	78	20	0	20	60	40	60
EO/BF	75	75	75	75	63	75	60	20	20	60	60	100
OVERALL	56	53	47	50	47	53	60	40	40	60	80	100
<u>"BEST" TEST</u>												
EO	69	69	66	69	69	72	0	20	20	0	0	0
BF	75	72	66	72	75	78	20	0	20	60	40	60
EO/BF	78	75	78	84	72	72	20	20	0	40	60	60
OVERALL	53	44	41	56	53	50	20	40	20	60	80	80

NOTE: + EO = eyes open, BF = blindfolded;
 ++ percentages based on 32 young and 32 elderly normals,
 5 vestibular patients, and 5 elderly fallers;
 +++ CS, LS and ML = cross-spectral, least squares and
 maximum likelihood models.

In general, the greatest success was achieved using the BF or test-C2 EO/BF results. Using the test-C2 EO data, one vestibular patient was classified correctly, but no fallers were identified. Using the BF data, the CS and ML models both allowed one vestibular patient and three elderly fallers to be identified. Using the test-C2 EO/BF data, three of the vestibular patients and all five elderly fallers were identified, using the CS and ML models respectively. In some cases, use of the "overall" criterion did improve the success rate; however, any improvement was small and was achieved at the expense of a very high false positive rate in the normal subjects.

7.1.5 Validation of the Statistical Models

In all of the regressions and ANOVA's discussed above, the residual plots and/or statistical tests gave no evidence to suggest that the residuals were not normally and independently distributed or that the variances were not uniform ($\alpha = 0.05$).

In the comparisons where subjects were treated as blocks, plots of the test results were constructed for each subject to assess possible interactions. In the comparison of system identification models, these plots gave no evidence of any serious interaction, as the subjects tended to show similar trends. However, in the comparison of tests, some subject-to-subject differences in the plotted trends were apparent, for the normal subjects. The Tukey test confirmed that there was significant subject-test interaction in the young subjects ($p < 0.001$), but not in the elderly subjects ($p > 0.05$).

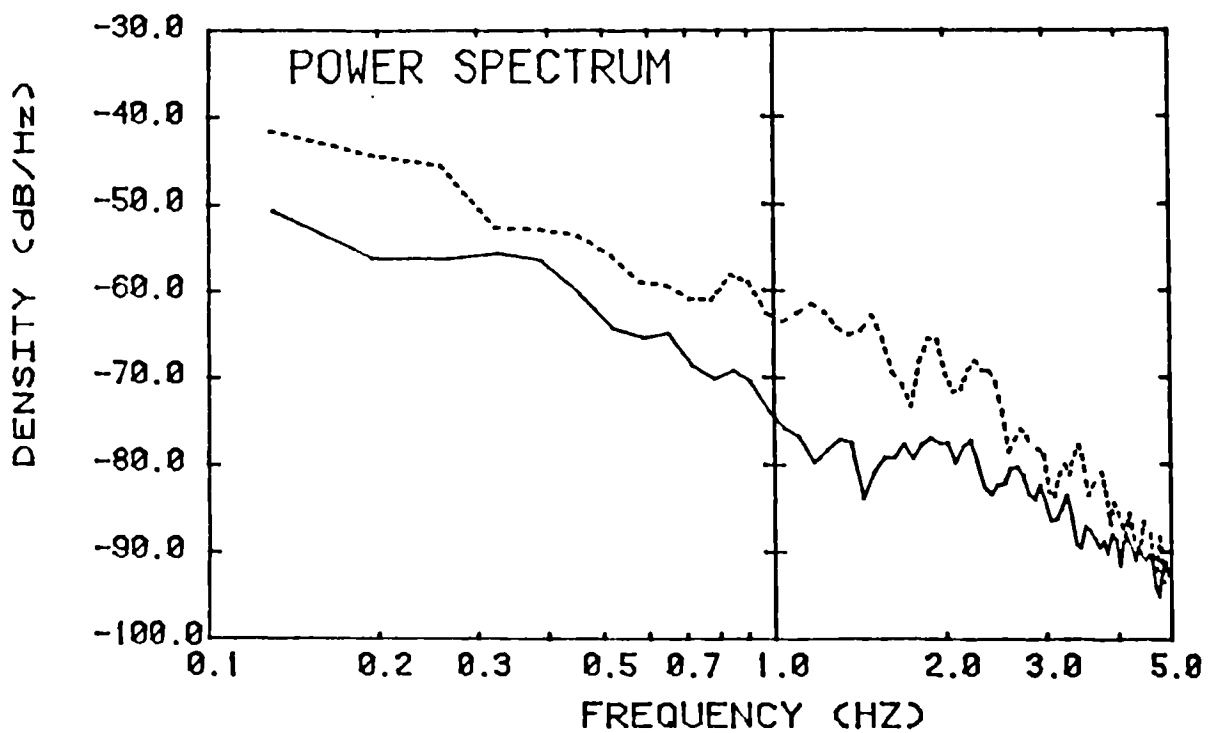
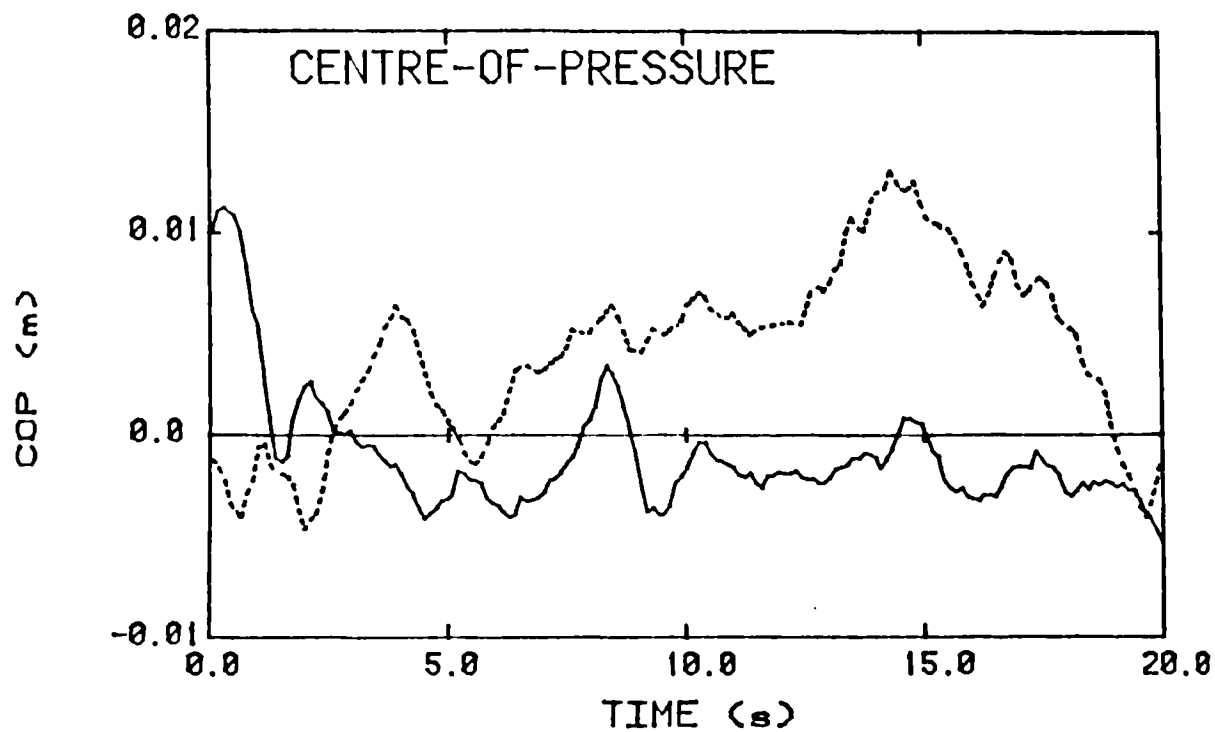


Fig 7.5 Example spontaneous sway results: time records of a-p COP displacement (initial 20 s of 77 s test) and corresponding power spectra estimates.

Legend: solid line - young male subject
dashed line - elderly female subject

7.2 SPONTANEOUS SWAY MEASURES

Examples of spontaneous sway data are plotted in figure 7.5. Segments of data (initial 20 s of the 77 s test) and corresponding power spectrum estimates are shown for typical young and elderly normal subjects.

As detailed in Section 6.7, the measures used to quantify spontaneous sway included the root-mean-square (RMS), range (RANGE), speed (SPEED) and mean frequency (MFREQ) of COP displacement, and the centroidal frequency (CFREQ) and dispersion (DISP) of the COP power spectrum. RMS, RANGE and SPEED were analyzed both with and without normalization with respect to the length of the base-of-support (BOS).

In order to apply the regression and ANOVA statistical methods, it was necessary to apply normalizing and "variance-stabilizing" transformations to the spontaneous sway data. This was true for all of the spontaneous sway measures, with the exception of DISP. CFREQ was transformed by a reciprocal cubic function. The remaining measures were transformed using the common logarithm function. In the following discussion, all references to the spontaneous sway measures (other than DISP) apply to the transformed versions, unless specified otherwise.

7.2.1 Comparison with Balance Test Responses

Table 7.6 summarizes the results of the linear regression of the spontaneous sway measures versus saturation amplitude (SA). The results are shown for the SA estimates derived using the CS, LS and ML models, based on the test-C2 data. Note that the R_a^2 values in the table are adjusted for degrees-of-freedom.

For the normal subjects, the linear regression accounted for only a small percentage of the variation in the spontaneous sway measures, as evidenced by the very small R_a^2 values. Nonetheless, in the young normals, the regressions were significant (i.e. the slope was not equal to zero) in some cases, namely for: RMS, RMS/BOS, RANGE and RANGE/BOS, using the LS and ML models for the SA data ($p < 0.05$). For SPEED/BOS, the regressions were marginally significant ($p < 0.1$). Neither SPEED, MFREQ, CFREQ nor DISP showed any significant linear relation to SA ($p > 0.1$).

TABLE 7.6

COMPARISON OF SPONTANEOUS SWAY MEASURES WITH SATURATION AMPLITUDE

SPONTANEOUS SWAY MEASURE +	SA MODEL ++	RESULTS OF REGRESSION VS SATURATION AMPLITUDE +++							
		YOUNG NORMALS		ELDERLY NORMALS		VESTIBULAR PATIENTS		ELDERLY FALLERS	
		T	Ra ² (%)	T	Ra ² (%)	T	Ra ² (%)	T	Ra ² (%)
log [RMS]	CS	-1.49	3.8	1.47	3.6	2.18	48.5	0.79	<0.1
	LS	-2.09*	9.8	0.89	<0.1	1.67	31.0	0.67	<0.1
	ML	-2.05*	9.3	1.24	1.7	1.96	41.5	0.97	0.0
log [RMS/BOS]	CS	-1.91	7.9	1.04	0.3	2.08	45.4	0.76	<0.1
	LS	-2.58*	15.5	0.48	<0.1	1.57	26.9	0.68	<0.1
	ML	-2.52*	14.8	0.82	<0.1	1.83	37.1	1.02	0.9
log [SPEED]	CS	-1.41	3.1	0.61	<0.1	1.14	6.7	1.38	18.5
	LS	-1.36	2.7	0.17	<0.1	0.59	<0.1	1.16	7.8
	ML	-1.35	2.6	0.45	<0.1	0.78	<0.1	1.32	15.5
log [SPEED/BOS]	CS	-1.83	7.0	0.07	<0.1	1.09	4.6	1.39	19.1
	LS	-1.82	6.9	-0.38	<0.1	0.56	<0.1	1.21	10.4
	ML	-1.80	6.7	-0.10	<0.1	0.74	<0.1	1.43	20.8
log [RANGE]	CS	-1.90	7.7	1.79	6.7	1.91	39.7	0.82	<0.1
	LS	-2.23*	11.3	1.52	4.0	1.32	15.7	0.67	<0.1
	ML	-2.15*	10.5	1.81	6.9	1.55	26.2	0.97	<0.1
log [RANGE/BOS]	CS	-2.29*	12.1	1.46	3.5	1.83	37.1	0.79	<0.1
	LS	-2.68*	16.7	1.20	1.4	1.26	12.9	0.68	<0.1
	ML	-2.59*	15.6	1.49	3.7	1.48	23.0	1.02	1.0
log [MFREQ]	CS	-0.07	<0.1	-1.26	1.9	-1.39	18.8	1.22	10.8
	LS	0.75	<0.1	-0.99	<0.1	-3.84*	77.4	1.11	5.3
	ML	0.71	<0.1	-1.14	1.0	-2.75	62.1	0.65	<0.1
1/[CFREQ] ³	CS	0.95	<0.1	-1.57	4.5	-1.75	34.0	-1.32	15.8
	LS	0.66	<0.1	-1.04	0.3	-0.89	<0.1	-1.21	10.2
	ML	0.68	<0.1	-1.31	2.2	-1.13	6.6	-1.46	22.2
DISP	CS	-0.82	<0.1	1.45	3.4	1.62	29.0	1.43	20.7
	LS	-0.56	<0.1	0.89	<0.1	0.79	<0.1	1.27	13.5
	ML	-0.60	<0.1	1.18	1.2	1.03	1.5	1.50	23.8

NOTE: + RMS, SPEED, RANGE and MFREQ = root-mean-square value, average speed, peak-to-peak range, and mean frequency of COP displacement; CFREQ and DISP = centroidal frequency and dispersion of COP displacement power spectrum; COP = centre-of-pressure;
 ++ SA = saturation amplitude; CS, LS and ML = cross-spectral, least squares and maximum likelihood models;
 +++ T: T-test for significance of regression; degrees of freedom = 30 for normal groups, 3 for balance-impaired groups; * indicates a significant regression, $p < 0.05$; $p > 0.05$ in all other cases; Ra² is coefficient of determination, adjusted for degrees of freedom.

For the elderly normals, the regression was marginally significant for RANGE, using either the CS or ML model ($p < 0.1$). For this variable, the sign of the regression slopes was opposite to that seen in the young normals. None of the other variables showed any significant linear relation to SA ($p > 0.1$).

Compared to the normal subject results, the regressions of the vestibular patient data tended to show larger R_a^2 values (with the exception of SPEED and SPEED/BOS, for which the regressions produced low R_a^2 values in both groups of subjects). Nonetheless, only MFREQ showed a statistically significant linear relationship to SA. The regression for MFREQ was significant ($p < 0.05$) for the LS model and marginally significant ($p < 0.1$) for the ML model. None of the other variables showed any significant linear relation to SA ($p > 0.1$).

Compared to the normal subjects, the analysis of the elderly faller data tended to show larger R_a^2 values for SPEED, SPEED/BOS, MFREQ, CFREQ and DISP. However, none of the regressions was even marginally significant ($p > 0.2$).

7.2.2 Responses in Normal Subjects

Descriptive statistics and the results of the ANOVA are listed in table 7.7. There was no significant interaction for any of the spontaneous sway measures ($p > 0.1$); therefore, the separate influences of age and sex can be assessed.

Significant age differences were found for SPEED and SPEED/BOS ($p < 0.01$) and for RANGE, RANGE/BOS, DISP and CFREQ ($p < 0.05$). For MFREQ, the age differences were marginally significant ($p < 0.1$), while RMS and RMS/BOS showed no significant age differences ($p > 0.1$). In all of the measures, the estimated mean (i.e. the untransformed value) was higher for the elderly subjects.

Sex differences were significant for RMS ($p < 0.05$), for SPEED ($p < 0.01$), and for CFREQ and DISP ($p < 0.001$). For RANGE, the differences were marginally significant ($p < 0.1$). In all cases, the higher mean values (untransformed) occurred in the males. For RMS, SPEED and RANGE, normalization with respect to BOS eliminated the sex differences ($p > 0.1$).

TABLE 7.7

SPONTANEOUS SWAY: AGE AND SEX DIFFERENCES IN NORMALS

SPONTANEOUS SWAY MEASURE +	MEAN \pm STANDARD DEVIATION ++			
	YOUNG	ELDERLY	MALES	FEMALES
RMS (mm)	4.08 \pm 1.88	4.56 \pm 1.97	4.74 \pm 2.03	3.91 \pm 1.74
RMS/BOS (%)	1.68 \pm 0.790	1.86 \pm 0.785	1.83 \pm 0.781	1.71 \pm 0.800
SPEED (mm/s)	5.08 \pm 3.17	6.20 \pm 2.12	6.42 \pm 3.17	4.86 \pm 1.97
SPEED/BOS (%/s)	2.08 \pm 1.27	2.52 \pm 0.816	2.48 \pm 1.24	2.12 \pm 0.890
RANGE (cm)	2.28 \pm 1.15	3.00 \pm 1.93	2.98 \pm 1.97	2.30 \pm 1.09
RANGE/BOS (%)	9.42 \pm 4.90	12.1 \pm 7.19	11.5 \pm 7.41	10.0 \pm 4.85
MFREQ (Hz/10)	2.22 \pm 0.673	2.59 \pm 0.838	2.44 \pm 0.665	2.37 \pm 0.883
CFREQ (Hz/100)	8.30 \pm 3.46	8.82 \pm 2.53	9.60 \pm 3.84	7.52 \pm 1.23
DISP (/100)	4.34 \pm 1.93	5.31 \pm 1.64	5.70 \pm 1.74	3.94 \pm 1.51

SPONTANEOUS SWAY MEASURE +	AGE	F-VALUES +++	
		SEX	INTERACTION
log [RMS]	1.39	4.35 *	0.354
log [RMS/BOS]	1.31	0.728	0.237
log [SPEED]	7.98 **	7.43 **	0.496
log [SPEED/BOS]	7.50 **	1.95	0.338
log [RANGE]	4.44 *	3.89	1.25
log [RANGE/BOS]	4.29 *	0.813	1.03
log [MFREQ]	3.82	0.385	0.00661
1/[CFREQ] ³	5.31 *	20.7 ***	1.40
DISP	6.11 *	20.3 ***	0.700

NOTE: + RMS, SPEED, RANGE and MFREQ = root-mean-square value, average speed, peak-to-peak range, and mean frequency of COP displacement; CFREQ and DISP = centroidal frequency and dispersion of COP displacement power spectrum; COP = centre-of-pressure;

++ 16 males and 16 females in each age group;

+++ F-VALUES: test for significant differences between means due to age, sex or age-sex interaction; degrees of freedom = 1,60;

* $p < 0.05$, ** $p < 0.01$, *** $p < 0.001$; $p > 0.05$ in all other cases.

7.2.3 Identification of Balance-Impaired Individuals

Table 7.8 lists percentile scores for the vestibular patients and elderly fallers, based on the spontaneous sway measures. The results of the subject classification are summarized in table 7.9.

Two of the five vestibular patients were identified correctly (at the $\alpha = 0.25$ criterion) using either RMS, SPEED, RANGE, RMS/BOS and RANGE/BOS. The remaining sway measures were each able to identify only one vestibular patient as being balance-impaired.

Using either SPEED, SPEED/BOS or MFREQ, four of the five elderly fallers were identified correctly (at the $\alpha = 0.25$ criterion or better). Using DISP, two of the five were identified correctly. The remaining sway measures each identified only one of the five elderly fallers as being balance-impaired.

7.2.4 Validation of the Statistical Models

For the transformed data, the residual plots and/or statistical tests gave no evidence to suggest that the residuals (for the ANOVA and regression analyses described above) were not independent and normally distributed or that the variances were not uniform ($\alpha = 0.05$).

TABLE 7.8

SPONTANEOUS SWAY: CLASSIFICATION OF BALANCE-IMPAIRED SUBJECTS

SUBJECT	PERCENTILE SCORE BASED ON SPONTANEOUS SWAY MEASURE +								
	TIME DOMAIN MEASURES						FREQUENCY MEASURES		
	NON-NORMALIZED			NORMALIZED ++			LOG MFREQ	$\frac{1}{\text{CFREQ}^3}$	DISP
LOG RMS	LOG SPEED	LOG RANGE	LOG RMS	LOG SPEED	LOG RANGE				
vestibular patients:									
V1	88*	76*	91**	81*	69	85*	30	26	71
V2	21	23	22	17	19	18	50	73	29
V3	18	60	22	15	53	19	96**	66	40
V4	99***	99***	99***	98***	99***	99***	87	1***	98***
V5	3	9	4	2	4	2	84	79	22
elderly fallers:									
F1	66	91**	70	70	94**	74	80	39	63
F2	63	96***	59	74	99***	69	92*	16	84
F3	1	16	3	2	20	3	97**	85	15
F4	50	99***	52	52	99***	54	99***	13	91*
F5	91**	99***	86*	92**	99***	88*	98***	4**	97**

NOTE: + RMS, SPEED, RANGE and MFREQ = root-mean-square value, average speed, peak-to-peak range, and mean frequency of COP displacement; CFREQ and DISP = centroidal frequency and dispersion of COP displacement power spectrum; COP = centre-of-pressure; ++ normalization with respect to length of base-of-support; * balance-impaired at $\alpha = 0.25$ criterion, ** at $\alpha = 0.1$, *** at $\alpha = 0.05$ (two-tailed for MFREQ, CFREQ and DISP; one-tailed for other measures).

TABLE 7.9

SPONTANEOUS SWAY: SUMMARY OF SUBJECT CLASSIFICATION ($\alpha = 0.25$)

SPONTANEOUS SWAY MEASURE +	PERCENTAGE OF SUBJECTS CLASSIFIED CORRECTLY ++			
	YOUNG NORMALS	ELDERLY NORMALS	VESTIBULAR PATIENTS	ELDERLY FALLERS
log [RMS]	75	78	40	20
log [RMS/BOS]	78	81	40	20
log [SPEED]	78	72	40	80
log [SPEED/BOS]	78	75	20	80
log [RANGE]	75	81	40	20
log [RANGE/BOS]	72	81	40	20
log [MFREQ]	72	81	20	80
1/[CFREQ] ³	81	72	20	20
DISP	75	66	20	40

NOTE: + RMS, SPEED, RANGE and MFREQ = root-mean-square value, average speed, peak-to-peak range, and mean frequency of COP displacement; CFREQ and DISP = centroidal frequency and dispersion of COP displacement power spectrum; BOS = length of base-of-support; COP = centre-of-pressure;
 ++ percentages based on 32 young and 32 elderly normals, 5 vestibular patients and 5 elderly fallers.

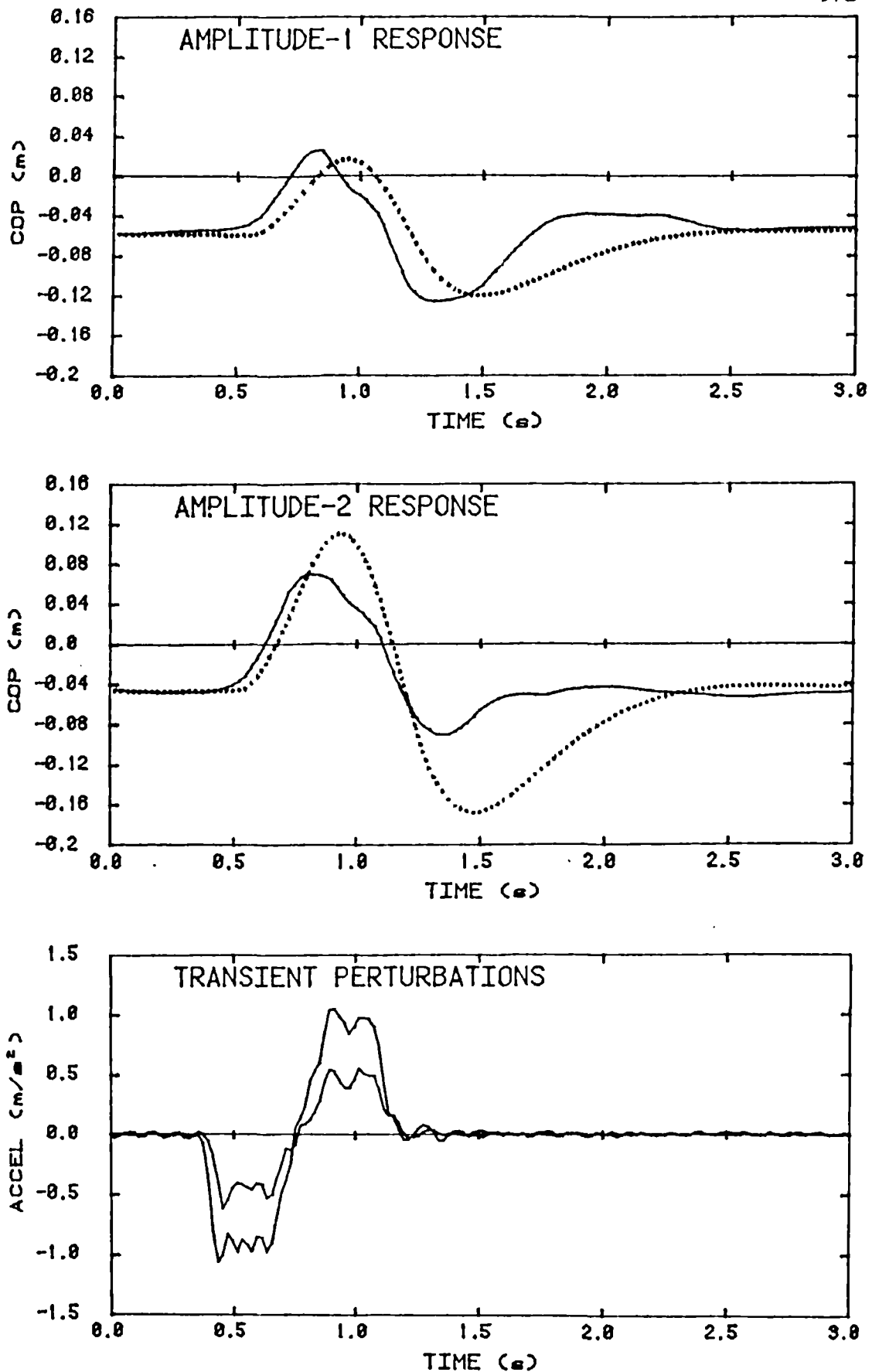


Fig 7.6 Example transient test results: actual and predicted values.

top - COP displacement due to amplitude-1 perturbation (0.5 m/s^2)
 middle - COP displacement due to amplitude-2 perturbation (1.0 m/s^2)
 bottom - amplitude-1 and -2 platform accelerations

Note: solid lines - actual data; dotted lines - predictions using cross spectral model, test-C2 data

7.3 TRANSIENT RESPONSES

Example data from two transient tests are shown in figure 7.6. The data were obtained from tests on the same subject, at pulse amplitudes of 0.5 m/s² and 1.0 m/s². Also shown are examples of the corresponding transient response predictions (CS model, test-C2 data).

To assess whether the desired perturbation amplitudes were consistently achieved in the tests, the mean values and coefficients of variation (standard deviation divided by the mean) were estimated, based on the measured values of the peak backward platform acceleration. Using the acceleration data sampled at 16.7 Hz, the mean amplitudes were 0.496, 0.976 and 1.46 m/s², corresponding to desired amplitudes of 0.5, 1.0 and 1.5 m/s², respectively. The corresponding coefficients of variation were 3.5%, 1.9% and 1.4%. Although the peak values obtained from the data sampled at 100 Hz were linearly related to the 16.7 Hz results ($R_a^2 = 91.2\%$; regression significant at $p < 0.001$), the 100 Hz values were consistently higher. Using the 100 Hz data, the mean amplitudes were 0.776, 1.20 and 1.63 m/s². The corresponding coefficients of variation were 12.8%, 7.8% and 5.1%.

7.3.1 Dependence of Actual Response on Perturbation Amplitude

Table 7.10 summarizes the results of the linear regression analysis of response "gain" (peak forward COP displacement divided by peak backward platform acceleration) versus perturbation amplitude (peak backward platform acceleration). The analyses were limited to the lowest three perturbation amplitudes, as no subjects were able to maintain balance in any tests at the higher amplitudes. The results shown in the table (and discussed below) were obtained using the acceleration data that were sampled at 16.7 Hz. Very similar results were achieved using the data that were sampled at 100 Hz.

In the full regression model, each subject was allotted an individual slope and intercept. Compared to the full model, a reduced model having only a single common slope was significantly

TABLE 7.10

TRANSIENT RESPONSE: REGRESSION VERSUS PERTURBATION AMPLITUDE

REGRESSION	R _a ² (%) +	POOLED SLOPE	F-VALUES	
			ZERO SLOPE ++	COMMON SLOPE +++
<u>FULL MODEL +++++</u>				
gain vs amplitude +++++	87.8	-0.0600	35.5 ***	3.98 ***
log [gain] vs log [amplitude]	92.2	-0.508	57.0 ***	4.08 ***
gain vs 1/√amplitude	91.0	0.105	49.9 ***	4.75 ***
<u>REDUCED MODEL</u>				
gain vs amplitude	81.1	-0.0707	532. ***	
log [gain] vs log [amplitude]	87.8	-0.521	881. ***	
gain vs 1/√amplitude	84.9	0.106	697. ***	

NOTE: + R_a²: coefficient of determination, adjusted for degrees of freedom;
 ++ test for zero slope is equivalent to test for significance of regression; degrees of freedom = 26 and 111 for full model, 1 and 136 for reduced model;
 +++ test for common slope: degrees of freedom = 25 and 111;
 +++++ full model fits a separate slope and intercept for each subject; reduced model fits a single common slope;
 +++++ gain = [peak COP displacement (m)]/[peak acceleration (m/s²)]; amplitude = peak acceleration (m/s²);
 *** indicates p<0.001; p>0.1 in all other cases.

poorer in accounting for the variation in the data ($p < 0.001$). Nonetheless, even in the reduced model, the test for zero slope was significant ($p < 0.001$), indicating a linear relationship between response gain and perturbation amplitude. The pooled regression slope was negative; therefore, on the average, the gain decreased with increasing perturbation amplitude.

Regression of the logarithm of the response gain versus the logarithm of the amplitude revealed a significant linear relationship ($p < 0.001$), with a pooled slope approximately equal to -0.5 . This result implies that the relationship between gain and perturbation amplitude is an inverse square root function. Indeed, regression versus the inverse square root of the acceleration yielded increases in both the R_a^2 and F-values, compared to the linear function. However, the hypothesis of a common slope was still rejected ($p < 0.001$).

7.3.2 Comparison of Actual and Predicted Responses

Table 7.11 lists descriptive statistics for the percentage error between the actual and predicted values of the peak COP displacement, as a function of the perturbation amplitude. As above, the analysis was limited to the lowest three perturbation amplitudes. Note that the CS-model predictions were derived using the acceleration data that were sampled at 100 Hz, whereas the LS- and ML-model predictions were derived using the data that were sampled at 16.7 Hz (see Section 6.8).

The ANOVA and pairwise comparisons confirmed the results that seem evident in the tabulated statistics, namely that: (1) the best agreement was achieved at the smallest transient perturbation amplitude, and (2) the percentage error grew larger as the perturbation amplitude was increased. Regardless of the model (CS, LS or ML) or the data (test-C2 or "best" test) used to estimate the model, the ANOVA demonstrated highly significant differences between the mean percentage error values at the three perturbation amplitudes ($p < 0.001$). The pairwise comparisons indicated that all three mean values were significantly different from each other

TABLE 7.11

COMPARISON OF ACTUAL AND PREDICTED TRANSIENT RESPONSE

MODEL FOR PREDICTIONS +	PERTURBATION AMPLITUDE (m/s ²) ++	PERCENTAGE ERROR BETWEEN PREDICTED AND ACTUAL RESPONSE +++	
		MEAN ± SD +++++	RANGE
<u>TEST C2</u>			
CS model	0.5	18.2 ± 20.6	-21.0 : 77.3
	1.0	70.5 ± 27.0	18.8 : 139.
	1.5	102. ± 26.1	59.8 : 143.
LS model	0.5	14.4 ± 20.3	-25.2 : 90.0
	1.0	66.7 ± 25.3	18.3 : 135.
	1.5	92.7 ± 27.0	39.9 : 152.
ML model	0.5	13.2 ± 21.1	-26.0 : 91.5
	1.0	64.9 ± 26.3	16.8 : 132.
	1.5	89.4 ± 27.6	38.3 : 144.
<u>"BEST" TEST</u>			
CS model	0.5	17.8 ± 21.2	-18.3 : 84.1
	1.0	69.5 ± 24.5	23.1 : 133.
	1.5	100. ± 24.0	61.5 : 138.
LS model	0.5	15.6 ± 20.6	-18.1 : 92.7
	1.0	69.0 ± 25.6	23.4 : 148.
	1.5	94.1 ± 26.4	47.6 : 147.
ML model	0.5	13.7 ± 20.7	-20.9 : 89.7
	1.0	66.2 ± 26.6	20.5 : 152.
	1.5	89.9 ± 26.7	44.0 : 148.

NOTE: + CS, LS and ML = cross-spectral, least squares and maximum likelihood models;
 ++ amplitude of backward acceleration pulse;
 +++ % error in peak COP displacement =
 (100%)(predicted peak - actual peak)/(actual peak);
 +++++ mean and standard deviation (SD) estimates based on 71, 60 and 32 tests for amplitudes 0.5, 1.0 and 1.5 m/s², respectively.

($p < 0.01$). The data in figure 7.6 serve to further illustrate the effects of increase in perturbation amplitude.

7.3.3 Functional Definition of the Base-of-Support

Table 7.12 displays results from the stepwise regression of peak anterior COP displacement (in those tests in which heel-lift was observed) versus foot dimensions. Separate analyses were performed for: (1) right COP and right foot dimensions, (2) left COP and left foot dimensions, and (3) overall COP and average foot dimensions.

In each iteration of the stepwise regression, the variable with the largest F-value was added to the model, and the F-values of the variables already in the model were recalculated. Each F-value indicates whether the coefficient (i.e. the slope) is significantly different from zero.

The table shows the results of the first three iterations. In all of the analyses, the length of the foot was the dominant variable. Using foot-length as the only independent variable, the regression models accounted for approximately 80% of the variation in the peak COP values. Furthermore, the regressions were highly significant ($p < 0.001$). The offsets (*y-intercepts*) were not significantly different from zero, indicating a proportional relationship between foot-length and the functional length of the BOS ($p > 0.05$).

Inclusion of additional variables yielded no significant improvements in the regression models, as evidenced by the small F-values associated with the added variables ($p > 0.05$) and by the lack of improvement in the R_a^2 values. (Note that the R_a^2 values were adjusted for degrees-of-freedom so as to yield approximately unbiased estimates of the population R^2 despite changes in the number of parameters in the regression model.)

7.3.4 Validation of the Statistical Models

Plots of the residuals for the ANOVA and regression models used in the above analyses gave no indication that the residuals were not independent and normally distributed or that the variances

TABLE 7.12

STEPWISE REGRESSION: MAXIMUM CENTRE-OF-PRESSURE DISPLACEMENT
VERSUS FOOT DIMENSIONS

MODEL	OFFSET +		R _a ² (%) ++	F-VALUE +++	REGRESSION VARIABLES +++++		
	COEFF	F-VALUE			VARIABLE	COEFF	F-VALUE
<u>OVERALL CENTRE-OF-PRESSURE</u>							
1	-0.0153	0.980	81.4	229. ***	L	0.947	229. ***
2	-0.0169	1.19	81.4	114. ***	L MT1	1.12 -0.206	34.6 *** 0.9
3	-0.0217	1.44	81.1	75.3 ***	L MT1 L-A	0.967 -0.190 0.203	8.1 ** 0.7 0.3
<u>LEFT CENTRE-OF-PRESSURE</u>							
1	-0.00948	0.348	79.0	197. ***	L	0.923	197. ***
2	-0.0123	0.578	79.3	101. ***	L MT1	1.09 -0.197	55.8 *** 1.6
3	-0.0154	0.672	78.9	66.0 ***	L MT1 MT5	1.08 -0.224 0.0701	51.7 *** 1.7 0.1
<u>RIGHT CENTRE-OF-PRESSURE</u>							
1	-0.0229	2.28	82.8	252. ***	L	0.980	252. ***
2	-0.0272	2.82	82.7	125. ***	L MT1-A	0.903 0.173	64.3 *** 0.7
3	-0.0240	2.04	82.5	82.9 ***	L MT1-A MT5	0.967 0.170 -0.121	46.1 *** 0.6 0.5

NOTE: + offset (or y-intercept) is constant term in regression; units = m; F-value tests whether offset is non-zero, degrees of freedom = 1,50;
 ++ R_a²: coefficient of multiple determination, adjusted for degrees of freedom;
 +++ F-value: test for significance of regression; degrees of freedom = m,51-m where m = number of independent variables;
 +++++ variables: L = length of foot; A, MT1 and MT5 = distances between ankle, first metatarsal head and fifth metatarsal head from back of foot, respectively; dimensions of left foot used in analysis of left COP, dimensions of right foot used in analysis of right COP, average dimensions used in analysis of overall COP; coefficients (i.e. slopes) are dimensionless; F-value tests for non-zero slope, degrees of freedom = 1,51-m; COP = centre-of-pressure;
 *** indicates p<0.001; ** indicates p<0.01; p>0.1 in all other cases.

were not uniform. For the comparison of actual and predicted transient responses, plots of percentage error versus perturbation amplitude gave no reason to suspect serious subject-amplitude interaction.

CHAPTER 8. DISCUSSION

8.1 RATIONALE FOR THE EXPERIMENTAL AND ANALYTICAL METHODOLOGY

8.1.1 The Test Perturbation

The rationale behind the selection and design of the test perturbation was discussed in detail in Chapters 3 and 5. The major points are summarized here.

Direct simulation of the transient perturbations that actually cause falls was rejected, because of potential safety problems and the possibility of inducing anticipatory adaptations that would not occur in actual falls. Instead, a continuous waveform was used in the balance test. To simulate the unpredictable nature of fall-provoking perturbations, a pseudorandom (PRN) waveform was selected. PRN waveforms are preferred to random (RAN) waveforms, because RAN tests require longer measurement times in order to "average out" the inherent statistical variability. Furthermore, because PRN waveforms are "self-windowing", truncation error ("leakage") is avoided. By designing the PRN signal to comprise a small number of frequency components, none of which were small-integer multiples, it was possible to minimize harmonic and intermodulation distortion (due to nonlinearity in the posture control system) in the linear transfer function estimates. In selecting the power spectrum, bandwidth, amplitude and duration of the test perturbation, consideration was given to the need for persistent excitation, accurate system identification, stationarity, and subject safety and tolerance.

Although the same spectrum, bandwidth and duration were selected for all subjects, the most appropriate perturbation amplitude was expected to be subject-dependent. In general, the perturbation amplitude should be as large as possible, within the constraints of subject safety and tolerance, in order to maximize the signal-to-noise ratio in the measurements and to minimize the influence of sensory threshold nonlinearities. In addition, if the assumed linear sub-saturation operating range of the posture control system is in fact substantially nonlinear, then it may be desirable to maximize the perturbation amplitude in order to minimize errors in the prediction of large-amplitude transient

response (see Section 8.6.5). The testing protocol was designed to iterate toward the most appropriate amplitude for each subject, starting with a conservatively small value estimated from the pilot tests.

8.1.2 The Testing Procedures

The testing procedures were detailed in Section 6.3. The rationale is presented here.

The subjects were tested unshod so as to eliminate variability due to differences in footwear. The tests were performed in stocking feet, rather than barefoot, for subject comfort and hygiene (no problems with slipping were observed). Forcing subjects to adopt an arbitrary test position might interfere with balancing responses, as well as causing discomfort; therefore, subjects were allowed to select their foot spacing and angulation. Foot tracings were used to detect changes from the initial foot position and to allow the same positioning to be repeated in subsequent tests.

Although initial posture could not be controlled rigorously, a standard set of instructions was given prior to each test in order to minimize variation, particularly, *attempts to increase stability through gross changes such as crouching*. The subjects were instructed to hold their arms at their sides so as to minimize the tendency to wave the arms or touch the safety handrails. To ensure consistent test-to-test and subject-to-subject visual and vestibular input, the subjects were instructed to look straight ahead, using a poster as a visual target.

"Muzak" ® (i.e. bland monotonous background music) was played (through headphones) to mask auditory cues from the platform motor, as well as distracting sounds from the laboratory environment. The music was also intended to relax the subjects and to distract them from making voluntary modifications to their balancing responses. In order to prevent possible music-induced increases in spontaneous sway (e.g. Edwards, 1947), music was not played during the spontaneous sway tests, although the headphones were still worn so as to muffle external noises.

Fatigue-related changes in response were minimized by allowing

seated rests between tests and by limiting the length of each test (5 minutes for RAN tests, 3 minutes for PRN tests) and the length of each testing session (maximum of 60 minutes for the young subjects, 30 minutes for the elderly subjects).

For safety, the subjects were warned in advance that the platform would begin to move. In the transient tests, the warning-test interval was controlled to vary in a random manner (between 3 and 8 s), in order to minimize anticipatory manoeuvres.

8.1.3 The Experimental Protocol

The protocol included a spontaneous sway test, a PRN learning test, PRN tests at two different amplitudes and a RAN test. All of these tests were performed with eyes open (EO). In addition, a blindfolded (BF) test was performed, using the PRN waveform. A different waveform realization was used in each PRN test in order to maximize unpredictability. The primary goal of the present experiments was to detect inter-subject differences; therefore, all subjects were tested using the same protocol, without randomizing the order of the tests. Randomization of test order would be necessary to allow true test-related differences to be completely distinguished from "order effects" (i.e. adaptation, fatigue); however, this might tend to mask the inter-subject differences.

Spontaneous sway was measured to allow the balance test responses to be compared to more traditional measures of postural stability. The PRN learning trial was included to allow the subjects to gain familiarity with the test procedure and the testing environment. Because substantial changes in postural "set" (e.g. tonic levels of muscle co-contraction) were expected to occur between the first test and subsequent tests, the learning trial prevented this source of variability from affecting the results of the study. The protocol was designed to iterate safely toward the most appropriate amplitude for each subject, by starting with a conservatively small amplitude (based on pilot results) and then either increasing or decreasing the amplitude of subsequent tests, depending on the tolerance of the subject. The RAN test was included to ensure that there were no sharp peaks or troughs in the

frequency response of the posture control system that might pass undetected in the PRN tests, as a result of the larger intervals between the frequency components in the PRN signal. Although it was recognized that a thorough investigation of the effects of changes in visual conditions was beyond the scope of the present work, a blindfolded test was included to obtain some preliminary information about the influence of vision on the balance test responses.

In addition to the tests described above, the young normal subjects were tested using transient waveforms. The objective of these tests was to provide data that would allow: (1) the ability of the continuous-waveform tests to predict transient response to be evaluated, (2) the actual linearity of the posture control system over the assumed linear (i.e. sub-saturation) operating range to be assessed, and (3) functional definitions for the base-of-support (BOS) to be explored. For safety reasons, the elderly subjects were not tested. Furthermore, only backward platform translations were used. These perturbations are safer than forward translations because they cause the subjects to pitch forward, in which case it is much easier to grab the safety handrail. As a further safety precaution, the perturbation amplitudes were tested in ascending order, stopping when the subject could no longer maintain balance.

8.1.4 The Methods of Analysis

In order to determine the balance test "score" (i.e. the saturation amplitude, SA), an input-output model was estimated from the balance test data and then used to predict the peak centre-of-pressure (COP) response to a unit transient pulse in platform acceleration. The SA was calculated by relating the predicted peak COP response (ΔCOP) to the length of the BOS. The SA represents the pulse amplitude at which the resulting COP displacement would saturate (or equal the length of) the BOS (assuming that the initial COP location was at the opposite end of the BOS).

Typically, transient behaviour is characterized by the response to an impulse or step input. Neither is a realistic

simulation of actual postural perturbations. An acceleration impulse would require an infinite accelerating force; an acceleration step represents an ever-increasing ramp in velocity. Furthermore, the peak step response reflects only some of the dynamic characteristics of the control system. For example, in a second order system, the peak step response is independent of the natural frequency of the system. Whereas an acceleration impulse is equivalent to a velocity step, an acceleration pulse produces a less abrupt, ramped change in velocity. Thus, for example, an acceleration pulse might approximate a slip or a trip, where there is a sudden (but not instantaneous) change in the relative velocity between the feet and the upper body. Based on these considerations, the SA was defined in terms of a pulse acceleration input. Note that the selected pulse duration (0.06 s) would excite the system over the same frequency range used in the PRN balance test, since a pulse of this duration has a power spectrum that is flat up to approximately 5 Hz (e.g. Doebelin, 1980).

Although the COP on each foot may saturate its BOS independently, the ability to generate stabilizing ankle moments or shear forces during the balance test will not be fully compromised until both feet saturate; therefore, the SA was defined using the overall COP, rather than analyzing each foot separately. The length of the BOS was defined as the average foot length, since analysis of the transient tests failed to provide a more accurate functional definition. Although many of the predicted transient responses showed a small return overshoot in the COP response (i.e. a small sway in the direction opposite to the initial sway response), the overshoot was much smaller than the initial COP displacement and was therefore less likely to cause BOS saturation; hence, the SA estimates were based on the initial COP displacement alone. See Section 8.6.4 for a further discussion of the SA estimation methodology.

By modelling the posture control system as a linear transfer function cascaded with a saturation-like nonlinearity, the problem of quantifying postural stability was reduced to a linear system identification problem. This is important because linear models have a tremendous advantage over nonlinear models in terms of

analytical simplicity and ease of interpretation.

Three methods were used to identify the linear input-output model from the balance test data. The cross-spectral (CS) method involved estimation of the nonparametric frequency response. Plots of the frequency response were useful in checking the data for obvious errors and in determining appropriate parametric model structures. To allow prediction of pulse response, the frequency response was fitted with a parametric transfer function model, using the coherence function as a weighting factor. For the RAN and "non-harmonic" PRN inputs used here, the coherence indicates (at least approximately) the relative amount of "noise" in the output (see Appendix B) and therefore reflects the degree of confidence in the frequency response estimate at each frequency.

The CS method is an example of the "classical" frequency response approach to system identification. In recent years, a plethora of sophisticated, parametric, time-domain methods has appeared (e.g. Eykhoff, 1982). The data were re-analyzed using two of these methods, least squares (LS) and maximum likelihood (ML), to determine whether the CS results could be improved.

Much of the recent work in the system identification field has been highly theoretical, and relatively few discussions of practical engineering applications are available. Åström and Wittenmark (1984), in reviewing the several studies that have attempted to compare the different system identification methods, concluded that there is no method that is universally best and that the choice of method is not crucial. Their recommendations included the ML method. The LS method is useful for generating the initial parameter estimates required for the ML method, and can be used as a system identification method in its own right, although estimation errors are likely to arise due to correlation in the residuals (Hsia, 1978).

The form of the model used in the CS method (i.e. a rational, polynomial, Laplace-domain transfer function cascaded with a dead-time element) is justified in Appendix A.1.1. The form of the discrete-time model used in the LS and ML methods can be derived from the Laplace-domain model using the bilinear transform approximation.

A number of methods exist for determining the most appropriate model structure, i.e. equation order and dead time (e.g. Söderström, 1977). The Akaike method was chosen because of its simplicity. The Akaike criterion (AIC) avoids the problem of "overfitting" by penalizing model complexity. Although the theoretical development of the AIC has been rooted in the time domain, the same method was applied in fitting the parametric transfer function to the nonparametric frequency response estimates (CS method).

The Akaike method requires comparison of the candidate model structures. Upper bounds for the equation order and dead time were estimated through inspection of the nonparametric frequency response plots. For the LS and ML methods, the maximum equation order was set at a higher value (i.e. the limit imposed by the system identification software) in order to "whiten" the residuals, if necessary (Hsia, 1978).

See Section 8.6.3 for a further discussion of the system identification methods.

8.2 BALANCE TEST RESPONSES

8.2.1 Age and Sex Differences in Normal Subjects

Because of the physiological changes that are known to occur in ageing (e.g. decrease in nerve conduction velocity; deterioration of visual, vestibular and somatosensory function; reduction in muscle strength), one would expect to find age-related differences in postural stability (see Section 2.4.2). Accordingly, deterioration in balancing synergies (Woollacott et al, 1982a, 1982b and 1986; Wolfson et al, 1986), increased sway in response to rotational platform perturbations (Holliday and Fernie, 1985), and increase in spontaneous postural sway (Sheldon, 1963; Hasselkus and Shambes, 1975; Black et al, 1977; Overstall et al, 1977; Fernie and Holliday, 1978; Era and Heikkinen, 1985; Hayes et al, 1985) have been demonstrated in elderly subjects.

In general agreement with these findings, the present experimental results did in fact demonstrate highly significant differences between young and elderly normals, with reduced stability (i.e. smaller SA) predicted for the elderly under both EO

and BF conditions. Analysis of variance (ANOVA) of the dead-time parameter in the CS model showed significantly higher values in the elderly subjects (e.g. mean of 0.117 s versus 0.091 s in test C2; $p < 0.001$). Simulations demonstrated that small increases in dead time can lead to substantial decreases in SA (see Appendix A.3.4); therefore, at least some of the age-related differences in SA can be attributed to the slowing of the postural responses. The simulations also demonstrated that age-related changes in height and weight and/or reductions in feedback gain could also contribute to a decrease in SA in the elderly.

Whereas some investigators have found eyes-closed balance tests to show greater age dependency (Potvin et al, 1980), others have found eyes-open tests to be a more sensitive measure of the effects of ageing (Stones and Kozma, 1987). Although the present results did find highly significant age differences in both EO and BF tests, the significance levels were in fact substantially higher in the EO condition.

Although sex-related differences in the sensorimotor subsystems are well known (e.g. lower muscle strength in females), the influence of sex on overall postural performance is poorly documented. A review of the literature failed to find any perturbation studies that have rigorously examined this issue. As discussed later in Section 8.3.3, most spontaneous sway experiments have found no significant sex differences, or have failed to analyze this factor. In one of the few studies to report significant sex differences, Overstall et al (1977) found increased spontaneous sway in females; however, it is not clear to what extent their measure of sway ("total angular movement" at the waist, a-p direction) can be used to compare the postural stability of subjects of differing body dimensions. Moreover, some of the sex differences that they observed could be due to the larger proportion of fallers included in the female subject group.

Epidemiological evidence suggests that elderly females have a higher incidence of falls than males (see Section 2.4.3); however, this finding is not necessarily indicative of the postural stability in normal nonfallers.

The present experimental results showed no significant differences in the SA of the normal males and females. Although males did in fact exhibit a higher mean value for ΔCOP (the peak COP displacement in the predicted unit pulse response), the sex-related differences were eliminated in calculating the SA, by relating ΔCOP to the length of the BOS.

8.2.2 Comparison of Tests

Test-related differences in response may occur as a result of changes in the test conditions, i.e. visual stimulus, perturbation amplitude and perturbation waveform. Alternatively, changes in balancing strategy (i.e. postural synergy, initial posture or tonic postural "set") or voluntary movements may cause test-to-test variation that is unrelated to the test conditions. If these changes occur in a random manner, they will tend to mask true inter-test differences. If the changes occur systematically (due to adaptation or fatigue), then true test-related differences will be distorted. Because of the potential for systematic "order effects" in the present protocol, caution must be exercised in analyzing test-to-test differences.

Caution must also be exercised because of statistical considerations. Because there was only one observation per "cell", subject-test interaction could not be included in the ANOVA model. However, Tukey's test for interaction showed that there was in fact significant subject-test interaction for the young normal subjects. Failure to account for this interaction in the ANOVA model means that the statistical tests are less likely to detect test-to-test differences that do exist (Neter et al, 1985c). On the other hand, any significant differences that are detected will be valid, in an average sense. There may, however, be substantial subject-to-subject differences.

The results showed significantly higher SA values in the RAN and BF tests (tests C4 and C5, respectively) for both the young and the elderly normal subjects. The results of the BF tests will be discussed in detail in the next section. The RAN and PRN results are expected to differ, due to waveform-dependent differences in

the transfer function estimation errors. These errors are discussed in detail in Section 5.3.1 and in Appendix B.

The RAN tests were included to ensure that there were no sharp peaks or troughs in the frequency response that might pass undetected in the PRN tests. Visual inspection of the RAN-test frequency response plots showed no evidence of sharp peaks or troughs for any of the subjects tested; therefore, the PRN-test results were judged to be reliable in this regard.

In comparing the PRN tests, it should be noted that a different realization of the PRN waveform was used in each PRN test (in order to maximize unpredictability). If the sub-saturation postural responses are substantially nonlinear, then the SA estimates may be dependent on the particular waveform realization used in the test (see Section 8.6.5). In order to minimize the influence of system nonlinearity, the PRN realizations were designed for minimum peak factor. Moreover, the peak factor was approximately the same for all of the different realizations. Thus, it seems unlikely that the differences in waveform realization would lead to significant test-to-test differences in the SA estimates.

For the elderly normals, the results showed no significant differences between the three PRN tests: the learning test, the "amplitude 1" test and the "amplitude 2" test (tests C1, C2 and C3, respectively). The failure to detect significant differences cannot be attributed to subject-test interaction, as these subjects showed no significant interaction. Note that three of the elderly subjects were tested at a lower amplitude in test C3 because they executed compensatory motions in test C2; therefore, comparison of tests C2 and C3 will not give a valid assessment of the influence of perturbation amplitude.

For the young normals, the results showed significant differences between tests C1 and C3 or between tests C2 and C3, depending on the system identification model. These results are valid, but because of the subject-test interaction, other differences may have gone undetected. All of the young normals

were tested at the mid-range amplitude in tests C1 and C2, and at the highest amplitude in test C3. Hence, the test-to-test differences may be a result of the differences in amplitude (indicating nonlinearity in the posture control system and/or amplitude-dependent adaptations). Alternatively, the differences may be due to order effects.

The differences in the findings for the young and elderly subjects may be due to a greater tendency for the young subjects to modulate their balancing responses in accordance with their expectations of the postural threat (see Section 8.6.6). Conceivably, the same level of modulation does not occur in the elderly because the perceived postural threat remains high in these subjects, in spite of repeated testing or changes in amplitude.

A small number of subjects executed compensatory motions during the tests (i.e. two young normals in test C1, one in test C3 and two in test C4; one elderly normal in test C1, three in test C2, six in test C3, one in test C4 and two in test C5). Any compensatory motions will tend to degrade the SA estimates; however, in all of the cases cited here, the manoeuvres were judged to be relatively minor and of short duration (e.g. lifted heels or touched handrail momentarily). If the manoeuvres had been more extensive, then the results would have been excluded from the analysis.

8.2.3 Influence of Vision

The experiments demonstrated an increase in predicted stability in the BF test. Approximately 85-90% of the normal subjects showed an increase in SA when blindfolded, and the mean BF SA was found to be significantly larger than the mean EO SA. Since the increases in SA when blindfolded (test C5) were generally much larger than the differences between the other PRN test results (tests C1, C2 and C3), it seems unlikely that "learning" effects are the reason for the improvement. Because stability actually increased in the later BF test, fatigue is not a reasonable explanation, either.

Possibly, subjects overcompensate for the loss of visual input by increasing the "stiffness" of the posture control system,

through increases in the gain of the vestibular and somatosensory feedback or through various other mechanisms. Increases in reflex gain under visual deprivation have in fact been demonstrated (Ishida and Imai, 1980; Ishida and Miyazaki, 1985). Alternatively, the overcompensation for loss of vision might result from changes in balancing synergy. It is interesting to note that similar overcompensations have been reported for other sensorimotor deficits, e.g. the finding that unilateral below-knee amputees sway less than normal subjects (Gauthier-Gagnon et al, 1986; Vittas et al, 1986); similar mechanisms may be involved. The modulation of balancing responses is discussed further in Section 8.6.6.

An alternative explanation lies in the conflict between the otoliths and the other sensory modalities that occurs during the balance test, as discussed in Chapter 3 (see also Section 8.6.1). Experiments in which visual feedback was either "nulled out" or "enhanced" (through servo-control of the visual surround) have demonstrated that unexpected incongruence between visual and other sensory modalities can lead to attenuation of muscle responses (Nashner and Berthoz, 1978). Accordingly, if the otoliths do in fact contribute to rapid balancing responses, then the otolith-vision conflict could conceivably lead to decreased stability during eyes-open tests.

In disagreement with the present results, spontaneous sway studies have shown that eye closure results in increased sway in most normal subjects, in terms of COP displacement (e.g. Black et al, 1982) or displacement of the body (e.g. Dornan et al, 1978). Perturbation experiments have also found increased body sway and/or COP displacement when vision is deprived (e.g. Ishida and Imai, 1980; Andres, 1982; Tokita et al, 1984). The disagreement in results may be due to differences in: (1) the measured response variables (body sway does not necessarily correlate with COP displacement), (2) the order of testing, (3) the perturbation characteristics, (4) the instructions given to the subjects, (5) the postural "set" or "stiffness" of the subjects (which may depend on (2), (3) and (4)), and/or (6) the visual conditions. With regard to visual conditions, the present test protocol differed from that typically used in other perturbation

experiments, in that the visual field moved with the platform and vision-deprivation was achieved by means of a blindfold.

As discussed above, the moving visual field creates a conflict between the vestibular otoliths and the other sensory modalities. In moving-platform tests that use a stationary field, the otolith and visual inputs "agree", but the absolute-motion information provided by these sensors now "conflicts" with the relative-sway information provided by the somatosensory and semicircular canal inputs. This type of test might simulate the "sensory context" of falls occurring during gait or in riding a moving vehicle (while looking at the stationary external environment). Balancing strategies that subjects have learned to deal with these situations may differ considerably from their responses to perturbations during stationary stance. These differences may account for some of the disagreement in experimental results. See Section 8.6.1 for a further discussion of this issue.

If subjects are allowed to view both the platform and the surrounding stationary environment, then they have sufficient visual information to distinguish the platform motion from their own sway. This additional information may facilitate anticipatory improvements in balancing performance. Analogous results have been described in visual tracking experiments, where adaptive responses occur when subjects are presented with displays of the target trajectory, in addition to displays of tracking error (Sheridan and Ferrell, 1981a). In a balance test, the additional visual information may allow subjects to determine the limits of the range of platform motion and to thereby predict when changes in direction are about to occur (in point of fact, subjects may be able to estimate the limits of platform motion by viewing the stationary environment alone, and may not need to see the platform itself).

In visual deprivation tests, the method by which vision is deprived would seem to be important. Stiffening compensations may diminish in tests which rely on voluntary eye-closure, rather than blindfolding, as subjects are aware that they can easily restore visual input by opening their eyes should they feel that their balance is threatened.

The EO/BF ratio was found to be significantly lower in the normal elderly subjects, compared to the young normals (test-C2 data, LS and ML models). Although, on the average, both EO and BF results were lower in the elderly subjects, the age-related decrease was disproportionately larger for the EO test. This finding could be a result of the deterioration in vision that occurs in ageing. The elderly subjects were in fact found to have significantly poorer visual acuity ($p < 0.01$; mean of 20/35 in the elderly subjects, 20/25 in the young subjects; Snellen visual acuity score, better eye, with corrective lenses if normally worn). Alternatively, the result may be due to age-related differences in response modulation, e.g. elderly subjects may tend to stiffen more than young subjects when deprived of vision (see Section 8.6.6). In contrast to the present results, Dornan et al (1978) found no age-related differences in the EO/BF ratio, in their measurements of spontaneous body sway.

Blindfolding tended to reduce the coherence in the frequency response estimates. The decreases in coherence when blindfolded may reflect increases in extraneous movements unrelated to the perturbation (e.g. spontaneous sway).

8.2.4 Balance Test Responses in the Balance-Impaired Groups

For the vestibular patients and elderly fallers, failure to detect significant test-to-test differences may be due, in part, to the small numbers of subjects tested. Nonetheless, the vestibular patients tended to show results that were similar to those observed in the normals, with larger SA values in tests C4 and C5. In contrast to the normals, however, the mean SA in test C1 was large and, as a result, did not differ significantly from tests C4 and C5. For the elderly fallers, the analysis was limited to tests C1, C2 and C5. For these subjects, the most striking result was the similarity between the mean SA estimates for the EO (test C2) and BF (test C5) tests, in contrast to the strong influence of blindfolding seen in the other subject groups.

One vestibular patient (test C3) and one elderly faller (tests C1, C2 and C5) executed compensatory motions during the tests. With one exception, the manoeuvres were judged to be

relatively minor and of short duration, as was the case for the normal subjects. In test C1 for elderly faller F2, however, the manoeuvres were more extensive; hence, this result was excluded from the analysis.

With the exception of one vestibular patient, the eyes-open balancing performance of the balance-impaired subjects was similar to that of the normal subjects. The major differences between the subject groups appeared in the BF tests and in the EO/BF ratio. Note that the small numbers of subjects in the balance-impaired groups severely limit the statistical power (i.e. the ability to detect differences) with which the subject groups can be compared. For this reason, the statistical analyses focussed on the identification of the balance-impaired subjects on an individual basis.

Nonetheless, t-test comparisons of the subject groups were performed. These analyses failed to show any significant differences between the vestibular patients and the young normals ($p > 0.1$). In comparing the elderly fallers to the elderly normals, no significant differences were found for the EO or BF data. However, because the elderly fallers failed to show a strong increase in SA when blindfolded, the mean EO/BF ratio was found to be significantly higher in these subjects (e.g. test C2, ML model; $p < 0.05$).

Although four of the five elderly fallers showed an increase in SA when blindfolded, the changes were very small. In fact, on the average, there was no significant difference between the EO and BF tests for the elderly faller subjects ($p > 0.1$), in contrast to the other subject groups (who performed better in the BF tests). The fallers all had relatively normal EO results, but four of the five tended to show sub-normal performance in the BF tests.

The above results can be explained in terms of deteriorated vision, deterioration in the nonvisual neural and sensorimotor subsystems, or a combination of the two factors.

(1) In the case of deteriorated vision, fallers may be forced to rely almost entirely on nonvisual feedback, but may be able to achieve relatively normal levels of eyes-open performance by means of stiffening

compensations. The presence or absence of visual inputs would have little effect on the postural performance.

(2) Alternatively, stiffness increases during eyes-open tests (to compensate for visual and/or nonvisual deterioration) may limit the degree to which further stiffening can occur when blindfolded.

(3) As a third possibility, fallers may actually increase their use of visual inputs to compensate for deterioration in the nonvisual subsystems. When vision is deprived, the same compensatory increase in feedback gain occurs as in normal subjects; however, the postural performance is now limited by the deterioration in the nonvisual sensorimotor subsystems, and the fallers are unable to achieve the overcompensation that occurs in normals.

This last explanation, i.e. that fallers have an increased reliance on visual inputs, is supported by the results of visual perception experiments, which found that fallers' perceptions of horizontality and verticality were more likely to be influenced by misleading visual cues, compared to nonfallers (Tobis et al, 1985).

The visual tests showed deteriorated visual acuity in the faller subjects. All five fallers were 20/40 or worse and two were poorer than 20/200 (Snellen visual acuity score, better eye, with corrective lenses if normally worn). In contrast, the mean acuity in the elderly normals was 20/35, with scores ranging from 20/20 to 20/100. These results would seem to contradict the argument above that fallers may have an increased reliance on visual inputs. If the fallers did in fact show a greater reliance on less accurate visual inputs, one might expect to see poorer performance in the EO tests, which was not the case. Note, however, that the vision tests performed here assessed only the static acuity, and did not assess the ability for visual motion detection. Furthermore, only central-field vision was tested. Peripheral vision may in fact play a more important role in postural control (see Section 2.1.4.3).

Four of the five vestibular patients showed an increase in SA when blindfolded. Compared to the elderly fallers, however, these

subjects showed a much greater degree of inter-subject variation. Of the three vestibular patients who were identified correctly, one subject performed poorly in both EO and BF tests, while the other two showed abnormal results only in the EO/BF ratio.

Although patients with vestibular deficits might be expected to show exaggerated balance impairment when blindfolded, due to an increased reliance on vision (Bles and deJong, 1986), increased utilization of somatosensory inputs can often mask the deficit. For example, Nashner et al (1982) found that differences in the spontaneous sway of normal subjects and patients with vestibular deficits were small even when vision was deprived, provided that somatosensory inputs were not disrupted. The results for the vestibular patients tested here provide only limited evidence for abnormally large reductions in stability under visual deprivation. Two patients exhibited a large EO/BF ratio (test-C2 data, CS model); however, these results did not occur consistently (i.e. when the modelling methodology was changed or when the "best" test data were used). Moreover, one of the patients showed the opposite effect, i.e. small EO/BF ratio.

8.2.5 Identification of Balance-Impaired Individuals

In using the balance test to identify the balance-impaired subjects, the greatest success was achieved using the BF data and, in particular, the EO/BF ratio. These results suggest that the degree of reliance on vision may play an important role in determining the relative stability of elderly fallers and patients with vestibular lesions. Although Stones and Kozma (1987) argue that vision-deprived tests may not generalize to the conditions encountered in everyday life, there is evidence that a sizeable proportion of falls do occur in poorly lit environments. For example, Wild et al (1980 and 1981) found that 10% of falls occurred in darkness and another 10% in dim light, in their elderly subject population. Although not a perfect simulation, the BF tests should give some indication of postural performance in these types of situations.

Note that the EO/BF ratio quantifies the relative influence of vision without reference to the BOS. As a result, errors in

defining and measuring the BOS (see Section 8.4.3) do not affect the EO/BF estimates. This factor may account, in part, for the better identification rates obtained in using the EO/BF ratio, compared to the results obtained using the BF data.

The test-C2 data provided somewhat greater success than the "best" test data. This can be attributed to the larger variance in the "best" test SA estimates. For the "best" test estimates, the subjects differed in terms of which test and perturbation amplitude were used to estimate their SA. Thus, the increased variance could be the result of order effects and/or amplitude dependence in the balancing performance.

The ML model was most successful in identifying the elderly fallers, while the CS model was most successful in identifying the vestibular patients. In a number of instances, the three models failed to agree. In order to determine which model gives the best predictions of relative stability, larger numbers of balance-impaired subjects must be tested.

The failure to identify all of the vestibular patients may be due to an absence of abnormal anterior-posterior (a-p) instability. The patients tested here were quite able to stand in normal situations; their impairment became evident only when attempting to stand on one leg or to stand or walk toe-to-heel, i.e. in situations where lateral instability was heightened. The testing protocol used in the present experiments was not designed to challenge lateral stability. In future, greater success in identifying patients with unilateral vestibular deficits might be achieved by including a medial-lateral (m-l) test perturbation in the protocol.

It should be noted that the five vestibular patients tested here were a heterogeneous group, in terms of the nature and "age" of their deficit and the degree of compensation that may have occurred. Since the balance test is a functional test, patients who have fully compensated for their deficits cannot be identified.

In screening the normal subjects, it was necessary to rely on the subjects' self-reports in order to identify medical disorders or deficits that might affect balance, as the medical records of these subjects could not be accessed (for ethical reasons). Thus,

misclassification error may have increased due to inadvertent inclusion of balance-impaired individuals in the normal subject groups.

Errors in identifying the elderly fallers may be due, in part, to errors in the selection of the faller subjects. Although the subjects are inferred to have balance impairments based on their history of falling, this is not necessarily true, as falls can result from other causes unrelated to balance impairment, for example: (1) transient physiological disturbances, (2) impaired ability to avoid ordinary environmental hazards, or (3) exposure to extraordinarily severe perturbations (see Section 2.4). The accuracy of the retrospective falling histories must also be questioned.

In spite of the potential errors in the selection of the elderly fallers, the balance test was able to identify 100% of the selected subjects as being balance-impaired, provided that a fairly high false positive rate (25%) was allowed. However, it should be cautioned that some of the differences between the fallers and the elderly normals that were detected by the balance test could be due to differences in the test protocol (i.e. smaller perturbation amplitude and fewer tests for some fallers). The more advanced age of the fallers might also be a factor. Although individuals with very recent falls (i.e. within the previous month) were screened from the study, the poor test results in the faller subjects may still be due, at least in part, to the debilitating effects of their falls. Subjects who are at-risk but have yet to experience a debilitating fall may present more subtle balance impairments.

It should be emphasized that the testing of the balance-impaired subjects performed in the present study was intended to provide only a preliminary evaluation of the balance test. The small numbers of balance-impaired subjects tested severely limit the accuracy with which the true misclassification rates can be estimated (Bartlett et al, 1986). In dealing with such small sample sizes, "outliers" (e.g. a faller whose fall was unrelated to any balance impairment, or a vestibular patient who has compensated for any a-p instability) have a profound influence on the estimated misclassification rates. Clearly, larger numbers

of balance-impaired subjects must be tested in order to provide a more definitive assessment of the balance test.

8.3 SPONTANEOUS SWAY

8.3.1 Comparison with Balance Test Responses

In comparing the spontaneous sway measures to the SA estimates, the linear relationships were in general quite weak. The strongest relations were found in the young normals, using the LS and ML models, for variables RMS, RANGE, RMS/BOS and RANGE/BOS (i.e. root-mean-square and peak-to-peak range of a-p COP displacement, both unnormalized and normalized with respect to the length of the BOS).

For the amplitude measures of sway (RMS and RANGE), larger values are expected to correlate with greater instability. Because the SA is instead a measure of stability, one would expect a negative slope in the relationship between these measures of spontaneous sway and the SA. Only in the young normal subjects was this found to be the case. The elderly normals, vestibular patients and elderly fallers either failed to show this trend or showed the opposite trend.

For the other sway measures, the regressions typically were found to lack statistical significance. Nonetheless, it is interesting to note that, almost without exception, the sign of the estimated regression slope for the elderly normal, vestibular patient and elderly faller subject groups was opposite to that seen in the young normal subjects.

The lack of success in demonstrating strong correlations between SA and spontaneous sway in the vestibular patients and elderly fallers may be due, at least in part, to the small number of subjects tested. Alternatively, the differences in the results of the different subject groups could be due to differences in response modulation or control system nonlinearity.

Conceivably, in the elderly normal, vestibular patient and elderly faller groups, the balance test results and spontaneous sway measures fail to correlate because of the varying extent to which the different subjects modulate their balancing strategies in the two testing situations. In particular, the more unstable

subjects may show a greater tendency to increase the stiffness of their posture control system during the balance tests, in order to prevent themselves from falling, but may show relatively normal levels of stiffness during the spontaneous sway tests, in the absence of a serious postural threat. Conversely, for the young normals, the two testing situations may represent equally low levels of postural threat; therefore, these subjects may tend to show similar balancing responses in both types of tests. Stiffness modulations are discussed further in Section 8.6.6.

An alternative explanation can be provided in terms of intrinsic control-loop nonlinearity. If there exist substantial inter-subject differences in the nature of the nonlinear amplitude-dependence, the larger-amplitude responses measured in the balance test will fail to correlate with the small-amplitude spontaneous sway results (viewing spontaneous sway as the response to very small, self-imposed perturbations). Conceivably, this scenario could be representative of the elderly normal, vestibular patient and elderly faller groups, where large subject-to-subject variation in nonlinear trends might occur. Conversely, the young normal subjects, a more uniform population, may tend to show similar nonlinear amplitude dependence. In this case, the test results at different amplitudes would tend to show greater correlation. The effects of nonlinearity on the balance test responses are discussed further in Section 8.6.5.

8.3.2 Age-Related Differences in Normal Subjects

The present results demonstrated significant increases in the range (RANGE) and average speed (SPEED) of spontaneous a-p COP displacement in elderly normal subjects; however, no significant age-related differences were found in the RMS values. The age-related increase in SPEED is in general agreement with results presented by Fernie and Holliday (1978), although their measure of sway involved the displacement at the hip and included both a-p and m-l displacements. Overstall et al (1977) demonstrated an age-related increase in the "total angular movement" (measured at the hip in the a-p direction), a measure which is proportional to the average speed of angular sway. Era and Heikkinen (1985)

reported age-related increases in the "total extent" of a-p and m-l COP sway during an 8 s test, a measure proportional to the average speed of COP displacement. Other investigators have demonstrated an age-related increase in the projected area of sway associated with shoulder movements (Sheldon, 1963) or COP displacement (Hasselkus and Shambes, 1975). In agreement with the present results, Hayes et al (1985) found no significant age-related differences in EO a-p RMS COP displacement, although they did find some small but significant age-related increases in the m-l direction.

The present results also demonstrated significant age-related differences in frequency-domain sway measures, i.e. increase in centroidal frequency (CFREQ) and dispersion (DISP) in the elderly subjects. In addition, there was a marginally significant increase in mean frequency (MFREQ) in these subjects. These findings appear to be in agreement with Hayes et al (1985), who reported increased high frequency content (between 2 and 5 Hz) in the sway power spectrum of some elderly subjects. In spite of the age-related differences in CFREQ and DISP, the shape of the power spectrum was found to be similar for all subjects. In no cases did the power spectrum show any pronounced peaks, *as have been reported in certain types of cerebellar lesions (Mauritz et al, 1979) and in disturbances of muscle afferentation (Aggashyan et al, 1973; Dichgans et al, 1975).*

Biomechanical factors could account for some of the age-related differences in the frequency content of the sway. For example, assuming inverted pendulum motion and proportional feedback control, the natural frequency of sway $\omega_n = \sqrt{(K - mgL) / J_0}$, where K is the feedback gain, mg is the body weight, L is the height of the centre-of-gravity and J_0 is the rotational inertia about the ankles (see Appendix A). As illustrated in table A.1, ageing is typically accompanied by increase in weight and decrease in height; rotational inertia may either increase or decrease. For a hypothetical "50th percentile male", the natural frequency of sway increases from $\omega_n = 0.25$ Hz to $\omega_n = 0.30$ Hz as a result of the changes in anthropometric properties that occur in ageing (based on the simple model

presented above, assuming a feedback gain $K = 900 \text{ Nm/rad}$). This example assumes that the feedback gain does not change with ageing; as indicated by the model, changes in gain will also affect the frequency of sway.

8.3.3 Sex-Related Differences in Normal Subjects

The experimental results indicated significant (or marginally significant) sex-related differences in all but one of the non-normalized spontaneous sway measures, with males exhibiting larger values for RMS, SPEED, RANGE, CFREQ and DISP. As discussed in Section 8.2.1, Overstall et al (1977) found significant sex differences in their measurements of "total angular movement", with higher values in the females. In contrast, several other investigators have failed to find any significant sex-related differences, in amplitude or area measures of spontaneous COP displacement (Njiokiktjien and de Rijke, 1971; Black et al, 1982) or in timed tests of one-legged balancing ability (Stones and Kozma, 1987).

In general, the literature on sex-related differences appears to be rather deficient. In most cases, investigators have either neglected to allow for possible sex effects (e.g. Fernie and Holliday, 1978; Daley and Swank, 1981), have limited their studies to a single sex (e.g. Hasselkus and Shambes, 1975; Era and Heikkinen, 1985), or have treated males and females separately without explicitly analyzing the sex differences (e.g. Terekhov, 1976; Hayes et al, 1985).

The sex differences found in the frequency measures may result, at least in part, from anthropometric factors (i.e. reduced weight, height and rotational inertia in females). These factors would affect the natural frequency of sway, as illustrated by the simple model presented in the previous section. Overstall et al (1977) have suggested that sex differences may result from differences in the body-mass/muscle-mass ratio. Such differences would affect the magnitude of the feedback gain (K) relative to the other terms in the model.

The sex differences in the time-domain sway measures were found to disappear when the variables were normalized with respect

to the length of the BOS. Although Hasselkus and Shambes (1975) performed a similar normalization in their analysis, the results cannot be compared, as they only tested females in their study. Lacking any compelling evidence to the contrary, it seems reasonable to assume that there exist no real differences in the postural stability of normal males and females. Based on this assumption, it can be argued that the normalized sway measure represents a more reasonable predictor of postural stability than the non-normalized measure.

8.3.4 Identification of Balance-Impaired Individuals

In using the time-domain spontaneous sway measures to identify the vestibular patients, all of the measures (except for SPEED/BOS) were able to identify two of the five patients. In using the frequency measures, only one patient was identified correctly. In general agreement with this lack of success, Nashner et al (1982) found only small differences in the spontaneous sway of patients with vestibular deficits compared to normal controls. Their sway measure was the integral of the rectified a-p body angle, normalized with respect to the "maximum possible". Similarly, Hufschmidt et al (1980) found only small increases in eyes-open RMS sway, sway path and projected area of sway in patients with vestibular lesions, using the combined a-p and m-l COP displacement as the measure of sway. They also found a small decrease in the mean frequency of sway in the vestibular patients; however, the present results suggest the opposite tendency.

For the elderly fallers, the greatest success was achieved using SPEED, SPEED/BOS or MFREQ. Using any of these measures, four of the five fallers were identified correctly, at a high level of confidence. Using a combination of SPEED (or SPEED/BOS) and MFREQ as the predictor variables, all five fallers would be identified correctly. The remaining sway measures were each able to identify only one or two of the fallers.

Kirshen et al (1984) found significantly increased RMS COP sway (both a-p and m-l) in a group of elderly fallers; however, their findings must be questioned, as the much larger variance exhibited by the fallers violates the assumptions of the ANOVA

model that they used. Using a linear function of eyes-closed a-p and m-l RMS sway and a-p range of sway, they were able to identify 9 of 17 fallers and 37 of 49 controls correctly. They did not present the results obtained using eyes-open data. The present results showed relatively normal (or better than normal) values for eyes-open RMS and RANGE in four of five elderly fallers.

Fernie et al (1982) found a significantly higher mean value for the speed of sway in a population of fallers, but attained a success rate of only 57% in using this measure to identify individual fallers (Bartlett et al, 1986). In contrast, the present results showed SPEED to be a very good predictor of falling. The disagreement may lie in methodological differences. Fernie and coworkers measured the combined a-p and m-l hip displacement, rather than a-p COP displacement, and their measurements were limited to very low frequencies. In addition, there is reason to suspect that the faller subjects that they tested had more subtle balance impairments than the subjects tested here.

8.4 TRANSIENT TEST RESPONSES

8.4.1 Linearity

The results of the transient tests showed a strong amplitude dependence in the sub-saturation balancing performance. In particular, the gain of the response (i.e. the peak COP displacement divided by the peak acceleration) was found to decrease as the perturbation amplitude was increased. The dependence of response gain on perturbation amplitude was described quite well, on the average, by an inverse square root function. As discussed below, however, it is not clear to what extent the observed amplitude dependence was a result of adaptation to the testing protocol.

In the transient tests, the perturbation amplitudes were tested in ascending order, stopping when the subject could no longer maintain balance. This protocol was adopted as a safety precaution; however, as a result, "true" amplitude-dependent changes, due to nonlinearity in the posture control system, may be confounded by adaptation and fatigue. Fatigue would seem to be

unlikely, as the decreasing response gain seen in the later large-amplitude tests implies more effective, rather than less effective, balancing responses. Adaptive effects, however, could be an important factor.

In their transient tests, Horak et al (1985) found that postural synergies were modulated to achieve more effective balancing responses when the perturbations were predictable, and that amplitude-dependent influences disappeared when the amplitudes were randomized. Moore et al (1986) found that subjects adapted to a predictable transient perturbation by leaning either forward or backward, prior to the start of the test. By leaning in the direction of the anticipated centre-of-gravity (COG) displacement, the muscles are prestretched, thereby increasing the muscle stiffness and facilitating the stretch reflex response. Leaning in the opposite direction increases the time available for the stabilizing response (before the limits of stability are reached) and allows the initial moment due to the body weight to be used to oppose the perturbation. These and other anticipatory adaptations are discussed further in Section 8.6.6.

Note that, in the transient tests performed here, the onset of platform motion was controlled to occur at a random interval after warning the subject. Although this prevented the subjects from making effective anticipatory motions, it did not prevent the types of adaptations described above.

The use of anticipatory adaptations and the effectiveness of these adaptations might be expected to increase progressively, as a gradual learning and "fine-tuning" process. The use of these adaptations might also be expected to increase with the anticipated level of postural threat, i.e. the perturbation amplitude. This would be quite possible, since the subjects were warned in advance of each new increase in amplitude. Amplitude-related adaptations will tend to confound any amplitude dependence due to nonlinearity in the posture control system. Because the amplitudes were tested in ascending order, progressive adaptations will have a similar confounding effect.

To evaluate possible adaptive effects, an ANOVA was performed for each perturbation amplitude, treating the response gain and

trial number as the dependent and independent variables, respectively, and blocking on subjects. For the lowest perturbation amplitude, there were highly significant trial-related changes in response ($p < 0.001$). Pairwise comparisons of the mean values showed that the response gain decreased by a significant amount with each new trial ($p < 0.01$). At the higher amplitudes, however, there were no significant differences between trials ($p > 0.1$). These results suggest that learning and fine-tuning of the adaptive responses takes place over the first few trials, at the lowest amplitude, and is essentially completed by the start of the trials at the next amplitude.

Analysis of the variation of initial COP location with trial number confirmed that adaptive processes occurred. In many subjects, the initial COP location tended to move backward with increasing trial number, i.e. subjects increasingly leaned in a direction opposite to the anticipated COG displacement. In almost all of the subjects, the largest change occurred between the first and subsequent trials.

Note that these results support one of the criticisms of transient testing that motivated the use of a continuous-waveform in the balance test, namely, that anticipatory effects may confound the results when repeated testing is performed. Even if the direction of perturbation is randomly varied, subjects can still improve their stability by leaning in one direction or the other. Depending on the direction of leaning and the direction of the perturbation, stability will be increased either through prestretching of the muscles or presetting of the COG location, as discussed earlier. In contrast, in a continuous-waveform test, anticipatory leaning is unlikely to influence stability beyond the first few "strokes" of platform motion.

Even though the above considerations indicate that anticipatory adaptations account for at least some of the apparent amplitude dependence in the postural responses, this amplitude dependence could also be a result of nonadaptive nonlinearities "built into" the control system. One example would be nonlinear gain control, whereby a secondary feedback loop acts to modulate the feedback gain in the primary loop. Nashner (1970) found it

necessary to incorporate this type of nonlinearity into his model of the posture control system in order to attain agreement with observed balancing responses. Sensory thresholds are another possibility. Simulation of inverted pendulum responses suggested that the transient perturbations would exceed reported displacement thresholds in the somatosensors and otoliths, angular acceleration thresholds in the semicircular canals, and visual velocity thresholds; however, the influence of rate thresholds in the muscle spindles was not resolved (see Appendix A.3.6). It is conceivable that these thresholds are exceeded only at larger perturbation amplitudes, and that this factor contributes to the amplitude dependence observed in the balancing responses.

8.4.2 Comparison of Actual and Predicted Response

For the smallest transient amplitude, the input-output model derived from the PRN balance test data predicted the peak transient response to a reasonable degree of accuracy (mean error $\approx 15\%$, standard deviation $\approx 20\%$). Note that the RMS amplitude of the PRN perturbation was substantially lower than the transient amplitude (i.e. 0.1 m/s^2 versus 0.5 m/s^2); therefore, this result implies that the posture control system can be approximated by a linear system over this range of amplitudes.

For larger transient perturbations, however, the predictions derived from the balance test were poor. This result is not surprising, in view of the amplitude dependence observed in the transient responses. However, as discussed in the previous section, it is not clear to what extent the apparent amplitude dependence is the result of adaptation to the experimental protocol, and to what extent the nonadaptive behaviour of the posture control system is truly nonlinear.

8.4.3 Functional Definition of the Base-of-Support

Estimation of the SA requires a definition for the length of the BOS. Functionally, subjects are not able to utilize the entire foot as a BOS (Whitney, 1962). For an idealized rigid foot, generation of stabilizing ankle moment will not cause the foot to rotate (i.e. heel-lift or toe-lift) until the COP reaches the perimeter of the BOS (see Appendix A). For a real foot, however,

the maximum COP excursion may be limited by other factors. As the COP approaches the end of the foot, the load becomes concentrated over a smaller area of tissue; conceivably, at some point, a pressure tolerance threshold could be exceeded, thereby exciting a nociceptive withdrawal reflex. For forward sway, COP displacement beyond the metatarsophalangeal (MTP) joints requires a moment to be generated at these joints; therefore, maximum COP excursion may be limited by the strength of the MTP musculature.

The results from the transient tests were analyzed in an attempt to derive a functional definition for the BOS in terms of measurable anatomical dimensions. For safety reasons, the transient tests were limited to backward platform translations which displace the COP forward; therefore, only the anterior limit of the BOS was investigated here. The anterior functional limit of the BOS was defined by the maximum COP displacement in those transient tests where heel-lift was observed to occur.

The best functional definition for the BOS was found to be a linear proportional function of the total foot length. The functional definition was not improved by including measurements of other foot dimensions. The lack of improvement may be due, in part, to the inaccuracies in the measurements of these dimensions, due largely to the difficulty in locating the appropriate anatomical landmarks.

Note that the methods used to determine the functional BOS yield only an approximate definition. The true functional length of the BOS may depend on a number of other factors. For example, large foot rotations will cause the MTP joints to extend to the limit of their range of motion. In this case, the MTP muscle strength is no longer a limiting factor, as the required moment can be generated by the passive stiffness of the muscles and connective tissues. Thus, the maximum COP excursion may increase in tests where larger foot rotations occur. The posterior functional limit of the BOS may also be dependent on the magnitude of foot rotation, since the most posterior point of contact will shift as the calcaneous "rolls" backward.

8.5 AN ASSESSMENT OF THE POSTURE CONTROL MODEL

8.5.1 Relation to Current Theories of Postural Control

As discussed in Chapter 3, postural control is thought to involve two distinct modes of operation (Droulez et al, 1985). Within a particular "operating range", the posture control system functions in a continuous, closed-loop, servocontrol mode. In this "conservative" mode of operation, the control loop acts to maintain the system in the vicinity of a desired state. When the limits of the operating range are exceeded, the system switches to a discontinuous, "projective" mode of operation. The projective mode must define the next objective and then select an appropriate motor program, from a pre-established repertoire, to achieve the transition into the conservative operating range associated with the new objective state. The projective mode involves a higher level of neural processing than the conservative mode.

Although the projective mode could in theory be "switched on" at any point, the involvement of higher-level neural centres would be expected to result in slower and hence less effective balancing responses, compared to the conservative mode. Furthermore, it would seem desirable to leave the higher centres free to perform other high-level functions. Therefore, it seems plausible that the posture control system would normally utilize the conservative mode of operation to the greatest extent possible.

Droulez et al (1985) argue that the organization of postural responses into a small number of stereotyped synergic patterns (e.g. Nashner, 1977) is totally compatible with a servocontrolled, conservative mode of operation. Even though selection and triggering operations are involved, sensory feedback is still used to continuously modulate and update a process acting to maintain the system at or near a desired state.

In the posture control model developed here, the limits of the conservative operating range are represented by the finite length of the BOS. When the COP reaches these limits, the posture control system must switch to the projective mode of operation in order to maintain stability. Based on the arguments developed above, the most effective posture control system is expected to maximize use of the conservative mode of operation. In quantifying the size of

the conservative operating range (i.e. the range of perturbations that can be withstood without saturating the BOS), the SA characterizes the potential for the posture control system to remain in the conservative mode, and hence compares postural performance and stability in this regard.

Although the kinematics of falls occurring during gait and while standing differ considerably, there exists experimental evidence which suggests that the posture control responses are similar. Nashner (1980) found that small perturbations applied during gait produced responses which tended to maintain the normal ankle rotation trajectory, similar to the responses observed when perturbations were applied during stance. Although Berger et al (1984) found that larger perturbations produced complex bilateral responses that differed considerably from those occurring during stance, these results are not inconsistent with the posture control model. In gait, as in stance, larger perturbations cause BOS saturation, at which point more complex balance-recovery manoeuvres must be executed in order to prevent a fall. Whereas the sub-saturation balancing responses in stance would be triggered by deviation from an expected body position or posture, the responses during gait (or other voluntary activities) would be triggered by deviation from an expected trajectory of body motion (Nashner, 1980).

Sensations of BOS saturation could conceivably act to trigger the more complex projective balancing responses. These sensations could be transduced directly by the plantar mechanoreceptors or derived from a combination of other sensory inputs. The trigger would be activated only when the BOS saturation (occurring in either foot) represents a deviation from the expected COP position or trajectory (for that foot). Thus, the trigger would be overridden during the BOS saturation that occurs routinely in the course of the gait cycle (Grundy et al, 1975) and other voluntary activities.

Note that the BOS saturation trigger is not a necessary feature of the posture control model. The projective balancing responses might be triggered by an entirely different mechanism (e.g. a "tilt" threshold transduced by the otoliths and neck

proprioceptors). Regardless of the mechanism used to trigger the projective responses, the model predicts that the relative stability of the control system is related to the potential to remain in the conservative operating range. If, however, the projective trigger consistently "pre-empts" the ability to utilize this potential, then the model may fail to yield accurate predictions of actual postural performance.

One of the more attractive features of the posture control model is that the relative stability of the system is characterized independent of the nature of the balancing strategy. According to the model, the most effective strategies will result in the smallest COP displacement, in the course of maintaining stability. In contrast to a number of other posture control models, there is no need to assume a particular form of response (e.g. inverted pendulum motion).

Nashner and coworkers (Nashner and McCollum, 1985; Horak and Nashner, 1986) have identified two major balancing strategies: the ankle synergy and the hip synergy (see Section 2.3.4). In contrast to the ankle synergy, the hip synergy generates large shearing forces but relatively small COP excursions. These authors recognized that the finite-BOS nonlinearity will limit stability for ankle synergy responses; however, for the hip synergy, they suggested that the frictional properties of the support surface may be the limiting factor, because of the need to generate large shearing forces. In situations where friction is adequate, the posture control model suggests that the hip synergy will be a more effective balancing strategy. Because of the relatively small COP excursions, the hip synergy will maintain postural stability while minimizing the probability of BOS saturation. This raises the interesting possibility that decreased stability may result from an overreliance on the ankle synergy. If this is true, then it might prove possible to retrain balance-impaired subjects to better utilize the hip synergy.

8.5.2 Limitations

The posture control model provides no basis for assessing the ability to utilize projective-mode balance-recovery manoeuvres.

However, conservative- and projective-mode performance might be expected to correlate to some extent. Although the modes differ in terms of neural processing, both rely on the same sensory and motor sub-systems; hence, deterioration in these sub-systems would be expected to affect the performance of both modes.

The model emphasizes the importance of saturation-like nonlinearities in determining postural stability. Although the finite-BOS nonlinearity is hypothesized to be the dominant saturation-like nonlinearity affecting postural stability, it is possible that others could predominate. One example would be the limitation on shear force imposed by the frictional properties of the support surface, as discussed in the previous section. Based on everyday experience, however, this seems unlikely to be a limiting factor, except in situations where the surface is very slippery. The strength limitations of the ankle muscles could be another important saturation-like nonlinearity; however, experiments in which the length of the BOS was varied (by means of specially designed "boots") have provided some preliminary evidence that the finite-BOS limitation is reached before the strength limitations of the ankle muscles (Maki and Fernie, 1986).

In the posture control model, the limits of the conservative operating range are defined in terms of BOS saturation. Once the COP reaches the perimeter of the BOS, generation of additional stabilizing ankle moment (in the ankle synergy) or shearing force (in the hip synergy) will cause the foot to rotate. The model postulates that this dictates a projective switch to a new balancing strategy. Although analysis of a linearized two-link model confirmed that the sub-saturation system does become unstable at this point (see Appendix A.1.2), simulations that included certain nonlinear properties apparently have shown that it is possible to stabilize a two-link system using a single moment-generator (Nashner, 1981). It is not clear, however, whether such stabilization can be achieved using the sub-saturation control strategy, or whether a projective switch to a new control strategy is required.

Regardless, experimental evidence indicates that the additional stabilization that occurs during the foot rotation that

follows BOS saturation is relatively small. In transient testing, most subjects adopted projective strategies (i.e. grabbed a handrail, waved their arms or moved their feet) in order to cope with a further increase in amplitude (i.e. an increment of 0.5 m/s^2) beyond the amplitude at which foot rotation first occurred. Other subjects used these projective strategies even at the lowest amplitude at which foot rotation first occurred. Thus, even if the BOS saturation limits do not coincide exactly with the limits at which projective responses must be adopted (i.e. the limits of the conservative operating range), they can be viewed as a reasonable approximation of these limits.

8.5.3 Validation of the Posture Control Model

The posture control model was developed to provide a conceptual framework for the development of a balance testing methodology. Like many conceptual models, it is not amenable to direct experimental validation.

Indirect evidence for the importance of the finite-BOS nonlinearity can be derived by comparing the SA results with results obtained using ΔCOP , which characterize the performance of the posture control system without reference to the BOS. The ΔCOP values were found to be less successful in identifying the balance-impaired subjects (e.g. one of five elderly fallers was identified correctly, test C5, ML model, 25% false positive rate; in comparison, the SA identified three of the five fallers correctly). Furthermore, in contrast to the SA, ΔCOP was found to depend significantly on sex, with larger values in the males. Since there is no evidence to support the implication that males are less stable than females, the SA would seem to be a more reasonable measure of stability. Similar evidence was found in the spontaneous sway measures. Sex-related differences in the spontaneous sway measures were eliminated after normalization with respect to the length of the BOS.

It should be pointed out, however, that normalization with respect to other anthropometric parameters (e.g. height) could also act to eliminate sex-related differences. If one accepts the premise that true sex differences in postural stability do not

exist, then the absence of sex differences is a necessary, but not sufficient, condition for validating the posture control model.

8.6 AN ASSESSMENT OF THE BALANCE TEST

8.6.1 The Test Perturbation

Data presented by Wild et al (1981) suggest that falls are almost equally likely to occur during gait as during ordinary activities of daily living (ADL). Ideally then, the balance test perturbation should simulate the kinematics and sensory input of both gait and ADL perturbations.

A horizontal acceleration of the platform on which the subject stands approximates the kinematics of these perturbations in that it creates a relative acceleration between the feet and the upper body. However, because the balance test is performed during two-footed stance, the simulation of the kinematics of gait perturbations is less than ideal. A large proportion of gait falls are expected to occur when the body weight is supported predominantly or entirely by one foot. Furthermore, in gait, postural stability is not a result of muscle responses alone, as the momentum of the body can act to return the centre-of-gravity to a stable position over the BOS.

In a fall from a stationary standing posture, all sensory inputs will be derived from the swaying motion of the body relative to the external environment. In a fall that occurs during gait, the visual and otolith inputs will provide absolute-motion information which no longer correlates directly with the relative sway-motion information provided by the somatosensory and semicircular canal inputs. Thus, the "sensory context", i.e. the manner in which the data from the different sensory modalities is interpreted and utilized, will be different in these two situations.

In the balance test, most of the sensory inputs provide relative sway-motion information and thereby simulate the sensory context of falls occurring during stance. The major incongruence lies in the otoliths, which measure absolute head acceleration, i.e. the platform acceleration plus the sway-related acceleration of the head relative to the platform. Similarly, there may be some

incongruence in the response of the semicircular canals, to the extent that they are influenced by the linear acceleration of the head. Because they transmit the platform acceleration to the body, the shearing forces on the feet will also fail to correlate with the swaying motion of the body.

Thus, accurate simulation of the sensory input of stance falls is not achieved in the plantar mechanoreceptors or in the vestibular organs. However, it is not clear to what extent plantar mechanoreceptors actually sense shearing forces, much less the role that these sensory cues might play in postural control. Although the semicircular canals may be influenced by linear accelerations, there is no question that the predominant response is to the angular motion of the head (Wilson and Melvill Jones, 1979a) which results from the body sway. Thus, the incongruent influence of the platform acceleration is unlikely to have a major effect on the canal response. The effect of the incongruence between the otoliths and other senses cannot be predicted at the present time. Nashner (1971) has argued that the otoliths do not contribute to relatively rapid balancing responses, because of their slow dynamic response and their inability to distinguish between gravitational and inertial stimuli. In contrast, experimental evidence suggests that the otolith-spinal reflex response to vertical accelerations does play a role in the control of rapid movements (e.g. Wilson, 1985); however, the evidence is much less clear in the case of horizontal accelerations.

Because the visual field is controlled to move with the platform, the visual input during the balance test provides relative sway-motion information. If, instead, a stationary visual field were used, both the visual and otolith inputs would provide absolute-motion information, while the somatosensors and semicircular canals would continue to provide (primarily) relative sway-motion information. This type of test simulates the sensory context of falls during gait.

However, it should be noted the stationary-field test may suffer from a loss of unpredictability. For example, when using a continuous-waveform perturbation, subjects may be able to estimate the limits of the platform range of motion and thereby anticipate

when changes in direction are imminent (see Section 8.2.3). Furthermore, neither type of platform test, moving visual field or stationary field, will provide a perfect simulation of the sensory inputs during gait falls. Because the sensory inputs associated with gait are not simulated, the effect of the sensory cues may be altered, due to nonlinear interactions between gait-related and sway-related stimulation. For example, sensory thresholds, not reached during sway alone, may be exceeded by the additional stimulation that would occur during gait.

The limitations of the balance test in simulating gait-related kinematics and sensory input are a necessary consequence of the decision to use a continuous-waveform perturbation. As discussed in Chapter 3, this decision was based on: (1) concern for the safety of the subjects, and (2) concern that transient testing could lead to adaptive and anticipatory responses that would not occur in actual falls. Nonetheless, as discussed in Section 8.5.1, there is evidence that the balancing responses that occur in gait and in stance are similar in organization, at least for small perturbations. Thus, in spite of the limitations of the balance test in simulating gait perturbations, the balance test performance may be indicative of the sub-saturation responses to small gait perturbations. As in stance, more complex responses are required once BOS saturation occurs.

Note that the pilot tests that were conducted to determine the perturbation characteristics involved a small number of young healthy subjects; hence, the results do not necessarily reflect the optimal perturbation characteristics for other subject groups. The experiences in testing the larger, more varied group of subjects have indicated a number of changes that should be made in future tests, particularly those involving balance-impaired individuals. These changes are discussed in Section 8.7.

Note also that the eye-object distances during the balance tests were relatively small (approximately 0.7 m a-p, 0.4 m laterally) and therefore may be a less than ideal simulation of typical falling situations. For larger eye-object distances, the effectiveness of the visual contribution to postural stabilization decreases (Brandt et al, 1986).

8.6.2 Measurement and Computational Accuracy

8.6.2.1 Sources of error

The accuracy of the ΔCOP and SA estimates is dependent on: (1) the accuracy of the acceleration, COP and BOS measurements, (2) the data sampling rate and reconstruction method, and (3) the accuracy of the system identification algorithms.

The measurement errors were detailed in Chapter 4. Conservatively, the error standard deviations were 1.5 mm for the COP measurements and 0.05 m/s² for the acceleration measurements. The estimates for the SA were also affected by error in the measurement of the foot dimensions. This error was estimated to be within approximately ± 1 mm.

Note that the COP errors were determined separately for each force plate. The overall COP (CO), used in the SA estimates, is related to the left and right COP values (CL and CR) as follows:

$$\text{CO} = (\text{FL CL} + \text{FR CR}) / (\text{FL} + \text{FR})$$

where FL and FR are the vertical forces on the left and right feet. The error (E) in the overall COP can be estimated from the Taylor series expansion for CO, as follows:

$$\begin{aligned} E &= \text{CO}(\text{CL} \pm \Delta\text{C}, \text{CR} \pm \Delta\text{C}, \text{FL} \pm \Delta\text{F}, \text{FR} \pm \Delta\text{F}) - \text{CO}(\text{CL}, \text{CR}, \text{FL}, \text{FR}) \\ &= \pm \Delta\text{C} \partial\text{CO}/\partial\text{CL} \pm \Delta\text{C} \partial\text{CO}/\partial\text{CR} \pm \Delta\text{F} \partial\text{CO}/\partial\text{FL} \pm \Delta\text{F} \partial\text{CO}/\partial\text{FR} \\ &\quad \pm \Delta\text{C}^2 \partial^2\text{CO}/\partial\text{CL}^2 \pm \dots \end{aligned}$$

where ΔC and ΔF are the errors in the COP and vertical force measurements, respectively (for simplicity, the error magnitudes are assumed to be the same for each force plate). The upper bound on the error in the overall COP can be estimated by summing the absolute values of the first-order terms in the Taylor series, since the higher order terms will be relatively small (Doebelin, 1975). Using this approach, the upper bound is determined to be:

$$|E| \leq |\Delta\text{C}| + |\text{CL} - \text{CR}| |\Delta\text{F}| / |\text{FL} + \text{FR}|$$

Because $|\Delta\text{F}|/|\text{FL} + \text{FR}|$ is small (see table 4.2 in Chapter 4), the second term in the above expression will be negligible, even in the atypical case where CL and CR differ appreciably. Thus, the upper bound on the error in the overall COP is approximately equal to

$|\Delta C|$, the error in the separate force plate COP measurements.

Note that mean errors in the measurements will not influence the system identification. In the CS method, changes in the mean level of the data affect only the "DC" value of the frequency response, which was not used in fitting the transfer function model. In the LS and ML methods, the starting values of the data were subtracted prior to analysis. Random input and output measurement error result in increased variance in the transfer function estimates. In addition, random input measurement error creates a bias error in the estimates; however, the bias will be small provided that the measurement noise is small relative to the actual input signal (Bendat and Piersol, 1980).

In order to prevent aliasing, the sampling rate must exceed the highest frequency content in the signals by a factor of two. Thus, since the data were sampled at a rate of 16.7 Hz, the COP and acceleration signals should have minimal energy at frequencies above 8.35 Hz (the "aliasing frequency"). In practical measurement situations, it is impossible to completely eliminate all signal power above the aliasing frequency; therefore, there will always be some degree of aliasing error, the magnitude of which depends on the steepness of the "roll-off" in the signal spectrum (Gardenhire, 1964).

Any aliasing error in the balance test data is expected to be very small. Power spectral analysis of the unfiltered data showed a sharp cut-off in the acceleration spectrum at 5 Hz (the intended upper frequency limit), while the COP power tended to decrease with increasing frequency (e.g. -50 dB between 0.1 and 5 Hz). The anti-aliasing filters produced an additional roll-off of 40 dB/decade beyond 6 Hz. Small peaks in the unfiltered spectra at 13 Hz and 60 Hz were attenuated by these filters (-15 dB at 13 Hz, -40 dB at 60 Hz). Although the anti-aliasing filters produce a small degree of amplitude and phase distortion in the input and output measurements (i.e. below 5 Hz), the distortion tends to "cancel out" in estimating the input-output transfer function.

The error associated with the reconstruction of the continuous pulse response waveform from the discrete data (generated using the input-output model) affects the accuracy with which ΔCOP , the peak

value in the predicted unit pulse response, can be determined. The reconstruction error depends on the sampling rate (relative to the frequency content of the waveform) and the method used to interpolate between the data points. In the present analysis, the peak value was selected from the discrete data, a method which implies linear interpolation between data points. Gardenhire (1964) found linear interpolation to produce RMS errors comparable to those obtained using more complex interpolation schemes, but did not evaluate the errors in determining peak values.

Although the sampling rate must be sufficiently high to minimize aliasing and reconstruction error, an excessively high sampling rate can lead to numerical errors, as the system identification algorithm may become ill-conditioned (Isermann, 1980).

Because the system identification methods involve iterative algorithms, the final results are only an approximation to the true solution. In addition, there may be errors associated with the selection of the model structure (i.e. equation order and dead time). Additional inaccuracy may result from computer rounding error and truncation error (i.e. approximation of mathematical functions by truncated series). Although they are small, rounding and truncation errors can have a large impact in ill-conditioned computations. The bilinear transformation, used to generate the unit pulse response prediction in the CS method, is an approximation; however, comparison with results derived directly, using the inverse Laplace transform, showed negligible error.

8.6.2.2 Simulation of effects of errors

In order to estimate the effects of the sources of error described above on the Δ COP estimates, the analysis algorithms were performed using simulated data. To generate these data, the posture control system was represented as a second-order system, a digital bilinear transform simulation was performed to generate the COP output in response to a PRN platform acceleration input, and a random number generator was used to add simulated measurement noise (Gaussian, zero mean) to the input and output signals. The simulated data were generated using a sample interval of 1 ms, and

TABLE 8.1

RESULTS OF SIMULATION OF MEASUREMENT AND COMPUTATIONAL ERROR

SAMPLE INTERVAL (s)	NOISE (STD DEV) +		% ERROR IN Δ COP ++		
	ACCEL (m/s ²)	COP (mm)	CS MODEL	LS MODEL	ML MODEL
0.06	0.0	0.0	0.190	- 0.439	- 0.467
	0.05	1.5	- 4.09	- 1.55	- 9.92
	0.0025	1.5	- 0.304	22.9	- 1.58
	0.05	1.0	- 3.98	- 5.66	- 9.57
	0.0025	1.0	- 0.183	16.7	- 1.29
0.015	0.0	0.0	0.216	0.450	0.0302
	0.05	1.5	- 0.522	-13.7	- 4.06
	0.0025	1.5	0.397	74.4	- 0.351
	0.05	1.0	- 0.550	-15.4	- 3.89
	0.0025	1.0	0.246	62.8	- 0.230

NOTE: + ACCEL = acceleration (input), COP = centre-of-pressure (output); noise was Gaussian, with zero mean and standard deviation (STD DEV) as indicated;
 ++ % error = (100%)(simulation Δ COP - true Δ COP)/(true Δ COP);
 Δ COP = peak COP displacement in the unit pulse response;
 simulated system was second order (damping coefficient = 1.1, natural frequency = 1.0 Hz, dc gain = -0.2) with zero dead time; CS, LS and ML = cross-spectral, least squares and maximum likelihood models.

the input and output values were then resampled to simulate sampling rates of either 16.7 Hz or 66.7 Hz.

Table 8.1 summarizes the results of the error simulations. The listed values represent the percentage error between the algorithm-computed and true values for ΔCOP . For the results shown in the table, the algorithms were constrained to use the correct model structure (second order, zero dead time).

For the ML method, the results indicated that the error in the ΔCOP predictions due to measurement inaccuracy, sampling and reconstruction error, and computational error was on the order of 10%. Reduction in accelerometer inaccuracy (to 0.0025 m/s^2 , a value attainable with a force-balance accelerometer) reduced the error to about 1.6%, while increase in the sampling rate to 66.7 Hz further reduced the error to 0.35%. Decrease in the COP error standard deviation (to 1 mm, a less conservative estimate of the force plate inaccuracy) yielded only small improvements.

The errors in the CS method were smaller than the ML errors, but tended to show the same trends in response to changes in sampling rate and measurement error.

The LS method produced accurate results in the absence of measurement noise, but otherwise tended to yield large errors in the predicted peak response. The small errors that occasionally occurred would seem to be purely coincidental, as the COP waveforms predicted by the LS analysis differed substantially from the theoretical result. In all simulations where measurement noise was included, the residuals were found to be highly correlated, indicating that the model estimates were biased. In the analysis of the actual experimental data, where the model order was not constrained, selection of a higher model order would tend to "whiten" the residuals (Hsia, 1978); therefore, such large errors are not expected to have occurred in the experimental results.

In the above results, the models were constrained to have the correct structure. When instead the algorithms were allowed to select the model structure, the LS and ML methods invariably overestimated the equation order and often produced erroneous estimates for the dead time as well, resulting in large errors in the ΔCOP predictions. In contrast, the CS method usually selected

the correct model structure.

The above findings are not unexpected, as the Akaike criterion (used to determine the model structure) is known to overestimate the order of time-domain models when a "true" linear finite-order system exists, but provides good results when the goal is to find an approximating model for a more complex system (Shibata, 1976). Thus, it is misleading to extrapolate from the simulation, where the "true" system was of finite order, to the actual measurement situation, where no such "true" system existed. The experimental results suggest that errors in the determination of the model structure did not have a major influence on the Δ COP predictions, as the CS method, an entirely different analytical approach, was found to produce results that were generally very similar to the LS and ML results.

In estimating the SA from the Δ COP prediction, the error in measuring the length of the foot results in a small additional error. For example, if Δ COP = 0.720 m and BOS = 0.260 m (typical values), then an error of 1 mm in the BOS measurement produces a change of 0.4% in the SA estimate.

8.6.3 System Identification Methods

The CS method requires much less computation than the LS or ML methods. For example, to analyze a single test, the combined LS/ML method typically required 4 hours of computer time (VAX 11/730, 1 Mbyte memory), compared to 20 minutes for the parametric CS model and 30 s for the nonparametric frequency response. The CS method has the disadvantage of being statistically inefficient, because of the large number of parameters that are estimated (i.e. a frequency response gain and phase value at each of the 128 frequencies in the FFT, in addition to the parameters in the fitted transfer function) (Jenkins and Watts, 1968). The LS and ML models require estimation of considerably fewer parameters, and therefore should result in more accurate (i.e. smaller variance) parameter estimates.

LS models are accurate provided that the residuals are "white" (i.e. independent); otherwise, the parameter estimates are biased (Hsia, 1978). Increases in model order tend to whiten the residuals. Statistical testing (using the run test; $\alpha = 0.01$)

revealed in almost all cases that the residuals were significantly correlated, even when high-order models were fit. The resulting bias error may explain why the LS Δ COP predictions were found to differ significantly from the CS and ML estimates.

The ML method requires that the residuals are both independent and normal. Although the residuals for the ML model were found to be independent in most of the subjects ($\alpha = 0.01$), the residuals were found to be non-normal in almost all cases (using the chi-square goodness-of-fit test; $\alpha = 0.01$). Fortunately, this violation may not have a large impact on the results, as Gustavsson's (1972) experience suggests that the ML method does not depend critically on the normality assumption.

Comparison of the three system identification models revealed, in general, good agreement in the estimates for the peak pulse response. The poorest agreement was in the BF (test C5) data, in the comparisons with the CS model. Because blindfolding often reduced the coherence at the low and/or high ends of the frequency range and because the coherence was used as a weighting factor in fitting the parametric CS models to the frequency response estimates, the changes in coherence would have a substantial effect on the CS estimates. This may explain the disagreement, since the LS and ML estimates would be much less directly affected by the changes in coherence.

Occasionally, the CS estimates differed substantially from the LS and ML values. In these cases, the pulse response predicted by the CS model was found to include a step change in COP. Unlike the immediate step changes in COP that can occur passively (as a result of the shearing forces on the feet), these steps were delayed, associated with the active muscle-generated response (see Appendix A.3.1). Since muscles cannot generate forces instantaneously, the CS results were judged to be inappropriate. Apparently, in these cases, the AIC criterion resulted in an inappropriate model structure. Use of the model structure with the next lowest AIC value produced pulse response predictions that showed much better agreement with the LS and ML results.

The simulation results presented in the previous section showed the CS method to yield the most accurate Δ COP predictions.

The superior performance of the CS method might be due to: (1) the smaller sample interval used in reconstructing the unit pulse response (0.01 s instead of 0.06 s), and/or (2) more accurate dead-time estimates (the CS method allowed the dead time to be estimated as a continuous variable, whereas the LS and ML methods required the dead time to be an integer multiple of the sample interval). Although the inherent statistical inefficiency of the CS method is expected to result in less accurate parameter estimates than the time-domain methods, it should be noted that the input-output behaviour is often relatively insensitive to errors in the parameter values (Isermann, 1980).

Nonetheless, in view of the large errors that can occasionally occur, the CS method should be used with caution. It is probably best suited for preliminary data evaluation or other applications where computational expense must be minimized. Of the two time-domain methods, the ML results are expected to be more accurate, because of the non-white residuals and resulting bias in the LS estimates.

8.6.4 Estimation of the Saturation Amplitude

In an actual fall, BOS saturation (i.e. the "true" SA) will depend on the location of the COP at the time of the perturbation, as well as the dynamic COP displacement associated with the balancing response. Lacking quantitative *a priori* information about the most probable initial COP location, the nominal SA estimates do not account for this factor.

In many of the predicted pulse responses, a small overshoot occurred as the COP returned to the starting value (e.g. see fig 7.1 in Chapter 7). This overshoot is much smaller than the initial COP displacement and is therefore unlikely to cause BOS saturation. Accordingly, the SA estimates were based on the initial ΔCOP and did not include the return overshoot. SA estimates based on peak-to-peak ΔCOP were in fact found to be less successful in identifying the balance-impaired subjects (e.g. two of the five elderly fallers were identified correctly, test C5, ML model, false positive rate of 25%; in comparison, the SA estimates based on the initial ΔCOP identified three of the five fallers

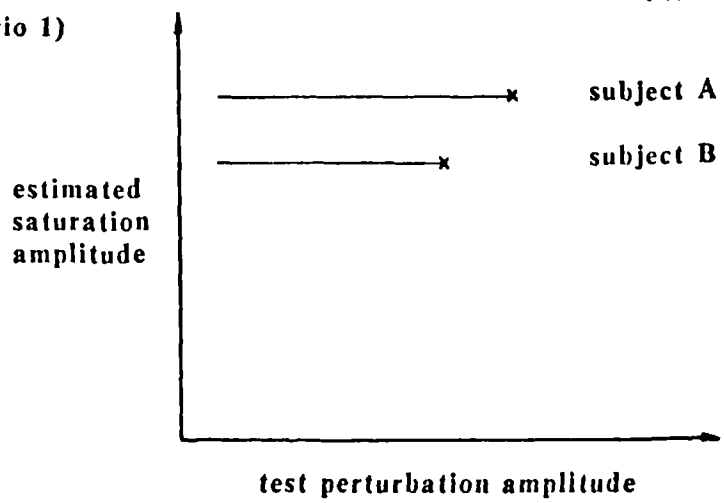
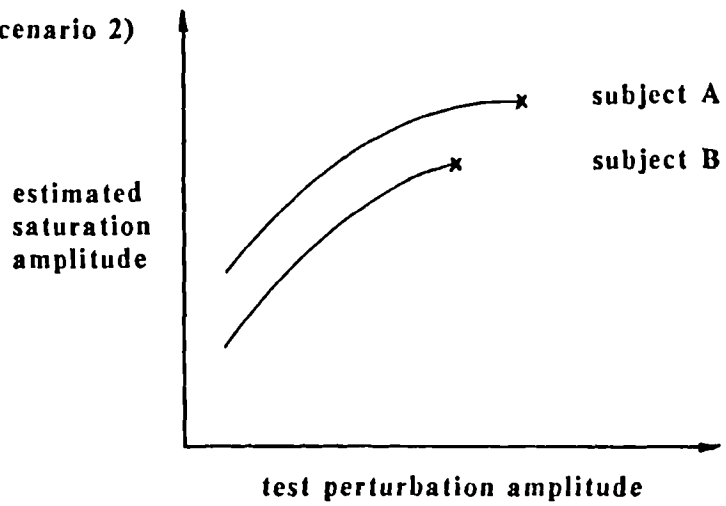
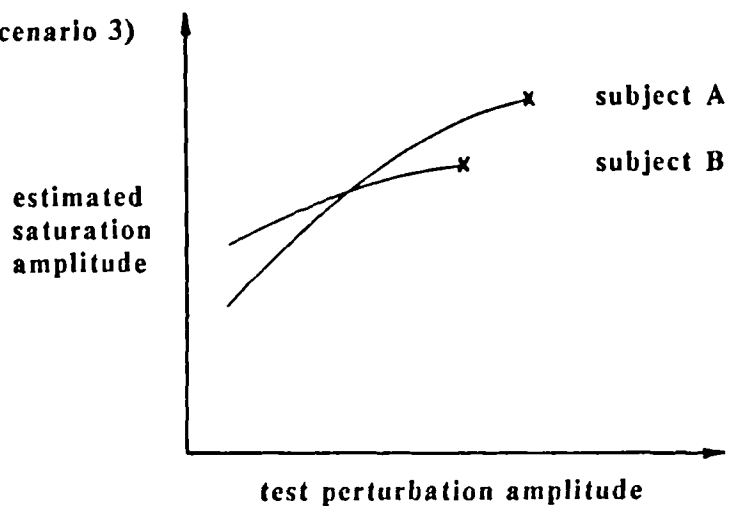
LINEAR SYSTEM (scenario 1)**NONLINEAR SYSTEM (scenario 2)****NONLINEAR SYSTEM (scenario 3)**

Fig 8.1 Influence of nonlinearity on saturation amplitude estimates (x indicates the true saturation amplitude).

correctly).

The best functional definition for the length of the BOS was found to be a proportional linear function of total foot length; therefore, the SA was estimated by defining the BOS to be equal to the average foot length. The inaccuracies inherent to this approximation may contribute to the error in the SA estimates (see Section 8.4.3).

8.6.5 Linearity

The balance testing methodology is based on an assumption that the posture control system is approximately linear for perturbation amplitudes ranging from the test amplitude up to the amplitude at which BOS saturation would actually occur. For a nonlinear system, the dynamic performance is dependent on the input amplitude and waveform. Thus, nonlinearity will cause the SA estimates to become dependent on the perturbation amplitude used in the balance test, and will further affect the SA estimates by reducing the accuracy with which the transient pulse response (used to estimate the SA) can be predicted from the continuous-waveform test.

The amplitude dependence issue is illustrated in figure 8.1. In order to consider this issue separately from the waveform dependence, it is assumed that the SA is estimated directly, using a transient pulse as the test perturbation. Thus, by definition, the SA estimate is equal to the true value at the perturbation amplitude which actually causes BOS saturation to occur (assuming an initial COP location at the opposite end of the foot).

Three scenarios are depicted in the figure: (1) a linear system, (2) a nonlinear system where all subjects show similar (i.e. approximately parallel) nonlinear trends, and (3) a nonlinear system where subjects show differing nonlinear trends. For the linear system, accurate results will be achieved regardless of the perturbation amplitude used in the test. In the nonlinear scenarios, small-amplitude tests will fail to yield accurate predictions of large-amplitude response. Nonetheless, in scenario-2, the inter-subject differences are independent of the test perturbation amplitude; hence, the results allow useful comparative evaluations, provided that all subjects are tested at

the same amplitude. In scenario-3, the inter-subject differences are highly dependent on the test perturbation amplitude. In this case, the results of the balance test will fail to be meaningful, even on a comparative basis, unless the induced balancing responses approach the BOS saturation limits. This requires close matching of the test perturbation amplitude to the balancing capabilities of each subject.

Provided that the transient pulse response is measured directly, the estimated SA for a nonlinear system will approach the true value as the test amplitude approaches the amplitude that actually causes BOS saturation. In the balance test, however, the transient response is predicted from a linear model estimated using a continuous-waveform perturbation. The continuous waveform excites the posture control system over a wide operating range, and the resulting model is a linearized version of the actual dynamic characteristics "averaged" over this operating range. Increasing the amplitude of the continuous waveform will help to make the linearized model more representative of large-amplitude behaviour, however, for a nonlinear system, the error in the large-amplitude transient response predictions can never be completely eliminated.

Direct measurements of transient response seemed to indicate substantial nonlinearity in the sub-saturation postural responses. The linear transfer functions derived from the steady-state balance tests predicted small-amplitude transient response reasonably well, but overestimated the large-amplitude response. Although the amplitude dependence was fairly well represented by a common nonlinear function, there was also evidence to suggest significant subject-to-subject differences in the nonlinear trends. In interpreting these results, however, it must be re-emphasized that it is not clear to what extent the amplitude dependence observed in the transient tests was a result of adaptation to the protocol, rather than nonlinearity in the control mechanisms.

The PRN test results did not allow for an accurate assessment of linearity, as they too may have been confounded by adaptive effects. In the pilot experiments, where order effects were eliminated by randomized order of testing, the results suggested approximate linearity for PRN RMS amplitudes exceeding 0.1 m/s^2

(the mid-range amplitude in the main experiments); however, these results were based on a very limited number of subjects.

Since the issue of nonlinearity could not be resolved based on the present data, two separate experimental analyses were performed. To allow for scenario-2, the analysis was performed using the data from test C2, in which all subjects (except one faller) were tested at the same amplitude. In this case, the SA estimates are viewed as a comparative measure of postural performance. To allow for scenario-3, the analysis was repeated using the "best" test (i.e. largest tolerated amplitude) for each subject. Regardless of the linearity scenario, use of the "best" test data has the advantage of providing an improved signal-to-noise ratio in the measurements.

Use of the test-C2 data was found to be more successful in identifying the balance-impaired subjects than the "best" test data. Note, however, that only one amplitude "iteration" was performed for each subject; therefore, the maximum amplitude tested may not be representative of the maximum balancing capabilities of each subject. In addition, the "best" test results may have been degraded by order effects, since subjects differed in terms of which test was used to estimate their SA.

8.6.6 Modulation of Balance Test Responses

Experimental evidence suggests that balancing responses may be modulated according to the context of the balancing task, i.e. previous experience and current expectations about the perturbation, the available sensory information and the support surface conditions (e.g. Nashner, 1976; Horak et al, 1985; Horak and Nashner, 1986; Moore et al, 1986). The response modulation may be achieved through changes in the feedback gain(s) of the control system. Alternatively, there may be a change in balancing synergy. In addition to gain adjustments, this would involve changes in the pattern and relative timing of the muscle activation.

Conceptually, the feedback gain sets the "stiffness" of the posture control system. Stiffness modulation could occur through a number of mechanisms. The stiffness of the muscle actuators could

be increased through co-contraction of antagonist muscle groups or through muscle pre-stretching (e.g. by leaning). Whereas co-contraction or pre-stretching might influence the excitability of the muscle somatosensors, the spindle sensitivity and threshold could also be modulated separately through the gamma motoneuron system. Conceivably, stiffness can also be modulated through adjustment of the neural feedback gain "pre-settings" associated with the different sensory channels. In physiological terms, this could occur through tonic facilitation or inhibition of the various postural reflexes. One example of stiffness modulation through neural gain adjustments would be the "reweighting" of sensory inputs that appears to occur when one or more sensory channels is blocked or disrupted (Nashner et al, 1982). Another example would be the habituation of inappropriate destabilizing responses that occurs during repeated exposure to rotational platform perturbations (Nashner, 1976).

For simplicity, in the earlier discussions of stiffness modulation (Sections 8.2.3 and 8.3.1), it was tacitly assumed that increases in stiffness lead to improved stability, i.e. increased SA. In point of fact, it is also possible to explain improvements in SA in terms of stiffness decreases. Apparently, the effect of a given stiffness modulation is dependent on the stiffness level. As demonstrated in inverted-pendulum simulations (see Appendix A.3.5), stiffening beyond the optimum stiffness may actually lead to increased COP displacement. Conversely, at supra-optimal stiffness levels, decrease in stiffness may yield a reduced COP displacement.

Changes in balancing synergy could influence the balance test results, since the ankle synergy is expected to produce larger COP displacements than the hip synergy (see Section 8.5.1). Horak and Nashner (1986) observed that the ankle synergy was employed during tests on normal support surfaces, but found that shortening the surface resulted in more complex patterns that were apparently a combination of the ankle and hip synergies. After repeated practice, some of the subjects showed a progressive shift to a pure hip synergy. Although Horak and Nashner studied only the effects of support surface, it seems likely that other context-related factors (e.g. perturbation amplitude) could also affect the synergy

selection. In addition, stiffness modulation may have an interacting influence. For example, co-contraction may tend to "rigidify" the hip, thereby interfering with the use of the hip synergy.

It is not clear to what extent response modulation is an automatic adaptive process (i.e. part of a fixed control hierarchy) or a result of conscious, voluntary, anticipatory adjustments. It may be that some of the modulation mechanisms are voluntary (e.g. leaning, co-contraction) and others are automatic (e.g. reweighting of sensory inputs). A randomized series of tests in which a subject was instructed to either relax or co-contrast his leg muscles confirmed that a voluntary strategy such as this can lead to significant changes in the balance test results ($p < 0.01$; mean SA of 0.486 when relaxed, 0.420 when co-contracted; ML model).

Response modulation is apparently influenced by the subject's perception of the postural threat that the perturbation represents, i.e. the perturbation amplitude. This is supported by Horak et al (1985), who found that amplitude-dependent modulation of balancing responses disappeared when the amplitudes were randomized. Thus, although the amplitude dependence described in the previous section could be due to intrinsic control-loop nonlinearity, amplitude-dependent response modulation is another possible explanation.

Ideally, in order to accurately predict falling liability, the balance test would evoke the same balancing strategy (i.e. synergy and stiffness level) that would occur in typical falling situations. In balance tests that lack an adequate postural threat, relatively stable subjects may tend to adopt a "sloppy" control strategy. In order to evoke more realistic responses in the balance test, it may be necessary to more closely match the level of perturbation to the balancing capabilities of each subject.

Conversely, it is desirable to eliminate compensations that are unlikely to occur in actual falling situations. One such compensation would be the anticipatory leaning found to occur in transient testing (Moore et al, 1986); however, this adaptation is not expected to provide any benefit in the continuous-waveform

balance test beyond the first few "strokes" of the perturbation. This is supported by the results of a randomized series of tests in which a subject was instructed to either lean forward or assume a normal posture prior to the start of each balance test. The leaning had no significant effect on the SA estimates ($p > 0.1$).

Since co-contraction is an inefficient and fatiguing strategy (Winter, 1978), one can argue that it would not be used to increase stability during normal activities, except possibly for short periods where the balance threat is heightened (e.g. walking in an unfamiliar darkened room). However, experimental evidence shows that substantial co-contraction may in fact occur during the normal gait cycle. Olney (1985) reported a mean co-contraction index of 23% (at the ankle) during the stance phase, while Falconer and Winter (1985) reported a mean value of 42% during the weight acceptance phase and 24% during the push-off phase (the co-contraction index represents the percentage of total flexion and extension muscle moment that is "wasted" in co-contraction). It is not clear whether similar co-contraction occurs during other activities of daily living (ADL), or whether the levels of co-contraction that might occur during the balance test are at all comparable to that occurring during gait or ADL. It may prove useful to account for co-contraction occurring during the balance test by normalizing the balance test response with respect to the relative co-contraction level. Note, however, that this normalization process may be confounded if the relationship between SA and co-contraction level is not monotonic.

8.6.7 Repeatability

If the balance test is to be used in studying factors that influence postural control, then it is important that the results show good test-to-test repeatability. If the test is to be used as a monitoring tool, then the day-to-day repeatability must be good.

Pilot tests suggested that large test-to-test changes may occur between the first and subsequent tests (see Appendix C). In general, however, the pilot tests indicated relatively small levels of random test-to-test variability, with the coefficient of variation (CV) ranging from 2 to 19% (average of 6.6%). There was

no evidence of significant test-to-test trends that might suggest adaptation or fatigue. Two of six subjects showed evidence of day-to-day trends. Otherwise, day-to-day repeatability was good, with the CV ranging from 2 to 20% (average of 7.7%). Further testing of larger numbers of subjects is needed to substantiate the pilot results.

In the main experiments, the EO PRN tests on the elderly normals gave no evidence to suggest significant test-to-test trends. However, the results of the young normals were less conclusive. For these subjects, there were significant differences between tests C2 and C3 or between tests C1 and C3, depending on the system identification model; however, these differences may have been a result of the change in perturbation amplitude, rather than adaptive effects. As discussed in Section 8.6.5, perturbation amplitude will affect the SA estimates if the assumed linear operating range of the posture control system is substantially nonlinear. There were in fact no significant differences between tests C1 and C2, which were performed at the same amplitude.

8.6.8 Validation of the Balance Test

The practical utility of the balance test can be validated by assessing its sensitivity in identifying disordered or deteriorated postural control and by comparing this sensitivity to that of the more traditional (and simpler) spontaneous sway measurements.

In the preliminary evaluations performed here, the BF balance test results and the EO/BF ratio were reasonably successful in identifying vestibular patients and elderly fallers. However, in using the EO data alone, the results were poor. Greater success was achieved using certain spontaneous sway measures. Unfortunately, because BF spontaneous sway was not measured in the present study, the two testing methodologies cannot be compared with regard to vision-deprived balancing performance.

Although Kirshen et al (1984) found eyes-closed measurements of spontaneous sway to provide the best discrimination of fallers from controls, Bartlett et al (1986) obtained the same misclassification rates using either eyes-open or eye-closed data. In contrast to Bartlett's results, the SA misclassification rates

were highly dependent on the visual conditions. It may be that the balance test is a more sensitive measure of the influence of visual factors on postural performance. A comparative evaluation of the two testing methodologies under both visual conditions is needed.

For the normal subjects, the age-related differences seen in the spontaneous sway measures were not as pronounced as the age-related differences in the balance test results (i.e. $0.005 < p < 0.05$ in the spontaneous sway measures compared to $p < 0.001$ or $p < 0.0001$ in the balance test results). This result suggests that the balance test may be a more sensitive measure of the deterioration in balance that is expected to occur in normal ageing.

The balance test may also have an advantage over spontaneous sway measures in terms of repeatability. As discussed in the previous section, pilot experiments found day-to-day and test-to-test CV's ranging from 2 to 20% (average of 7 to 8%). In comparison, Black et al (1982) reported CV's ranging from 14% to 86% (average of 40-45%) in repeating their measurements of spontaneous COP displacement on five consecutive days, while Holliday and Fernie (1979) found a reduction of 25% in the average speed of spontaneous hip displacement over five consecutive days of testing. For repeated same-session tests, Hufschmidt et al (1980) reported mean CV's ranging from 25 to 60% in their measures of spontaneous COP sway (i.e. RMS sway, sway path, projected area of sway and mean frequency of sway).

Note that the larger intra-individual variation will not necessarily degrade the utility of the spontaneous sway test, provided that inter-subject differences or differences resulting from changes in test conditions (e.g. visual deprivation) are also proportionately larger. Experimental evidence, however, suggests that this may not be the case. For example, the spontaneous sway test and the balance test were found to yield comparable age-related differences, i.e. both tests showed differences of approximately 10-30% in comparing the mean results for the young and elderly normals.

8.7 SUGGESTED IMPROVEMENTS TO THE BALANCE TEST

8.7.1 The Perturbation Platform

The simulation of the effects of measurement and sampling error on the balance test results indicated that substantial improvements could be achieved by reducing the error in the acceleration measurements (to 0.0025 m/s^2) and by increasing the sampling rate (to 66.7 Hz). The increased accuracy in the acceleration measurements could be provided by a servo force-balance accelerometer. The increased sampling rate could be achieved using a dedicated data acquisition and control system.

Foot placement could be facilitated by means of a mechanism that could be slid into contact with the perimeter of the feet. By incorporating linear potentiometers into the design, automatic measurement of the maximum a-p and m-l dimensions of the BOS could be achieved. This system would improve the accuracy of the BOS measurements and would help to detect and prevent test-to-test changes in foot position. For safety, the device would have to be removed during the tests, or else designed to provide minimal restraint of foot movements (e.g. to allow stepping).

In testing particularly apprehensive subjects, it was sometimes difficult to persuade these subjects not to touch the safety handrails during the tests. This problem might be solved by slightly increasing the handrail-to-subject distance, so that subjects would have to either lean or take a small step in order to grab the handrail. Alternatively, the handrails might be replaced by a safety harness. However, as discussed in Section 4.2.4, the harness would have to be carefully designed so as to minimize any sensory feedback and to distribute the restraining forces in such a way as to prevent injury.

Apprehension might be reduced by mounting the platform so that the surface is flush with the surrounding floor and by locating the platform in a "friendlier" nontechnical environment. The use of a safety harness may actually tend to increase apprehension in some subjects; pilot tests are needed to evaluate this possibility.

Although a poster was used as a central visual target, the peripheral visual field comprised blank styrofoam panels. Both central and peripheral visual stimuli could be better controlled by

covering all surfaces of the visual field with patterns of dots (or other markings) with known spatial frequency content. More realistic simulations of typical falling situations might be achieved by increasing the spatial frequency content of the peripheral visual field. Increasing the eye-object distances might also help to improve the simulation of actual falls.

To facilitate experiments on the effects of changes in visual conditions, the visual surround should be redesigned. By using an adjustable framework with removable panels, the eye-object distances and spatial frequency content could be readily changed. By mounting the framework on a separate carriage, the movement of the visual surround could be divorced from the platform motion. Thus, the surround could remain stationary, it could be linked to move with the platform, or it could be controlled to move independently (e.g. servo-driven to null out visual cues).

8.7.2 The Testing Procedure and Protocol

Since none of the RAN tests conducted to date showed any evidence of sharp peaks or troughs in the frequency response, the test procedure could be expedited by eliminating the RAN test.

Some of the elderly fallers found the *three-minute tests* difficult to tolerate; therefore, the duration of the test should be reduced. Two minutes might be a reasonable compromise between tolerance and estimation accuracy.

For some of the fallers, the 0.1 m/s^2 amplitude was too large; therefore, the first tests should be conducted at a smaller amplitude (e.g. 0.05 m/s^2). Testing all subjects at the same amplitude is useful, as it provides a basis for comparison of subjects independent of any assumptions of linearity in the balancing responses (see Section 8.6.5).

In addition, more accurate simulation of balancing behaviour in falling situations might be achieved by more closely matching the perturbation amplitude to each subject's capabilities. This would help to reduce errors due to possible nonlinearity in the sub-saturation balancing responses, and would tend to prevent subjects from adopting a "sloppy" control strategy (see Sections 8.6.5 and 8.6.6).

The difficulty lies in determining the balancing capabilities of each subject. Simply increasing the testing amplitude until the subject "bails out" (i.e. grabs a handrail or moves his/her feet) will tend to increase the apprehension of the subjects and may also jeopardize their safety. Moreover, the decision to "bail out" may occur well before the true limits of stability are reached. An improved approach would be based on determining the amplitude at which the maximum anterior or posterior COP displacement exceeds some pre-determined threshold (e.g. 75% of the foot length). This amplitude could be determined by quickly "ramping" through a series of very short tests of increasing amplitude. A full-duration test would then be performed at the determined amplitude.

As discussed in Section 8.6.6, it may be useful to minimize the effects of anticipatory changes in co-contraction level by normalizing the test results with respect to relative co-contraction level. The relative co-contraction could be defined as the mean co-contraction measured during the balance test divided by the mean co-contraction measured during quiet standing. In order to quantify co-contraction, the balance test procedure would include bilateral electromyographic (EMG) measurements from appropriate antagonist muscle pairs (e.g. tibialis anterior and gastrocnemius).

To better identify direction-dependent impairments, the balance testing protocol could include both a-p and m-l perturbations. The m-l perturbations could be achieved by standing the subjects "sideways" on the platform. Although this would preclude separate measurements of the COP for each foot, such measurements are not essential in the balance tests.

8.8 DIRECTIONS FOR FUTURE RESEARCH

Although the results presented here are encouraging, the ultimate assessment of the balance test as a predictor of falling liability in the elderly must come through a study of a large, randomly-selected elderly population. In order to obtain accurate fall data, the falling history of the subjects would be monitored prospectively, following the balance test. The possibility of using other measures (e.g. gait, vision, etc.) in combination with

the balance test results to obtain improved predictions of falling liability should be explored.

Future experiments should include measurements of spontaneous postural sway, to allow the balance test to be compared further with more traditional (and simpler) measures of postural stability. The possibility of normalizing the balance test results with respect to co-contraction level could be explored by including agonist-antagonist EMG measurements in the test protocol. To better identify direction-dependent impairments, both a-p and m-l perturbations could be used.

Further transient testing is needed to assess the ability of the balance test to predict large-amplitude transient response. Anticipatory effects could be minimized by randomizing the direction of the perturbation and/or the order in which the different amplitudes are tested. EMG measurements could be included to allow assessment of anticipatory co-contraction. For safety, the experiments would be limited to young healthy adults (as in the present study). In addition, a safety harness would be used, accepting the limitation that the harness would probably provide some degree of sensory feedback.

The ability of the balance test to identify patients with various balance-impairments needs further investigation. The utility of m-l perturbations could be explored, particularly with reference to identification of patients with unilateral vestibular deficits. Improved identification of unilateral deficits might be achieved through separate analysis of the two feet, which would allow left/right asymmetries to be assessed.

The balance test could be further validated by testing normal subjects under altered conditions. If the balance test is a good predictor of postural stability, it should identify changes in response resulting from the altered states. Moreover, the detected changes should agree with existing knowledge. Ankle proprioception, plantar pressure cues and ankle stiffness could be altered by standing the subjects on a compliant surface (e.g. foam rubber). More selective disruptions could be achieved through ischemic blocking of ankle proprioception (i.e. by applying a tourniquet to the lower leg). Alternatively, plantar

mechanoreceptor input could be altered by standing the subjects on beds of ball bearings and varying the diameter and spacing of the bearings. Topical anaesthetics or ice baths could be used to impair mechanoreceptor function. The effects of drugs and medications could also be tested.

In addition to validating the posture control model and balance testing methodology, further testing of normal subjects under altered conditions and patients with balance deficits may yield more fundamental information about the organization of postural responses and the contributions of the different sensory modalities.

Of particular interest is disruption of the plantar mechanoreceptors. The contribution of these *sensors to postural* control has been little studied; however, they may play an important role, particularly if BOS saturation does in fact trigger projective balancing responses. Conceivably, the mechanoreceptors would provide the posture control system with the necessary information about the COP location relative to the BOS limits. In this context, it is interesting to note that some investigators have found that direct COP measurements are needed to stabilize lower-limb neuroprostheses (Chizeck et al, 1985).

Another area for further study involves the effects of changes in visual conditions on the balance test responses. Tested conditions could include blindfolding, voluntary eye-closure, visual input from the platform frame of reference (surround moves with the platform), visual input from the external frame of reference (stationary surround), and unrestricted visual input (subject allowed to view both platform and stationary environment). Such a study might help to explain the differences between the present results and other results reported in the literature, and could lead to further improvements in the balance testing methodology.

Once its validity as a predictor of postural stability has been established, the balance test can be used to investigate different factors that might contribute to falling and to develop methods for preventing falls. Examples of factors that could be studied include environmental lighting, drugs, hypoxia,

environmental pollutants, noise, footwear and orthoses. At this point, work could also begin on refining the balance testing methodology and instrumentation into a simple clinical tool for identifying functional balance impairments and screening potential fallers.

CHAPTER 9. SUMMARY

A balance testing methodology was developed, based on a posture control model which defines relative stability by the degree to which a transient postural perturbation would cause the centre-of-pressure on the feet to approach the limits of the base-of-support. To minimize anticipatory adaptations and to ensure subject safety, the balance test uses a small-amplitude continuous random or pseudorandom perturbation. The data are used to identify an input-output model, which is then used to predict large-amplitude transient response.

To simulate the kinematics and sensory cues of typical falling situations, the test perturbation was selected to be an anterior-posterior acceleration of a platform on which the subject stands, with a visual surround that moves with the platform. The perturbation platform was designed to have the amplitude and bandwidth capabilities needed to perturb balance to the point of instability. The design requirements were estimated, in part, from the results of digital simulations of balancing responses. Static and dynamic tests were performed to assess the accuracy of the force plates and accelerometer mounted on the platform carriage.

The waveform, power spectrum, bandwidth, amplitude and duration of the perturbation signal were selected to satisfy requirements for persistent excitation, accurate identification, stationarity, and subject safety and tolerance. Pilot experiments were performed to aid in the selection of the perturbation parameters, and to assess the repeatability of the balance test responses.

In using the balance testing methodology to test 64 young and elderly normal healthy adult subjects, the following results were demonstrated:

- (1) highly significant age-related differences, with decreased stability predicted for the elderly under both eyes-open and blindfolded conditions;
- (2) no significant sex-related differences;
- (3) significant increase in predicted stability when blindfolded, on the average and in the vast majority of subjects.

Although the differences between the results obtained using three different system identification methods (cross-spectral, least squares and maximum likelihood) were generally small, errors in model structure determination occasionally led to inappropriate results when using the cross-spectral method.

In using the balance test to identify balance-impaired individuals, the blindfolded results and eyes-open/blindfolded ratio provided higher success rates than the eyes-open results. Depending on the modelling method, the balance test was able to identify correctly up to three of five vestibular patients and five of five elderly fallers, at a false positive rate of 25% in the normal subjects. With the exception of one vestibular patient, all of the balance-impaired subjects showed relatively normal levels of performance during eyes-open tests.

Generally, the balance test results were found to be weakly correlated with measures of eyes-open spontaneous postural sway. For the normal young adults, however, certain amplitude measures of spontaneous sway showed agreement with the balance test scores. Significant age-related differences in spontaneous sway were detected in the normal subjects, although the differences were not as pronounced as those demonstrated in the balance test results. Significant sex-related differences disappeared when the amplitude measures of sway were normalized with respect to the length of the base-of-support. In using the eyes-open spontaneous sway measures to identify the balance-impaired subjects, up to two of five vestibular patients and four of five elderly fallers were identified correctly, at a false positive rate of 25% or better in the normal subjects.

Direct measurements of transient response in the young normal subjects revealed a substantial decrease in the gain of the response with increasing perturbation amplitude. The transient response predictions derived from the balance test results provided reasonably accurate predictions of small-amplitude transient response, but were found to overestimate the peak response to larger transient perturbations. It is not clear, however, to what extent the transient test results were confounded by amplitude- and/or order-dependent adaptations. In using the transient

response results to define the functional length of the base-of-support in forward sway, the best definition was found to be a proportional function of the total foot length.

The lack of correlation between the balance test results and measures of spontaneous postural sway and the increases in predicted stability found in the blindfolded tests suggest that subjects may modulate their control strategy according to the circumstances of the balancing task. The transient test results, order effects notwithstanding, are suggestive of intrinsic nonlinearity in the posture control system or, alternatively, amplitude-dependent response modulations. In order to improve the predictions of postural performance in actual falling situations, it may be necessary to more closely match the test perturbation amplitude to the balancing capabilities of each subject. Nonetheless, even if the balance test fails to yield predictions of postural stability that are accurate in an absolute sense, it still provides a basis for comparing the postural performance of different individuals in relative terms.

In conclusion, the balance testing methodology developed in this thesis appears to provide a sensitive functional measure of the changes in postural control that are known to occur in normal ageing. Although it shows promise as a tool for identifying balance-impaired individuals, larger numbers of balance-impaired subjects must be tested to provide more conclusive evidence than the preliminary evaluation performed here. Future experiments should include measurements of spontaneous postural sway, to allow the balance test results to be compared further with more traditional (and simpler) measures of postural stability.

LIST OF REFERENCES

- Aggashyan RV, Gurfinkel VS, Mamasakhlisov GV and Elner AM (1973), Changes in spectral and correlation characteristics of human stabilograms at muscle afferentation disturbance. *Agressologie* 14D:5-9.
- Akaike H (1974), A new look at the stochastic model identification. *IEEE Trans Automatic Control* AC-19:716-723.
- Allum JHJ and Budingen HJ (1979), Coupled stretch reflexes in ankle muscles: an evaluation of the contributions of active muscle mechanisms to human postural stability. *Prog Brain Res* 50:185-195.
- Allum JHJ and Keshner EA (1986), Vestibular and proprioceptive control of sway stabilization, in "Disorders of Posture and Gait", eds W Bles and T Brandt, Elsevier, Amsterdam, pp 19-40.
- Allum JHJ and Pfaltz CR (1985), Visual and vestibular contributions to pitch sway stabilization in the ankle muscles of normals and patients with bilateral peripheral vestibular deficits. *Exp Brain Res* 58:82-94.
- Allum JHJ, Mauritz K and Vogele H (1982), The mechanical effectiveness of short-latency reflexes in human triceps surae muscles revealed by ischaemia and vibration. *Exp Brain Res* 48:153-156.
- Andres RO (1982), Diagnostic implications of induced body sway, in "Nystagmus and Vertigo", eds V Honrubia and MAB Brazier, Academic Press, New York, pp 191-204.
- Andres RO and Anderson DJ (1980), Designing a better postural measurement system. *Am J Otolaryngol* 1:197-206.
- Aniansson A, Grimby G and Rundgren A (1980), Isometric and isokinetic quadriceps muscle strength in 70-year-old men and women. *Scand J Rehabil Med* 12:161-168.
- Ashley MJ, Gryfe CI and Amies A (1977), A longitudinal study of falls in an elderly population: 2. Some circumstances of falling. *Age Ageing* 6:211-220.
- Åström KJ (1980), Maximum likelihood and prediction error methods. *Automatica* 16:551-574.
- Åström KJ and Wittenmark B (1984), Computer controlled systems: theory and design, Prentice-Hall, Englewood Cliffs, New Jersey, Chap 13.
- Baker SP and Harvey AH (1985), Fall injuries in the elderly, in "Symposium on Falls in the Elderly: Biologic and Behavioural Aspects", eds TS Radebaugh, E Hadley and R Suzman, WB Saunders, Philadelphia (*Clin Geriatr Med* 1:501-512).

- Barin K (1980), An empirical evaluation of the one-link inverted pendulum model of human postural dynamics, MS Thesis, Ohio State University, Columbus, Ohio.
- Barin K (1983), An experimental study of multi-link models of human postural dynamics and control, PhD Thesis, Ohio State University, Columbus, Ohio.
- Bartlett SA, Holliday PJ, Maki BE and Fernie GR (1986), On the classification of a geriatric subject as a faller or non-faller. *Med Biol Eng Comput* 24:219-222.
- Begbie GH (1967), Some problems of postural sway, in "Myotatic, Kinaesthetic and Vestibular Mechanisms", eds AVS Dereuck and J Knight, Ciba Foundation Symposium, JA Churchill, London.
- Belanger M and Patla AE (1984), Corrective responses to perturbation applied during walking in humans. *Neurosci Lett* 49:291-295.
- Bendat JS and Piersol AG (1971a), *Random data: analysis and measurement procedures*, Wiley-Interscience, New York, pp 122-125.
- Bendat JS and Piersol AG (1971b), *Random data: analysis and measurement procedures*, Wiley-Interscience, New York, Chaps 5,6.
- Bendat JS and Piersol AG (1980), *Engineering applications of correlation and spectral analysis*, Wiley-Interscience, New York, Chaps 4,5.
- Bensel CK and Dzendolet E (1968), Power spectral density analysis of the standing sway of males. *Perception Psychophysics* 4:285-288.
- Berger W, Dietz V and Quintern J (1984), Corrective reactions to stumbling in man: neuronal coordination of bilateral leg muscle activity during gait. *J Physiol* 357:109-125.
- Berthoz A, Pavard B and Young LR (1975), Perception of linear horizontal self-motion induced by peripheral vision (linear vection): basic characteristics and visual-vestibular interactions. *Exp Brain Res* 23:471-489.
- Black FO, O'Leary DP, Wall C and Furman J (1977), The vestibulo-spinal stability test: normal limits. *Trans Am Acad Ophthalmol Otol* 84:549-560.
- Black FO, Wall C, Rockette HE and Kitch R (1982), Normal subject postural sway during the Romberg test. *Am J Otolaryngol* 3:309-318.
- Bles W and deJong JMBV (1986), Uni- and bilateral loss of vestibular function, in "Disorders of Posture and Gait", eds W Bles and T Brandt, Elsevier, Amsterdam, pp 127-139.
- Box GEP and Jenkins GM (1976), *Time series analysis: forecasting and control*, Holden-Day, San Francisco, Chap 11.

- Brandt T, Paulus W and Straube A (1986), Vision and posture, in "Disorders of Posture and Gait", eds W Bles and T Brandt, Elsevier, Amsterdam, pp 157-175.
- Brauer D and Seidel H (1980), The autoregressive structure of postural sway. *Agressologie* 21E:101-104.
- Brocklehurst JC, Robertson D and James-Groom P (1982), Clinical correlates of sway in old age - sensory modalities. *Age Ageing* 11:1-10.
- Brodal A (1981), *Neurological anatomy*, third edition, Oxford University Press, New York, Chap 2.
- Brown KT (1980), Physiology of the retina, in "Medical Physiology, Fourteenth Edition", ed VB Mountcastle, CV Mosby, St Louis, pp 504-543.
- Brown JE and Frank JS (1987), Influence of event anticipation on postural actions accompanying voluntary movement. *Exp Brain Res* (in press).
- Camana PC, Hemami H and Stockwell CW (1977), Determination of feedback for human posture control without physical intervention. *J Cybernetics* 7:199-226.
- Campbell MJ, McComas AJ and Pitito F (1973), Physiological changes in ageing muscles. *J Neurol Neurosurg Psychiatry* 36:174-182.
- Campbell AJ, Reinken J, Allan BC and Martinez GS (1981), Falls in old age: a study of frequency and related clinical factors. *Age Ageing* 10:264-270.
- Carlsöö S (1972), *How man moves: kinesiological methods and studies*, Heinemann, London.
- Carter G and Ferrie JF (1979), A coherence and cross spectral estimation program, in "Programs for Digital Signal Processing", IEEE Press, New York.
- Cernacek (1980), Stabilography in neurology. *Agressologie* 21D:25-29.
- Chan CW, Jones GM, Kearney RE and Watt DG (1979), The 'late' electromyographic response to limb displacement in man: I. Evidence for supraspinal contribution. *Clin Neurol* 46:173-181.
- Chaney RE (1965), Whole body vibration of standing subjects, Boeing Company, Report No. BOE-D3-6779, Wichita, Kansas. As quoted by McCormick EJ (1976), "Human Factors in Engineering and Design (Fourth Edition)", McGraw-Hill, New York, p 385.

- Chao EY (1978), Experimental methods for biomechanical measurements of joint kinematics, in "CRC Handbook of Engineering in Medicine and Biology", eds BN Feinberg and DG Fleming, Chemical Rubber Co., Cleveland, Ohio, pp 385-411.
- Chizeck HJ, Selwan PM and Merat FL (1985), A foot pressure sensor for use in lower extremity neuroprosthetic development, at "RESNA 8th Annual Conference", Memphis, Tennessee.
- Cordo PJ and Nashner LM (1982), Properties of postural adjustments associated with rapid arm movements. *J Neurophysiol* 47:287-302.
- Daley ML and Swank RL (1981), Quantitative posturography: use in multiple sclerosis. *IEEE Trans Biomed Eng* BME-28:668-671.
- Davies CTM and White MJ (1983), Contractile properties of elderly human triceps surae. *Gerontology* 29:19-25.
- Dichgans J, Mauritz KH, Allum JHJ and Brandt T (1975), Postural sway in normals and atactic patients: analysis of the stabilizing and destabilizing effects of vision. *Agressologie* 17C:15-24.
- Diener HC, Dichgans J, Bootz F and Bacher M (1984), Early stabilization of human posture after a sudden disturbance: influence of rate and amplitude of displacement. *Exp Brain Res* 56:126-134.
- Dietz V, Mauritz KH and Dichgans J (1980), Body oscillations in balancing due to segmental stretch reflex activity. *Exp Brain Res* 40:89-95.
- Do MC, Breniere Y and Brenguier P (1982), A biomechanical study of balance recovery during the fall forward. *J Biomech* 15:933-939.
- Doebelin EO (1975), *Measurement systems: application and design*, McGraw-Hill, New York, Chap 3.
- Doebelin EO (1980), *System modelling and response: theoretical and experimental approaches*, John Wiley and Sons, New York, Chap 6.
- Dorfman LJ and Bosley TM (1979), Age-related changes in peripheral and central nerve conduction in man. *Neurology* 29:38-44.
- Dornan J, Fernie GR and Holliday PJ (1978), Visual input: its importance in the control of postural sway. *Arch Phys Med Rehabil* 59:586-591.
- Drillis R and Contini R (1966), Body segment parameters, Report No. 1163-03, Office of Vocational Rehabilitation, Department of Health, Education and Welfare, New York. As quoted by Roebuck JA, Kroemer KHE and Thomson WG (1975), "Engineering Anthropometry Methods", Wiley-Interscience, New York, Chap 6.

Droulez J, Berthoz A and Vidal PP (1985), Use and limits of visual vestibular interaction in the control of posture, in "Vestibular and Visual Control on Posture and Locomotor Equilibrium", eds M Igarishi and FO Black, Karger, Basel, Switzerland, pp 14-21.

Edwards AS (1947), Body sway and nonvisual factors, J Psychol 23:241-254. As quoted by Hinchcliffe R (1983), in "Hearing and Balance in the Elderly", ed R Hinchcliffe, Churchill Livingstone, New York, pp 227-250.

Eklund G (1969), Influence of muscle vibration on balance in man. Acta Soc Medica Upsala 74:113-117. As quoted by Nashner LM (1981), in "Handbook of Behavioural Neurobiology, Volume 5, Motor Coordination", eds AL Towe and ES Luschei, Plenum Press, New York, pp 527-565.

Electrocraft (1980), DC motors, speed controls and servo systems (fifth edition), Electrocraft Corporation, Hopkins, Minnesota.

Elnor AM, Popov KE and Gurfinkel VS (1972), Changes in stretch reflex system concerned with the control of postural activity of human muscles. Agressologie 13D:19-24.

Era P and Heikkinen E (1985), Postural sway during standing and unexpected disturbance of balance in random samples of men of different ages. J Gerontol 8:287-295.

Exton-Smith AN (1977), Clinical manifestations, in "Care of the Elderly: Meeting the Challenge of Dependency" eds AN Exton-Smith and J Grimley Evans, Academic Press, London, pp 41-57.

Eykhoff P (1974), System identification: parameter and state estimation, John Wiley and Sons, London, Chap 10.

Eykhoff P (1982), On the coherence among the multitude of system identification methods, in "Identification and System Parameter Estimation", eds GA Bekey and GN Saridis, Pergamon Press, Oxford, pp 31-42.

Falconer K and Winter DA (1985), Quantitative assessment of co-contraction at the ankle joint in walking. Electromyogr Clin Neurophysiol 25:135-149.

Fernie GR and Holliday PJ (1978), Postural sway in amputees and normal subjects. J Bone Joint Surg 60A:895-898.

Fernie GR, Gryfe CI, Holliday PJ and Llewellyn A (1982), The relationship of postural sway in standing to the incidence of falls in geriatric subjects. Age Ageing 11:11-16.

Gabell A, Simons MA and Nayak USL (1985), Falls in the healthy elderly: predisposing causes. Ergonomics 28:965-975.

- Gantchev G and Popov V (1973), Quantitative evaluation of induced body oscillations in man. *Agressologie* 14C:91-93.
- Gantchev G, Dunev S and Draganova N (1972a), On the problem of the induced oscillations of the body. *Agressologie* 13B:51-55.
- Gantchev G, Dunev S and Draganova N (1972b), On the spontaneous and induced body oscillations, in "Motor Control", eds AA Gydkov, NT Tankov and DS Kosarov, Plenum Press, New York, pp 179-194.
- Gardenhire LW (1964), Selecting sample rates. *Instrumentation Technology* 11:59-64.
- Gauthier-Gagnon C, St-Pierre D, Drouin G and Riley E (1986), Augmented sensory feedback in the early training of standing balance of below-knee amputees. *Physiotherapy Canada* 38:137-142.
- Ghez C and Shinoda T (1978), Spinal mechanisms of the functional stretch reflex. *Exp Brain Res* 32:55-68.
- Gibb J (1982), The fundamentals of signal analysis. Application Note 243, Hewlett Packard, Palo Alto, California.
- Gillis B, Gilray K, Lawley H, Mott L and Wall JC (1986), Slow walking speeds in healthy young and elderly females. *Physiotherapy Canada* 38:350-352.
- Golliday CL and Hemami H (1976), Postural stability of the two degree-of-freedom biped by general linear feedback. *IEEE Trans Automatic Control* AC-21:74-79.
- Gonshor A and Melvill Jones G (1976), Extreme vestibulo-ocular adaptation induced by prolonged optical reversal of vision. *J Physiol (Lond)* 256:381-414.
- Goodwin GC and Payne RL (1977), Dynamic system identification, Academic Press, New York, Chap 6.
- Gordon M, Huang M and Gryfe CI (1982), An evaluation of falls, syncope, and dizziness by prolonged ambulatory cardiographic monitoring in a geriatric institutional setting. *J Am Geriatr Soc* 30:6-12.
- Graupe D (1976), Identification of systems, Van Norstrand Reinhold, New York, Chap 4.
- Graybiel A and Fregly AR (1966), A new quantitative ataxia test battery. *Acta Otolaryngol* 61:292-312.
- Grimby G and Saltin B (1983), The ageing muscle. *Clin Physiol* 3:209-218.

- Grimes DL (1979), An active multi-mode above-knee prosthesis controller, PhD Thesis, Massachusetts Institute of Technology, Cambridge, Massachusetts.
- Grundy M, Tosh PA, McLeish RD and Smidt L (1975), An investigation of the centres of pressure under the foot while walking. *J Bone Joint Surg* 57B:98-103.
- Gryfe CI, Amies A and Ashley MJ (1977), A longitudinal study of falls in an elderly population: I. incidence and morbidity. *Age Ageing* 6:201-210.
- Guimaraes RM and Isaacs B (1980), Characteristics of the gait in old people who fall. *Int Rehabil Med* 2:177-180.
- Gurfinkel VS (1973), Physical foundations of stabilography. *Agressologie* 14C:9-14.
- Gurfinkel VS, Lipshits MI, Mori S and Popov KE (1976), The state of the stretch reflex during quiet standing in man. *Prog Brain Res* 44:473-486.
- Gustavsson I (1972), Comparison of different methods for identification of industrial processes. *Automatica* 8:127-142.
- Hasselkus BR and Shambes GM (1975), Aging and postural sway in women. *J Gerontol* 6:661-667.
- Hatze H (1980), Neuromusculoskeletal control systems modeling: a critical survey of recent developments. *IEEE Trans Automatic Control* AC-25:375-385.
- Hayes KC, Spencer JD, Lucy SD, Riach CL and Kirshen HJ (1985), Age-related changes in postural sway, in "Biomechanics IX-A", eds DA Winter, RW Norman, RP Wells, KC Hayes and AE Patla, Human Kinetics Publishers, Champaign, Illinois, pp 383-387.
- Hemami H and Jaswa VC (1978), On a three-link model of the dynamics of standing up and sitting down. *IEEE Trans Syst Man Cybern* SMC-8:115-120.
- Herman R (1970), The myotatic reflex: clinico-physiological aspects of spasticity and contracture. *Brain* 9:273-312.
- Hibino R (1980), The role of tonic stretch reflex during standing in man. *Nagoya J Med Sci* 43:15-24.
- Hinchcliffe R (1983), Epidemiology of balance disorders in the elderly, in "Hearing and Balance in the Elderly", ed R Hinchcliffe, Churchill Livingstone, New York, pp 227-250.
- Holliday PJ and Fernie GR (1979), Changes in the measurement of postural sway resulting from repeated testing. *Agressologie* 20:225-228.

- Holliday PJ and Fernie GR (1985), Postural sway during low frequency floor oscillation in young and elderly subjects, in "Vestibular and Visual Control in Posture and Locomotor Equilibrium", eds M Igarashi and FO Black, Karger, Basel, Switzerland, pp 66-69.
- Honjo S and Furukawa R (1957), The goniometer test. *Ann Otol Rhinol Laryngol* 66:440-458.
- Horak FB and Nashner LM (1986), Central programming of postural movements: adaptation to altered support-surface configurations. *J Neurophysiol* 55:1369-1381.
- Horak FB, Diener HC and Nashner LM (1985), Influence of stimulus parameter and set on human postural strategies. *Soc Neurosci Abstr* 11:704.
- Houk JC (1976), An assessment of stretch reflex function. *Prog Brain Res* 44:303-314.
- Houk JC and Henneman E (1974), Feedback control of muscle: introductory concepts, in "Medical Physiology, Thirteenth Edition", ed VB Mountcastle, CV Mosby, St Louis, pp 608-616.
- Hsia TC (1978), System identification: least-squares methods, Lexington Books, Lexington, Massachusetts, Chaps 6,7.
- Hufschmidt A, Dichgans J, Mauritz KH and Hufschmidt M (1980), Some methods and parameters of body sway quantification and their neurological applications. *Arch Psychiatry Neurol Sci* 228:135-150.
- Inman VT and Isman RE (1969), Anthropometric studies of the human foot and ankle. *Bulletin of Prosthetics Research* 10:97-129.
- Isaacs B (1983), Falls in old age, in "Hearing and Balance in the Elderly", ed R Hinchcliffe, Churchill Livingstone, New York, pp 373-388.
- Isermann R (1980), Practical aspects of process identification. *Automatica* 16:575-587.
- Ishida A and Imai S (1980), Responses of the posture-control system to pseudo-random acceleration disturbances. *Med Biol Eng Comput* 18:433-438.
- Ishida A and Miyazaki S (1985), Identification of the posture control system using records during quiet stance, in "Vestibular and Visual Control on Posture and Locomotor Equilibrium", eds M Igarashi and FO Black, Karger, Basel, Switzerland, pp 70-73.
- Jenkins GM and Watts DG (1968), Spectral analysis and its applications, Holden-Day, Oakland, California, Chap 10.

Kandel ER and Schwartz JH (1981), Principles of neural science, Elsevier/North-Holland, New York.

Kennedy WJ and Gentle JE (1980), Statistical computing, Marcel Dekker, New York, Chap 6.

Kenshalo DR (1979), Changes in the vestibular and somesthetic systems as a function of age, in "Sensory Systems And Communication In The Elderly (Aging Vol 10)", eds JM Ordy and K Brizzee, Raven Press, New York, pp 269-282.

Kirshen AJ, Cape RDT, Hayes KC and Spencer JD (1984), Postural sway and cardiovascular parameters associated with falls in the elderly. J Clin Exp Gerontol 6:291-307.

Koozekanani SH, Stockwell CW, McGhee RB and Firoozmand F (1980), On the role of dynamic models in quantitative posturography. IEEE Trans Biomed Eng BME-27:605-609.

Kornzweig AL (1980), Progress in ophthalmology for the elderly since the 1971 White House Congress on Aging. Mt Sinai J Med 47:197-204.

Larsson L, Grimby G and Karlsson J (1979), Muscle strength and speed of movement in relation to age and muscle morphology. J Appl Physiol 46:451-456.

Leibowitz HW and Shupert C (1985), Spatial orientation mechanisms and their implications for falls, in "Symposium on Falls in the Elderly: Biologic and Behavioural Aspects", eds TS Radebaugh, E Hadley and R Suzman, WB Saunders, Philadelphia (Clin Geriatr Med 1:571-580).

Lestienne F, Soechting J and Berthoz A (1977), Postural readjustments induced by linear motion of visual scenes. Exp Brain Res 28:363-384.

Lexell J, Henriksson-Larsen K, Winblad B and Sjostrom M (1983), Distribution of different fiber types in human skeletal muscles: effects of aging studied in whole muscle cross sections. Muscle Nerve 6:588-595.

Lipsitz LA (1985), Abnormalities in blood pressure homeostasis that contribute to falls in the elderly, in "Symposium on Falls in the Elderly: Biologic and Behavioural Aspects", eds TS Radebaugh, E Hadley and R Suzman, WB Saunders, Philadelphia (Clin Geriatr Med 1:637-648).

Litvintsev AI (1973), Mechanisms of man's vertical posture control. Agressologie 14B:17-21.

McGhee RB and Kuhner MB (1970). On the dynamic stability of legged locomotion systems, in "Advances in External Control of Human Extremities", Yugoslav Committee for Electronics and Automation, Belgrad, Yugoslavia, pp 342-442. As quoted by Koozekanani et al (1980), IEEE Trans Biomed Eng BME-27:605-609.

MacLennan WJ, Timothy JI and Hall MRP (1980), Vibration sense, proprioception and ankle reflexes in old age. J Clin Exp Gerontol 2:159-171.

Maki BE and Fernie GR (1986) The finite base-of-support non-linearity and its relationship to postural instability, at "Eighth International Symposium on Posturography", Amsterdam.

Maki BE, Rosen MJ and Simon SR (1985), Modification of spastic gait through mechanical damping. J Biomech 6:431-443.

Mauritz KH, Dichgans J and Hufschmidt A (1979), Quantitative analysis of stance in late cortical cerebellar atrophy of the anterior lobe and other forms of cerebellar ataxia. Brain 102:461-482.

Metropolitan Life (1978), Statistical Bulletin 59(3):10-12. As quoted by Morse JM (1986), Can J Public Health 77:21-25.

Meyer M and Blum E (1978), Quantitative analysis of postural reactions to induced body oscillations. Agressologie 19A:30-31.

Montgomery DG (1984a), Design and analysis of experiments (second edition), John Wiley and Sons, New York.

Montgomery DG (1984b), Design and analysis of experiments (second edition), John Wiley and Sons, New York, pp 85-99.

Moore SP, Horak FB and Nashner LM (1986), Influence of stimulus anticipation on human postural responses, at "North American Society for Psychology of Sport and Physical Activity", Phoenix, Arizona.

Morse JM (1986), Computerized evaluation of a scale to identify the fall-prone patient. Can J Public Health 77:21-25.

Nashner LM (1970), Sensory feedback in human postural control, ScD Thesis, Massachusetts Institute of Technology, Cambridge, Massachusetts.

Nashner LM (1971), A model describing vestibular detection of body sway motion. Acta Otolaryngol 72:429-436.

Nashner LM (1972), Vestibular posture control model. Kybernetik 10:106-110.

Nashner LM (1976), Adapting reflexes controlling the human posture. Exp Brain Res 26:59-72.

Nashner LM (1977), Fixed patterns of rapid postural responses among leg muscles during stance. *Exp Brain Res* 30:13-24.

Nashner LM (1980), Balance adjustments of humans perturbed while walking. *J Neurophysiol* 44:650-664.

Nashner LM (1981), Analysis of stance posture in humans, in "Handbook of Behavioural Neurobiology, Volume 5, Motor Coordination", eds AL Towe and ES Luschei, Plenum Press, New York, pp 527-565.

Nashner LM (1982), Equilibrium testing of the disoriented patient, in "Nystagmus and Vertigo: Clinical Approaches to the Patient with Dizziness", eds V Honrubia and MAB Brazier, Academic Press, New York, pp 165-178.

Nashner LM and Berthoz A (1978), Visual contribution to rapid motor responses during postural control. *Brain Res* 150:403-407.

Nashner LM and Cordo PJ (1981), Relation of automatic postural responses and reaction-time voluntary movements of human leg muscles. *Exp Brain Res* 43:395-405.

Nashner LM and McCollum G (1985), The organization of human postural movements: a formal basis and experimental synthesis. *Behav Brain Sci* 8:135-172.

Nashner LM and Wolfson P (1974), Influence of head position and proprioceptive cues on short latency postural reflexes evoked by galvanic stimulation of the human labyrinth. *Brain Res* 67:255-268.

Nashner LM and Woollacott M (1979), The organization of rapid postural adjustments of standing humans: an experimental-conceptual model, in "Posture and Movement", eds RE Talbott and DR Humphrey, Raven Press, New York, pp 243-257.

Nashner LM, Black FO and Wall C (1982), Adaptation to altered support and visual conditions during stance: patients with vestibular deficits. *J Neurosci* 2:536-544.

Nashner LM, Woollacott M and Tuma G (1979), Organization of rapid responses to postural and locomotor-like perturbations of standing man. *Exp Brain Res* 36:463-476.

National Safety Council (1979), Accident facts, National Safety Council, Chicago.

Neter J, Wasserman W and Kutner MH (1985a), Applied linear statistical models (second edition), RD Irwin, Homewood, Illinois.

Neter J, Wasserman W and Kutner MH (1985b), Applied linear statistical models (second edition), RD Irwin, Homewood, Illinois, Chap 18.

- Neter J, Wasserman W and Kutner MH (1985c), Applied linear statistical models (second edition), RD Irwin, Homewood, Illinois, pp 779-782.
- Nichols TR and Houk JC (1973), Reflex compensation for variations in the mechanical properties of muscle. *Science* 181:182-184.
- Nickens H (1985), Intrinsic factors in falling among the elderly. *Arch Intern Med* 145:1089-1093.
- Njiokiktjien CH (1980), The current state of posturography in neurology. *Agressologie* 21D:31-33.
- Njiokiktjien CH and deRijke W (1971), The recording of Romberg test and its application in neurology. *Agressologie* 13C:1-7.
- O'Brien M, Power K, Sanford S, Smith K and Wall J (1983), Temporal gait patterns in healthy young and elderly females. *Physiotherapy Canada* 35:323-326.
- Ogata K (1970a), Modern control engineering, Prentice-Hall, Englewood Cliffs, New Jersey, Chap 9.
- Ogata K (1970b), Modern control engineering, Prentice-Hall, Englewood Cliffs, New Jersey, p 539.
- Ogata K (1970c), Modern control engineering, Prentice-Hall, Englewood Cliffs, New Jersey, Chap 6.
- Okubu J (1980), The review of posturography in Japan. *Agressologie* 21D:3-24.
- Olney SJ (1985), Quantitative evaluation of cocontraction of knee and ankle muscles in normal walking, in "Biomechanics IX-A", eds DA Winter, RW Norman, RP Wells, KC Hayes and AE Patla, Human Kinetics Publishers, Champaign, Illinois, pp 431-436.
- Overstall PW, Exton-Smith AN, Imms FJ and Johnson AL (1977), Falls in the elderly related to postural imbalance. *Br Med J* 1:261-264.
- Panero J and Zelnik M (1979), Human dimension and interior space, Whitney Library of Design, New York.
- Perry BC (1982a), Falls among the elderly living in high-rise apartments. *J Fam Pract* 14:1069-1073.
- Perry BC (1982b), Falls among the elderly: a review of the methods and conclusions of epidemiologic studies. *J Am Geriatr Soc* 30:367-371.
- Potvin AR, Syndulko K, Tourtellotte WW, Lemmon JA and Potvin JH (1980), Human neurologic function and the aging process. *J Am Geriatr Soc* 28:1-9.

- Prudham D and Evans JG (1981), Factors associated with falls in the elderly: a community study. *Age Ageing* 10:141-146.
- Pyykkö I, Starck J, Scholtz H, Mayer E, Aalto H and Enebom H (1986) Evaluation of vestibular deficiency using posturography, in "Vertigo, Nausea, Tinnitus and Hearing Loss in Cardiovascular Diseases", eds CF Claussen and MV Kirtane, Elsevier, Amsterdam, pp 363-370.
- Rabiner LR, Schafer RW and Dlugos D (1979), Periodogram method for power spectrum estimation, in "Programs for Digital Signal Processing", IEEE Press, New York.
- Rake H (1980), Step response and frequency response methods. *Automatica* 16:519-526.
- Roberts TDM (1978), Neurophysiology of postural mechanisms, Butterworths, London.
- Roth PR (1971), Effective measurements using digital signal analysis. *IEEE Spectrum* 8:62-70.
- Roy SH, Bailin MT, Slecker MM and DeLuca CJ (1985), Modelling postural sway in man: experimental evidence for a random process model of quiet standing. *Soc Neurosci Abstr* 11:704.
- Ryan TA, Joiner BL and Ryan BF (1982), Minitab reference manual, Pennsylvania State University, University Park, Pennsylvania, pp 48-49.
- Scheibel AB (1979), Aging in human motor control systems, in "Sensory Systems and Communication in the Elderly", eds JM Ordy and K Brizzee, Raven Press, New York, pp 297-310.
- Sehested P and Severin-Nielsen T (1977), Falls by hospitalized elderly patients: causes, prevention. *Geriatrics* 32:101-108.
- Seidel RC (1975), Transfer-function-parameter estimation from frequency response data - a fortran program, Technical Report NASA TMX-3286, National Technical Information Service, Springfield, Virginia.
- Sheldon JH (1960), On the natural history of falls in old age. *Br Med J* 2:1685-1690.
- Sheldon JH (1963), The effect of age on the control of sway. *Gerontol Clin* 5:129-138.
- Sheridan TB and Ferrell WR (1981a), Man-machine systems: information, control, and decision models of human performance, MIT Press, Cambridge, Massachusetts, Chap 13.

- Sheridan TB and Ferrell WR (1981b), Man-machine systems: information, control, and decision models of human performance, MIT Press, Cambridge, Massachusetts, Chap 9.
- Shibata R (1976), Selection of the order of an autoregressive model by Akaike's information criterion. *Biometrika* 63:117-126.
- Soames RW and Atha J (1980), The validity of physique-based inverted pendulum models of postural sway behaviour. *Ann Hum Biol* 7:145-153.
- Söderström T (1977), On model structure testing in system identification. *Int J Control* 26:1-18.
- Spiriduso WW (1980), Physical fitness, aging and psychomotor speed: a review. *J Gerontol* 35:850-865.
- Stark L (1968), Neurological control systems, Plenum Press, New York, Chap 2.
- Stearns SD (1975), Digital signal analysis, Hayden, Rochelle Park, New Jersey, Chap 11.
- Stockwell CW, Koozekanani SH and Barin K (1981), A physical model of human postural dynamics. *Ann NY Acad Sci* 374:722-730.
- Stones MJ and Kozma A (1987), Balance and age in the sighted and blind. *Arch Phys Med Rehabil* 68:85-89.
- Strejc V (1980), Least squares parameter estimation. *Automatica* 16:535-550.
- Strenge H and Hedderich J (1982), Age-dependent changes in the central somato-sensory conduction time. *Eur Neurol* 21:270-276.
- Terekhov Y (1976), Stabilometry and some aspects of its applications: a review. *Biomed Eng* 11:12-15.
- Tinetti ME, Williams TF and Mayewski R (1986), Fall risk index for elderly patients based on number of chronic disabilities. *Am J Med* 80:429-434.
- Tobis JS, Nayak L and Hoehler F (1981), Visual perception of verticality and horizontality among elderly fallers. *Arch Phys Med Rehabil* 62:619-622.
- Tobis JS, Reinsch S, Swanson JM, Byrd M and Scharf T (1985), Visual perception dominance of fallers among community-dwelling older adults. *J Am Geriatr Soc* 33:330-333.
- Tokita T, Miyata H and Fujiwara H (1984), Postural response induced by horizontal motion of a platform. *Acta Otolaryngol [Suppl] (Stockh)* 406:120-124.

- Traub MM, Rothwell JC and Marsden CD (1980), Anticipatory postural reflexes in Parkinson's disease and other akinetic-rigid syndromes and in cerebellar ataxia. *Brain* 103:393-412.
- van den Bos A (1974), Estimation of parameters of linear systems using periodic test signals, PhD thesis, Delft University of Technology, Delft, The Netherlands, Chap 2.
- van den Bos A and Krol RG (1979), Synthesis of discrete-interval binary signals with specified Fourier amplitude spectra. *Int J Control* 30:871-884.
- van Lunteren A (1979a), Identification of human operator describing function models with one or two inputs in closed loop systems, PhD thesis, Delft University of Technology, Delft, The Netherlands, Chap 3.
- van Lunteren A (1979b), Identification of human operator describing function models with one or two inputs in closed loop systems, PhD thesis, Delft University of Technology, Delft, The Netherlands, Chap 4.
- van Lunteren A (1985), Personal communication, Department of Mechanical Engineering, Delft University of Technology, Delft, The Netherlands.
- Vanmarcke EH (1972), Properties of spectral moments with applications to random vibration. *J Eng Mech Div, ASCE* 98:425.
- Vittas D, Larsen K and Jansen EC (1986), Body sway in below-knee amputees. *Prosthet Orthot Int* 10:139-141.
- Waller J (1974), Injury in the aged: clinical and epidemiological implications. *NY State J Med* 74:2200.
- Walpole RE and Myers RH (1972), Probability and statistics for engineers and scientists, MacMillan, New York, pp 263-266.
- Walsh EG (1973), Standing man, slow rhythmic tilting, importance of vision. *Agressologie* 14C:79-85.
- Watanabe I and Okubo J (1981), The role of the plantar mechanoreceptor in equilibrium control. *NY Acad Sci* 374:855-864.
- Webster JG (1978), Amplifiers and signal processing, in "Medical Instrumentation, Application and Design", ed JG Webster, Houghton Mifflin, Boston, Chap 3.
- Welch PD (1967), The use of fast fourier transform for the estimation of power spectra: a method based on time averaging over short, modified periodograms. *IEEE Trans Audio Electrostatics*, AU-15:70-73.

- Westheimer G (1980), The eye, in "Medical Physiology, Fourteenth Edition", ed VB Mountcastle, CV Mosby, St Louis, pp 481-503.
- Whipple RH, Wolfson LI and Amerman PM (1987), The relationship of knee and ankle weakness to falls in nursing home residents: an isokinetic study. J Am Geriatr Soc 35:13-20.
- Whitney RJ (1962), The stability provided by the feet during maneuvers whilst standing. J Anat 96:103-111.
- Wieslander J (1980), IDPAC commands - user's guide, Department of Automatic Control, Report CODEN: LUTFD2/(TFRT-3157)/1-108/(1980), Lund Institute of Technology, Lund, Sweden.
- Wild D, Nayak USL and Isaacs B (1980), A study of falls in old people at home, Report to the Dept of Health and Social Security (UK).
- Wild D, Nayak USL and Isaacs B (1981), Description, classification and prevention of falls in old people at home. Rheumatol Rehabil 20:153-159.
- Wilson VJ (1985), Otolith-spinal reflexes, in "Vestibular and Visual Control on Posture and Locomotor Equilibrium", eds M Igarishi and FO Black, Karger, Basel, Switzerland, pp 177-185.
- Wilson VJ and Melvill Jones G (1979a), Mammalian vestibular physiology. Plenum Press, New York, Chap 3.
- Wilson VJ and Melvill Jones G (1979b), Mammalian vestibular physiology. Plenum Press, New York, Chap 7.
- Wilson VJ and Peterson BW (1980), The role of the vestibular system in posture and movement, in "Medical Physiology, Fourteenth Edition", ed VB Mountcastle, CV Mosby, St Louis, pp 813-836.
- Winter DA (1978), Energy assessments in pathological gait. Physiotherapy Canada 30:183-191.
- Winter DA (1979a), Biomechanics of human movement, Wiley-Interscience, New York, pp 150-152.
- Winter DA (1979b), Biomechanics of human movement, Wiley-Interscience, New York, Chap 4.
- Winter DA (1979c), Biomechanics of human movement, Wiley-Interscience, New York, Chap 6.
- Winter DA (1979d), Biomechanics of human movement, Wiley-Interscience, New York, Chap 7.
- Wolfson LI, Whipple R, Amerman P and Kleinberg A (1986), Stressing the postural response: a quantitative method for testing balance. J Am Geriatr Soc 34:845-850.

Woollacott MP, Shumway-Cook AT and Nashner LM (1982a), Changes in the postural response system with aging. Soc Neurosci Abstr 8:838.

Woollacott MP, Shumway-Cook AT and Nashner LM (1982b), Postural reflexes and aging, in "The Aging Motor System", eds JA Mortimer, FJ Pirozzola and GJ Maletta, Prager, New York, pp 98-119.

Woollacott MP, Shumway-Cook AT and Nashner LM (1986), Aging and postural control: changes in sensory organization and muscular coordination. Int J Aging Hum Dev 23:81-98.

Wyke B (1979), Cervical articular contributions to posture and gait: their relation to senile disequilibrium. Age Ageing 8:251-258.

Young A, Stokes M and Crowe M (1984), Size and strength of the quadriceps muscles of old and young women. Eur J Clin Invest 14:282-287.

Young A, Stokes M and Crowe M (1985), The size and strength of the quadriceps muscles of old and young men. Clin Physiol 5:145-154.

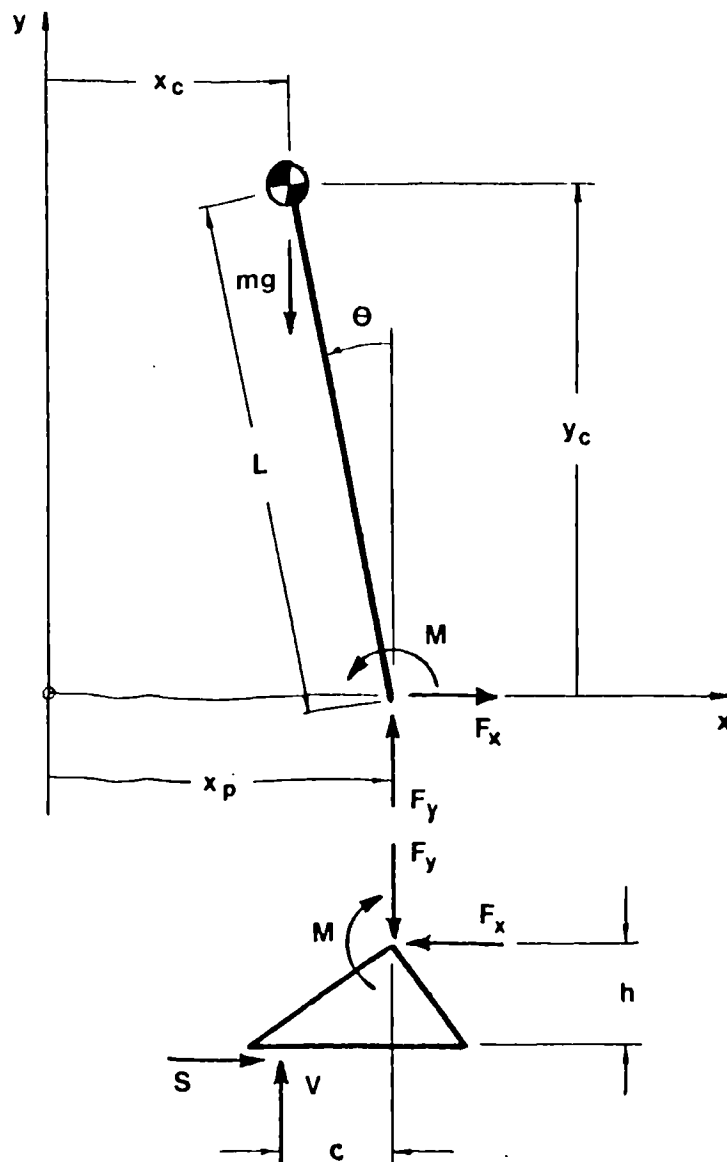


Fig A.1 Free-body diagram: single-link sub-saturation model.

- Legend:
- x_p - platform position
 - x_c - anterior-posterior position of centre-of-gravity
 - y_c - vertical position of centre-of-gravity
 - θ - ankle angle
 - c - displacement of centre-of-pressure
 - M - muscle-generated ankle moment
 - F_x - horizontal joint reaction force
 - F_y - vertical joint reaction force
 - S - horizontal ground reaction force
 - V - vertical ground reaction force
 - m - body mass
 - g - acceleration due to gravity

Note: L and h are anthropometric dimensions; rotational inertia about ankle axis = J_o , about centre-of-gravity = J_c ; mass, weight and rotational inertia of foot assumed to be zero.

APPENDIX A. ANALYSIS AND SIMULATION OF THE POSTURE CONTROL SYSTEM

A.1 DERIVATION OF A SIMPLIFIED DYNAMIC MODEL

As detailed in Section 2.1, the posture control system acts to regulate the position of the skeletal linkage in the presence of destabilizing perturbations resulting from gravitational, inertial and/or externally-applied forces. Stabilizing moments are generated at the joints of the linkage by means of feedback control loops, where the visual, vestibular and somatosensory systems function as the transducers, the spinal and supraspinal neural centres function as the controllers, and the muscles function as the actuators.

A.1.1 Single-Link Sub-Saturation Model

In the simplest biomechanical model, the dynamics of the skeletal linkage are represented by a single-link inverted pendulum with a single degree-of-freedom, the ankle angle θ . A triangular foot is included in order to analyze the ground reaction forces, but does not contribute to the dynamics. This model approximates the sub-saturation dynamics of the ankle synergy (see Section 2.3.4), where ankle rotation is the predominant motion and the centre-of-pressure (COP) displacement does not reach the limits of the base-of-support (BOS).

Figure A.1 shows a free-body diagram of an inverted pendulum situated onboard the moving perturbation platform. Using the nomenclature defined in the figure, the dynamic equations are derived as follows:

$$x_c(t) = x_p(t) - L\sin\theta(t)$$

$$\ddot{x}_c(t) = \ddot{x}_p(t) + L\dot{\theta}^2(t)\sin\theta(t) - L\ddot{\theta}(t)\cos\theta(t) \quad (1)$$

$$y_c(t) = L\cos\theta(t)$$

$$\ddot{y}_c(t) = -L\ddot{\theta}(t)\sin\theta(t) - L\dot{\theta}^2(t)\cos\theta(t) \quad (2)$$

$$F_x(t) = m\ddot{x}_c(t) \quad (3)$$

$$F_y(t) = m\ddot{y}_c(t) + mg \quad (4)$$

$$M(t) = J_c\ddot{\theta}(t) - LF_y(t)\sin\theta(t) - LF_x(t)\cos\theta(t) \quad (5)$$

For small θ , $\sin \theta \approx \theta$ and $\cos \theta \approx 1$. Using this approximation and retaining only the linear terms, the above equations become:

$$\ddot{x}_c(t) \approx \ddot{x}_p(t) - L\ddot{\theta}(t) \quad (6)$$

$$\ddot{y}_c(t) \approx 0 \quad (7)$$

$$F_x(t) \approx m\ddot{x}_p(t) - mL\ddot{\theta}(t) \quad (8)$$

$$F_y(t) \approx mg \quad (9)$$

$$M(t) \approx J_0\ddot{\theta}(t) - mgL\theta(t) - mL\ddot{x}_p(t) \quad (10)$$

where $J_0 = J_c + mL^2$. Equation (10) demonstrates that an acceleration of the platform on which the inverted pendulum stands is equivalent to applying a destabilizing moment, $mL\ddot{x}_p(t)$, to the "body link". In the Laplace domain, equation (10) becomes:

$$M(s) \approx (J_0s^2 - mgL)\theta(s) - mL A(s) \quad (11)$$

where $A(s) = s^2X_p(s)$ is the platform acceleration and s is the Laplace operator.

For the simplest control model, the stabilizing muscle-generated ankle moment $M(s)$ is a function of the ankle angle θ , i.e. $M(s) = -H(s)\theta(s)$. Thus, equation (11) can be re-arranged to form the closed-loop transfer function:

$$\frac{\theta(s)}{A(s)} \approx \frac{mL}{J_0s^2 + H(s) - mgL} \quad (12)$$

Since the mass and weight of the feet are small, the ground and ankle reaction forces are approximately equal. Using this approximation (i.e. $F_x \approx S$ and $F_y \approx V$), the COP $C(s)$ and the ankle angle $\theta(s)$ are related by the following equation:

$$\begin{aligned} M(s) &\approx hF_x(s) - C(s)F_y(s) \\ &\approx h(mA(s) - mLs^2\theta(s)) - mgC(s) \\ &= -H(s)\theta(s) \end{aligned} \quad (13)$$

Eliminating $\theta(s)$ from equations (12) and (13) yields:

$$\frac{C(s)}{A(s)} \doteq (1/g) \frac{h(J_0 - mL^2)s^2 + (h + L)H(s) - mgLh}{J_0s^2 + H(s) - mgL} \quad (14)$$

To represent the most important characteristics of the control system, the feedback element $H(s)$ should include: (1) a gain, to represent the combined gain of the sensory transducers, neural processors and muscle actuators; (2) a time delay (or dead time), to account for neural synaptic delays, nerve conduction time and central processing time; and (3) a lag term, to account for dynamic effects in the development of the muscle tension (Sheridan and Ferrell, 1981b). Thus, as a first-order approximation, $H(s) = K e^{-\tau s} / (T_m s + 1)$.

A more realistic model of the feedback element would account for dynamic effects in the sensors, in addition to the muscle dynamics. Assuming that the functional stretch reflex is the predominant control loop (Nashner, 1981), then the dynamics of the muscle spindles must be represented (assuming the spindles to be the predominant sensors). Using Nashner's (1970) lead-lag model of the spindle response, the feedback element becomes:

$$H(s) = K e^{-\tau s} \frac{(T_L s + 1)}{(T_m s + 1)(T_s s + 1)} \quad (15)$$

A common approximation is to neglect the ankle moment due to the horizontal shearing force, $F_x(t)$ (e.g. Ishida and Imai, 1980). For the linearized model, the moment due to the horizontal force is $mh\ddot{x}_c(t)$, whereas the moment due to the vertical force is $mc(t)(g + \ddot{y}_c(t))$. It can be argued that $\ddot{x}_c(t)$ and $\ddot{y}_c(t)$ are small compared to g under most conditions (whereas h and $c(t)$ are of the same order of magnitude); therefore, the net ankle moment can be approximated by $mgc(t)$, i.e. the ankle moment is proportional to the COP displacement. In this case, equation (14) becomes:

$$\frac{C(s)}{A(s)} \doteq (L/g) \frac{H(s)}{J_0s^2 + H(s) - mgL} \quad (16)$$

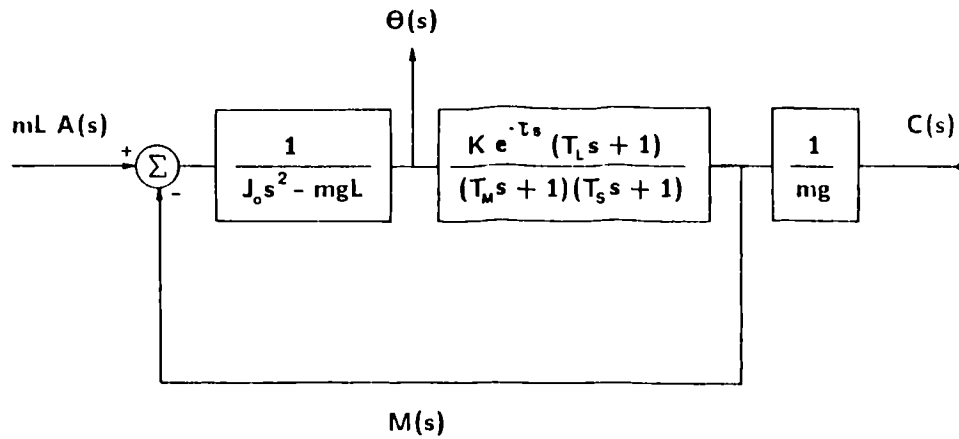


Fig A.2 Approximate linear model of the posture control system.

- Legend:
- s - Laplace operator
 - $A(s)$ - platform acceleration
 - $\theta(s)$ - ankle angle
 - $C(s)$ - centre-of-pressure displacement
 - $M(s)$ - muscle-generated ankle moment
-
- m - body mass
 - L - height of centre-of-gravity
 - J_o - rotational inertia about ankle axis
 - g - acceleration due to gravity
-
- K - feedback gain
 - τ - dead time
 - T_L - feedback lead time constant
 - T_M - muscle lag time constant
 - T_S - spindle lag time constant

The validity of this approximation is explored in Section A.3.1. The simplified and linearized control model represented by equation (16) is diagrammed in figure A.2.

If desired, the ankle angle and COP transfer functions can be reduced to a polynomial form by using the approximation that $e^{-\tau s} \approx 1 - \tau s$ (for small τ). Substituting equation (15) into equations (12) and (14), the transfer functions become:

$$\frac{\theta(s)}{A(s)} \approx \frac{mL}{a_0} \frac{T_m T_s s^2 + (T_m + T_s)s + 1}{a_4 s^4 + a_3 s^3 + a_2 s^2 + a_1 s + 1} \quad (17)$$

$$\frac{C(s)}{A(s)} \approx \frac{b_0}{a_0 g} \frac{b_4 s^4 + b_3 s^3 + b_2 s^2 + b_1 s + 1}{a_4 s^4 + a_3 s^3 + a_2 s^2 + a_1 s + 1} \quad (18)$$

where:

$$a_4 = (J_0 T_m T_s) / a_0$$

$$a_3 = J_0 (T_m + T_s) / a_0$$

$$a_2 = (J_0 - mgL T_m T_s - K T_L \tau) / a_0$$

$$a_1 = [K(T_L - \tau) - mgL(T_m + T_s)] / a_0$$

$$a_0 = K - mgL$$

$$b_4 = [h(J_0 - mL^2) T_m T_s] / b_0$$

$$b_3 = [h(J_0 - mL^2)(T_m + T_s)] / b_0$$

$$b_2 = [h(J_0 - mL^2) - mgLh T_m T_s - K T_L \tau (h + L)] / b_0$$

$$b_1 = [K(T_L - \tau)(h + L) - mgLh(T_m + T_s)] / b_0$$

$$b_0 = K(h + L) - mgLh$$

Neglecting the ankle moment due to F_x , equation (18) becomes:

$$\frac{C(s)}{A(s)} \approx \frac{K L e^{-\tau s}}{a_0 g} \frac{T_L s + 1}{a_4 s^4 + a_3 s^3 + a_2 s^2 + a_1 s + 1} \quad (19)$$

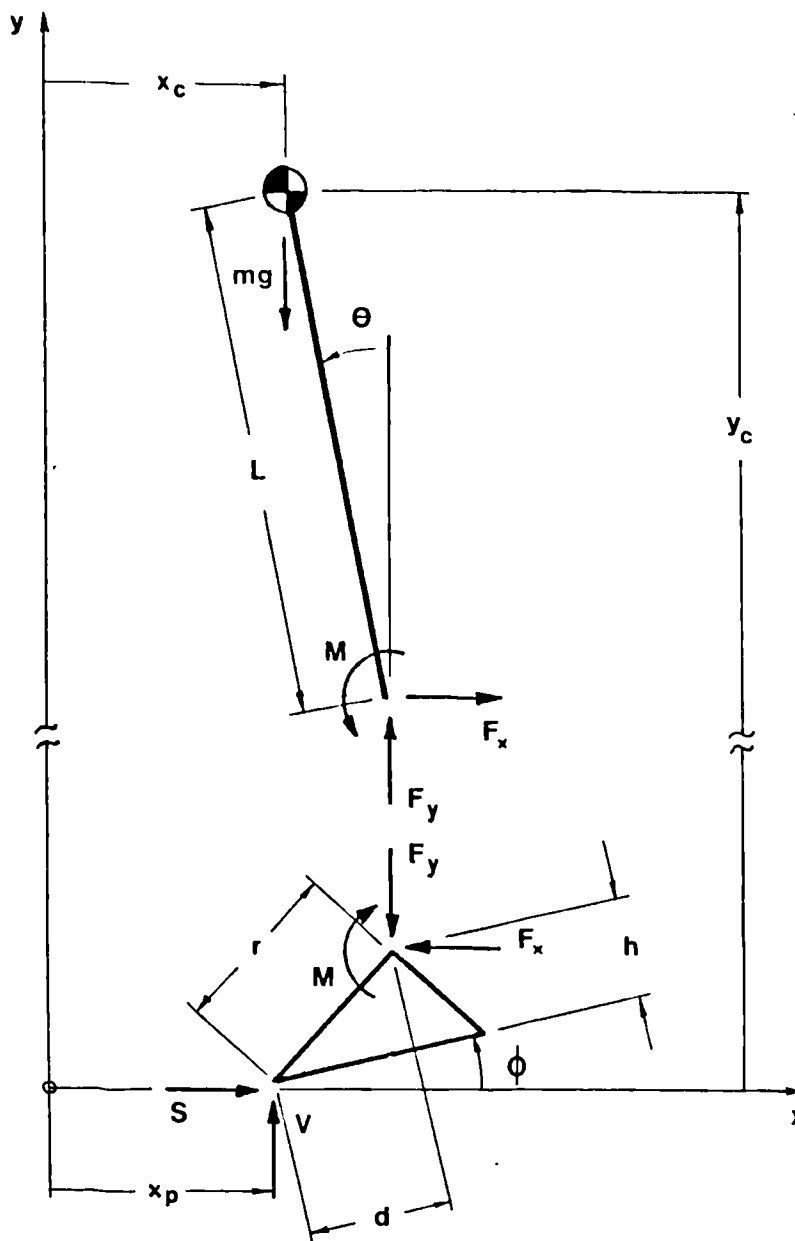


Fig A.3 Free-body diagram: two-link saturated base-of-support model.

- Legend:
- x_p - platform position
 - x_c - anterior-posterior position of centre-of-gravity
 - y_c - vertical position of centre-of-gravity
 - ϕ - foot angle
 - θ - body angle
 - M - muscle-generated ankle moment
 - F_x - horizontal joint reaction force
 - F_y - vertical joint reaction force
 - S - horizontal ground reaction force
 - V - vertical ground reaction force
 - m - body mass
 - g - acceleration due to gravity

Note: L , r , d and h are anthropometric dimensions; rotational inertia about ankle axis = J_o , about centre-of-gravity = J_c ; mass, weight and rotational inertia of foot assumed to be zero.

A.1.2 Two-Link Saturated Base-of-Support Model

Once the COP reaches the limits of the BOS, the single-link inverted pendulum model no longer applies. At this point, attempts to increase the stabilizing muscle moment at the ankle will cause the foot to rotate; therefore, the foot dynamics must now be included in the model. The model for forward sway is shown in figure A.3.

The dynamic equations for each link are derived using the same free-body approach as applied earlier in equations (1) to (10). Using the nomenclature defined in figure A.3, the linearized small-angle equations for the "body link" are as follows:

$$F_x(t) \cong m\ddot{x}_p(t) - mL\ddot{\theta}(t) - mh\ddot{\phi}(t) \quad (20)$$

$$F_y(t) \cong mg + md\ddot{\phi}(t) \quad (21)$$

$$M(t) \cong J_0\dot{\theta}(t) - mgL\theta(t) - mL\ddot{x}_p(t) + mhL\ddot{\phi}(t) \quad (22)$$

Neglecting the mass, weight and rotational inertia of the feet, the corresponding equations for the "foot link" are:

$$S(t) \cong F_x(t) \quad (23)$$

$$V(t) \cong F_y(t) \quad (24)$$

$$M(t) \cong -mr^2\ddot{\phi}(t) + mgh\phi(t) + mh\ddot{x}_p(t) - mdg - mhL\ddot{\theta}(t) \quad (25)$$

As before, the muscle-generated moment $M(t)$ is produced by the feedback control loop, i.e. $M(s) = -H(s)\theta(s)$. Note, however, that the angle θ is no longer equal to the ankle angle, but now reflects the orientation of the body relative to the gravitational reference frame. Feedback of this type could be provided by the vestibular and/or visual sensors. Assuming, for simplicity, that $H(s) = K(T_Ls + 1)$, then the characteristic equation for the two-link system (equations (22) and (25)) is:

$$\begin{aligned} 0 = & [J_0mr^2 - (mhL)^2]s^4 + [KT_L(mr^2 + mhL)]s^3 \\ & + [mr^2(K - mgL) - mghJ_0 + Kmhl]s^2 - [mghKT_L]s + mgh(mgL - K) \quad (26) \end{aligned}$$

If instead the feedback is a function of the ankle angle ($\theta - \phi$), then the characteristic equation becomes:

$$\begin{aligned}
 0 = & [J_0mr^2 - (mhL)^2]s^4 + [KT_L(J_0 + mr^2 + 2mhL)]s^3 \\
 & + [mr^2(K - mgL) + J_0(K - mgh) + 2KmhL]s^2 \\
 & - [mgKT_L(h + L)]s + mg(mghL - K(h + L))
 \end{aligned} \tag{27}$$

Both of the linear feedback schemes presented (i.e. feedback of either body angle or ankle angle) result in unstable systems, as evidenced by the presence of negative coefficients in the characteristic equation (e.g. Ogata, 1970c). Inclusion of the lag and dead time terms previously included in the feedback element (see equation (15)) would tend to further destabilize this system. Note, however, that this linearized two-link model will only apply up to the point at which the ankle reaches the limits of its range of motion.

For example, consider a forward fall. A stabilizing plantar-flexion (i.e. extension) moment generated at the ankle will cause the foot to rotate forward, pivoting about the point of contact at the toes. If the stabilizing ankle moment is insufficient to arrest the forward rotation of the body, then a fall will occur (assuming that no stepping, grasping or waving manoeuvres are executed).

If, however, the ankle moment does arrest and reverse the forward rotation of the body, then the ankle will be driven into plantar-flexion as the foot continues to rotate forward. Once the limit of the plantar-flexion range of motion is reached, the two-link system is reduced to a single link rotating about the toes. This single-link system is unstable and has no capacity for active stabilization, as any plantar-flexion moment generated by the ankle muscles is negated by the passive stiffness of the connective tissues. At this juncture, depending on the angle of inclination and the angular momentum, the single-link system may either rotate forward (leading to a fall) or backward. If backward rotation occurs, then it may be possible to regain stability if, through an appropriate sequence of ankle dorsi-flexion and backward foot rotation, the system returns to its original foot-flat

TABLE A.1

SIMULATION PARAMETERS

	YOUNG (25-34)		ELDERLY (65-74)	
	MALES	FEMALES	MALES	FEMALES
body mass (kg):				
5th percentile	58.5	46.3	53.1	48.1
50th percentile	76.6	59.0	73.0	65.8
95th percentile	101.2	86.6	93.9	88.9
body height (m):				
5th percentile	1.636	1.516	1.593	1.461
50th percentile	1.753	1.618	1.697	1.565
95th percentile	1.875	1.709	1.801	1.664
rotational inertia (kg-m ²): +				
5th percentile	55.2	37.5	47.5	36.2
50th percentile	83.1	54.5	74.1	56.8
95th percentile	125.4	89.2	107.4	86.8
feedback parameters (s):				
dead time	0.100	0.100	0.110	0.110
muscle lag time constant	0.100	0.100	0.100	0.100
spindle lag time constant	0.100	0.100	0.100	0.100
lead time constant	0.400	0.400	0.400	0.400

+ NOTE: rotational inertia is about the flexion-extension ankle axis; calculated from height and mass percentile values using formulae presented by Winter (1979a).

inverted pendulum configuration.

The foregoing analysis suggests that, under certain circumstances, subjects may be able to restore balance even though toe-rise (backward falls) or heel-rise (forward falls) occurs. This prediction is supported by experimental observations of responses to transient perturbations. As indicated above, this phenomenon may be a result of complex control strategies involving the ankle or a combination of joints; however, other more simple explanations are also possible.

For backward falls, the small increase in the length of the BOS that occurs as the calcaneus "rolls" backward could explain small gains in stability. For forward falls, the additional stability may involve the metatarsophalangeal (MTP) joints. Normally, displacement of the COP beyond the MTP joints requires an active muscle moment to be generated at these joints; hence, limitations on MTP muscle strength limit the maximum COP excursion. Raising the heels, however, may extend the MTP joints to the limit of their range of motion, so that a much larger moment can now be supported by the passive stiffness of the muscles, ligaments and other connective tissues.

A.2 SIMULATION METHODS

Digital simulations were performed based on the single-link model derived in Section A.1.1 (i.e. equations (12), (14), (15) and (16)). In order to simulate responses in the time domain, difference equations were derived from the Laplace-domain transfer functions using the bilinear transform approximation: $s = (2/\Delta t)(z-1)/(z+1)$, where Δt is the sample interval and z^{-1} is the backward shift operator (e.g. Stearns, 1975). The simulations were performed using a sample interval of 0.002 s.

The responses to pseudorandom (PRN), random (RAN) and transient platform accelerations were simulated; the details of the acceleration signals are provided in Sections 5.4.3 and 6.1. Responses to unit acceleration pulses were also investigated.

The model parameters used in the simulations are listed in table A.1. The anthropometric values were chosen to represent selected percentiles of young and elderly males and females (Panero

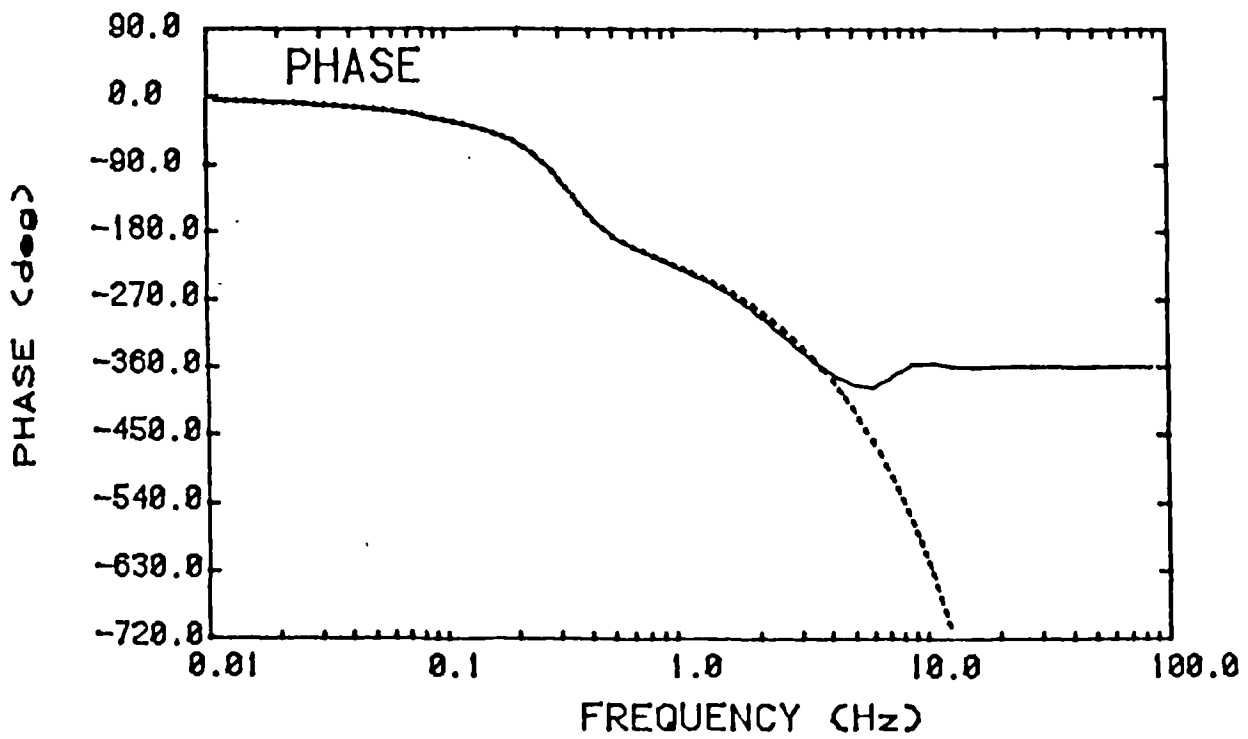
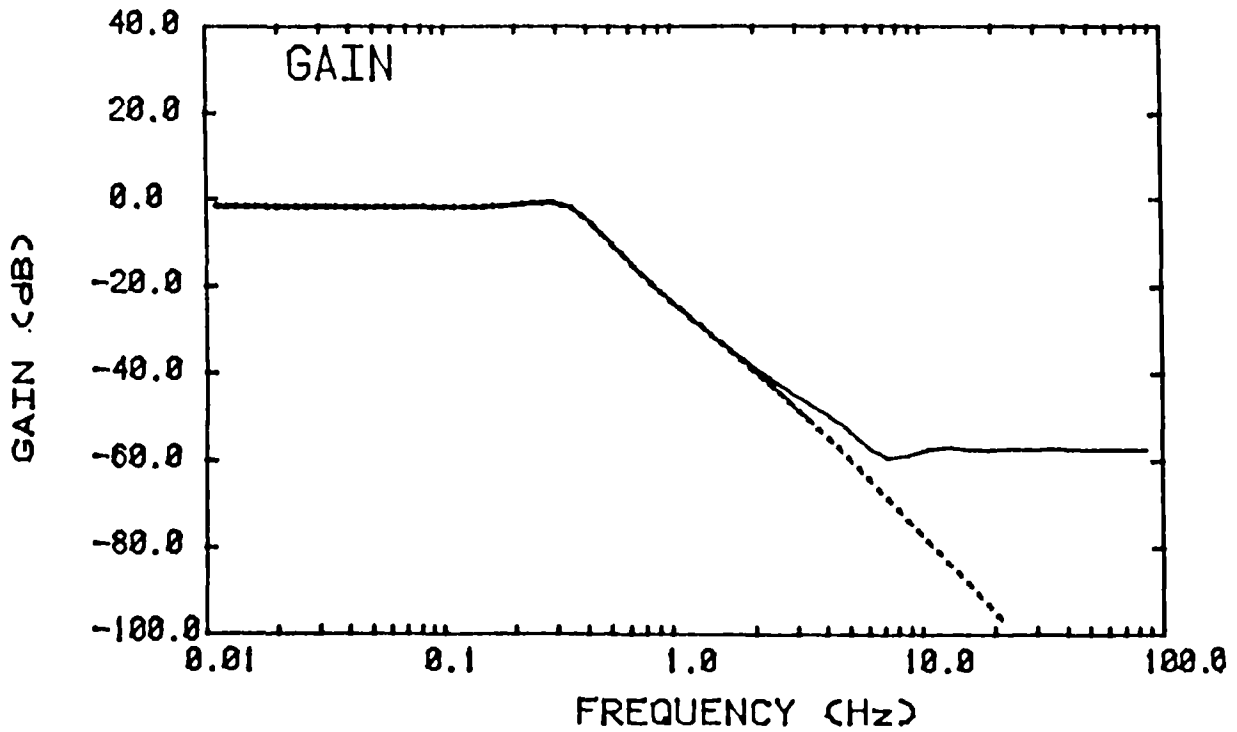


Fig A.4 Example frequency response
 (input = platform acceleration, output = COP displacement;
 50th percentile young female).

Legend: solid line - shear forces included in simulation
 dashed line - no shear forces

and Zelnik, 1979). Rotational inertias about the ankle were calculated using data tabulated by Winter (1979a), and the centre-of-gravity (COG) height was assumed to be 56.7% of the body height (Drillis and Contini, 1966). For the feedback element, the time delay (or dead time) values were estimated from electromyographic (EMG) latencies in the ankle muscles measured in response to sudden perturbations (Woollacott et al, 1986). The lag time constants in the feedback element were taken from Nashner's work (1970). For each simulation, the feedback gain and lead time constant were selected to ensure system stability. Note that adjustment of the lead time constant is equivalent to adjustment of the angular velocity feedback gain.

In searching for appropriate gain and lead values, stability was determined by solving for the poles of the approximate transfer functions (17) and (18). Relative stability was quantified by estimating the gain and phase margins from the open-loop transfer function $M(s)/(mLA(s)) = H(s) / (J_0 s^2 - mgL)$.

A.3 SIMULATION RESULTS

A.3.1 Influence of Shear Forces

Example simulation results are shown in figures A.4 and A.5. These results were derived from a simulation of a 50th percentile young female. Figure A.4 shows the frequency responses derived from transfer functions (14) and (16), i.e. with and without the shear force terms. Example pulse responses are plotted in figure A.5. Three pulse durations were simulated: 0.002 s, 0.02 s and 0.2 s. In each case, the amplitude of the pulse was equal to $1/\text{duration}$ (m/s^2). Each pulse began at 0.1 s.

Neglecting the ankle moment due to the shear force has negligible effect on the frequency response, except at higher frequencies (i.e. above 5 Hz). In the pulse response, inclusion of the shear force terms superimposes a coincident pulse on the COP response; otherwise, the shearing force has a negligible effect. The COP pulse is equal in duration to the acceleration pulse, with an amplitude proportional to the acceleration amplitude. For the longer-duration, smaller-amplitude unit pulses, the amplitude of

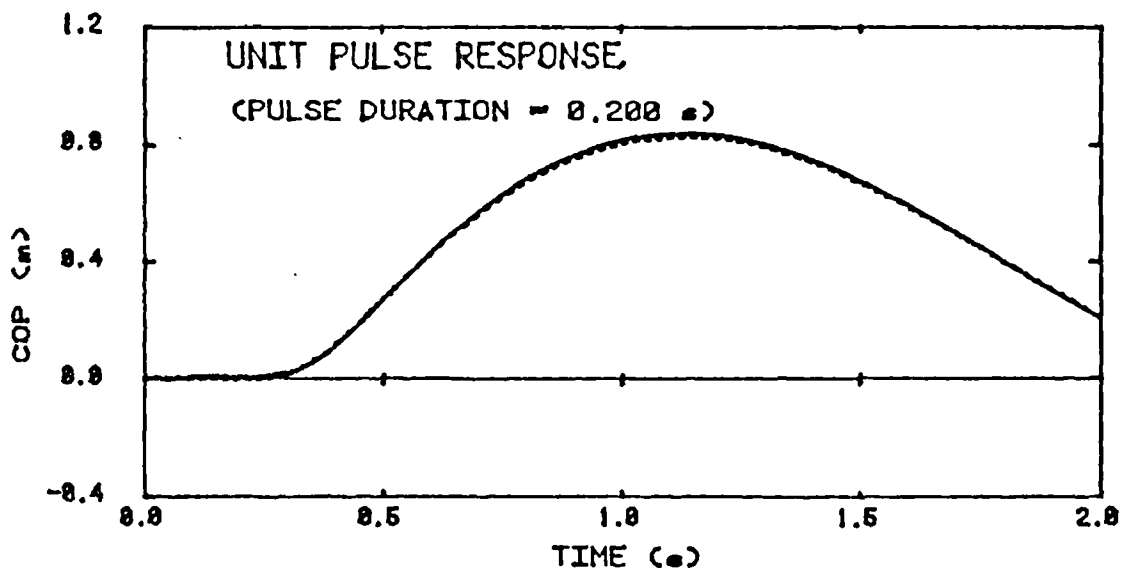
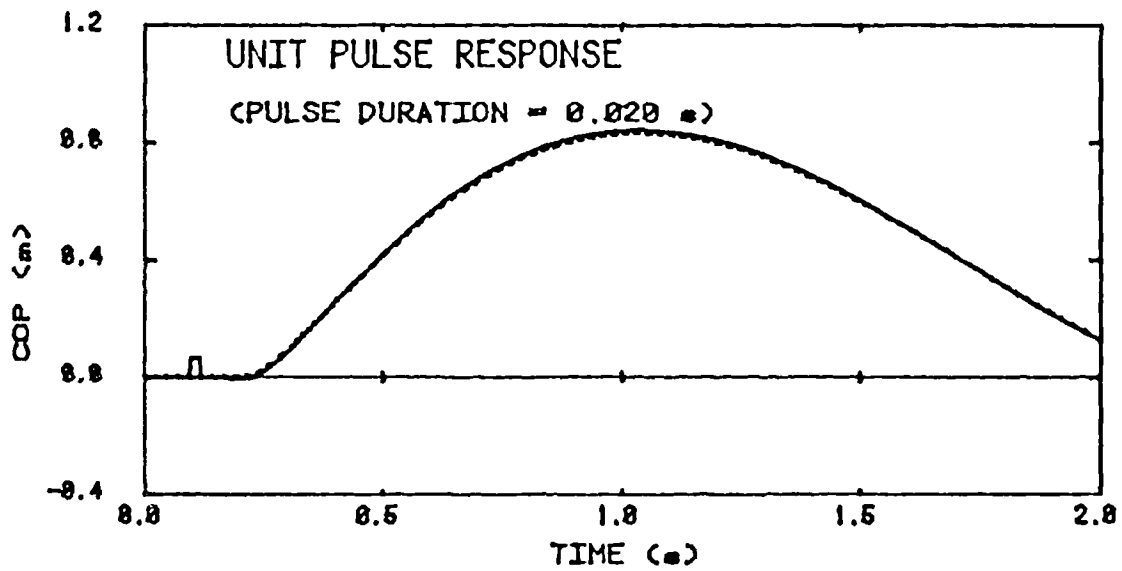
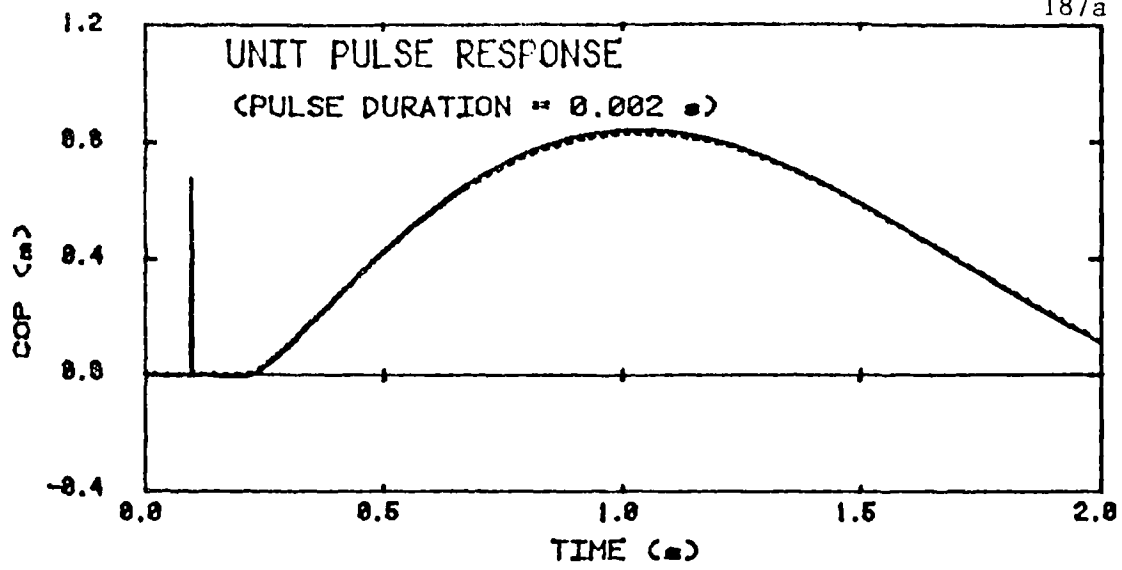


Fig A.5 Example unit pulse responses (COP)
(50th percentile young female).

Legend: solid line - shear forces included in simulation
dashed line - no shear forces

the COP pulse is very small.

These results can be predicted from the transfer functions using the initial value theorem. For a true acceleration impulse, the theorem predicts an impulse in the COP response, but only when the shear force terms are included (i.e. transfer function (14)). For an acceleration step (i.e. the leading edge of a pulse), the theorem predicts a COP step of magnitude $(hA_0/g)(1 - mL^2/J_0)$, where A_0 is the amplitude of the step. Except for very "sharp" (i.e. large-amplitude, short-duration) acceleration pulses, the COP step is small compared to the subsequent COP displacement, as illustrated in figure A.5.

The initial COP displacement prevents the foot from rotating by counteracting the moment due to the applied shearing force. It is a passive mechanical event, totally unrelated to any active balancing responses. (These active responses are delayed, due to the dead time in the feedback loop.) The simulations demonstrate that, for pulses of duration 0.02 s or greater, the passive component of the response is negligible. Pulse durations of this order of magnitude are expected to represent more realistic simulations of actual fall-provoking perturbations than very short pulses. In the balance test, the peak COP displacement is estimated in response to a pulse of duration 0.06 s; therefore, the balance test results should reflect the efficacy of active balancing responses.

In all of the results that follow, the pulse and frequency response simulations were based on transfer function (14), i.e. the contribution of the shear force to the net ankle moment was included.

A.3.2 Perturbation Bandwidth Requirements

Figure A.6 shows frequency response plots for the $C(s)/A(s)$ transfer function, for three different values of the feedback gain. The corresponding unit pulse responses are also shown. The lowest and highest gain values are very close to the stability limits. The other gain value lies approximately mid-way between these extremes. Although these particular plots were obtained from a simulation of a 50th percentile young female, similar results were

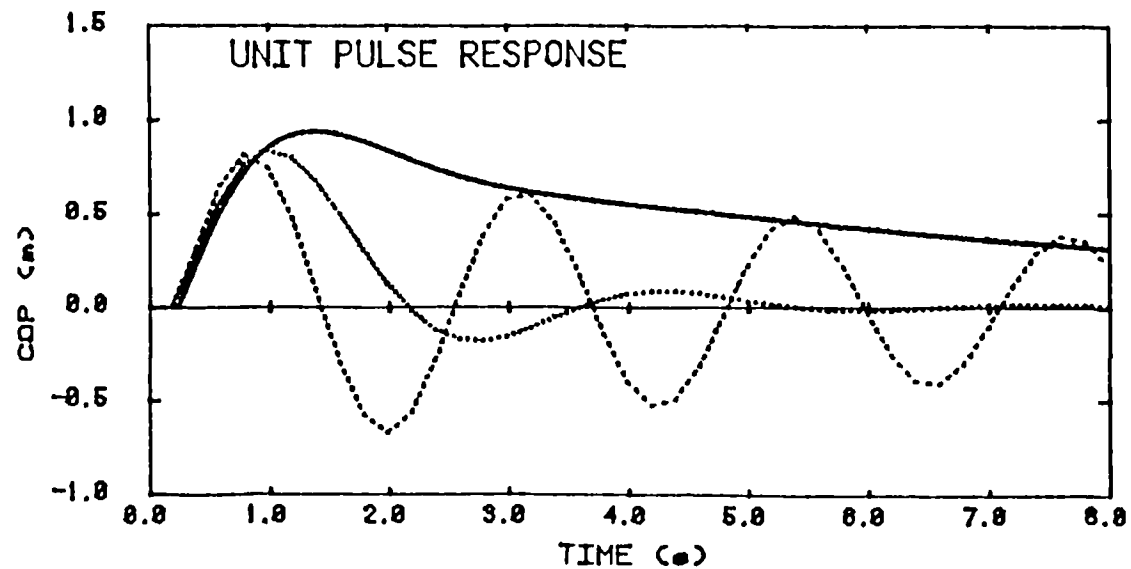
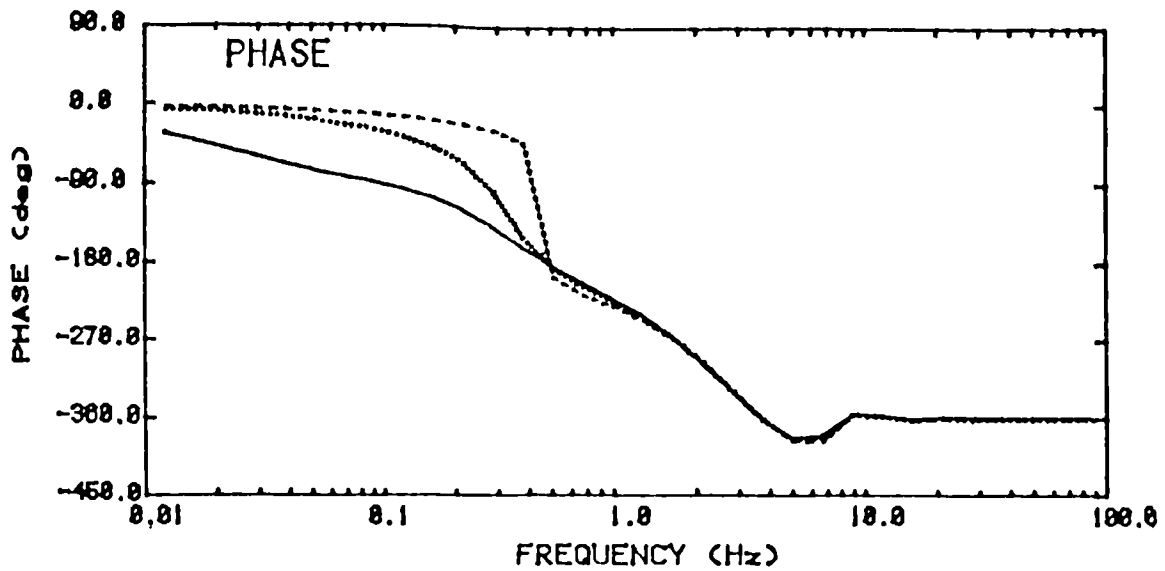
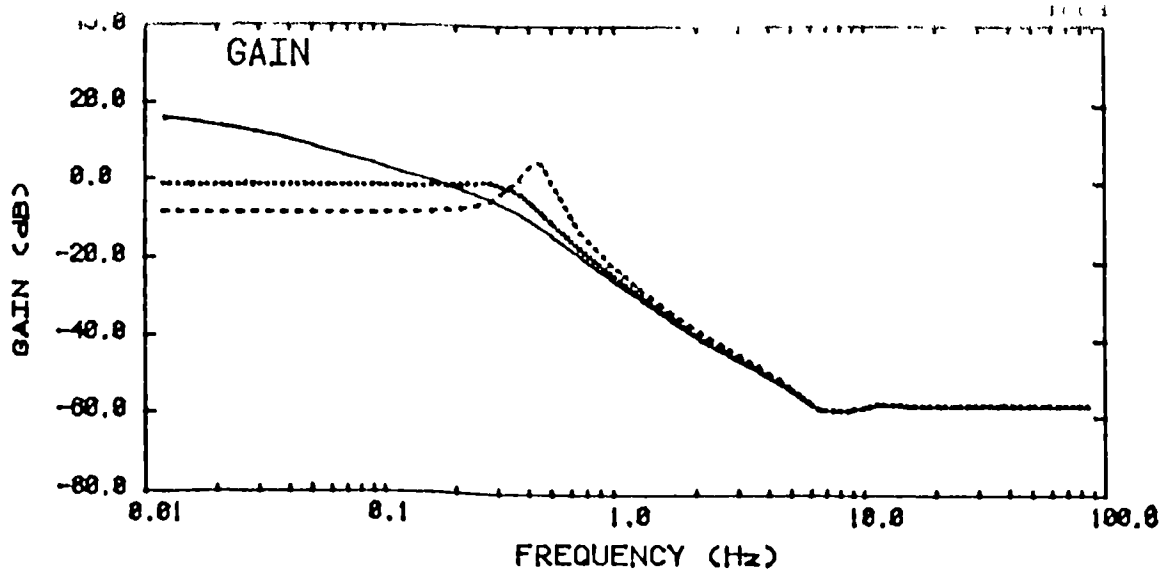


Fig A.6 Effects of changes in feedback gain (50th percentile young female; pulse duration = 0.2 s).

Legend: solid line - gain = 500 N-m/rad
 dotted line - gain = 550 N-m/rad
 dashed line - gain = 650 N-m/rad

obtained in simulations of other subject groups.

For all three gain values, the frequency response shows very substantial attenuation (50 to 80 dB) at frequencies higher than 5 Hz. Since there is no reason to expect increased perturbation power at frequencies above 5 Hz (see Section 5.3.3); the system behaviour at these higher frequencies is of very limited functional significance.

For the two higher gain values, the frequency response shows a flat low-frequency asymptote. The frequency response gain appears to "flatten out" at frequencies lower than 0.2 Hz. This result suggests that the lower bandwidth limit of the perturbation should be somewhat less than 0.2 Hz in order to allow the low-frequency asymptote to be identified.

For the lowest gain value, no low-frequency asymptote is apparent, even at frequencies as low as 0.01 Hz; however, this gain value is probably not realistic. As is evident in the unit pulse response, the small gain results in a highly overdamped system. The extremely long settling time that results does not agree with observed balancing responses.

Based on the above simulation results, it appears that a perturbation bandwidth of 0.1-5.0 Hz would be sufficient to identify the dynamic characteristics of the posture control system relevant to relatively rapid balancing responses.

A.3.3 Perturbation Amplitude Requirements

In designing the perturbation platform, it was necessary to estimate the maximum acceleration, velocity, range of motion, thrust and power requirements. Simulations were performed to estimate these values. The goal was to determine the perturbation characteristics that would ensure loss of balance, i.e. that the COP would reach the limits of the base-of-support (BOS).

The simulations used the transient, RAN and PRN acceleration waveforms described in Section 5.4.3. Extreme anthropometric values were selected to ensure conservative design estimates, i.e. a 5th percentile female and a 95th percentile male were both simulated. Although the larger mass of the male subject might be expected to result in larger thrust and power requirements, it is

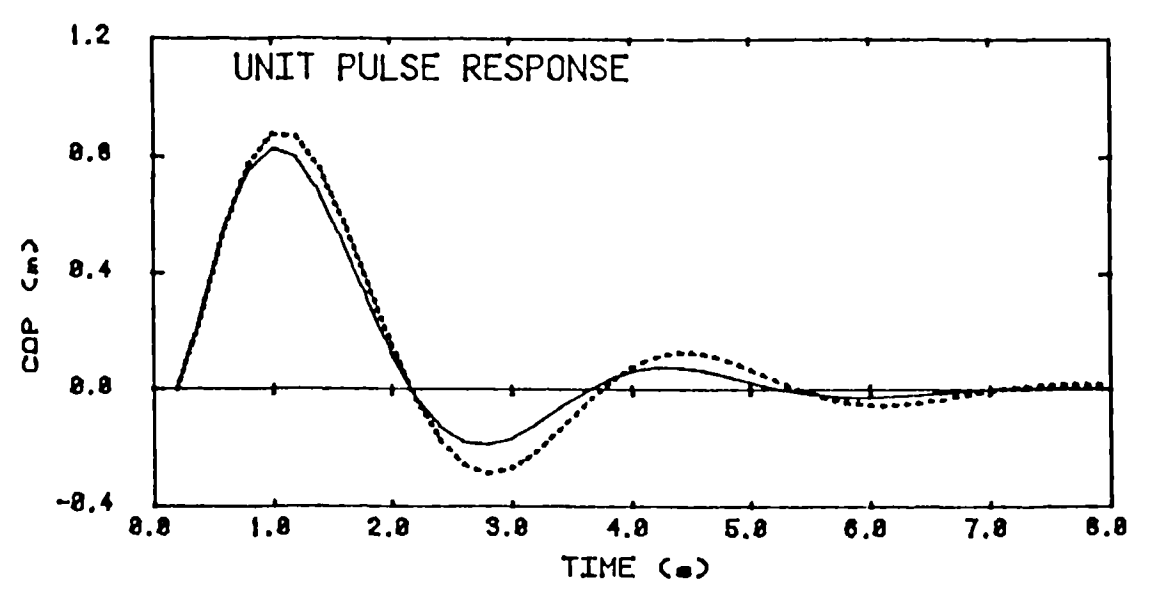
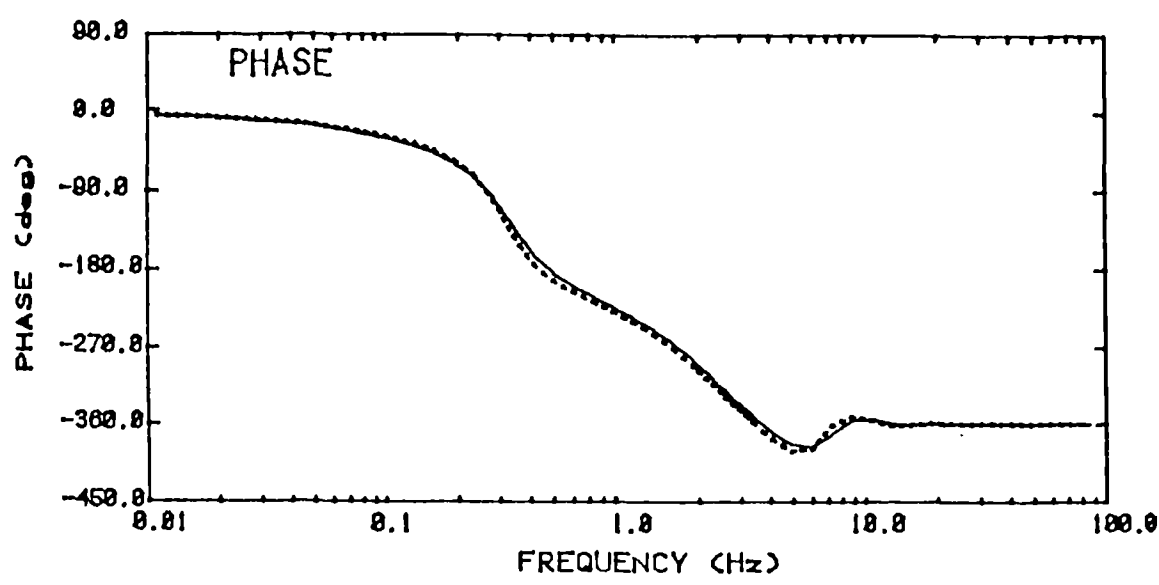
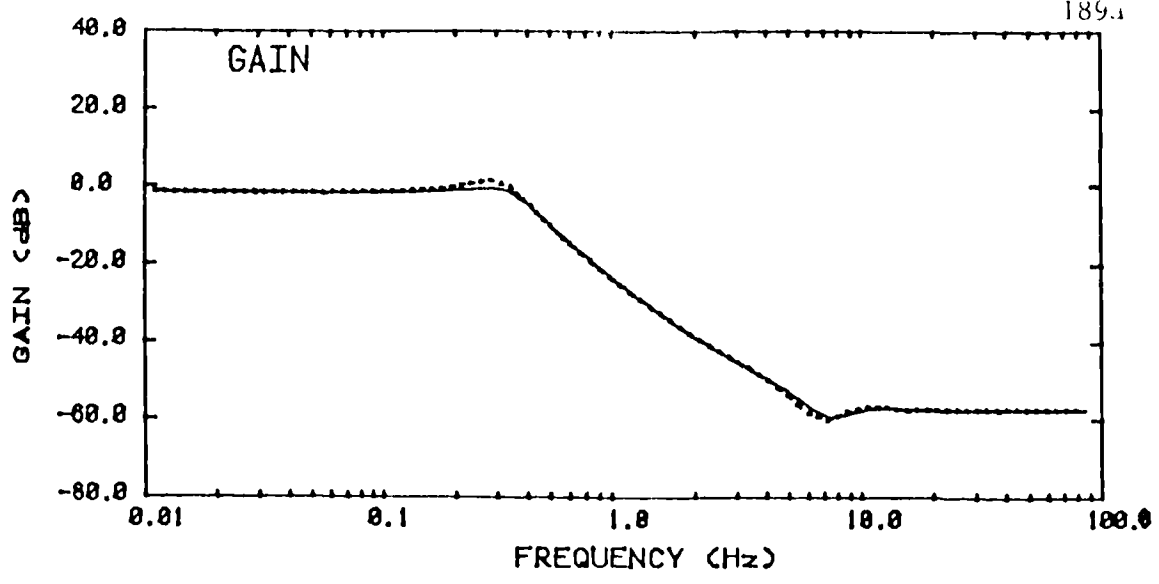


Fig A.7 Effects of changes in dead time
(50th percentile young female; gain = 550 N-m/rad;
pulse duration = 0.2 s).

Legend: solid line - dead time = 0.100 s (young)
dashed line - dead time = 0.110 s (elderly)

conceivable that the lower COG of a small female could raise the thrust and power requirements.

The maximum perturbation amplitude was estimated as the amplitude required for BOS saturation to occur. For the PRN and RAN perturbations, the criterion called for the peak-to-peak COP displacement to equal the foot length. For the transient perturbation, the criterion was based on the peak COP, to simulate the worst case where the subject would be "leaning back on his heels" at the start of a backward platform motion. The foot length was estimated to be 15.2% of the body height (Drillis and Contini, 1966).

The required thrust (F_x) was estimated from equation (8) and the power was calculated as the product of the thrust and the platform velocity. The 95th percentile male proved to be the limiting case, requiring greater thrust and power than the 5th percentile female. The following requirements were determined: (1) maximum acceleration of 1.5 m/s^2 , (2) maximum speed of 0.45 m/s , (3) maximum thrust of 0.12 kN , (4) maximum power of 15 W , and (5) maximum range of 0.39 m . The limiting values of the design requirements were all based on the transient waveform simulations, with the exception of the range requirement, which was based on the RAN waveform. Note that the power and thrust estimates represent the values that must be transmitted to the subject, and do not include losses occurring in the platform drive train.

A.3.4 Effects of Ageing on Balancing Responses

The physiological changes that occur in ageing are expected to result in deterioration in postural performance. In particular, increased COP displacement is expected to occur as a result of: (1) decrease in feedback gain, due to a reduction in sensory acuity and/or muscle strength, and (2) increase in the feedback dead time, due to reduced nerve conduction velocity and increased central processing time. In addition, the decrease in height and increase in weight that typically occur in ageing might be expected to influence the efficacy of the balancing responses.

The effects of changes in feedback gain were illustrated in Section A.3.2, and are discussed in more detail in the next

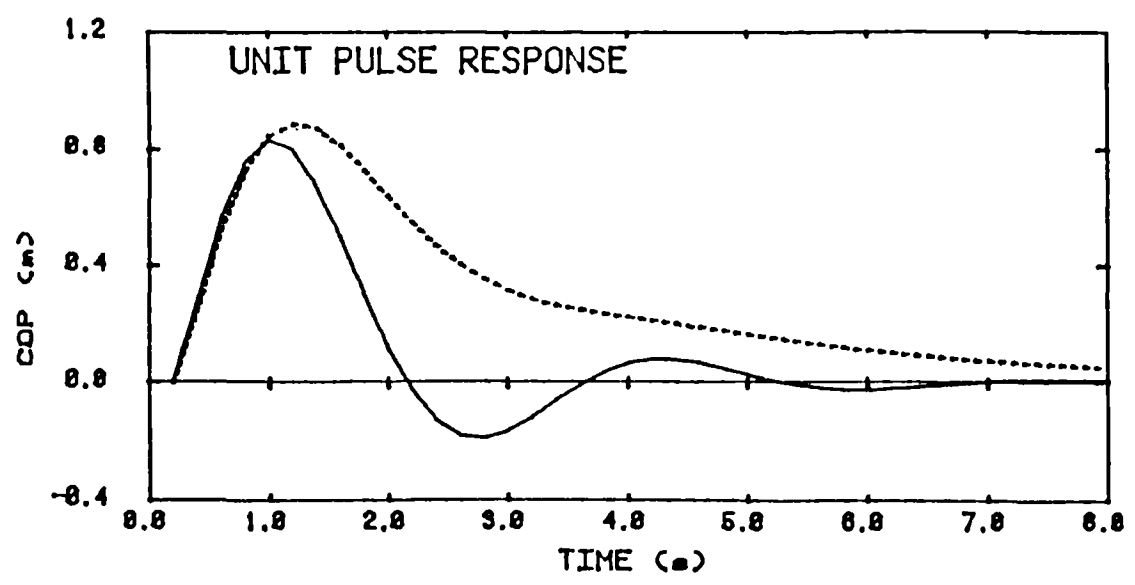
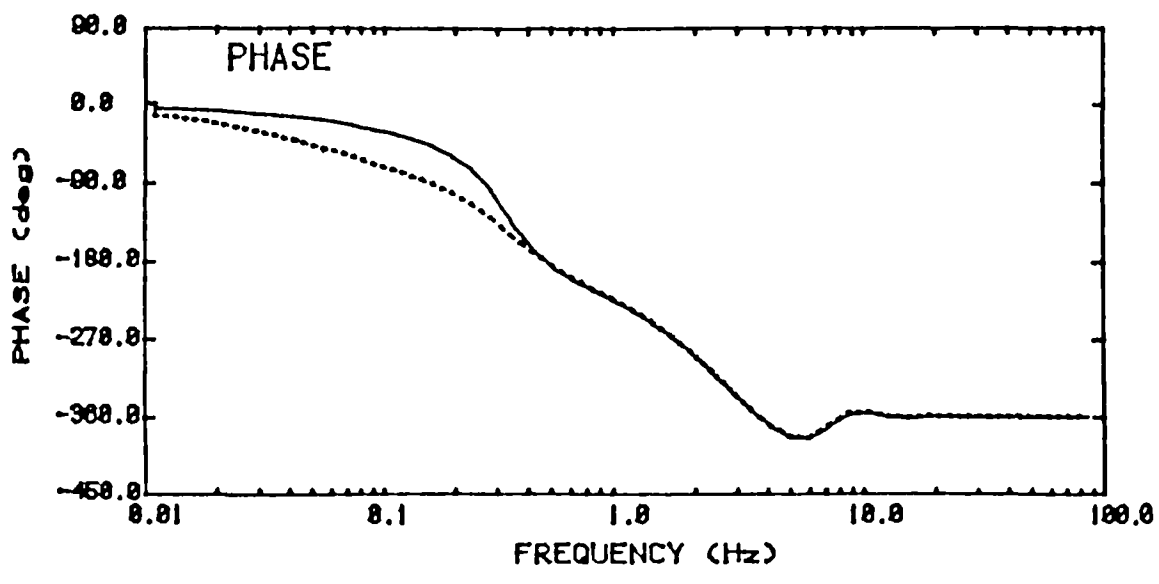
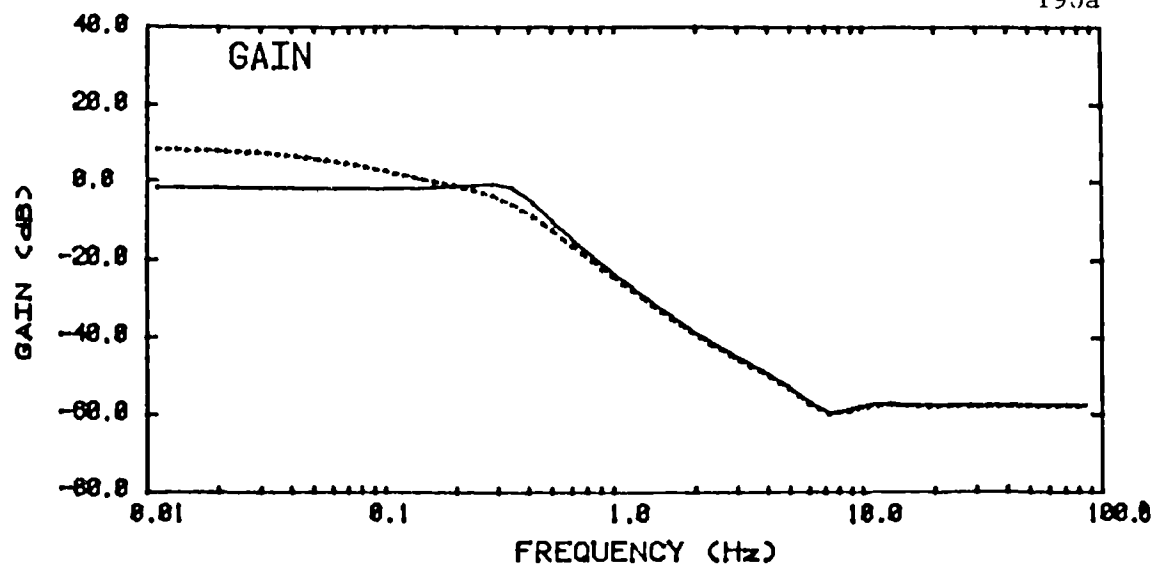


Fig A.8 Effects of changes in height and weight (dead time = 0.1 s; gain = 550 N-m/rad; pulse duration = 0.2 s).

Legend: solid line - 50th percentile young female
dashed line - 50th percentile elderly female

section. Figure A.7 illustrates the effects of increase in dead time, while figure A.8 illustrates the effects of height and weight changes. In each figure, the $C(s)/A(s)$ frequency response and the unit pulse response are presented for a 50th percentile female.

Even though the 10 ms increase in dead time had relatively little effect on the frequency response, it did increase the peak pulse response substantially (6.5%).

The effects of the changes in height and weight were also substantial, producing an increase of 7.0% in the peak pulse response. The anthropometric changes affect both the rotational inertia and the destabilizing moment due to the body weight. For 50th percentile females, the anthropometric changes associated with ageing produce a small increase in rotational inertia (thereby increasing stability) and a substantial increase in body weight moment (thereby decreasing stability). As illustrated in figure A.8, the net result was a decrease in stability (i.e. increased COP displacement in the pulse response). It should be noted that the concept of a "50th percentile female" was used here only for illustrative purposes. In reality, percentiles can be defined only in terms of a specific measurement; the "50th percentile female" does not exist.

The above results suggest that the increase in dead time and the changes in anthropometric characteristics expected to occur in ageing could both tend to reduce postural stability, assuming that no compensatory increase in feedback gain occurs.

A.3.5 Effects of Changes in Feedback Gain

The effects of changes in feedback gain on the COP responses were illustrated in figure A.6, for three different gain values. Figure A.9 shows the variation of the peak COP and ankle angle in the unit pulse response as a function of feedback gain. The most extreme gain values plotted are very close to the limits of stability. Once again, the results shown were obtained from simulations of a 50th percentile young female; similar results were obtained from simulations of other subject groups.

The peak angular displacement decreases monotonically as the feedback gain is increased. In contrast, the COP response has a

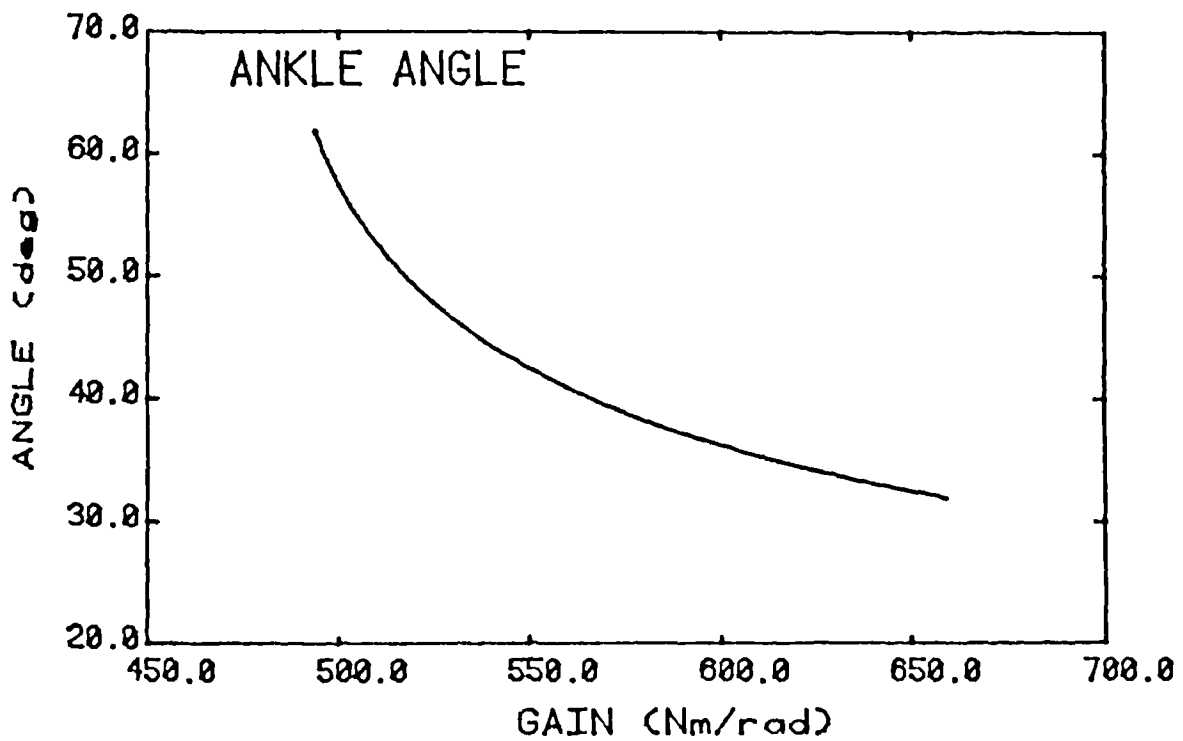
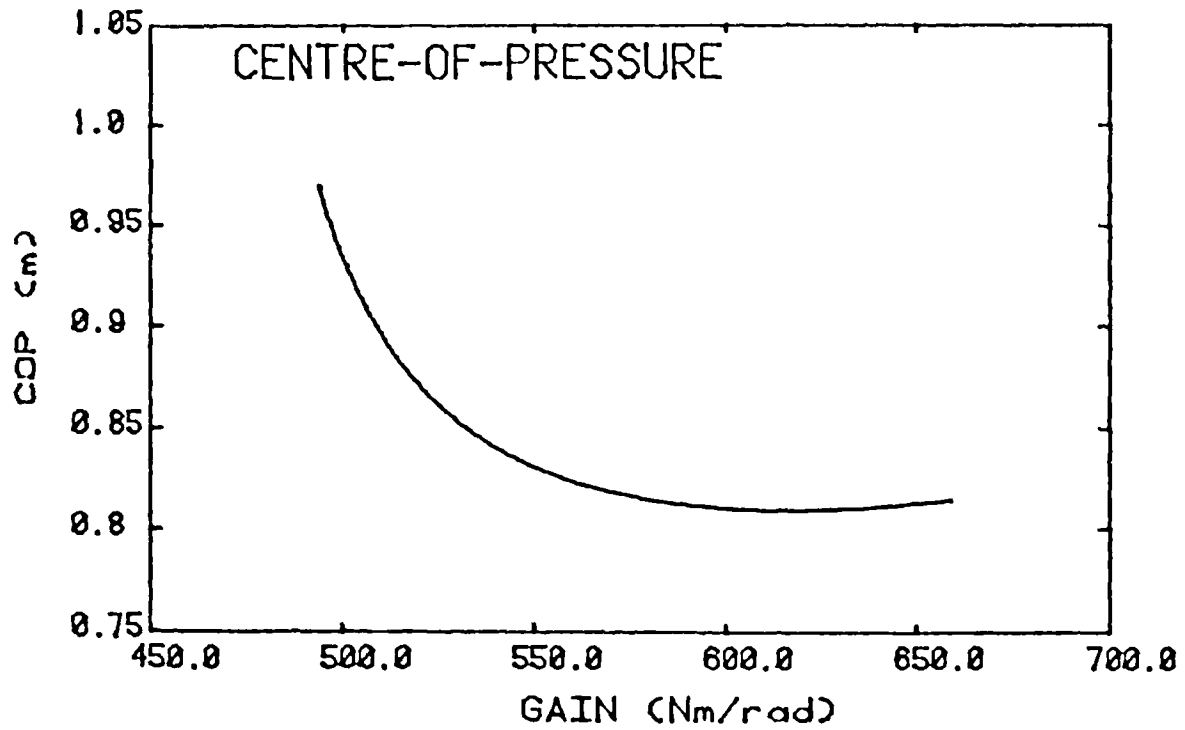


Fig A.9 Effect of feedback gain on peak responses
(subject: 50th percentile young female; pulse duration = 0.2 s).

distinct minima. The corresponding gain value represents a control strategy that is optimal, in that a stable response is achieved while minimizing the COP displacement. By minimizing the COP displacement, the likelihood of saturating the BOS is also minimized and, according to the experimental hypothesis, postural stability is maximized.

The plots in figure A.9 illustrate that the effects of compensatory changes in control system "stiffness", achieved through modulation of the feedback gain, are dependent on the gain level. Below the optimal gain, increases in gain will produce decreases in both angular sway and COP displacement. Above the optimal gain, increases in gain will still produce decreased angular sway, but the COP displacement will now increase (slightly). This finding could explain the lack of correlation between the results of the present study, where COP was measured, and the results of other studies which measured sway displacements of the body (see Section 8.2.3).

A.3.6 Sensory Thresholds

The balance testing methodology requires that the small-amplitude perturbation used in the test elicits posture control responses similar in nature to those elicited by the relatively large perturbations that cause falls. In order for this to be true, the test perturbation must provoke motions that exceed the pertinent sensory thresholds. Simulations were performed to determine whether the perturbation amplitudes estimated from the results of the pilot tests (and later used in the balance tests) were sufficient to exceed known threshold values.

The functional stretch reflex is thought to be triggered by the muscle spindles and by joint and cutaneous somatosensors (Nashner, 1981). Nashner and Cordo (1981) found an ankle rotation rate of 2.5 deg/s to be the minimum necessary to elicit this response. Elner et al (1972) reported a somewhat higher threshold of 20 deg/s. Seated ankle rotation experiments have demonstrated that reflex-induced ankle moment increases markedly once the ankle rotational velocity exceeds approximately 75 deg/s (Herman, 1970; Maki et al, 1985), although it appears that this threshold-like

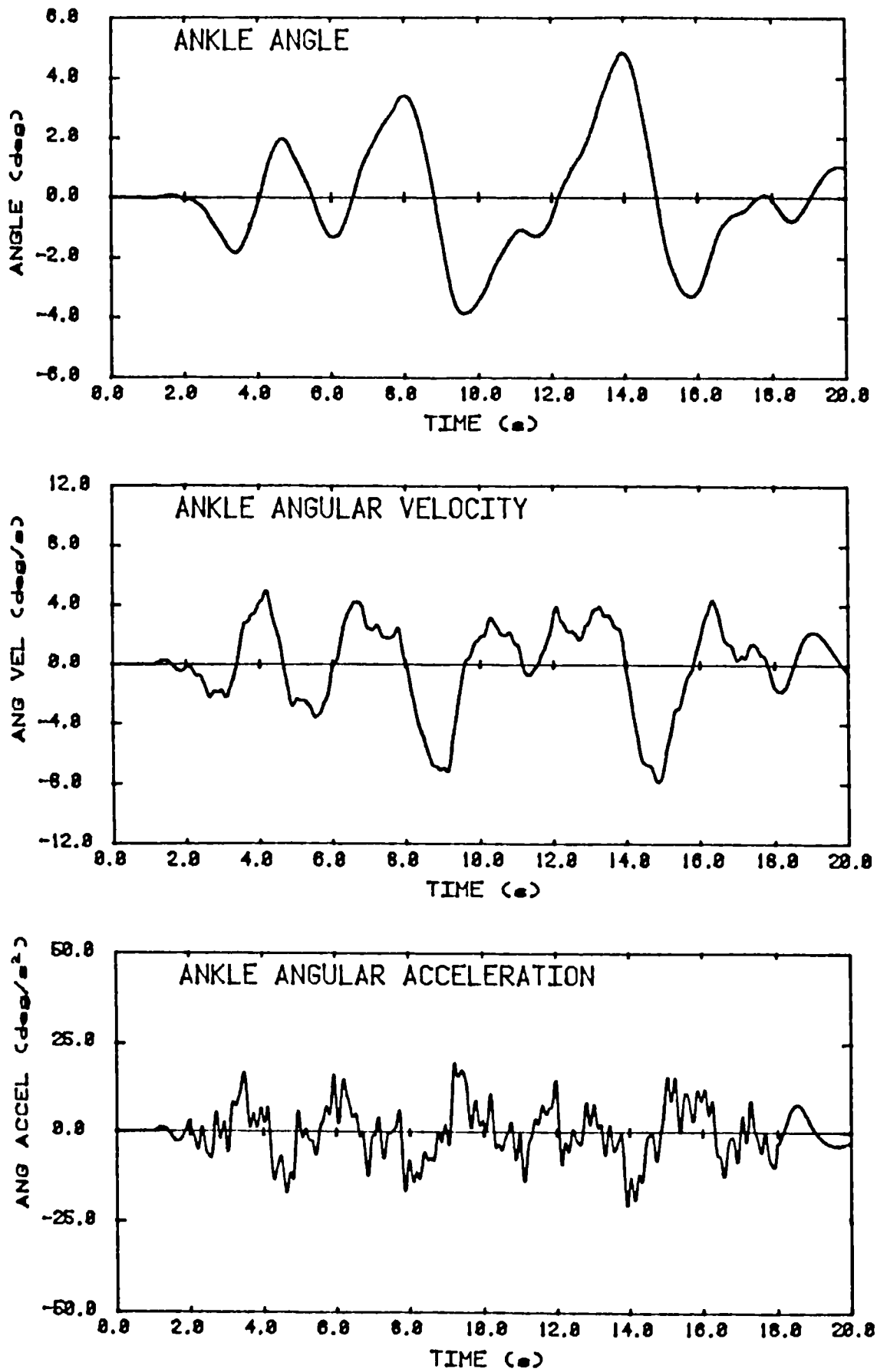


Fig A.10 Ankle kinematics: pseudorandom perturbation (50th percentile young female; gain = 550 N-m/rad).

effect may be inhibited during stance and gait. In terms of ankle displacement, Nashner (1970) reported a threshold of 0.1 degrees in the joint receptors, but no significant threshold in the spindles. Gurfinkel et al (1976) concluded that an ankle rotation of 2 deg is more than sufficient to activate the muscle spindles.

As illustrated in figure A.10, the simulated inverted pendulum response to a PRN perturbation with a root-mean-square (RMS) amplitude of 0.1 m/s^2 does exceed the reported angular displacement thresholds, but exceeds only the lower estimates for the angular velocity thresholds. As shown in figure A.11, similar results were obtained using the smallest transient perturbation (peak amplitude of 0.5 m/s^2). The RMS ankle angle displacement was 1.90 deg for the PRN perturbation and 1.89 degrees for the transient perturbation. In terms of angular velocity, the RMS values were 2.86 and 4.28 deg/s for the PRN and transient perturbations, respectively.

Thresholds of 0.05 deg/s^2 and 0.29 deg have been reported for the semicircular canals and otoliths, respectively (Nashner, 1970). For an inverted pendulum, the angular rotation at the head is equal to that occurring at the ankle. Thus, the results shown in figures A.10 and A.11 apply, indicating that the test perturbation does indeed exceed the reported threshold values. The RMS angular acceleration values were 6.98 and 14.7 deg/s^2 , for the PRN and transient perturbations, respectively. As listed above, the corresponding RMS angular displacements were 1.90 and 1.89 deg.

Although visual thresholds have not been reported directly, an upper limit is estimated to be 1 cm/s, the minimum rate at which subjects were able to detect linear motion of a visual surround (Berthoz et al, 1975). For an inverted pendulum, the rate of visual motion is approximately equal to the product of the eye height and the ankle angular velocity. Both the PRN and transient waveforms exceeded the estimated threshold, with RMS values of 7.2 cm/s and 10.8 cm/s, respectively.

A.4 LIMITATIONS OF THE SIMULATION MODEL

The derivations presented in Section A.1.1 were based on a linearized inverted pendulum model of the biomechanics. The

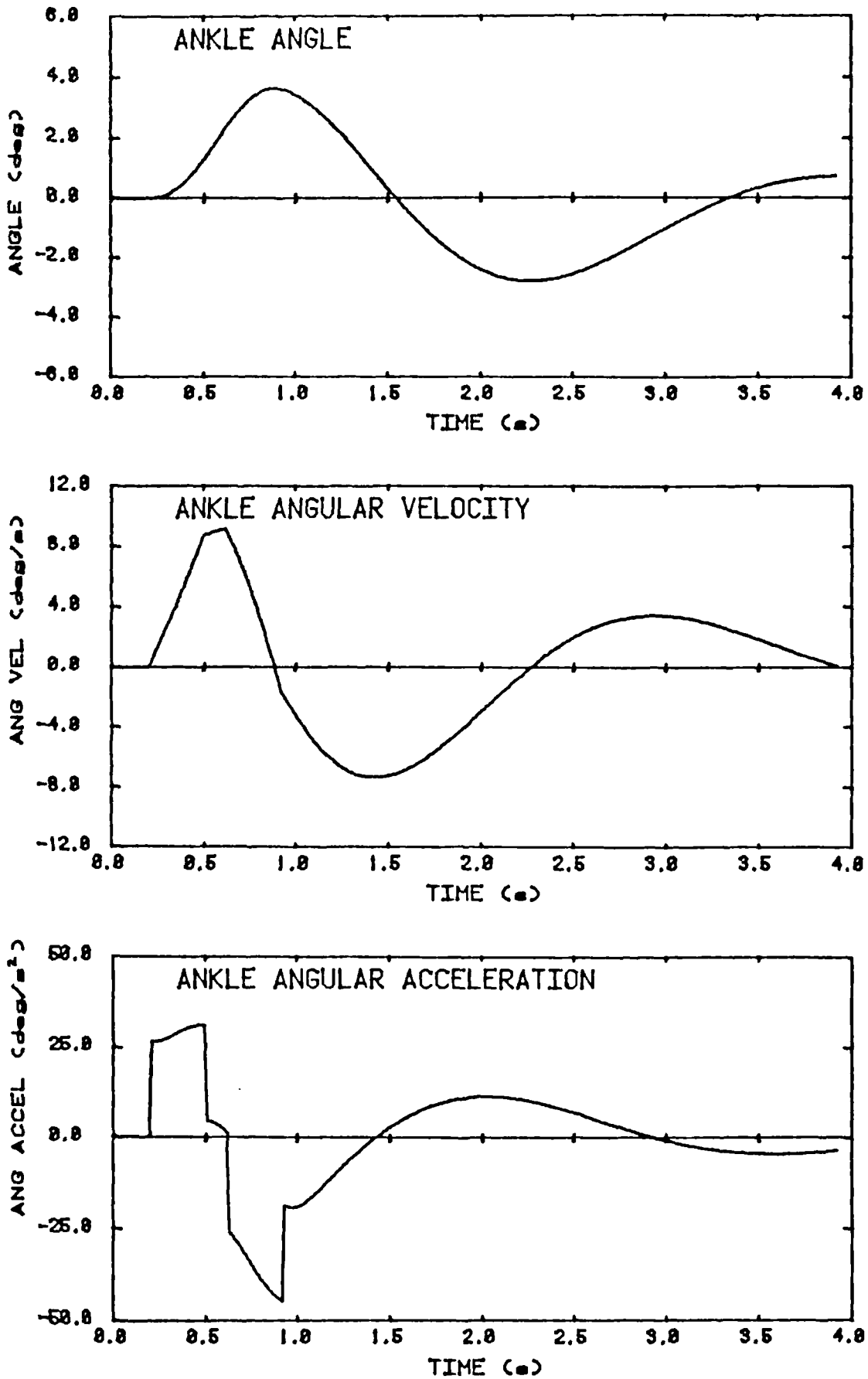


Fig A.11 Ankle kinematics: transient perturbation (50th percentile young female; gain = 550 N-m/rad).

control system was also assumed to be linear. Even though experimental evidence suggests that linearity may be a poor approximation (e.g. see Section 8.4.1), linear models were used here because of the tremendous advantage that they provide over nonlinear models in terms of computational simplicity and ease of interpretation.

The inadequacies of the inverted pendulum model have been documented by a number of investigators (see Section 2.1.1). In contrast, Nashner and McCollum (1985) have identified the inverted pendulum "ankle synergy" as an important balancing strategy. In any case, use of a multi-link model requires additional assumptions about the cross-coupling terms in the feedback, and errors introduced by these assumptions could well negate any benefits derived from a more realistic biomechanical model. The inverted pendulum was therefore selected as a first-order approximation of the multi-link dynamics.

In deriving the dynamic equations for the inverted pendulum, small-angle approximations were used in order to obtain linear equations. Assuming the length of the BOS and the height of the COG to be 15% and 60% of the body height respectively (Drillis and Contini, 1966), static BOS saturation will occur at an ankle angle of approximately 14 deg (i.e. $\tan^{-1} [0.15/0.6]$). In dynamic situations, the saturation angle will be even smaller. Thus, small-angle approximations are appropriate for a model of sub-saturation balancing responses.

It should be noted that, for simplicity, the passive muscle stiffness and viscosity were omitted from the model. The passive muscle properties are expected to have relatively little influence, except for very small sway displacements (i.e. spontaneous sway), where the passive stiffness may be sufficiently high to stabilize the inverted pendulum (Nashner, 1981).

From the above discussion, it is evident that the approximations in the simulation model limit the accuracy of the results and require that caution be exercised in any extrapolation of the results to actual postural performance. It should be emphasized that the purpose of the simulations was only to provide: (1) very approximate estimates, to aid in specifying design

requirements for the perturbation platform, (2) theoretical justification for certain aspects of the posture control model and balance testing methodology, and (3) possible explanations for some of the experimental findings. Detailed simulation of the posture control system is beyond the scope of the present work.

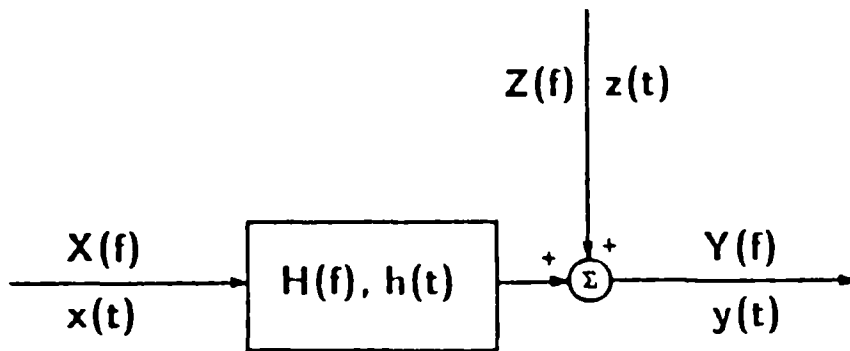


Fig B.1 The measurement problem.

APPENDIX B. SYSTEM IDENTIFICATION WITH PSEUDORANDOM INPUTS

Some authors have suggested that the coherence function can be used to assess the accuracy with which input and output measurements can be related by a noise-free linear nonparametric transfer function (or frequency response) model (Bendat and Piersol, 1971b and 1980; Roth, 1971). These authors limited their discussion to random inputs; however, other investigators have applied the same methods to pseudorandom inputs. In this appendix, it will be shown that this approach is not valid, particularly when using pseudorandom inputs with harmonic frequency content. Not only is the transfer function estimate biased, but the coherence function estimate does not indicate the "goodness-of-fit" of the linear model.

B.1 THEORY

The measurement problem is illustrated in figure B.1. The transfer function, $H(f)$, relates the linear output of the system to the input stimulus, $X(f)$. The measured output, $Y(f)$, is equal to the linear output plus a noise, $Z(f)$. Here, $X(f)$, $Y(f)$ and $Z(f)$ are the Fourier transforms of the time histories $x(t)$, $y(t)$ and $z(t)$, respectively, where f denotes frequency. $Z(f)$ represents the combined effects of: (1) measurement noise in the output transducer, (2) output due to unmeasured inputs (uncorrelated with $x(t)$), and (3) distortion products generated by nonlinearities in the system (Bendat and Piersol, 1971b; Roth, 1971). For simplicity, measurement noise in the input transducer is assumed to be negligible.

The nonparametric transfer function, $H(f)$, can be estimated from the spectral density relationships between the input and output signals, as follows (Jenkins and Watts, 1968; Bendat and Piersol, 1971b and 1980; Roth, 1971):

$$\hat{H}(f) = \hat{G}_{xy}(f) / \hat{G}_{xx}(f) \quad (1)$$

where $G_{xy}(f) = \lim_{T \rightarrow \infty} (2/T) E[X^*(f,T)Y(f,T)]$ is the expected value of the cross spectrum and $G_{xx}(f) = \lim_{T \rightarrow \infty} (2/T) E[X^*(f,T)X(f,T)]$ is the expected value of the input auto power spectrum (T is the duration, E is the expected value operator, "*" indicates a complex conjugate,

"^" indicates an estimate). The coherence function, $\gamma^2(f)$, is estimated as follows:

$$\hat{\gamma}^2(f) = [\hat{G}_{xy}(f)\hat{G}_{xy}^*(f)] / [\hat{G}_{xx}(f)\hat{G}_{yy}(f)] \quad (2)$$

The power spectra must be estimated from finite-duration measurements of $x(t)$ and $y(t)$. These estimates can be obtained by dividing the total data record into N equal-length segments (of duration T), computing the spectral estimates for each data segment and then averaging the N estimates (Bendat and Piersol, 1971b and 1980). Equations (1) and (2) become:

$$\hat{H}(f) = \frac{[(2/NT)\sum_{k=1}^N X_k^*(f,T)Y_k(f,T)]}{[(2/NT)\sum_{k=1}^N X_k^*(f,T)X_k(f,T)]} \quad (3)$$

$$\hat{\gamma}^2(f) = \frac{[(2/NT)\sum_{k=1}^N X_k^*(f,T)Y_k(f,T)] [(2/NT)\sum_{k=1}^N X_k(f,T)Y_k^*(f,T)]}{[(2/NT)\sum_{k=1}^N X_k^*(f,T)X_k(f,T)] [(2/NT)\sum_{k=1}^N Y_k^*(f,T)Y_k(f,T)]} \quad (4)$$

Since $Y_k(f,T) = H(f)X_k(f,T) + Z_k(f,T)$, equations (3) and (4) become:

$$\hat{H}(f) = H(f) + \hat{G}_{xz}(f)/\hat{G}_{xx}(f) \quad (5)$$

$$\hat{\gamma}^2(f) = \frac{\hat{G}_{xx}(f) [|H(f)|^2 \hat{G}_{xx}(f) + H(f)\hat{G}_{xz}(f) + H^*(f)\hat{G}_{zx}(f)] + |\hat{G}_{xz}(f)|^2}{\hat{G}_{xx}(f) [|H(f)|^2 \hat{G}_{xx}(f) + H(f)\hat{G}_{xz}(f) + H^*(f)\hat{G}_{zx}(f) + \hat{G}_{zz}(f)]} \quad (6)$$

where $\hat{G}_{xz}(f) = (2/NT)\sum_{k=1}^N X_k^*(f,T)Z_k(f,T)$, etc.

B.1.1.1 Random Input

If $x(t)$ is random, then the component of $z(t)$ associated with the distortion products generated by nonlinearities in the system will also be random. Although these distortion products may still bias the transfer function estimates (Bendat and Piersol, 1971b and 1980), their contribution to $\hat{G}_{xz}(f)$ and $\hat{G}_{zx}(f)$ will tend to "average out" (Gibb, 1982). As a result, since the other components of $z(t)$ are uncorrelated with $x(t)$, $\hat{G}_{xz}(f)$ and $\hat{G}_{zx}(f)$

will tend to become small as N is increased. Thus, *approximately*:

$$\hat{H}(f) \rightarrow H(f) \quad (7)$$

$$\hat{\gamma}(f)^2 \rightarrow \frac{|H(f)|^2 G_{xx}(f)}{|H(f)|^2 G_{xx}(f) + G_{zz}(f)} \quad (8)$$

That is, the estimate for $H(f)$ will approximate the true value, and the estimated coherence function will be approximately equal to the fraction of output power attributable to the linear transfer function, at each frequency. Increasing degrees of nonlinearity in the system will create increased distortion products and hence increase in $G_{zz}(f)$. From equation (8) above, this will result in reduced coherence. Thus, for a random input, coherence estimates will reflect the "goodness-of-fit" of the linear transfer function model (as well as the presence of measurement noise and/or unmeasured inputs).

B.1.2 Pseudorandom Input

Pseudorandom inputs are periodic. If the period of a pseudorandom input, $x(t)$, is equal to the duration of the data segment, T , then the spectral estimates of the input data segments will not vary, that is, $X_k(f, T) = X_0(f, T)$ for $k = 1, N$. Moreover, distortion products generated by nonlinearities in the system will also have period T . In this case, the noise estimate for each data segment, $Z_k(f, T)$, can be written as the sum of a random component, $R_k(f, T)$, and a periodic deterministic component, $D_0(f, T)$. The transfer function estimate now becomes:

$$\hat{H}(f) = H(f) + H_r(f) + [D_0(f, T)/X_0(f, T)] \quad (9)$$

where $H_r(f) = (1/NX_0(f, T)) \sum_{k=1}^N R_k(f, T)$ depends on the random component of the noise, but not the periodic component.

Similarly, equation (6) for the coherence estimate can be written as:

$$\hat{\gamma}^2(f) = \frac{A_x(f) + A_r(f) + A_d(f)}{A_x(f) + B_r(f) + A_d(f)} \quad (10)$$

where $A_r(f)$ and $B_r(f)$ depend on the random component of the noise, $A_d(f)$ depends on the deterministic component of the noise, and $A_x(f)$ does not depend on the noise. These terms are as follows:

$$A_x(f) = |H(f)|^2 \hat{G}_{xx}(f)^2$$

$$A_r(f) = (2/NT) \hat{G}_{xx}(f) [H(f)X_0(f,T) \sum_{k=1}^N R_k^*(f,T) + H^*(f)X_0^*(f,T) \sum_{k=1}^N R_k(f,T) + (1/N) \{ \sum_{k=1}^N R_k(f,T) \} \{ \sum_{k=1}^N R_k^*(f,T) \}]$$

$$A_d(f) = (2/NT) \hat{G}_{xx}(f) [ND_0(f,T)D_0^*(f,T) + D_0(f,T) \sum_{k=1}^N R_k^*(f,T) + D_0^*(f,T) \sum_{k=1}^N R_k(f,T) + NH(f)D_0^*(f,T)X_0(f,T) + NH^*(f)D_0(f,T)X_0^*(f,T)]$$

$$B_r(f) = (2/NT) \hat{G}_{xx}(f) [H(f)X_0(f,T) \sum_{k=1}^N R_k^*(f,T) + H^*(f)X_0^*(f,T) \sum_{k=1}^N R_k(f,T) + \sum_{k=1}^N R_k(f,T)R_k^*(f,T)]$$

If the system is perfectly linear, then $D_0(f,T) = D_0^*(f,T) = 0$ and $A_d(f) = 0$, and the coherence will approach the limit given in equation (8) as N increases. In this situation, the numerator of the coherence estimate represents the output of the linear transfer function, while the denominator represents the measured output, as in the random input case.

From equation (9), it is clear that deterministic noise, $D_0(f,T)$, due to nonlinearities in the system, will create bias in the transfer function estimate. Moreover, the presence of a nonzero $A_d(f)$ term in the numerator of the coherence estimate (equation (10)), means that the numerator no longer converges to the output of the linear transfer function, and the coherence no longer indicates the degree of nonlinearity in the system.

For many commonly used pseudorandom input signals (e.g. binary maximum-length sequences), energy is concentrated at discrete frequencies which are integer multiples of other frequency components in the signal. Harmonics generated in response to input energy at frequency f_1 will occur at frequencies that are integer

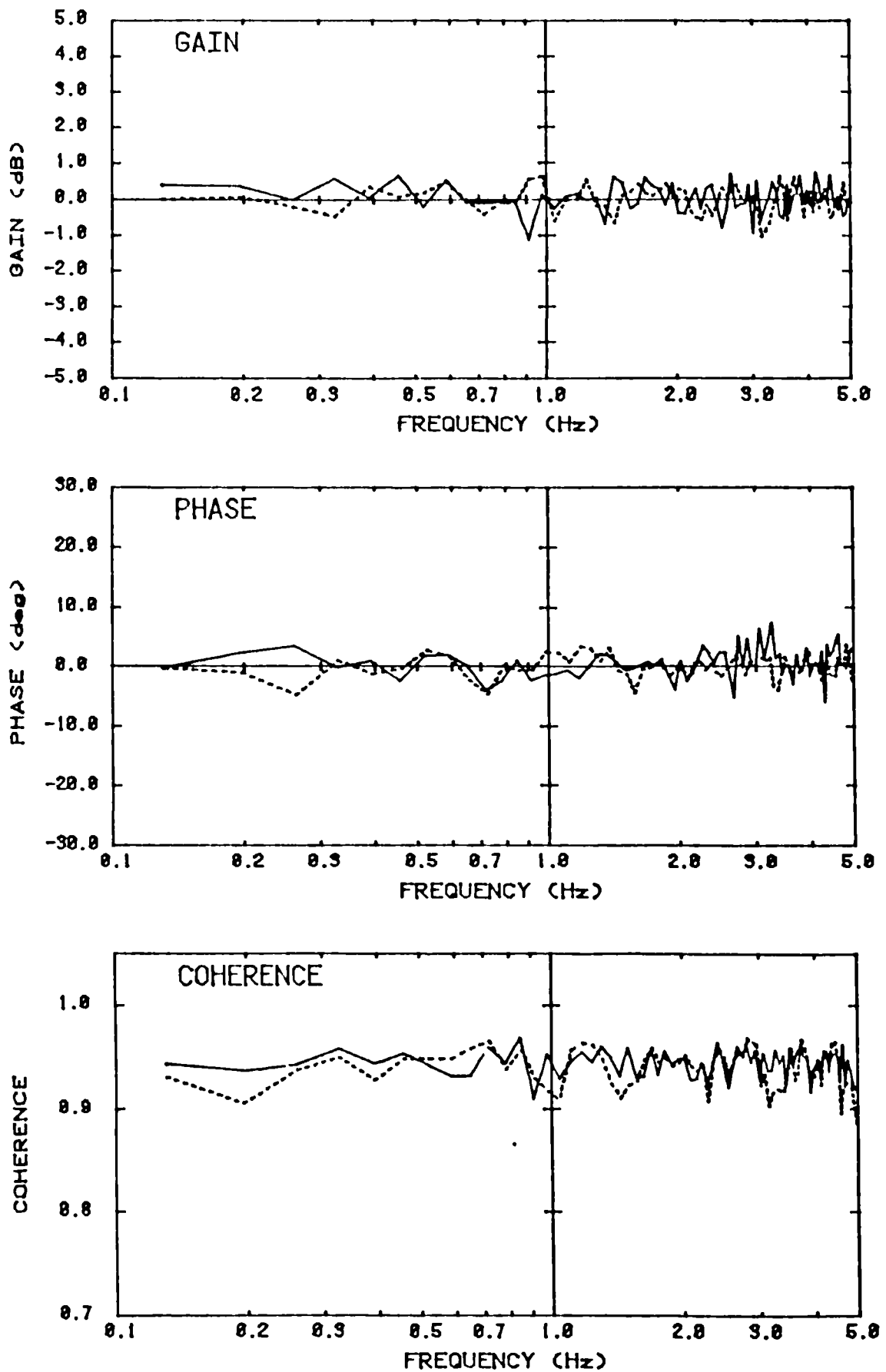


Fig B.2 Simulation results for purely random noise.

Legend: solid line - harmonic pseudorandom input (HPRN)
dashed line - random input (RAN)

multiples of f_1 (van Lunteren, 1985). In addition, intermodulation terms will be generated at frequencies that are sums and differences of the input frequencies (Gibb, 1982). The bias error in the transfer function estimate will occur at the harmonic and intermodulation frequencies.

The bias error can be reduced by using pseudorandom signals comprising a relatively small number of frequency components, none of which are integer multiples (i.e. harmonics) of other frequency components in the signal (van Lunteren, 1985). In this case, nonlinearities produce harmonics at frequencies that are not components of the input signal. By restricting the transfer function estimates to those frequencies present in the input, the harmonic distortion is prevented from biasing the results. In addition, the reduction in the number of frequency components in the input waveform leads to a reduction in the intermodulation distortion. For these nonharmonic inputs, the coherence function indicates approximately the amount of random noise, but cannot be used to assess linearity.

In practical measurement situations, use of true nonharmonic input signals may lead to other problems. In particular, any relatively wide intervals between the frequency components may allow sharp peaks or troughs in the transfer function to pass undetected. To achieve closer "spacing" of the frequency components (along the frequency axis), the input can be designed to eliminate only the small-integer frequency multiples. This will still effectively minimize harmonic distortion at the input frequencies, since the higher harmonics generated by nonlinearities tend to be relatively small in amplitude. In addition, in feedback control systems, the higher harmonics will tend to be attenuated by the low-pass elements in the control loop (Ogata, 1970b).

B.2 SIMULATION EXAMPLE

Digital simulations were performed in order to demonstrate the results derived above. In the simulations, the output is given by:

$$y(m\Delta t) = x(m\Delta t) + x^2(m\Delta t) + z(m\Delta t); \quad m = 1, M$$

where Δt is the sampling interval. The linear system has unity

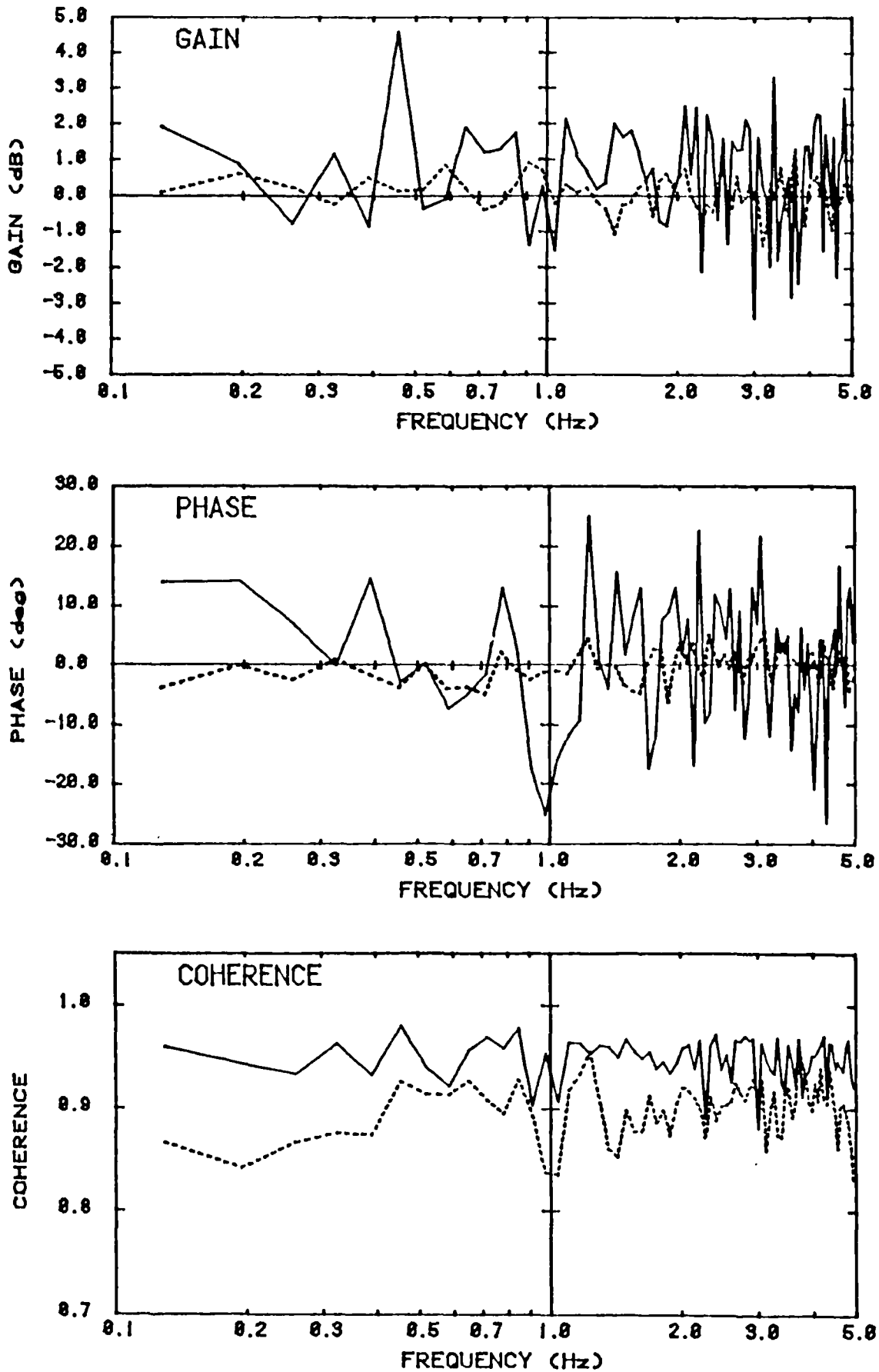


Fig B.3 Simulation results for random noise plus nonlinearity.

Legend: solid line - harmonic pseudorandom input (HPRN)
dashed line - random input (RAN)

gain and zero phase shift at all frequencies, i.e. $H(f) = 1$. The squared term simulates distortion products generated by nonlinearities in the system, while the zero-mean Gaussian noise, $z(t)$, represents random measurement noise in the output transducer as well as output due to unmeasured inputs (uncorrelated with $x(t)$).

Simulations were performed using three input signals: (1) a bandlimited and amplitude-limited approximation to Gaussian white noise (RAN); (2) a pseudorandom signal with harmonic frequency content (HPRN); and (3) a "nonharmonic" pseudorandom signal with limited harmonic content, i.e. only 4th and higher harmonics (NHPRN). The frequency composition of these signals was described in Section 5.4.3. All three inputs excited the system over the same frequency range, with the same power spectrum envelope and the same peak factor (ratio of peak value to root-mean-squared value). For each input, two simulations were performed: (1) random noise only, and (2) nonlinear distortion products plus random noise. The random noise, $z(t)$, was identical for all simulations.

The simulation generated $M = 5121$ data points, resulting in $N = 20$ 256-point segments. The transfer function and coherence estimates were then calculated, using a Fast Fourier Transform algorithm to implement the methods described in the previous section. For the random inputs, the data in each segment were windowed using a Hamming window to reduce distortion due to truncation of the data record. The pseudorandom inputs are "self-windowing" because the duration of each data segment is equal to the period (Gibb, 1982). Nonetheless, the pseudorandom data were analysed both with and without windowing, to ensure that differences in the random results were not due to the windowing.

Figure B.2 shows the transfer function and coherence estimates for the simulation using only random noise, without nonlinear effects. Note that both the RAN and HPRN results fluctuate about the true linear values ($|H(f)| = 1$; $\angle H(f) = 0$) in a similar manner. In both cases, the coherence was less than unity due to the presence of the random noise.

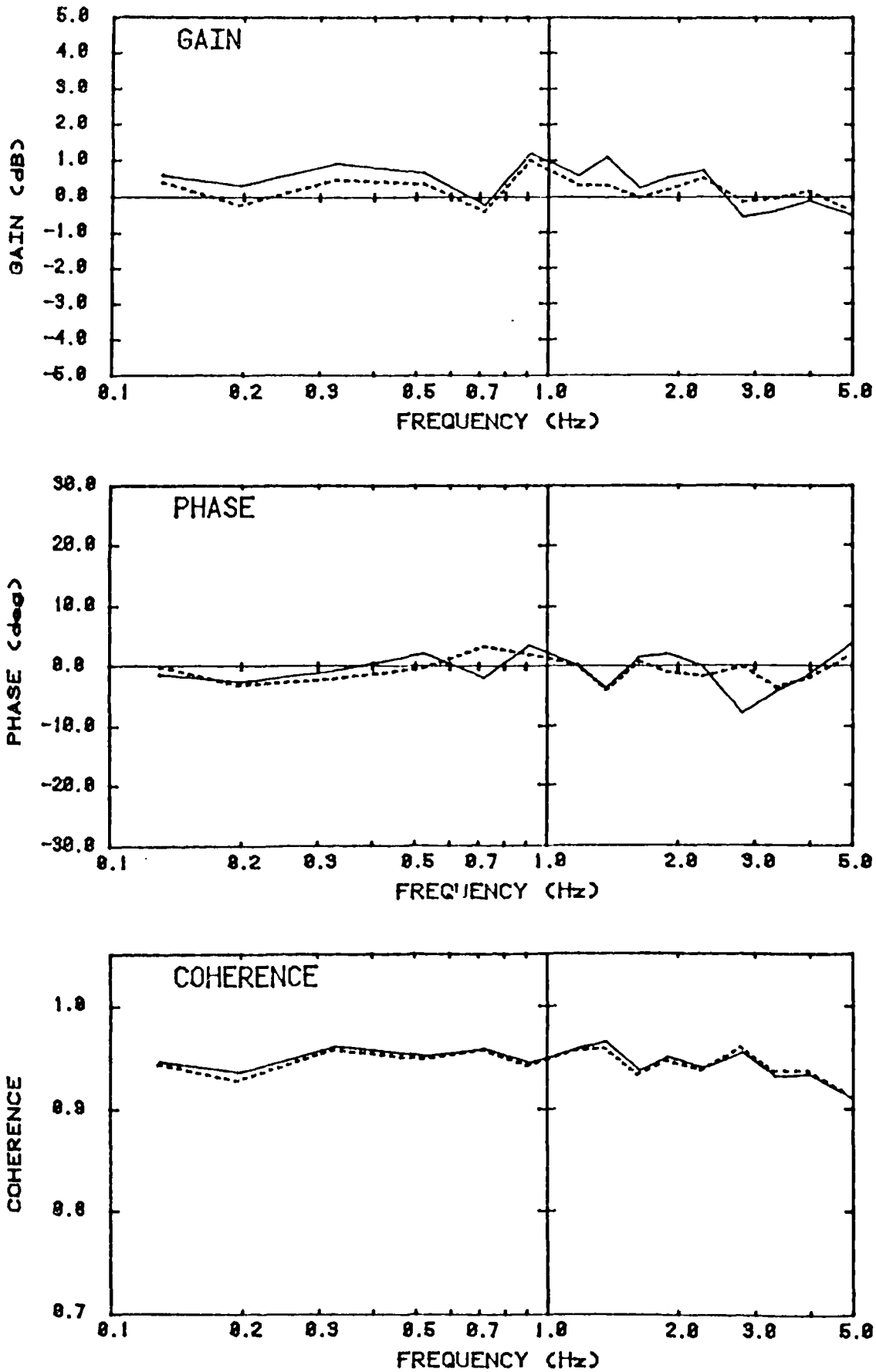


Fig B.4 Simulation results for "nonharmonic" pseudorandom input (NHPRN).

Legend: solid line - random noise plus nonlinearity
dashed line - random noise only

Figure B.3 shows the estimates when the nonlinear term was added to the simulation. For the HPRN input, the nonlinearity caused large errors in the transfer function estimates. Using an increased number of data segments to compute the estimates did not cause these errors to diminish. This result suggests a bias error. For the RAN input, inclusion of the nonlinearity had little effect on the transfer function estimates. Furthermore, increase in number of data segments was found to smooth out the fluctuations in the estimates, suggesting that the error is primarily random, rather than bias.

Using the RAN input, the coherence estimates decreased substantially when the nonlinearity was included in the simulation. Thus, the coherence function did indicate the linearity of the system. Using the HPRN input, the coherence estimates changed very little when the nonlinearity was included. Moreover, the small changes that did occur were not consistent, with increases occurring at some frequencies and decreases at others. These results demonstrate that use of coherence estimates to assess linearity will be erroneous for this type of input.

Figure B.4 demonstrates that the bias errors were much reduced when using the NHPRN input. In this case, inclusion of the nonlinearity had negligible effect on the transfer function and coherence estimates. Thus, the presence of the nonlinearity did not appreciably bias the transfer function estimates. The coherence function indicated the presence of the random noise, but did not reflect the nonlinear distortion.

B.3 CONCLUSION

In using random input signals to identify linear transfer function models of nonlinear systems, coherence estimates will reflect the degree of nonlinearity in the system. This is not true for pseudorandom inputs.

Use of pseudorandom inputs in which the frequency components are integer multiples of other frequency components in the signal will lead to biased estimates for the linear transfer function. By using true nonharmonic pseudorandom inputs, the bias error is much

reduced. In practical measurement situations, elimination of the lowest harmonics from the input achieves essentially the same result. In these cases, the coherence function indicates approximately the amount of random error in the transfer function estimates.

APPENDIX C. PILOT EXPERIMENTS TO ASSESS REPEATABILITY

C.1 INTRODUCTION

Pilot experiments were performed, using a small number of subjects, in order to gain some information about the test-to-test and day-to-day repeatability of the balance test results. Such information is needed if the balance test is to be used as a monitoring tool (e.g. to chart the progress of patients undergoing treatment). The primary objective here, however, was to gain information to aid in designing the testing protocol and selecting the perturbation waveform.

C.2 METHODOLOGY

C.2.1 Subjects

Six subjects were tested. All were healthy normal young adults, with no obvious or diagnosed neurological or musculoskeletal deficits. The subjects ranged in age from 28 to 34. There were three males and three females. None of the subjects had been tested previously on the perturbation platform.

C.2.2 Testing Procedure

The test procedure was identical to that used in the pilot experiments (see Section 5.4.2). Thus, for each test, the subject was instructed to stand relaxed, with feet comfortably spaced and arms at sides, and to look straight ahead. Headphones were used to listen to "Muzak"® so as to mask any auditory cues from the motor and to distract the subject from consciously modifying his/her motion. Prior to the first test, the outlines of the feet were traced, to allow the feet to be repositioned in the same location in subsequent tests.

Each test was approximately 5 minutes in duration. The platform motion was controlled to start and end gradually, with no sudden changes in acceleration. During the tests, the subjects were observed to determine whether they grabbed the handrail, waved their arms or moved their feet. At the end of each test, the subjects were allowed a 2-3 minute seated rest. The duration of each testing session was approximately 40 minutes.

C.2.3 Test Perturbations

Two waveforms were tested: harmonic pseudorandom (HPRN) and random (RAN). These waveforms were similar to those used in the pilot experiments performed to select the perturbation parameters (see Section 5.4.3).

To construct the RAN waveform, Gaussian white noise (generated by applying a normalizing transformation to the output of multiplicative congruential random number generator) was bandpass filtered, with cutoffs (-1 dB) at 0.4 and 4.7 Hz (-30 dB rejection at 0.3 and 5.0 Hz). The amplitude (prior to filtering) was limited to ± 3 standard deviations. The HPRN signal had a period of 15.36 s, and was constructed as a sum of equal-amplitude sinusoids having random phase angles uniformly distributed between 0 and 360 degrees. There were 68 sinusoids, spaced at equal frequency intervals of 0.065 Hz between 0.39 Hz and 4.75 Hz. Both waveforms had an RMS amplitude of 0.2 m/s². The peak factors of the HPRN and RAN waveforms were 2.29 and 3.46, respectively.

C.2.4 Protocol

Two males and one female were tested with the RAN waveform; one male and two females were tested with the HPRN waveform. Each subject was tested on five consecutive weekdays, five times on each day. Each subject was tested at approximately the same time of day on all five days. For each subject, the identical perturbation signal was used in all of the tests.

C.2.5 Analysis

For each test, a linear transfer function was fitted to the data, treating platform acceleration as the input and centre-of-pressure (COP) displacement as the output. The transfer function was then used to predict ΔCOP , the peak COP displacement in the unit pulse response. The transfer function was identified using cross-spectral, least squares and maximum likelihood methods. The analytical methods are discussed in detail in Sections 6.5 and 6.6.

The data for each subject were analyzed separately. Coefficients of variation were calculated to quantify the day-to-day, test-to-test and overall variability in the ΔCOP

TABLE C.1

TEST-TO-TEST AND DAY-TO-DAY VARIABILITY: COEFFICIENTS OF VARIATION

	COEFFICIENT OF VARIATION (%) +					
	PSEUDORANDOM WAVEFORM			RANDOM WAVEFORM		
	SUBJECT 1	SUBJECT 2	SUBJECT 3	SUBJECT 4	SUBJECT 5	SUBJECT 6
TEST-TO-TEST VARIABILITY						
day 1	3.84	3.06	14.1	5.56	8.78	8.01
day 2	9.00	2.30	3.00	1.92	5.51	6.19
day 3	4.53	2.07	6.28	3.74	10.7	8.49
day 4	6.35	5.78	19.1	4.48	7.18	9.26
day 5	4.42	5.01	9.70	2.47	15.5	3.65
mean	5.63	3.64	10.4	3.63	9.52	7.12
std dev	2.11	1.66	6.35	1.48	3.83	2.25
DAY-TO-DAY VARIABILITY						
test 1	11.8	5.09	20.1	5.72	3.93	7.78
test 2	9.41	3.87	4.42	3.32	5.34	5.91
test 3	10.2	3.29	9.02	2.21	12.4	9.61
test 4	13.2	1.14	18.4	6.85	4.67	5.98
test 5	11.4	4.54	7.43	4.23	13.7	4.69
mean	11.2	3.58	11.9	4.47	8.00	6.80
std dev	1.47	1.53	6.96	1.85	4.64	1.92
OVERALL VARIABILITY						
	10.6	3.82	12.6	4.59	10.7	7.16

NOTE: + coefficient of variation of Δ COP (predicted peak centre-of-pressure displacement in unit pulse response, maximum likelihood model); coefficient of variation = standard deviation / mean.

estimates. To assess trends in the ΔCOP estimates, multiple regression analysis was performed, using day, test and day-test interaction as the independent variables. Simple regression versus overall test number was also performed.

The analyses were performed using the Minitab software package (Pennsylvania State University, University Park, Pennsylvania). The details of the statistical methods are described by Neter et al (1985a). The assumptions of the regression analyses were tested using the methods outlined in Section 6.9.1.

C.3 RESULTS

For brevity, only the maximum likelihood results are presented here. Very similar results were obtained using the least squares and cross-spectral models.

The data from the HPRN and RAN tests are plotted as a function of the overall test number in figures C.1 and C.2, respectively. In the plots, data obtained from each day are connected by solid lines. Note that there are some missing data points, due to equipment malfunction (problems with the computer interface that were later corrected; see Section 4.4.3). Compensatory manoeuvres (i.e. grabbing handrail, moving feet or waving arms) were not observed in any of the tests.

The test-to-test, day-to-day and overall coefficients of variation are listed in table C.1. From the tabulated and plotted results, it is evident that the subjects differed considerably in terms of day-to-day, test-to-test and overall variability. In addition, there were often substantial day-to-day differences in test-to-test variability and test-to-test differences in day-to-day variability, as evidenced by the large standard deviations in the mean values. Subjects 2 (HPRN) and 4 (RAN) showed much lower and more consistent levels of variability than the other subjects.

For the first testing day, the plotted data for subject 3 (HPRN) and, to a lesser extent, subjects 4 and 6 (RAN) suggest a tendency for decreasing ΔCOP with increasing test number, with the largest changes occurring between the first and subsequent tests. Subject 5 (RAN) appears to exhibit the opposite trend. Note, however, that the result from the first test was lost for this

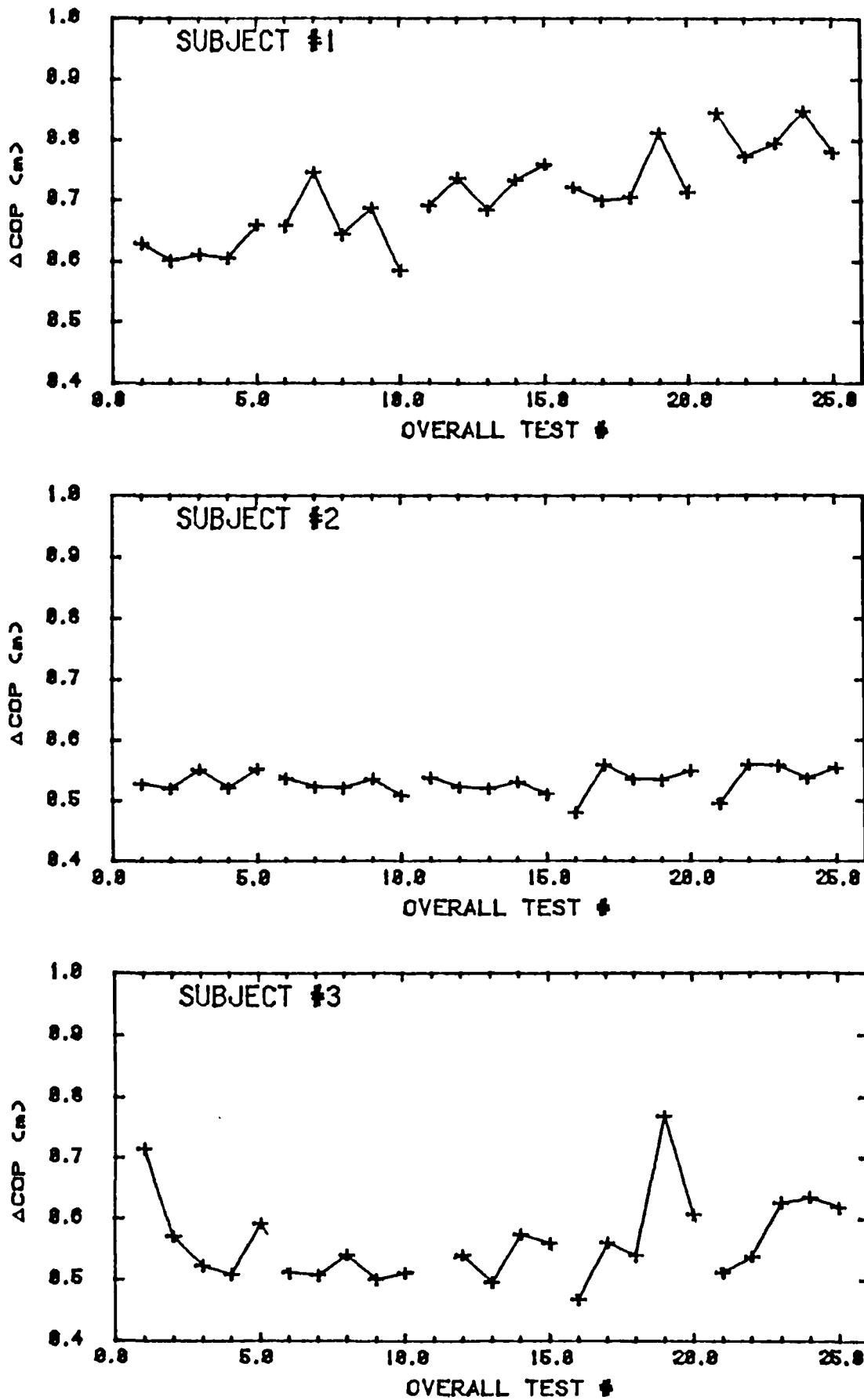


Fig C.1 Results of repeatability tests: pseudorandom waveform.

(Note: ΔCOP = peak centre-of-pressure displacement in unit pulse response, predicted using maximum likelihood model; solid lines connect data from same day.)

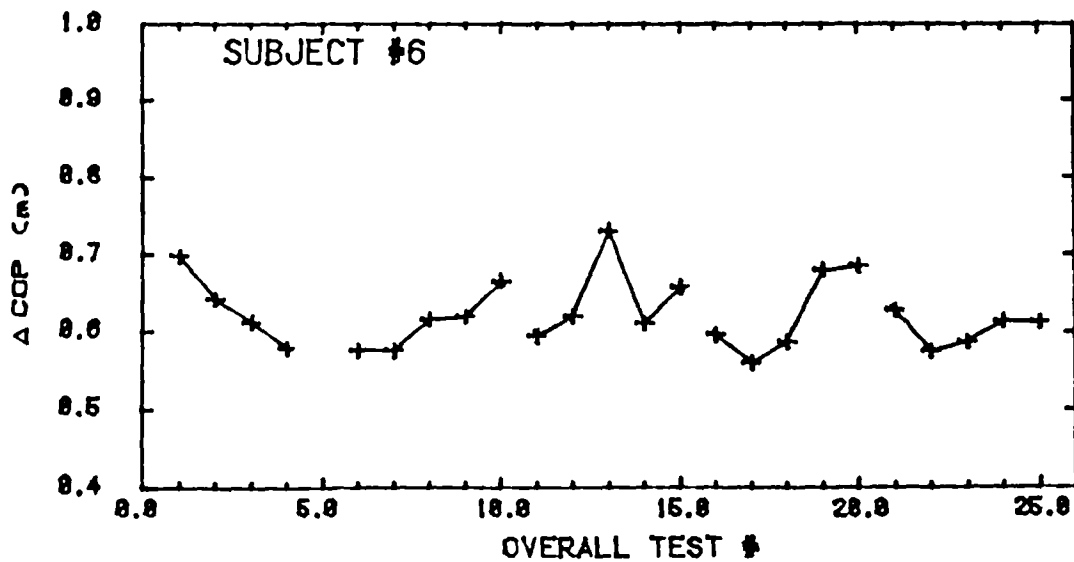
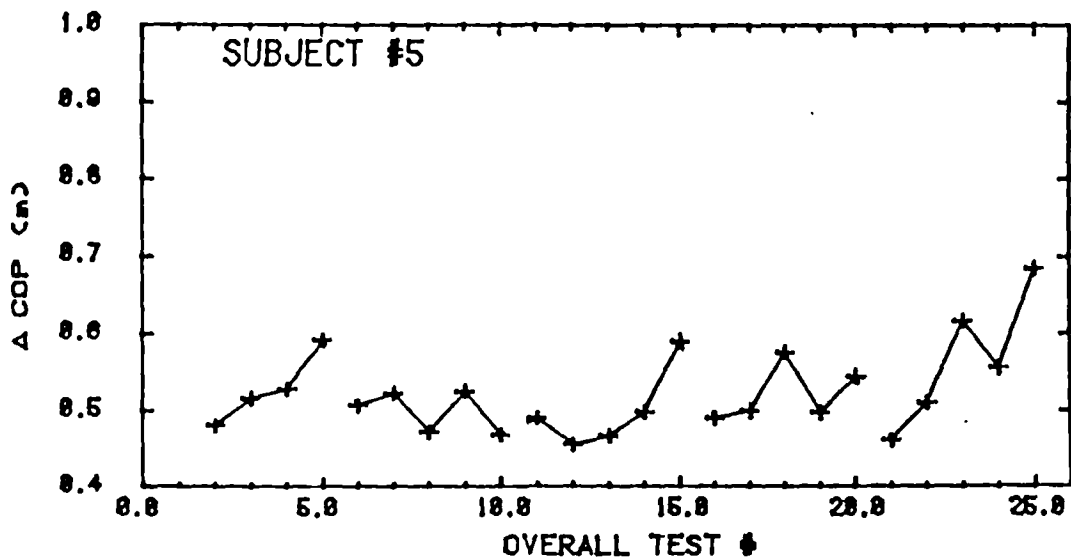
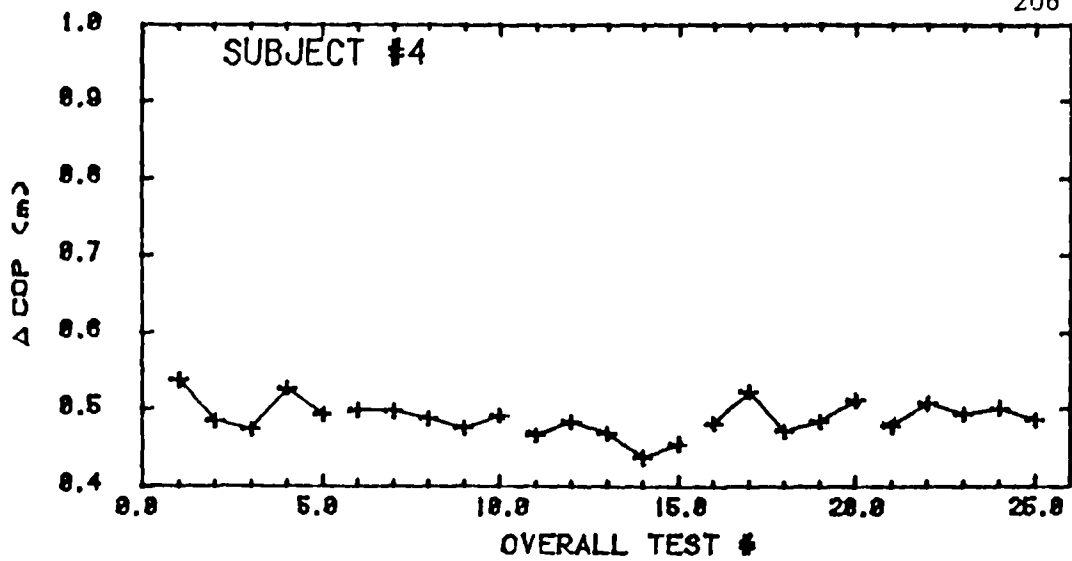


Fig C.2 Results of repeatability tests: random waveform.

(Note: Δ COP = peak centre-of-pressure displacement in unit pulse response, predicted using maximum likelihood model; solid lines connect data from same day.)

TABLE C.2

SUMMARY OF REGRESSION VERSUS DAY AND TEST NUMBER

WAVEFORM +	SUBJECT	SIMPLE	MULTIPLE REGRESSION ++		
		REGRESSION ++	DAY	TEST	INTER
<u>SLOPES: +++</u>					
HPRN	1	0.00848	0.0420	-0.00132	0.000655
	2	0.000483	-0.00554	-0.00401	0.00246
	3	0.00200	-0.0435	-0.0407	0.0173
RAN	4	-0.000415	-0.00678	-0.00758	0.00171
	5	0.00157	-0.00756	0.00176	0.00631
	6	-0.000522	-0.01932	-0.00558	0.00489
<u>T-VALUES: ++++</u>					
HPRN	1	7.19 ***	2.96 **	-0.09	0.15
	2	0.85	-0.83	-0.60	1.22
	3	1.02	-2.11 *	-1.96	2.79 *
RAN	4	-0.66	-0.88	-0.98	0.73
	5	1.88	-0.43	0.10	1.24
	6	-0.40	-1.28	-0.33	1.00

NOTE: + waveforms: HPRN = harmonic pseudorandom, RAN = random;
 ++ dependent variable = Δ COP (predicted peak centre-of-pressure displacement in unit pulse response, maximum likelihood model); for simple regression, independent variable = overall test number; for multiple regression, independent variables = day, test and day-test interaction;
 +++ units of regression slope = m/test, m/day or m/(day)(test);
 ++++ T-VALUE: T-test for zero slope; degrees of freedom = n-p, where n = number of data points (25 for subjects 1, 2 and 4; 24 for subjects 3, 5 and 6) and p-1 = number of independent variables;
 * p<0.05, ** p<0.01, *** p<0.001; p>0.05 in all other cases.

subject.

The results of the regression analysis are summarized in table C.2. Only two subjects showed significant trends. For subject 1 (HPRN), ΔCOP increased significantly with increasing overall test number ($p < 0.001$) and with increasing day ($p < 0.01$). This trend is also evident in the plotted data. Although subject 3 (HPRN) did show a significant day effect ($p < 0.05$), there was also significant day-test interaction ($p < 0.05$); therefore, for this subject, the day-to-day trend was dependent on the test number.

Except for subject 3, the diagnostic plots and tests gave no reason to suspect any serious violations of the assumptions of the regression model, i.e. that the data were normally and independently distributed with uniform variance. For subject 3, the increased variance apparent on days 1 and 4 would appear to violate the assumption of uniform variance; therefore, the regression results for this subject should be viewed with caution.

C.4 DISCUSSION

C.4.1 Adaptation to the Test Procedure

Systematic test-to-test differences may result from adaptation to the testing procedure and environment. Subjects who are initially apprehensive may tend to relax as they gain familiarity with the procedure, and may well modulate the "stiffness" of their posture control mechanisms in accordance with their level of anxiety and their expectations of the balance test. The day-to-day trend exhibited by subject 1 may be due to this type of adaptation. The same explanation may apply to the large change in response between the first and subsequent tests seen in subject 3.

Anticipatory changes in stiffness are probably not a realistic simulation of responses in actual falling situations, where the perturbation occurs suddenly and unexpectedly. Furthermore, because apprehension is expected to have a disproportionately large influence in the first test, where the subject "doesn't know what to expect", comparisons with subsequent tests may be confounded. See Section 8.6.6 for a more detailed discussion of this issue.

Based on these considerations, the test protocol was designed to minimize the "first test effect" by including a learning trial

in the protocol. Because the present experiments were to be limited to single-day testing, day-to-day trends were not a direct concern.

C.4.2 Adaptation to the Test Perturbation

Systematic test-to-test differences may also result from adaptation to the test perturbation, particularly if the waveform can be predicted by the subject. Pseudorandom waveforms are periodic and therefore can, in theory, be predicted. Although truly random waveforms are, by definition, unpredictable, the RAN waveform used in the tests is only an amplitude-limited approximation of true random noise and hence may also be predictable to some extent.

Because of the limited amount of data, the present results could not be analyzed for statistical differences between the two waveforms. However, the results give no reason to suspect any profound differences in predictability, as neither of the waveforms exhibited any significant test-to-test trends in the multiple regression analyses. In view of this finding, the significant day-to-day trend shown by subject 1 is probably a result of the adaptive effects described in Section C.4.1. The test-dependent day-to-day trends found in subject 3 could well be an artifact resulting from the "outlying" values obtained in tests 1 and 19.

C.4.3 Random Variability

Random test-to-test differences can occur as a result of random measurement and computational noise, and/or random changes in the balancing strategy adopted by the subject. The coefficients of variation presented in table C.1 reflect the influence of systematic trends, as well as random variation. Nonetheless, these results indicate that the test-to-test and day-to-day variability were generally quite small. For most subjects, the coefficients of variation were less than 10% and, in many cases, less than 5%. To put these values into perspective, they can be compared to the average change in response when blindfolded, which was found to be on the order of 10% (see table 7.3 in Chapter 7).

Occasionally, responses occurred that differed greatly from previous or subsequent responses, in particular, tests 1 and 19 for

subject 3. Whereas the test-1 result might be attributed to an adaptive effect, the test-19 result may reflect a radical change in balancing strategy that went undetected by the experimenter. The relatively large day-to-day coefficients of variation exhibited by subject 1 may be due largely to the significant day-to-day trend found in this subject.

If the random test-to-test variability is large, then it may be desirable to include, in the balance testing protocol, multiple tests for each subject, to allow averaging of the results. The present results suggest that the adaptive "first test effect" is potentially a much larger source of variation than the random variability, particularly for tests confined to a single day. Thus, in view of the testing time constraints imposed by other considerations such as subject fatigue and tolerance, multiple tests were not included in the protocol.

C.4.4 Limitations

The conclusions that can be drawn from these experiments are limited by the small numbers of subjects tested and, to a lesser extent, by the loss of data due to equipment malfunction. Nonetheless, the experiments did provide some useful information that was applied in designing the test protocol and test perturbation.

Although the results do give some indication of the test-to-test repeatability that can be expected in the balance tests, larger numbers of subjects must be tested. Furthermore, to attain a more realistic simulation of clinical applications, the tests should be repeated at longer intervals (e.g. weekly or monthly, instead of daily). Rather than using the identical perturbation signal in each test, the realization of the waveform should be varied from test to test (while preserving the same statistical and spectral properties), so as to minimize predictability.